The Role of the Deubiquitinase USP11 in Endocrine-Driven Breast Cancer

AUTHOR(S)

Lisa Dwane

CITATION

Dwane, Lisa (2018): The Role of the Deubiquitinase USP11 in Endocrine-Driven Breast Cancer. Royal College of Surgeons in Ireland. Thesis. https://doi.org/10.25419/rcsi.10803038.v1

DOI

10.25419/rcsi.10803038.v1

URL

https://repository.rcsi.com/articles/thesis/The_Role_of_the_Deubiquitinase_USP11_in_Endocrine-Driven_Breast_Cancer/10803038/1

The role of the deubiquitinase USP11 in endocrine-driven breast cancer

Lisa Dwane BSc (Hons)

Department of Molecular and Cellular Therapeutics

Supervisor: Prof. Darran O'Connor

Co-supervisor: Dr. Tríona Ní Chonghaile

RCSI

July 2018

A thesis submitted to the School of Postgraduate Studies, Faculty of Medicine and Health Sciences, Royal College of Surgeons in Ireland, in fulfilment of the degree of Doctor of Philosophy

Declaration

I declare that this thesis, which I submit to RCSI for examination in consideration of the award of a higher degree of Doctor of Philosophy is my own personal effort. Where any of the content presented is the result of input or data from a related collaborative research programme this is duly acknowledged in the text such that it is possible to ascertain how much of the work is my own. I have not already obtained a degree in RCSI or elsewhere on the basis of this work. Furthermore, I took reasonable care to ensure that the work is original, and, to the best of my knowledge, does not breach copyright law, and has not been taken from other sources except where such work has been cited and acknowledged within the text.

Signed _____

Student number _____

Date _____

Table of contents

Abbreviations

- 4-HT: 4-hydroxytamoxifen
- AF: Activating function
- AI: Aromatase inhibitor
- ANXA1: Annexin
- BARD1: BRCA1 associated RING domain 1
- BC: Breast cancer
- BCSS: Breast cancer-specific survival
- BLM: Bloom helicase
- BRCA1: Breast cancer type 1 susceptibility protein
- BRCA2: Breast cancer type 2 susceptibility protein
- CCD1: Cyclin D1
- CDK: Cyclin dependant kinase
- CEACAM1: Carcinoembryonic antigen-related cell adhesion molecule 1
- CKAP2L: Cytoskeleton Associated Protein 2 Like
- CYLD: Cylindromatosis
- DAVID: Database for Annotation, Visualization and Integrated Discovery
- DBD: DNA binding domain
- DDR: DNA-damage response
- DIAPH3: Diaphanous Related Formin 3
- DLR: Dual luciferase reporter
- DMEM: Dulbecco’s modified eagle’s medium
- DNA: Deoxyribonucleic acid
- DSB: Double strand breaks
- DUB: Deubiquitinase
- E1: Ubiquitin activating enzyme
- E2: Estradiol
- E2: Ubiquitin conjugating enzyme
- E3: Ubiquitin ligase
- EGFR: Epidermal growth factor receptor
- ERα: Estrogen receptor alpha
- ERβ: Estrogen receptor beta

- ES: Enrichment score
- FABP5: Fatty acid binding protein 5
- FASN: Fatty acid synthase
- FDA: Food and drug administration
- FPKM: Fragments per Kilobase of transcript
- GO: Gene ontology
- GREB1: Growth regulation by estrogen in breast cancer 1
- GSEA: Gene set enrichment analysis
- HDAC: Histone deacetylases
- HEK: Human embryonic kidney
- HER2: Human epidermal growth factor receptor 2
- HR: Homologous recombination
- HSP90: Heat shock protein 90
- IDC: Invasive ductal carcinoma
- IFIT1: Interferon-induced protein with tetratricopeptide repeats 1
- IFIT1: Interferon-induced protein with tetratricopeptide repeats 1
- ILC: Invasive lobular carcinoma
- INF: Interferon
- IP: Immunoprecipitation
- JAMM: Jabb1/MPN domain-associated metalloproteases
- KEGG: Kyoto encyclopaedia of genes and genomes
- KO: Knockout
- LBD: Ligand binding domain
- MAPK: Mitogen activated protein kinase
- METABRIC: Molecular Taxonomy of Breast Cancer International Consortium
- MIF: Macrophage migration inhibitory factor
- MINDY: Motif interacting with Ub-containing
- mTOR: Mammalian target of rapamycin
- MTT: 3-(4,5-Dimethylthiazol-2-yl)-2,5-Diphenyltetrazolium Bromide
- NCAPG: Non-SMC Condensin I Complex Subunit G
- NCAPH: Non-SMC Condensin I Complex Subunit H
- NCoR: Nuclear receptor corepressor

- NEMO: NF-κB essential modulator
- NF-κB: Nuclear factor kappa-light-chain-enhancer of activated B cells
- OS: Overall survival
- OTUB: Otubain
- OTUB1: Ovarian tumour deubiquitinase ubiquitin aldehyde binding 1
- PARP: Poly (ADP-ribose) polymerase
- PCA: Principal component analysis
- PCA: Principal component analysis
- PFS: Progression-free survival
- PgR: Progesterone receptor
- PI3K: Phosphoinositide 3-kinase
- PKIB: CAMP-Dependent Protein Kinase Inhibitor Beta
- PTM: Post-translational modification
- RFS: Recurrence-free survival
- RNA: Ribonucleic acid
- SDS-PAGE: Sodium dodecyl sulfate–polyacrylamide gel electrophoresis
- SEM: Standard error of the mean
- SERD: Selective estrogen receptor degrader
- SERM: Selective estrogen receptor modulator
- shRNA: Short hairpin RNA
- siRNA: Small interfering RNA
- SMRT: Silencing mediator for retinoid and thyroid receptors
- SRC: Steroid receptor coactivator
- TFF1: Tre foil factor 1
- TNBC: Triple-negative breast cancer
- TNM: Tumour, nodes, metastasis
- TOP2A: DNA topoisomerase 2-alpha
- TRAF2: TNF receptor-associated factor 2
- TRIM22: Tripartite Motif Containing 22
- TSA: Trichostatin A
- Ub: Ubiquitin
- UCH: Ubiquitin C-terminal hydrolase

- USP: Ubiquitin specific protease
- USP11: Ubiquitin-specific protease 11
- WHO: World health organisation
- WT: Wild type

Figures

Chapter 4

Chapter 5

Tables

Chapter 1

Chapter 2

Chapter 3

Chapter 4

Chapter 5

Summary

Approximately 80% of breast cancers overexpress the estrogen receptor α (ERα) and depend on this key transcriptional regulator for growth. The discovery of novel mechanisms controlling ERα function represent major advances in our understanding of breast cancer progression and potentially offer new therapeutic opportunities. Here, we investigated the role of deubiquitinating enzymes (DUBs), which remove ubiquitin moieties from proteins, in regulating ERα activity in breast cancer.

To identify DUBs involved in ERα transcriptional activity, an RNAi loss-of-function screen using a library of shRNA vectors targeting all 108 known or putative human DUB genes was performed. Suppression of the BRCA-associated DUB, USP11 was found to downregulate ERα transcriptional activity in ZR-75-1 cells and was the sole focus of this study.

Knockdown of USP11 in ZR-75-1 cells decreased ERα transcriptional activity and mRNA expression of ERα target genes. Furthermore, estradiol (E2) stimulation of these cells resulted in upregulation of USP11 in the nucleus and the formation of USP11 nuclear foci. IHC staining of a breast cancer tissue microarray (103 ER+ patients) and subsequent Kaplan-Meier analysis of this cohort revealed a significant association between high USP11 expression and poor overall ($p=0.030$) and breast cancer-specific survival ($p=0.041$). *In silico* analysis of publicly available breast cancer gene expression datasets further supported this observation. Interestingly, USP11 expression was upregulated in LCC1 cells, an isogenic, estrogen-independent model derived from MCF-7 cells. Knockdown of USP11 in LCC1 cells decreased the expression of multiple ERα target genes and cell cycle-associated genes, as determined by RNA sequencing (RNA-seq). Finally, knockdown of USP11 in ZR-75-1 cells induced significant changes in the proteome, as determined by liquid chromatography mass spectrometry (LC-MS).

This study, for the first time, determines a role for USP11 in ERα transcriptional activity. With further support, USP11 may represent a novel biomarker and therapeutic target in ERα-positive (ERα+) breast cancer.

Acknowledgements

Completing a PhD was the most rewarding yet difficult thing I have ever done and I would never have got to this stage without the ongoing support of many incredible people over the last 4 years. First of all, I'd like to say a huge thank you to my supervisor and mentor Prof. Darran O'Connor, for giving me the invaluable opportunity to pursue my career in breast cancer research. His advice and guidance over the last 4 years has been instrumental in the completion of this project and I am entirely grateful to have worked (and to continue to work) with him. I would also like to thank my co-supervisor Dr. Tríona Ní Chonghaile for her guidance and encouragement during my PhD. It is hugely important to any early-career female in academia to have a strong role model to look up to and Tríona certainly fulfils that role. I would like to thank Prof. William Gallagher for first introducing me in to the lab during my undergraduate studies for his guidance during my time in UCD. Importantly, I would like to thank the Irish Cancer Society and BREAST-PREDICT for funding my research and supporting me during these four years.

I would like to thank all of the incredibly talented scientists I have been lucky to work with during my PhD, especially to Brian, Sudip, Cami, Louise, Kate, Laoighse, Aisling, Bruce, Bo, Emer, Rut, and Marta. To my current lab members: Sudipto, thank you for your advice, encouragement and friendship during this time; I also apologise for always laughing at Brian's terrible jokes because I know this upsets you. Cami, you have been a breath of fresh air to this lab, thank you for being there and always pushing me to go to the gym when I don't want to go! Brian, I couldn't possibly put in to words how grateful I am to have you as a friend. Thank you for always keeping me smiling and shouting 'this is brand new information!!' at all of my poster sessions. We have been through so many ups and downs together in these last 5 years and I couldn't have done it without you. A big thank you to Seamus for always looking after me and making my last few months in the lab that little bit easier! A special thank you to Dr. Aisling O'Connor for mentoring me as an undergraduate and to Dr. Kate Connor and Dr. Laoighse Mulrane for helping me to find me feet in the early days of my PhD. To Dr. Catriona Dowling for getting back my thesis corrections in what I can only describe as world record time and to Elspeth Ward and Adam Lafferty… a bunch of incredible scientists and even more incredible friends! Come home…. Both of you!

I would like to thank all of my friends outside of the lab for their love and encouragement over the last 4 years. For the late night chats and dancing until the early hours at summer festivals, you all know who you are! These moments have kept me sane and I am so lucky to have a great network of friends around me. I want to say a very special thank you to Laura (Mammy Rice) for always supporting me and being proud of me.

Last but certainly not least, I want to thank my better half Dylan. Thank you for being my best friend and scientific advisor over these last four years; for reassuring me when experiments weren't working out and getting really excited for me when they were! You have helped me so much in my studies and this thesis wouldn't have been possible without your support. I can't wait to see where our academic careers take us in this world and I am so lucky to be taking this journey with you. And before you ask, no, we will not be starting a cancer immunology lab.

Finally, I want to thank my family for always believing in me and pushing me forward. To my parents, Marion and David Dwane, for making me the person I am today and always encouraging me to do my best. My mother's own journey with breast cancer inspired me to pursue this career and I hope that one day this small study can go on to help women like her.

This thesis is dedicated to my mother,
Marion Dwane, and to the memory of my father,
David Dwane

Chapter 1: General introduction

1.1 Breast Cancer

1.1.1 Introduction

Breast cancer (BC) is the most commonly diagnosed invasive cancer in women, with over 3,000 new cases occurring in Ireland each year. It is now estimated that one in eight Irish women will develop BC at some stage in their lifetime and these odds are rising rapidly. From 2015-2017, BC accounted for 30.1% of all cancers diagnosed in women, detected three times more frequently than lung or colorectal cancer. Despite the significant progress that has been made in the field over the last two decades, over 700 women in Ireland succumb to this complex, heterogeneous disease every year, making it the second leading cause of cancer-related mortality in Irish females (Figure 1.1) (NCRI, 2017). Advancements in our knowledge of BC pathogenesis are required in order to provide better management and care to patients and ultimately improve survival rates.

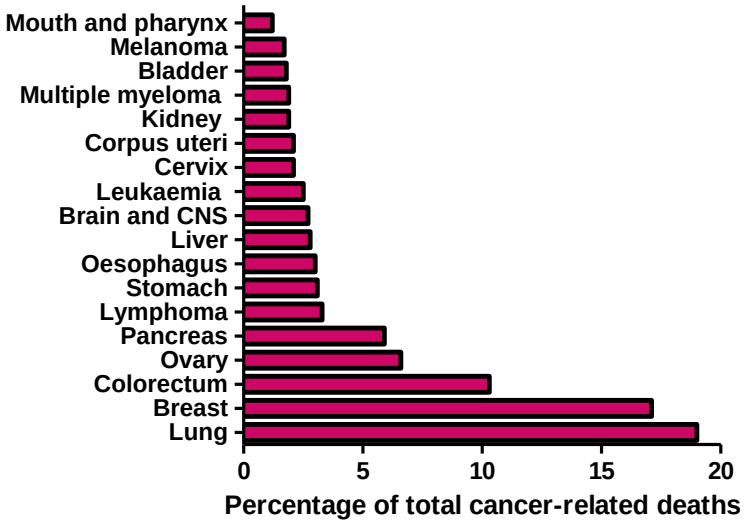

Figure 1.1: Breast cancer was the second most common cause of cancer-related mortality in females in Ireland 2012-2014 (NCRI, 2017).

There are a number of environmental and genetic factors that confer BC risk. The main risk factors for developing BC are being female and over the age of 50; others include age at first pregnancy (or no pregnancy at all), age at first menstruation and higher breast density (Eccles et al., 2013). Environmental factors, many of which are preventable, include alcohol and cigarette intake, poor diet and weight gain, shift work and hormone replacement therapy (McPherson et al., 2000).

Most breast cancers occur from sporadic genetic mutations, while only roughly 5-10% of cases are genetically inherited (Lalloo and Evans, 2012). Women with mutations in the DNA-damage repair (DDR) proteins, BRCA1 and BRCA2, have a 50-80% chance of developing breast and ovarian cancer in their lifetime. Both BRCA proteins are fundamental in homologous recombination (HR); a DNA double strand break (DSB) repair pathway which uses intact sister chromatids as a repair template (Roy et al., 2011). As HR protects the integrity of the genome, mutations within the pathway can lead to genome instability and as a result, carcinogenesis.

1.1.2 Breast cancer diagnosis, grading, staging

BC screening services have increased the incidence of early stage diagnoses. In Ireland, women between the ages of 50-69 are eligible for free mammographic screening every two years under the national BreastCheck screening programme (BreastCheck, 2018). If a lump is detected by mammography, a biopsy is taken and the sample is examined in the pathology laboratory. When diagnosed, BC is classified according to tumour stage and grade. Staging refers to the tumour size and how far the cancer has spread, while grading refers to how abnormal the tumour cells look following laboratory examination. The Tumour, Node, Metastasis (TNM) staging system is applied to a BC diagnosis, noting the size of the primary tumour and the presence of lymph node and distant metastases. Stages are then numbered 1-4; stage one being the earliest while stage 4 indicating distant metastasis from the breast (CRUK, 2017a).

Table 1.1: Breast cancer TNM staging

Tumour		Nodes		Metastasis	
TX	Tumour can't be measured of found	**NX**	Nodes can't be measured or found	**MX**	Metastasis can't be measured or found
T0	No evidence of primary tumour	**N0**	No lymph node metastasis	**M0**	No evidence of distant metastasis
Tis	*In situ* carcinoma	**N1**	Cancer cells present in 1 - 3 axillary lymph nodes	**M1**	Distant metastasis detected
T1	Tumour size is < 2 cm	**N2**	Cancer cells present in 4 - 9 axillary lymph nodes		
T2	Tumour size is between 2 cm - 5 cm	**N3**	Cancer cells present in > 10 axillary lymph nodes		
T3	Tumour size is > 5 cm				
T4	Tumour is any size with extension to the chest wall				
T4d	Inflammatory breast cancer				

1.1.3 Histological subtypes

BC is a highly heterogeneous disease encompassing many different subtypes and clinically, should not be treated as one disease. BC is histologically divided in to two main subtypes, invasive and *in situ* carcinoma. Invasive ductal carcinoma (IDC) is the most common infiltrating subtype, accounting for 70-80% of cases (Malhotra et al., 2010). This form of cancer originates in the milk ducts of the breast, migrates through the duct wall and as the name suggests, invades other breast tissue. Invasive lobular carcinoma (ILC) is a less common form of BC that originates in the milk-producing lobules of the breast, and accounts for 10-15% of all BC cases. ILCs often display characteristics associated with a good clinical prognosis, such as ERα positivity and low histological grade. Despite this, long term management of ILC can be difficult, as tumours are initially hard to detect, can be highly metastatic and as a result, ILC patients tend to have a worse outcome than other BC patients (McCart

Reed et al., 2015). *In situ* carcinoma is an early form of cancer and is often referred to as ‘pre-cancer’ of the breast. In cases of both ductal (DCIS) and lobular carcinoma *in situ* (LCIS), malignant cells have not invaded the breast tissue, making it a very treatable form of the disease

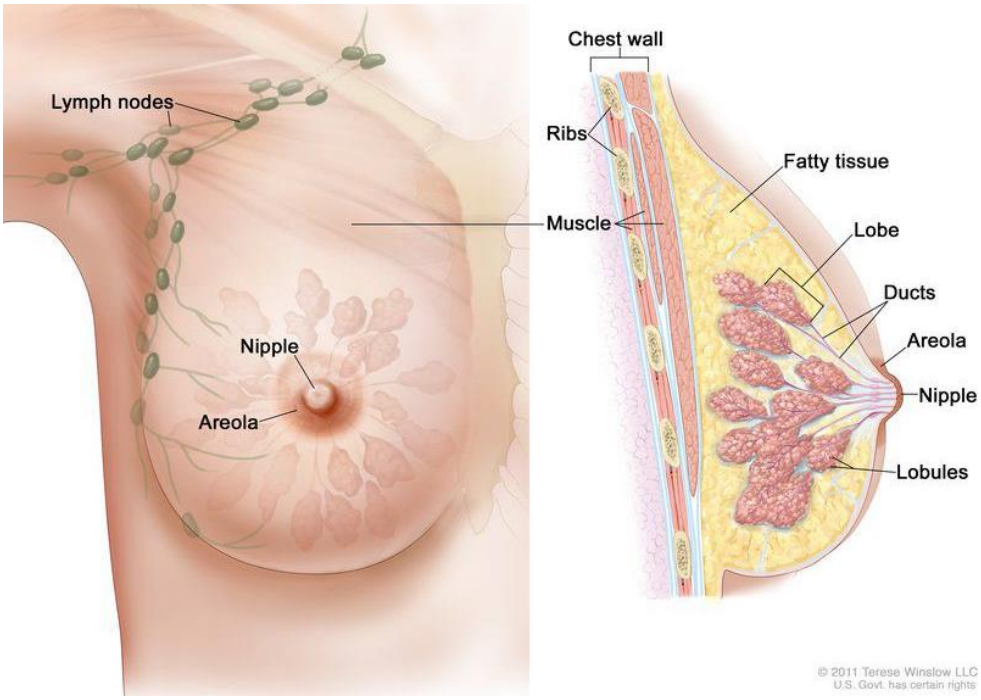

Figure 1.2: Anatomy of the female breast. *BC originates in either the milk-producing lobules (lobular carcinoma), or the ducts which carry the milk to the nipples (ductal carcinoma). The chest wall and axillary lymph nodes are often the first locations of BC metastasis. Image credit: National Breast Cancer Foundation.*

1.1.4 Molecular subtypes

Further classification of BC is made based on the molecular biology of a breast tumour. The use of immunohistochemical markers to categorise BC subtypes is common practise in the management and care of patients. Sørlie and colleagues were the first to categorise BC in to distinct, biological subtypes (Table 1.1) (Perou et al., 2000, Sorlie et al., 2001). Luminal tumour cells resemble those in the milk duct lumen, expressing luminal cytokeratins and hormone receptors. Luminal BC is classified in to at least two biological subtypes. Luminal A BCs are estrogen receptor alpha (ERα) or progesterone receptor (PgR) positive, human epidermal growth factor receptor 2 (HER2) negative, and have higher ERα target gene and lower proliferative marker expression than luminal B. Luminal B tumours are associated with a poorer

prognosis; they are ERα or PgR positive, HER2 positive or negative, and display a higher expression of proliferative markers such as Ki67 (Table 1.2).

The HER2 oncogene, from its first discovery (Coussens et al., 1985) to today's HER2-targeting therapies, has been one of the biggest success stories in the field of oncology. Roughly 25-30% of BCs have up to 100 times more expression of the HER2 transmembrane growth factor receptor (Moasser, 2007). HER2+ BCs have been generally associated with a poor prognosis, however, current and emerging HER2-targeting therapies are beginning to shift that trend.

Gene expression profiles of basal tumour cells resemble that of basal epithelial cells, lacking hormone receptor and HER2 expression, while expressing keratins, epidermal growth factor receptor (EGFR) and proliferative markers. Basal-like BC is often high grade and *TP53* mutations are common (Dai et al., 2015). While basal-like and triple-negative breast cancer (TNBC) are terms often used interchangeably, they are not synonymous. While most TNBCs are basal-like and vice versa, not all basal BCs lack ERα, PgR and HER2, and not all TNBCs have a basal expression profile (Badve et al., 2011).

Table 1.2: Five originally defined molecular BC subtypes (Dai et al., 2015)

Subtype	IHC status	Grade	Outcome
Luminal A	ER+/PgR+, HER2-, Ki67-	1/2	Good
Luminal B	ER+/PgR+, HER2-, Ki67+	2/3	Intermediate
	ER+/PgR+, HER2+, Ki67+		Poor
HER2+	HER2+, ER-, PgR-	2/3	Poor
Basal	ER-. PgR-, HER2-, basal marker+	3	Poor
Normal-like	ER-/PgR-, HER2-, Ki67-	1/2/3	Intermediate

In 2012, the genomic and transcriptomic analysis of over 2000 BC tumours further classified these molecular subtypes in to 10 integrated clusters. The Molecular Taxonomy of Breast Cancer International Consortium (METABRIC) study represented a major advancement in BC tumour classification, helping to tailor treatment to individual patients and providing rationale for the development of novel targeted therapies (Curtis et al., 2012, Dawson et al., 2013).

1.1.5 Breast cancer care and treatment

Perhaps the most effective treatment for any malignancy, to this day, is surgical removal of the tumour. There are two main types of BC surgery, mastectomy and wide local excision (lumpectomy), with or without the removal of axillary lymph nodes. Mastectomy, the removal of the entire breast, can range from total to radical mastectomy. While total mastectomy removes the breast tissue only, radical mastectomy removes the entire breast, lymph nodes and chest wall muscle. Lumpectomy involves the removal of the tumour and some of the surrounding normal tissue, conserving most of the breast. Most women receive radiotherapy following lumpectomy in order to irradiate any remaining tumour cells in the breast (Breastcancer.org, 2017).

Radiotherapy is the use of high energy x-rays directed at the breast to remove cancer cells. Radiotherapy also targets normal cells, which recover better than malignant cells due to their genomic stability. Radiotherapy is most commonly given after surgical resection of the tumour but can also be used prior to surgery to reduce tumour size. Radiotherapy can also be given as part of palliative care to relieve tumour-associated pain (Lutz et al., 2014).

The use of cytotoxic chemotherapy is common in the treatment of BC. Given systemically, it can target most rapidly dividing cells in the body- cancer and benign. It is for this reason that side effects associated with chemotherapy are quite severe; most patients suffer with alopecia, fatigue, nausea and constipation (ICS, 2015). Patients can receive neoadjuvant chemotherapy to shrink a tumour before surgery, and/or adjuvant chemotherapy to irradiate any remaining cancer cells. The most common chemotherapeutics used to treat BC include anthracyclines (doxorubicin and epirubicin), taxanes (paclitaxel and docetaxel), 5-fluorouracil, cyclophosphamide and carboplatin. A combination of two or three of these therapeutics are often administered in cycles (EBCTCG, 2005).

1.1.6 Targeted therapies: a personalised approach

In recent years, the most effective approach to treating BC has been tailoring the treatment to the unique biology of an individual's tumour. Utilising ERα, PgR and HER2 expression as predictive and prognostic markers is now standard of care following BC diagnosis. The discovery of these biomarkers has played a substantial role in the development of a number of novel targeted therapies, resulting in

significant improvements in the available treatment options for patients who display these tumour characteristics (Weigel and Dowsett, 2010).

As mentioned, the discovery and targeting of HER2 is one of oncology's biggest success stories. HER2 is one of four family members of epithelial tyrosine kinase receptors, to which it dimerises with to activate downstream growth signalling pathways (Incorvati et al., 2013). Trastuzumab (Herceptin®) was approved by the FDA in 1998 (Genentech, 1998) and was the first humanised monoclonal antibody approved for the treatment of metastatic BC. Monoclonal antibodies, or 'magic bullets', bind to their target epitope on a specific protein (in this case, HER2), blocking downstream growth signalling, while concurrently recruiting tumour-fighting immune cells (Vu and Claret, 2012). Owing to the success of trastuzumab, several other HER-targeting agents have progressed in to clinical use. For example, Lapatinib, which targets both HER1 and HER2 and is orally administered, was approved by the FDA in 2010. When combined with trastuzumab, overall survival (OS) of BC patients with HER2+, metastatic disease is extended by 4.5 months, on average (Blackwell et al., 2012). Pertuzumab, which blocks HER2/HER3 dimerisation, was approved in 2012 for HER+ metastatic BC following the results of the CLEOPATRA phase 3 clinical trial. Pertuzumab (Perjeta®), in combination with trastuzumab and docetaxel, extended progression free survival by an average of 6.1 months (Baselga et al., 2012). Trastuzumab-emtansine (TDM-1), is an antibody-drug conjugate, approved by the FDA in 2013 under the trade name Kadcyla® (Genentech, 2013). The immunoconjugate agent is a combination of trastuzumab and the microtubule-targeting chemotherapeutic emtansine (DM-1) (Incorvati et al., 2013). Thirty years of HER2 research and the introduction of targeted therapies has revolutionised the treatment of aggressive, HER2+ BC and has dramatically increased survival rates, as a result.

PgR is one of the most valuable biomarkers in BC diagnosis and management, however, PgR-targeted therapies have yet to make it in to the clinic. A leading-edge, preclinical study by Mohammad *et al.* suggests that stimulation of PgR with a PgR agonist, either endogenous progesterone or its synthetic form, can slow the growth of tumour cells and enhance sensitivity to tamoxifen (Mohammed et al., 2015). Activated PgR can change the location of ERα DNA binding and alter activity of the ERα complex in BC, as a result. This is the proposed explanation as to why ERα+/PgR+ patients tend to have a more favourable prognosis than ERα+/PgR-

patients (Baird and Carroll, 2016). PgR targeting is quite debatable, however, and further research is required to determine which BC patients can benefit from such therapy (Carroll et al., 2017). ERα targeted therapies, conceivably the most widely used and studied, will be explored in detail in the next section.

1.2 The Estrogen Receptor (ER)

1.2.1 Steroid receptor signalling

The first link between estrogen and BC was made in 1896, when physician George Beatson removed the ovaries of a 33-year old woman with advanced BC and consequently controlled her cancer growth (Clarke, 1998). Today we know that 70-80% of BCs display overexpression of ERα, making it one of the most significant biomarkers in the oncology field (Oosterkamp et al., 2014). The physiological functions of ER in human tissue are mediated by two receptor isoforms, ERα and ERβ (encoded by *ESR1* on chromosome 6 and *ESR2* on chromosome 14, respectively) (Lee et al., 2012). Both receptors share a common role in ovarian function, however their expression and function is diverse in other human tissues. In the breast and uterus ERα regulates cell proliferation, while ERβ counteracts this (Paterni et al., 2014). ER homology and differential expression in human tissue is outlined in Figure 1.3.

ERα, like other type 1 nuclear receptors, acts as a transcription factor when bound and activated by the steroid hormone estrogen. First, estrogen enters the cell and binds to cytoplasmic ERα, inducing dissociation from heat shock protein 90 (HSP90). When released, ERα homodimerises and translocates in to the nucleus. Here, ligand-bound ERα interacts with a number of cofactors which facilitate high-affinity binding to estrogen response element (ERE) palindromic sequences on DNA (Sever and Glass, 2013, Bjornstrom and Sjoberg, 2005) (Figure 1.4). Once bound, ERα can regulate the expression of estrogen-responsive genes and promote epithelial cell proliferation in normal mammary gland development. Deregulation of this process however, can result in uncontrolled proliferation and malignant formation (Le Romancer et al., 2011).

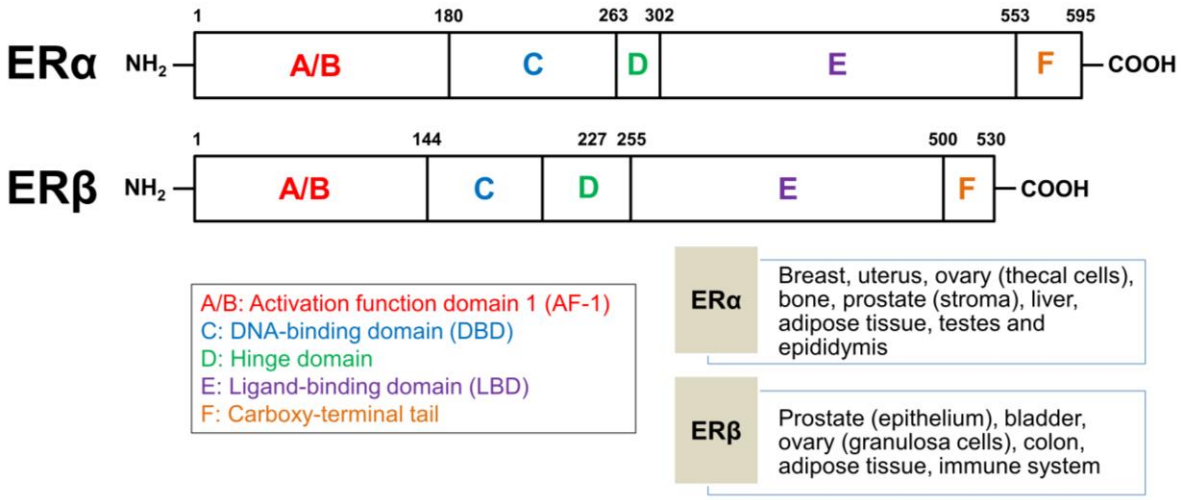

Figure 1.3: Sequence homology between ERα and ERβ and differential expression in human tissue. *Both ERs contain 5 domains with distinct functions. The N-terminal A/B domain contains AF-1, which plays a key role in transcriptional activity and interaction with cofactors. The C domain encodes the DBD, which binds to specific response elements on ER target genes. The D domain, or hinge region, is responsible for nuclear translocation. The E domain encodes the LBD where estrogen binds, as well as AF-2 which, similarly to AF-1, plays a role in transcription and cofactor recruitment. The function of the C-terminal F domain is poorly understood (Lee et al., 2012).*

As mentioned, ERα recruits a number of cellular cofactors in the nucleus which facilitate its function. The steroid receptor coactivator (SRC) family interacts with a number of ligand-bound nuclear receptors, including ERα, enhancing transcriptional activation. It is believed that SRC proteins play an active role in chromatin remodelling and recruitment of further transcription factors (Xu and Li, 2003). Moreover, aberrant SRC activity plays a key role in endocrine therapy resistance and metastatic BC (Browne et al., 2018). Corepressors, in contrast, repress ERα-mediated gene expression. Silencing mediator of retinoic acid and thyroid hormone receptors (SMRT) and its paralog, nuclear corepressor (N-CoR), play key roles in ERα-mediated gene repression. These proteins recruit further corepressors and histone deacetylases to repress ERα target gene expression (Varlakhanova et al., 2010).

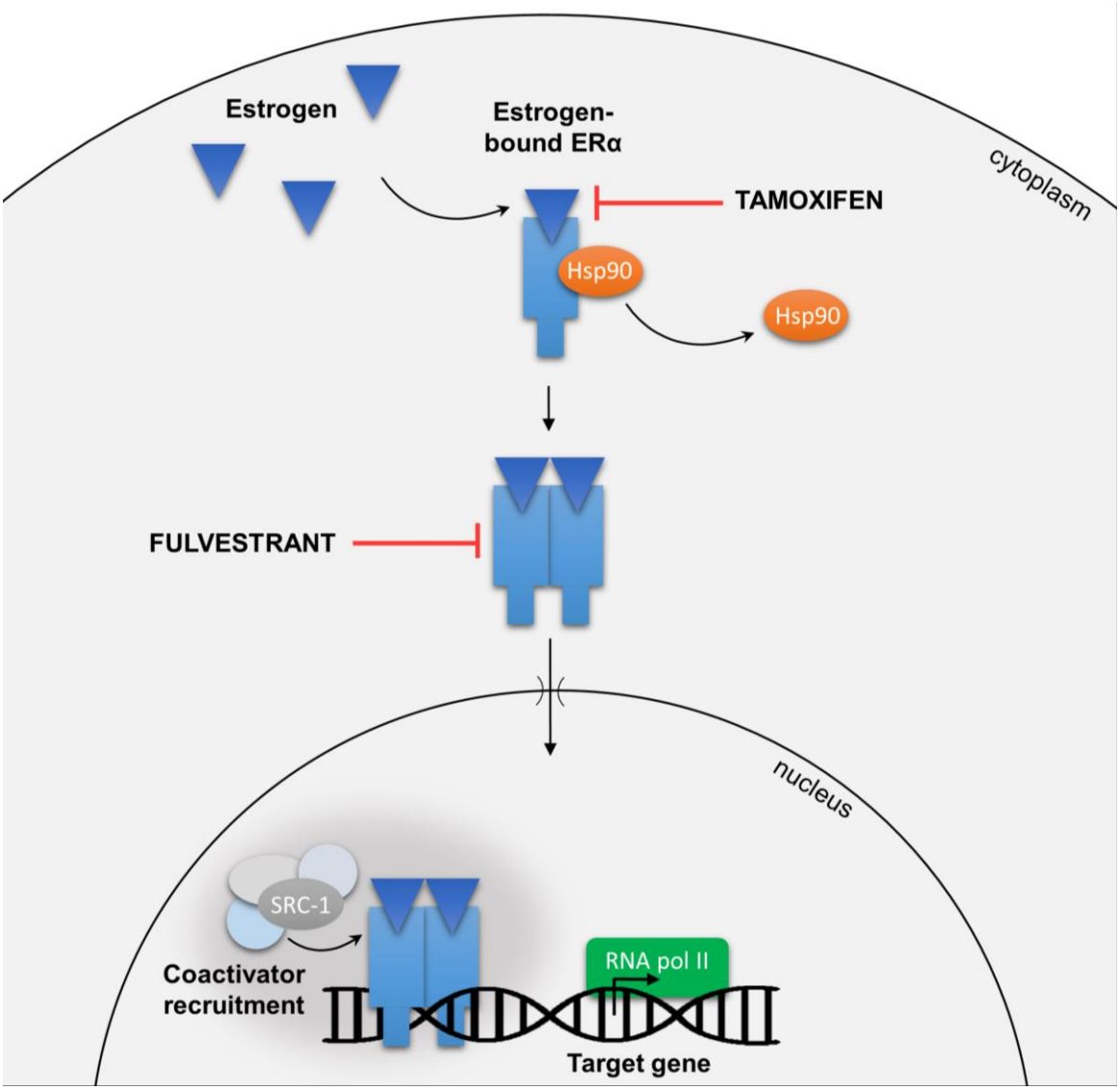

Figure 1.4: Overview of ERα signalling in BC. *Ligand-bound ERα dissociates from Hsp90, dimerises, and translocates to the nucleus. ERα binds to estrogen response elements, recruits coactivators and initiates transcription of target genes.*

1.2.2 ERα targeted therapies

ERα+ tumours are often associated with good prognosis and can be treated with anti-endocrine therapies which either promote receptor degradation (fulvestrant), block estrogen synthesis (aromatase inhibitors (AIs)) or antagonise the receptor (tamoxifen) (Maximov et al., 2013). Tamoxifen is a selective estrogen receptor modulator (SERM) that competes with estrogen for ERα in breast tissue and ultimately prevents the transcription of estrogen-responsive genes. The year 2017 marked the 40 year anniversary since the FDA approved the use of tamoxifen in ERα+ BC and it since has been one of the most prominent therapies in BC oncology.

Tamoxifen is a prodrug and is metabolised in the liver to its active forms, 4-hydroxytamoxifen (4-HT) and endoxifen. Estrogen-bound ERα adopts a structural conformation in which the LBD helix 12 forms a hydrophobic cleft containing AF-2 allowing for interaction with ERα coactivators. Tamoxifen binding shifts the conformation of helix 12 and as a result it binds to AF-2, attenuating coactivator binding and repressing ERα transcriptional activity (Clemons et al., 2002, Heldring et al., 2004). As a SERM, tamoxifen function is 'selective'. Tamoxifen acts as partial agonist in the uterus, therefore its long-term use can be associated with endometrial cancer. However, it can also be used to induce ovulation in women with fertility issues (Steiner et al., 2005). In BC, adjuvant tamoxifen treatment significantly reduces the rate of recurrence and reduces BC mortality, not only during the treatment period but for a decade following (Davies et al., 2013).

Other SERMs include raloxifene, which has a similar mechanism of action to tamoxifen but does not display agonist activity in the uterus (Dutertre and Smith, 2000). In 2007 raloxifene was FDA approved for both BC risk reduction and osteoporosis in postmenopausal woman (NIH, 2007). Toremifene, which also has a similar structure and function to tamoxifen, is approved for use in postmenopausal patients with advanced BC (Vogel et al., 2014).

Fulvestrant is a pure anti-estrogen. It reversibly binds to ERα momomers, preventing homodimerisation, hindering translocation in to the nucleus and inducing ERα degradation by the proteasome. Unlike tamoxifen, both AF-1 and AF-2 activating factor function is repressed and as a result, gene expression is inhibited. Furthermore, fulvestrant has no agonist function in human tissue, which represents a further advantage over tamoxifen (Carlson, 2005). Early clinical trials showed that fulvestrant was effective in BC patients previously treated with tamoxifen and aromatase inhibitors (AIs), leading to its FDA approval in 2002 (Ciruelos et al., 2014). In august 2017, the FDA approved fulvestrant as a monotherapy for ERα+, HER2- postmenopausal women who have not received any other endocrine therapy (AstraZeneca, 2017).

AIs do not directly act on or modulate ERα. Instead, they interfere with estrogen biosynthesis from androgens through suppression of the aromatase enzyme. AIs are often prescribed to postmenopausal women, where ovarian function is already suppressed. In premenopausal women, AIs have little effect on circulating estrogen due to high levels of aromatase substrate in the ovary (Fabian, 2007).

However, the completion of the Suppression of Ovarian Function Trial (SOFT) indicated that premenopausal, high-risk BC patients can benefit from the AI exemestane combined with ovarian suppression (Francis et al., 2015).

Third generation AIs in clinical use include anastrozole and letrozole, which reversibly bind to aromatase, while the steroidal AI exemestane irreversibly binds. A number of clinical trials have demonstrated the benefits of AI therapy, both as first line treatment and following tamoxifen treatment, and this is now recommended as the standard of care for postmenopausal BC patients (Winer et al., 2005).

Patient compliance to anti-endocrine therapy remains a serious issue in the oncology clinic and is associated with increased mortality. Previous studies have highlighted that 30-50% of patients discontinue their adjuvant therapy by the 4th year, often due to menopausal-like side effects (Wouters et al., 2013).

1.2.3 Resistance to ERα targeted therapies

Resistance to anti-endocrine therapies remains a clinically significant problem. Despite their therapeutic success in the adjuvant setting, almost half of patients will eventually relapse on endocrine intervention therapies. (Clarke et al., 2015). There are two major resistance classifications; *de novo*, when the patient does not respond to first line treatment, and acquired, when the patient initially responds but later relapses. There are a number of different mechanisms which confer resistance to anti-endocrine therapies, some of which are discussed below.

1.2.3.1 Nuclear receptor expression

The heterogenetic nature of breast tumours can mean there are a subpopulation of both ERα+ and ERα- cells. While anti-endocrine therapies might irradiate the ERα+ population, the ERα- cells can remain and proliferate. ERα loss over time occurs in ~20% of BC patients (Osborne and Schiff, 2011), meaning these tumours are no longer dependent on estrogen and don't respond to endocrine intervention. A number of different mechanisms have been proposed for ERα expression loss, including hypoxia, epigenetic silencing, the presence of p53 mutation and MAPK hyperactivation (Garcia-Becerra et al., 2012). However, the majority of drug sensitive ERα+ BCs that recur do continue to express ERα, and although they often respond to second or third line treatments, treatment failure is seen with increasing lines of therapy (Clarke et al., 2015).

The likelihood of anti-endocrine response is largely dependent on PgR expression. ERα+/PgR+ tumours are more common, and have a treatment response rate of ~70%. While it was initially assumed that PgR positivity was an indicator of active ERα function (which would respond well to therapeutic intervention), we now know that PgR affects ERα activity and alters DNA binding in BC (Mohammed et al., 2015). The loss of PgR in metastatic BC was associated with disease progression, indicating that PgR expression may be used as a biomarker in predicting response to endocrine therapy.

1.2.3.2 ERα mutations

Recurrent, ERα+ metastatic tumours often display anti-endocrine resistance and ERα mutation. The two most prevalent ERα mutations occur in the LBD (Y537N/C/S and D538G) (Martin et al., 2017), driving ligand-independent function and contributing to anti-endocrine resistance. Recently, Jeselsohn and colleagues elucidated the ERα mutant cistrome, highlighting differences between the estradiol-bound wild-type receptor and between both Y537S and D538G mutants. This highlighted the complexity of each mutation, provided a key insight in to mechanisms of resistance and revealed novel therapeutic targets in ERα mutant BC (Jeselsohn et al., 2018).

1.2.3.3 Coregulator function

As mentioned, aberrant coregulator activity is associated with anti-endocrine resistance. Coregulator recruitment is crucial in both agonist and antagonist activities of tamoxifen, the dysregulation of which can lead to resistance. SRC3 coactivator overexpression has been widely linked to tamoxifen resistance and it is overexpressed in many BC cell lines and tumours (Anzick et al., 1997). Furthermore, overexpression of SRC1 can convert tamoxifen activity from transcriptional repression to activation (Romano et al., 2010). Although extensively studied, the use of coregulators as predictive or prognostic markers is not clinically routine.

1.2.3.4 Growth pathways

The interplay of other cellular growth pathways can affect response to endocrine therapy, either by enhancing ERα signalling or bypassing it completely. HER2 overexpression and subsequent growth pathway activation has been associated with

poor response to anti-endocrine therapies (Clarke et al., 2015). *In vitro*, overexpression of HER2 in MCF-7s leads to ERα downregulation, tamoxifen agonist behaviour and therapy resistance (Garcia-Becerra et al., 2012). *In vivo*, HER2 crosstalk with SRC3 could also enhance the agonist activity of tamoxifen. Furthermore, fulvestrant-resistant tumours display both HER2 and MAPK upregulation (Massarweh et al., 2006), supporting their role in resistant pathways. Combining trastuzumab or gefitinib, an EGFR inhibitor, with anti-endocrine agents has shown promise *in vitro*, and may be a means of overcoming drug resistance in a subset of patients (Fan et al., 2015).

The phosphoinositide 3-kinase (PI3K) pathway has been extensively studied as an oncogenic mechanism in BC. PI3K/Akt/mTOR is hyperactivated in endocrine-resistant tumours and is known to confer therapy resistance. PI3K mutations are common in ER+ BC, occurring in roughly 30% of cases. Estrogen independent, ER+ cell lines are dependent on PI3K for growth, and mirror a clinical, anti-endocrine resistance phenotype (Fox et al., 2012). There are multiple pre-clinical models, supported by clinical evidence, for the use of PI3K pathway inhibitors in overcoming anti-endocrine therapy resistance. Everolimus, an mTOR inhibitor, has been shown to enhance the response to neoadjuvant letrozole. Furthermore, patients who had progressed on letrozole benefitted from everolimus combined with tamoxifen (Massarweh et al., 2006). The FDA approved everolimus for hormone receptor positive, HER2- advance BC in 2012 (NCI, 2012).

With these emerging reports of resistance mechanisms, there is a growing demand for alternative therapies to treat patients who don't respond to or develop resistance to current anti-endocrine therapies. Further understanding of the molecular mechanisms that control ERα activity can lead to the discovery of novel therapies for the treatment and management of ERα+ BC.

1.2.4 Post-translational regulation of ERα

Post-translational modifications (PTMs) can enhance or inhibit the functional ability of a protein and are essential for their physiological function within the cell (Wang et al., 2014). ERα is subject to multiple PTMs that can affect the stability, localisation and expression of the receptor. Perhaps the most widely studied PTM of ERα is serine phosphorylation, which is associated with both ligand-dependant and ligand-independent activation (Bunone et al., 1996), activation of ERα target genes (Cheng

et al., 2007), enhanced cofactor interaction (Shah and Rowan, 2005) and tamoxifen resistance (Thomas et al., 2008). There are 14 serine residues in the ERα N-terminal domain, many of which have been functionally characterised. Phosphorylation of S118 and S167 in the A/B AF-1 domain, are the best characterised. S118, which can be phosphorylated by MAPK, mTOR, CDK7 and EGFR, MAPK phosphorylation plays a role in coregulator binding and can enhance estradiol (E2) sensitivity. Importantly, hyperactivation of the MAPK pathway and subsequent S118 phosphorylation can drive ERα ligand-independent activity (Le Romancer et al., 2011, Anbalagan and Rowan, 2015).

S167 can by phosphorylated by MAPK, Akt and casein kinase 2 (CK2). Akt overexpression can increase S167 phosphorylation, enhancing tamoxifen resistance, ERα DNA-binding and interaction with SRC3 (Anbalagan and Rowan, 2015). S167 phosphorylation has also been implemented in tamoxifen resistance in endometrial cancer (Shah and Rowan, 2005).

Acetylation of ERα can either enhance or repress transcriptional activity of the receptor, depending on the modified lysine. Acetylation at K266, K302 and K303 is constitutive and is associated with ERα transcriptional inhibition. Unfortunately, little is known about the mechanisms that control acetylation of ERα. Interestingly, BRCA1 can repress ERα acetylation via the coactivator p300, while BRCA1/BARD1 represses ERα activity via monoubiquitination at K302, suggesting a PTM balance of ERα function mediated by BRCA1. (Ma et al., 2010). K266 and K268 are the main targets for p300 mediated acetylation, which were found to enhance both DNA binding and ligand-dependant activity (Kim et al., 2006).

Methylation can also occur on ERα at K302 by the methyltransferase SET7. SET7 methylation stabilises ERα and is important for the recruitment of the receptor to and the activation of target genes (Subramanian et al., 2008). ERα methylation is also involved in non-genomic signalling. Protein Arginine Methyltransferase 1 (PRMT1) transiently methylates the receptor at A260 and promotes its interaction with the p85 subunit of PI3K in the cytoplasm (Le Romancer et al., 2008).

Furthermore, methylation is associated with gene silencing when occurring at the promotor. Early reports describe differential methylation profiles of ERα in BC (Piva et al., 1990) and further state that the ERα promotor is methylated and could contribute to loss of ERα (Ottaviano et al., 1994). As discussed in section 1.2.3, the loss of ERα expression during BC treatment is associated with anti-endocrine

resistance. HDAC inhibitors, which can demethylate DNA and induce re-expression of a silenced gene, have received much scrutiny in cancer therapeutics. Interestingly, HDAC1 interacts with ERα and suppresses transcriptional activity via AF-2, suggesting a role in BC progression. Treatment with the HDAC inhibitor trichostatin A (TSA) can induce re-expression of ERα in ERα- BC cells, and may represent a viable therapeutic strategy in patients demonstrating ERα loss during therapy (Giacinti et al., 2006).

It is clear that post-translation modifications of ERα play a pivotal role in receptor function and BC pathogenesis. One modification of interest that has not received as much attention in this context is ubiquitination.

1.3 Ubiquitination

1.3.1 The Ubiquitination Pathway

Ubiquitination, a PTM involving the addition of a ubiquitin (Ub) moiety to a protein substrate, is the primary mechanism of protein turnover in the cell. Ub-mediated proteolysis has been extensively investigated for decades and indeed, the Nobel Prize in Chemistry was awarded to Aaron Ciechanover, Avram Hershko and Irwin Rose in 2004 for the discovery of this mechanism (Hershko and Ciechanover, 1998). Ubiquitination is a multistep process catalysed by three key enzymes; Ub activating enzyme (E1), Ub conjugating enzyme (E2) and Ub ligase (E3). Initially, the C-terminal carboxylate group of Ub is linked to E1 via a high energy thioester bond. E1 transfers Ub to one of its own cysteine residues, which is then shifted to a sulfhydryl group on one of the many E2 enzymes. Finally, E3 specifically catalyses the transfer of ubiquitin from E2 to a lysine residue on the substrate protein. The end result is a mono- or polyubiquitinated target protein, as illustrated in Figure 1.3 (Ciechanover et al., 2000, Berg et al., 2007, Dwane et al., 2017). As any of the seven lysine residues on the Ub molecule can be utilised to generate a polyubiquitin chain, different topologies can be produced with different functional consequences (Suryadinata et al., 2014). Polyubiquitin chains linked at lysine (K) residue 48 (K48) shuttle the tagged protein to the 26S proteasome; this degradative form of ubiquitination is often termed the ‘molecular kiss of death’ (Pickart, 2001, Pickart and Eddins, 2004). In contrast, monoubiquitination, and Ub chains of different topologies result in altered target protein functionality (Table 1.4).

Monoubiquitination, the addition of a single Ub molecule, is heavily involved in many proteasomal-independent functions of ubiquitination such as endocytosis (Haglund et al., 2003) and histone modification (Cole et al., 2015). Additionally, K63-linked polyubiquitination is one of the only non-degradative chain formations with a firmly established series of non-traditional functions, for example DDR (Messick and Greenberg, 2009), protein trafficking (Erpapazoglou et al., 2014), transcriptional regulation (Vallabhapurapu and Karin, 2009) and kinase signalling (Wang et al., 2012).

Spence and colleagues were the first to demonstrate that different Ub chain linkages engage in different functional roles by substituting each individual lysine residue on Ub for arginine in *Saccharomyces cerevisiae* and observing defects in DDR. Amino acid substitutions at K63 had no notable effect on protein turnover, indicating a role for K63-linked ubiquitination in non-degradative pathways (Spence et al., 1995). Despite this discovery, the rationale behind this differential functional role was initially unknown. It has since been established over the last two decades that the functional diversity of Ub linkages is largely dependent on the structural conformation of the polyubiquitin chain (Varadan et al., 2002). K48-linked chains have a closed, compacted confirmation due to the position of K48 relative to the C-terminus of Ub, allowing linking Ub molecules to form a hydrophobic interface that is critical for recognition by the 26S proteasome. Conversely, K63-linked chains have an extended conformation where the hydrophobic patches on the surface of the Ub molecule cannot interact with each other, leading to non-degradative roles (Varadan et al., 2002, Varadan et al., 2004).

Table 1.3: Functional consequences of different ubiquitination chain topologies (Dwane et al., 2017)

Chain formation	Functions
K48	Proteasomal degradation (Pickart, 1997)
K11	Proteasomal degradation (Xu et al., 2009) Regulation of cell division (Wickliffe et al., 2011)
K63	DNA damage repair (Messick and Greenberg, 2009) Protein trafficking (Erpapazoglou et al., 2014) Protein sorting (Lauwers et al., 2009) Regulation of transcription (Vallabhapurapu and Karin, 2009) Kinase signalling (Wang et al., 2012) Protein scaffolding (Wang et al., 2012) Oxidative stress response (Silva et al., 2015)
K27	DNA damage response (Gatti et al., 2015) Mitochondrial clearance (Geisler et al., 2010)
K29	Regulation AMPK-related kinases (Al-Hakim et al., 2008) Lysosomal degradation (Chastagner et al., 2006)
K6	BRCA1-mediated DNA damage repair (Morris and Solomon, 2004)
K33	Regulation AMPK-related kinases (Al-Hakim et al., 2008) DNA damage response (Elia et al., 2015)
Monoubiquitination	Endocytosis (Haglund et al., 2003) Intracellular localisation (Jura et al., 2006) Protein trafficking (Su et al., 2013) Histone modification (Cole et al., 2015) DNA damage repair (Gregory et al., 2003)

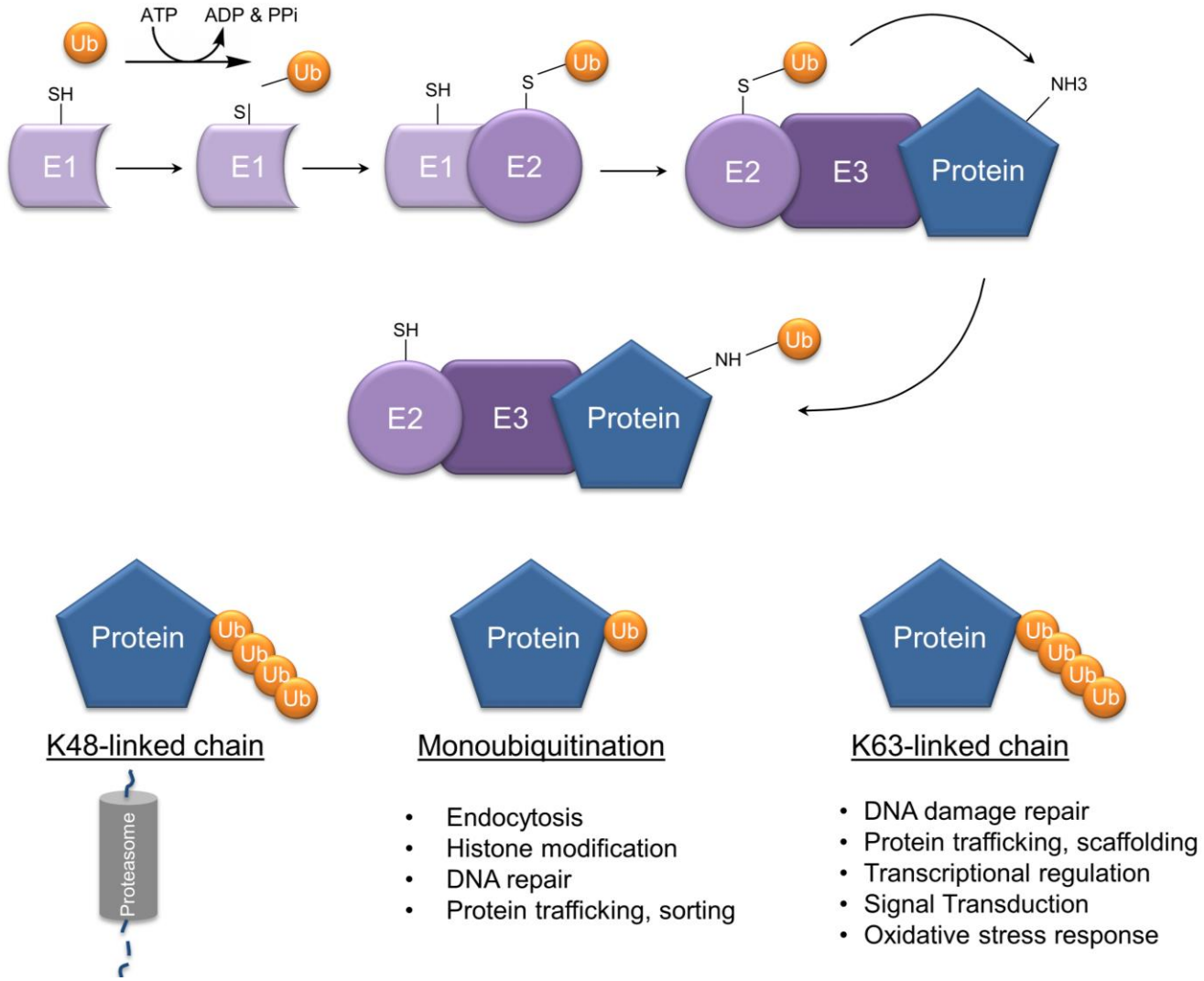

Figure 1.5: Functional consequence of different Ub chain topologies (Dwane et al., 2017).

Furthermore, the functional diversity of Ub chains has also been associated with the combinatorial effect of E2 and E3 enzymes. The human genome encodes for approximately 30 E2 enzymes within a single evolutionary family, while four distinct E3 families exist, accounting for an estimated 500-1000 ligases (Berg et al., 2007). These can form thousands of specific E2-E3 combinations, the pairing of which plays a crucial role in the type of Ub chain formed and the overall fate of the substrate. For example, the combinational role of UBE2D2 and UbcH5B results in the formation of a K48-linked chain which targets the substrate to the 26S proteasome, while UBE2N and Ubc13 act together to catalyse the formation of a K63-linked chain (van Wijk et al., 2009, Suryadinata et al., 2014). To further illustrate, the E2 enzyme UbcH5c creates a K48 linked chain when combined with E6-AP, however the same E2 enzyme generates a K6-linked chain when combined with BRCA1/BARD1 (Wu-Baer et al., 2003). Together, this highlights the complexity of the Ub pathway and illustrates the importance of this PTM in multiple cellular functions.

1.3.2 Ubiquitination and cancer

Since ubiquitination affects so many biochemical processes within the cell, it is not surprising that modifications in this system play a vital role in oncogenesis. The association of ubiquitination and cancer has come to a climax in recent years, owing to the unanticipated efficacy of proteasome inhibition in the clinic (Moreau et al., 2012). Bortezomib, the first proteasome inhibitor to be evaluated in human clinical trials, was approved by the US FDA in 2003 for the treatment of relapsed multiple myeloma and in 2006 for mantle cell lymphoma. Acting in a dose-dependent and reversible manner, bortezomib binds to and represses the activity of the 26S proteasome, leading to the accumulation of cell cycle regulatory proteins which render the cells more sensitive to apoptosis (Bold, 2004, Pellom and Shanker, 2012). A second generation of proteasome inhibitors have followed, including carfilzomib, which was approved in 2012 to treat multiple myeloma patients who have failed on prior therapies (Fostier et al., 2012) and more recently ixazomib, the first oral proteasome inhibitor (Moreau et al., 2016). Although inhibition of the proteolytic functions of the Ub system has been a success, they are mostly limited to the treatment of haematological malignancies, a subtype of cancer with a high rate of protein synthesis. With increased reports of drug resistance to add to their

limitations, there is a growing demand for the identification of novel druggable components of the Ub system. Recently, focus has shifted towards the role of deubiquitinating enzymes (DUBs) in oncogenic pathways, which may represent attractive therapeutic targets.

1.3.3 Deubiquitinases (DUBs)

Like most PTMs, ubiquitination is a reversible process. DUBs can reverse or edit the process of ubiquitination by hydrolysing the isopeptide bond between Ub and the substrate protein (He et al., 2016). DUBs remove Ub molecules from ubiquitinated proteins, preventing proteasomal degradation and stabilising the target. Moreover, DUBs also play a vital role in Ub recycling, generation of Ub precursors and protecting the proteasome from free Ub chains- which compete with ubiquitinated substrates (Amerik and Hochstrasser, 2004).

The mammalian genome encodes for over 100 DUBs, which are classified into six different groups based on their sequence and structure similarity (Table 1.4). Aside from the Jabb1/MPN domain-associated metalloproteases (JAMM) DUB family which are zinc metalloproteases, all DUBs are cysteine proteases, in which the enzyme active site requires the interaction between a catalytic triad. The largest and most diverse DUB family are the ubiquitin-specific proteases (USP); it is predicted that the human genome encodes over 50 of this class (Reyes-Turcu et al., 2009). The USP DUBs encode highly conserved Cys and His box motifs, which contain all catalytic triad residues. Ubiquitin C-terminal hydrolase (UCH) DUBs tend to hydrolyse smaller amides and esters at the C-terminal of Ub, as their name suggests (Amerik and Hochstrasser, 2004). The human genome encodes four UCH DUBs (Reyes-Turcu et al., 2009), including the BRCA-associated protein, BAP1. The ovarian tumour (OTU) DUB family are so called due to their homology with the ovarian tumour gene involved in *Drosophila* ovarian development. Fourteen are encoded in the human genome, however not all of these enzymes may possess DUB activity (Reyes-Turcu et al., 2009). The Josephin domain DUB family is characterised by the presence of a 180 residue alpha helical cysteine-protease domain-named the Josephin domain. Ataxin 3 (ATXN3) is the best characterised family member; this protein is mutated in spinocerebellar ataxia type 3, a neurodegenerative polyglutamine expansion disease (Amerik and Hochstrasser, 2004). ATXN3 targets both K48- and K63-linked Ub chains, with a preference for the

latter (Winborn et al., 2008). The JAMM DUB family is represented by a proteasomal subunit (the 'lid') and is the only DUB family to possess metalloprotease activity. Finally, the motif interacting with Ub-containing (MINDY) DUB family is the most recently discovered DUB family. MINDYs are cysteine proteases also, with a new, previously unannotated catalytic domain (Abdul Rehman et al., 2016).

Table 1.4: DUB families and examples

DUB family	Enzyme family	Example
Ubiquitin-specific protease (USP)	Cysteine proteases	USP11
Ubiquitin C-terminal hydrolase (UCH)	Cysteine proteases	UCHL1
Ovarian tumour (OTU)	Cysteine proteases	OTUB1
Josephin domain	Cysteine proteases	ATXN3
Motif interacting with Ub-containing (MINDY)	Cysteine proteases	FAM63A
Jabb1/MPN domain-associated metalloproteases (JAMM)	Metalloproteases	BRCC36

1.3.4 DUBs in oncogenic pathways

DUBs are often differentially expressed or activated in tumours, hence targeting them is of therapeutic interest. DUB mutations and chromosomal translocation can lead to aberrant signalling and activation of oncogenic pathways. One of the best studied oncogenic DUB mutations is that of the cylindromatosis gene (CYLD). CYLD is the primary susceptibility gene in familial cylindromatosis, an autosomal dominant genetic disorder which leads to the formation of multiple tumours on the scalp. This DUB negatively regulates NF-κB signalling by specifically deubiquitinating K63-linked Ub chains on TNF receptor-associated factor 2 (TRAF2) and NF-κB essential modulator (NEMO) (Kovalenko et al., 2003). Recently, USP7 is attracting much attention in the field following the development of specific, small molecule inhibitors (Turnbull et al., 2017). USP7 deubiquitinates and stabilises mouse double minute 2 homolog (MDM2), an oncogenic E3 ligase involved in p53 destabilisation. Targeting USP7 may be beneficial in the treatment of multiple cancers and immunological disorders (Kessler, 2014). Further examples of DUBs associated with cancer pathways are illustrated in Table 1.5.

Table 1.5: DUBs in oncogenic pathways

DUB	Role in cancer pathway	Reference
USP7	Stabilises the E3 ligase MDM2, in turn destabilising p53	(Kessler, 2014)
USP8	Regulates anti-apoptotic FLIP(S) in glioblastoma multiforme	(Panner et al., 2010)
USP15	Activates TGF-β signalling in glioblastoma, associated with a poor prognosis in glioblastoma patients	(Eichhorn et al., 2012)
USP17	Controls cell migration by controlling GTPase subcellular localisation	(de la Vega et al., 2011)
USP19	Stabilises the cyclin-dependent kinase inhibitor $p27^{Kip1}$	(Lu et al., 2011)
USP22	Promotes multidrug resistance by activating SIRT1/AKT/MRP1 pathways	(Ling et al., 2017)
USP28	Stabilises MYC in tumour cells	(Popov et al., 2007)
USP28	Stabilises LSD1 in breast cancer; a chromatin modulator that controls pluripotency	(Wu et al., 2013)
USP39	Essential for the viability of *KRAS*-dependant cancer cells; associated with a poor prognosis in lung and colon cancer	(Fraile et al., 2017)
USP44	Overexpression induces chromosomal instability, observed in T-ALL	(Zhang et al., 2011)
UCHL1	Upregulated in airways of cigarette smokers, overexpressed in over half of lung cancers	(Carolan et al., 2006)
BRCC36	Enhances cell survival following DNA-damage in a BRCA-dependant manner	(Dong et al., 2003)

The role of DUBs in nuclear receptor signalling is intriguing, yet limited. Interestingly, USP7 also regulates the androgen receptor (AR) in prostate cancer. USP7 deubiquitinates AR in an androgen-dependant manner, associating with AR at androgen responsive elements and facilitating chromatin binding (Chen et al., 2015).

Moreover, AR is also regulated by USP26 in a similar manner (Dirac and Bernards, 2010), highlighting an integral role for DUBs in AR signalling. With regard to ERα, information on how DUBs affect transcriptional activity is sparse.

1.3.5 ERα regulation by ubiquitination

Like all steroid receptors, ERα is ubiquitinated and its turnover is mediated by the ubiquitination-proteasomal pathway (UPP) (Nawaz et al., 1999). Agonist, antagonist and SERDs all effect ERα turnover in a differential manner. Estrogen-bound ERα has a half-life of 3-4 hours (Wijayaratne and McDonnell, 2001) and is degraded rapidly, as a result. Many groups have demonstrated that inhibition of ERα degradation can inhibit the function of the protein despite the abundance of the receptor, highlighting the importance of the UPP in ERα function (Stanisic et al., 2009, Le Romancer et al., 2011). On the other hand, unliganded ERα is very stable with a half-life of ~5 days. In order to maintain steady expression and eliminate misfolded proteins, ERα is targeted to the proteasome by interaction with heat-shock proteins, chaperones and HSP70 interacting protein. The SERD drugs function as anti-estrogens by inducing receptor degradation. Fulvestrant binds to ERα and induces it's dissociation from heat shock protein 90 (HSP90) and immobilisation to the nuclear matrix for degradation (Le Romancer et al., 2011).

ERα function is also regulated by deubiquitination. ERα is deubiquitinated by Otubain-1 (OTUB1), which negatively regulates its transcriptional activity in endometrial cancer cells. Moreover, OTUB1 regulates transcription of the ERα gene itself and can stabilise the receptor in the chromatin (Stanisic et al., 2009). Later, ubiquitin specific protease 9x (USP9x) was identified as an ERα interactor. USP9x attenuation was found to render BC cells resistant to tamoxifen, leading to the generation of a gene signature used to define patient outcome following adjuvant tamoxifen (Oosterkamp et al., 2014). These studies combined emphasise the importance of ubiquitination and deubiquitination in ERα function in BC and highlight an interesting topic worth exploring.

1.4 Aims and hypotheses

This project aims to explore the role of DUBs in endocrine-driven BC. It is hypothesised, that as a protein that is tightly regulated by post-translation modifications, that DUBs may play a key role in receptor regulation. It is envisioned that this comprehensive investigation will not only give us a better understanding of the role of DUBs in BC but may also open up new avenues to improve treatment options for patients suffering with this complex disease.

Chapter 2: Materials and Methods

2.1 Cell culture

2.1.1 Cell lines

ZR-75-1 cells were received from Prof. Rene Bernards (Netherlands Cancer Institute, Amsterdam, Netherlands). MCF7, LCC1 and LCC9 cells were received from Prof. Robert Clarke (Georgetown University Medical School, Washington DC, USA). HEK293T wild type and HEK293T USP11 knockout cell lines were received from Dr. Daniel Durocher (The Lunenfeld-Tanenbaum Research Institute, Mount Sinai Hospital, Toronto, Ontario, Canada). Cell lines were routinely tested for mycoplasma contamination using a MycoAlert detection kit (Lonza, UK).

Table 2.1: Cell line characteristics

Cell line	Source	Patient characteristics	Molecular characteristics
ZR-75-1	NKI	63 years old, Caucasian, female	ERα+, HER2+, high Ki67
MCF7	Georgetown University	69 years old, Caucasian, female	ERα+, HER2-, low Ki67
LCC1	Georgetown University	69 years old, Caucasian, female	ERα+ but estrogen independent, HER2-, low Ki67
LCC9	Georgetown University	69 years old, Caucasian, female	ERα+ but estrogen independent and anti-endocrine resistant, HER2-, low Ki67
HEK293T	Mount Sinai Hospital	Foetus	Contains the SV40 T-antigen

2.1.2 Cell culture medium

ZR-75-1, MCF7 and HEK293T cells were cultured in Dulbecco's Modified Eagle Medium (DMEM) (Sigma-Aldrich, St Louis, MO, USA) supplemented with 10% Foetal Bovine Serum (FBS) (v/v) (Gibco, Invitrogen, Carlsbad, CA, USA), 1% penicillin/streptomycin (v/v) (Gibco, Invitrogen) and 1% L-glutamine (Gibco, Invitogen). ZR-75-1 culture media was also supplemented with 1 nM estradiol (E2) (Sigma-Aldrich). LCC1 and LCC9 cells were cultured in phenol red-free DMEM (Sigma-Aldrich) supplemented with 5% charcoal/dextran-treated Foetal Bovine Serum (FBS) (v/v) (Gibco, Invitrogen), 1% penicillin/streptomycin (v/v) (Sigma-

Aldrich) and 1% L-glutamine (Gibco, Invitrogen). Experiments which required hormone depletion were also cultured in phenol red-free media.

2.1.3 Subcultivation

Subculturing of all cells took place in a Class II laminar flow hood under sterile conditions. All items placed in to the hood were sprayed with 70% v/v ethanol. Media was removed from cell culture dishes with a serological pipette. Cells were washed with Dulbecco's phosphate buffered saline (PBS) (Gibco, Invitrogen). Cells were then incubated in an appropriate volume of pre-warmed 1X trypsin EDTA (Sigma-Aldrich). The trypsin was neutralised with twice the volume of pre-warmed media, and a volume of cells was added to a new culture vessel in fresh culture medium. Both MCF7 and ZR-75-1 cell lines had a subculture ratio of 1:4 and were subcultured 2-3 times per week. LCC1 and LCC9 cells had a subculture ratio of 1:3 and were subcultured twice a week. HEK293T cells had a subculture ratio of 1:12 and were subcultured twice a week.

2.1.4 Preparation of cell stocks

A 70-80% confluent T175 cm^2 flask of cells was washed in PBS, trypsinised as described above and then centrifuged at 244 *x g* for 3 minutes in a 15 mL centrifuge tube. Media was aspirated and cells were resuspended in 1 mL DMEM containing 10% v/v dimethyl sulfoxide (DMSO) (Sigma-Aldrich) per cell stock; the number of cell stocks prepared was dependant on the cell line and confluency of the cells. Cells were subsequently transferred to a cryovial and placed into a Mr. Frosty freezing container (Thermo Fisher Scientific, Waltham, MA, USA) filled with isopropanol (Sigma Aldrich) to slow the decrease in temperature to approximately 1˚C per minute. The container was then placed in a -80˚C freezer. For long term storage, cells were moved to a liquid nitrogen cryopreservation container.

To thaw stocks, the cells were gently heated to 37˚C and added to 5 mL of media. Cells were centrifuged at 244 *x g* for 3 minutes, media was aspirated and cells were resuspended in fresh pre-warmed media. Media was replaced after 24 hours to remove any remaining DMSO.

2.1.5 Cell counting

Cell suspensions were counted using a haemocytometer. Cells were washed and trypsinised, centrifuged and resuspended in an appropriate volume of media, as described in section 2.1.4. Ten µL of this cell suspension was placed on the haemocytometer and cells were counted under the microscope. All four corner grids were counted and the average multiplied by 10^4 to account for the full volume of cell suspension on the haemocytometer. Using this method, an estimation of the number of cells in the full cell suspension was obtained.

2.2 RNA interference

2.2.1 Generation of stable USP11 knockdown cell lines

2.2.1.1 Bacterial transformation

A frozen stock of One Shot® TOP10 chemically competent *Escherichia coli* (Invitrogen) was left to gradually thaw on ice for 30 minutes. Two µL containing 50-100 ng of plasmid DNA (USP11 sh1-sh5, non-targeting control (NTC), psPAX, PMD.2G) was added to the culture and gently stirred with the pipette tip. The culture was incubated on ice for 30 minutes and subsequently heat shocked at 42 ˚C for 30 seconds. The culture was incubated on ice for a further 2 minutes. Two hundred and fifty µL of super optimal broth with catabolite repression (SOC medium) (Invitrogen) was then added to the culture without mixing. This was performed close to a Bunsen burner in order to maintain a sterile environment. The eppendorf containing the culture was placed in a incubating shaker and agitated horizontally at 37 ˚C for 1 hour. Fifty µL of the culture was added to one pre-warmed agar plate, while the remaining culture was added to the second to ensure adequate spacing of transformed colonies. The plates were left to incubate at room temperature for 5 minutes to allow the culture to soak into the agar, and subsequently incubated at 37 ˚C overnight.

2.2.1.2 Propagation of plasmid DNA

Five mL aliquots of lysogeny broth (LB, 20 g/L w/v (Sigma-Aldrich)), supplemented with 50 µg/mL w/v ampicillin (Thermo Fischer Scientific) were prepared in duplicate for each vector. Following overnight incubation of the plates described in section 2.2.1.1, an individual colony was selected with a pipette tip from each agar plate and used to inoculate the starter culture. The culture was agitated for 8 hours at 37 ˚C

until sufficiently cloudy. In the meantime, 100 mL aliquots of LB were prepared in conical flasks. Following incubation, 100 µL of the 5 mL culture was added to the prepared conical flasks and then agitated overnight at 37 ˚C. The following day, the culture was centrifuged at 3220 *x g* at 4 ˚C for 20 minutes. The supernatant was discarded and the pellet was frozen at -20 ˚C.

2.2.1.3 Extraction of plasmid DNA

Plasmid DNA was extracted using the PureYield™ Plasmid Midiprep System (Promega, WI, USA) as per manufacturer's instructions. The bacterial cell pellets were resuspended in cell resuspension solution. Three mL of cell lysis solution was added to the 15 mL centrifuge tube and the tube was inverted 3 times. The lysate was left to incubate for 3 minutes at room temperature before the addition of 5 mL of neutralisation solution was added. The centrifuge tube was inverted 5 times and the lysate was centrifuged at 3220 *x g* for 40 minutes. A column stack was assembled by nesting a clearing column into the top of a binding column. The column stack was placed onto the vacuum manifold and the cell lysate was added to the clearing column. The vacuum was applied to allow the lysate to pass through the clearing and binding membranes. The clearing column was removed and discarded and 5 mL of endotoxin removal wash was subsequently added to the binding column. The vacuum was applied to allow the wash to pass. Twenty mL of column wash was then added to the binding column and the vacuum was applied to allow the wash to pass. The vacuum was applied continuously for 30 seconds to dry the membrane. A 1.5 mL microcentrifuge tube with an open cap was applied to the base of the vacuum elution device. The DNA binding column was inserted and the elution device was attached to the vacuum. Five hundred µL of nuclease-free water (Promega) was added to the membrane and the vacuum was applied to elute the DNA. DNA quantity and quality was assessed using the NanoDrop UV-Vis spectrophotometer (Thermo Fischer Scientific).

2.2.1.4 Virus production by calcium phosphate transfection

HEK293T cells were seeded at 70-80% confluency in T75 cm^2 flasks 24 hours prior to viral production. The next day, 9 µg plasmid DNA (USP11 shRNA sh1-sh5, NTC) was combined with 9 µg psPAX viral packaging vector DNA, 4.5 µg pMD2.G envelope vector and 54 µL 2.5M calcium chloride (Sigma-Aldrich). shRNAs were

cloned in pKLO.1-puro plasmids (See Appendix 2 for vector maps). This combination was brought to a total volume of 450 µL with sterile H_2O. The DNA mix was then slowly introduced into 450 µL 2X HEPES buffer while continuously introducing air bubbles to the samples using a pipette aid; this was continued for 2 minutes following combination. Samples were subsequently incubated for 10 minutes at 37˚C to allow the DNA to precipitate. During this time, 10 mL fresh growth medium was added to the HEK 293T cells along with 12 µL of 25 mM chloroquine (Sigma-Aldrich). The DNA solution was then added to the cells. Following 8 hours incubation at 37˚C, the media on the cells was changed, and the cells were then left to incubate for a further 48 hours to allow for the production of viral particles. To harvest the virus following incubation, the media from the cells was removed and passed through a 0.45 µm filter. Viral particles were stored at -80˚C for further use.

2.2.1.5 Viral transduction

Target cells were seeded at approximately 40% confluency 24 hours prior to transduction. Viral particles were diluted in fresh media and gently added to the cells. After 24 hours, the viral particles were removed and cells were washed in PBS. The cells were then left to incubate for a further 24-48 hours before selection with puromycin (Sigma-Aldrich) (ZR-75-1: 3 µg/mL; MCF7: 2 µg/mL). Knockdown of USP11 was determined by Western blotting and quantitative real-time polymerase chain reaction (qRT-PCR).

2.2.2 siRNA transfection

Cells were seeded in complete media containing no antibiotics in a 6-well plate 24 hours prior to transfection. ZR-75-1 cells were seeded at 1 x 10^6 cells per well, while LCC1 and LCC9 cells were seeded at 0.7 x 10^6 cells per well. siRNA (30-50 µM) (Dharmacon, Lafayette, CO, USA) was diluted in serum-free DMEM (SFM) up to a volume of 125 µL prior to combination with lipofectamine 3000 (Invitrogen). Lipofectamine 2000 was diluted in SFM to a total of 125 µL, and both mixtures were left to incubate at room temperature for 5 minutes. Next, both mixtures were combined and incubated for 15 minutes at room temperature to allow lipofectamine 2000: siRNA complexes to form. During this time, media was removed from each well and replaced with 1.75 mL of fresh antibiotic-free media. Two-hundred and fifty µL of the lipofectamine 2000: siRNA complex was gently added in droplets to each

well and the plate was rocked back and forth to mix. Cells were incubated at 37˚C for 48-72 hours before gene knockdown was determined (120 hours for protein knockdown in some cases). This protocol was scaled up and down for larger and smaller plates, respectively.

2.3 Protein analysis

2.3.1 Protein extraction and quantification

Cells were washed with PBS before lysing in an appropriate volume of radioimmunoprecipitation (RIPA) buffer (50 mM Tris-HCl pH 7.4, 1% NP-40, 0.25% sodium deoxycholate, 150 mM NaCl, 1 mM EDTA) supplemented with complete mini EDTA-free protease inhibitor (Roche Diagnostics, Basel, Switzerland) and phosphatase inhibitor cocktail 3 (Sigma-Aldrich). Lysates were incubated on ice for 10 minutes, and then centrifuged at 18,800 *x g* for 15 minutes to remove cellular debris. The supernatant containing the protein was aliquoted and stored at -80˚C for further use. Protein was quantified using a bicinchoninic acid (BCA) protein assay as per manufacturer's instructions (Pierce, Illinois, USA).

2.3.2 SDS-PAGE

The composition of each gel is outline in table 1.1.

Protein samples were diluted in sterile H_2O to yield the same concentration of protein per sample. An appropriate volume of 4X NuPAGE Lithium Dodecyl Sulfate (LDS) buffer (Invitrogen), supplemented with 2.5% β-Mercaptoethanol (Sigma-Aldrich) was added to each sample. Samples were boiled at 100˚C for 5 minutes to allow for protein denaturation before loading onto the gel. SDS-PAGE was performed in 1X Tris Glycine running buffer (25 mM Tris, 250 mM glycine, 0.1% SDS) using a Bio-Rad Mini Protean III gel system (Bio-Rad Laboratories, Hercules, CA, USA). Gels were run for approximately 20 minutes at 90V through the stacking gel, followed by approximately 60 minutes at 120V through the resolving gel.

Table 2.2: Composition of SDS-PAGE gels

Resolving gel	**10% (mL)**	**12% (mL)**	**Stacking gel**	**5% (mL)**
Sterile H_20	4	3.3	Sterile H_20	6.8
30% acrylamide mix	3.3	4	30% acrylamide mix	1.7
1.5 M Tris (pH 8.8)	2.5	2.5	1.0 M Tris (pH 6.8)	1.25
10% SDS	0.1	0.1	10% SDS	0.1
10% ammonium persulfate	0.1	0.1	10% ammonium persulfate	0.1
N,N,N,N-tetramethylethylenedia-mine (TEMED)	0.004	0.004	N,N,N,N-tetramethylethylenedia-mine (TEMED)	0.01

2.3.3 Western blotting

Resolved proteins were transferred to a nitrocellulose membrane in 1X transfer buffer (25 mM tris, 190 mM glycine, 20% methanol) using a Bio-Rad Mini-Protean III electrophoretic transfer cell (Bio-Rad) at 300 mA for 90 minutes at 4˚C. Following transfer, membranes were blocked with either 5% (w/v) non-fat dried milk (Sigma-Aldrich) or 5% (w/v) BSA (Sigma-Aldrich), both prepared in 100 mL of 1X TBS-T (TBS buffer containing 0.1% (v/v) Tween 20 (Sigma-Aldrich)), and incubated with gentle agitation for 1 hour at room temperature. Membranes were then incubated in blocking buffer containing the primary antibody of choice overnight at 4˚C. All primary antibodies used can be found in table 2.2.

Following primary antibody incubation, membranes were washed with TBS-T four times, four minutes per wash, and subsequently incubated for 1 hour at room temperature with horseradish peroxidise (HRP)-conjugated secondary antibody (anti-mouse/anti-rabbit, Dako, Glostrup, Denmark) contained in blocking buffer. Membranes were again washed in TBS-T four times, four minutes per wash, and detection of HRP complexes was achieved by exposing the membranes to Enhanced Chemiluminescence (ECL) substrate (Pierce). Membranes were placed into an autoradiography cassette (Bio-Rad) and the signal was detected by exposure to X-ray film (Fujifilm, Tokyo, Japan). Membranes were also imaged using the Amersham Imager 600 (GE Healthcare Life Sciences, Marlborough, MA, USA).

Table 2.3: Primary antibodies

Antibody	Source	Catalogue number	Species	Molecular Weight	Blocking Buffer	Dilution
USP11	Bethyl Laboratories, Texas	A301-613A	Rabbit	115 kDa	BSA	1:5000
ERα (F10/D12)	Santa cruz biotechnology, TX, USA.	sc-8002/ sc-8005	Mouse	64-66 kDa	Milk	1:1000
ERα	Cell signalling technologies (Danvers, MA, USA)	D8H8	Rabbit	64-66 kDa	BSA	1:1000
PgR A/B	Cell signalling technologies	D8Q2J	Rabbit	118/90 kDa	BSA	1:1000
GAPDH	Abcam	Ab8245	Mouse	37 kDa	BSA	1:1000
Trimethyl histone H3	Active Motif, Belgium.	39535	Mouse	18 kDa	BSA	1:1000
β-actin	Abcam	Ab8227	Mouse	44 kDa	BSA	1:20,000

2.3.4 Immunoprecipitation (IP) assay

ZR-75-1 or HEK293T cells were grown in two 10 cm dishes per condition until 80-90% confluent. Cells were then washed with PBS and scraped into an appropriate volume of IP lysis buffer (50 mM HEPES pH 7.5, 100 mM NaCl, 1 mM EDTA, 10% glycerol, 0.5% NP40) supplemented with complete mini EDTA-free protease inhibitor (Roche Diagnostics, Basel, Switzerland) and phosphatase inhibitor cocktail 3 (Sigma-Aldrich). Protein was quantified using a BCA protein assay as per manufacturer's instructions (Pierce).

Protein A sepharose beads (Sigma-Aldrich) were pre-coupled to the antibody before the immunoprecipitation was carried out. Twenty five µL of beads were washed five times in chilled PBS-T, centrifuging between washes at 5,000 *x g* for 1 minute. Two µg of antibody was added to the beads in 1 mL PBS-T and samples were pre-coupled overnight at 4˚C with constant agitation. The next day, beads were washed twice in Sodium Borate (Sigma-Aldrich). For antibody cross-linking, beads were resuspended in dimethyl pimelimidate (DMP) (Sigma-Aldrich), dissolved in sodium borate, and incubated at RT with constant agitation for 30 minutes. To quench the cross-linking reaction, beads were washed once in ethanolamine and then incubated in fresh ethanolamine at RT with constant agitation for 2 hours. Beads were transferred to PBS and either stored at 4˚C or used immediately. To neutralise the beads, beads were resuspended in lysis buffer and incubated for 2 hours at 4˚C with constant agitation. Protein was precleared using IgG bound beads

for 1 hour at 4˚C with constant agitation. The supernatant was transferred to IP beads and incubated at 4˚C with constant agitation; overnight for endogenous IP and 3 hours for overexpression IP. The beads were washed 3 times in IP lysis buffer and resuspended in 25 µL LDS (supplemented with 10% β-mercaptoethanol). Samples were boiled for 8 minutes and centrifuged at full speed to collect the beads. Twenty µL of the supernatant was loaded onto the gel, along with pre-prepared input samples. Western blotting was performed to confirm immunoprecipitation and protein-protein interactions.

2.3.5 Cellular fractionation

Five x 10^6 cells were seeded were seeded in two 10 cm dishes. Once adhered, cells were transferred to phenol red-free DMEM containing 5% charcoal/dextran-treated FBS. After 48 hours, one of the two 10 cm dishes was stimulated with 1 nM E2, while the other dish remained under hormone-deprived conditions. Cellular fractions were generated using Qiagen's Cell Compartment kit, as per manufacturer's instructions. Extracts were analysed using Western blotting, with GAPDH and trimethyl histone H3 antibodies used as cytosolic and nuclear markers, respectively.

2.4 RNA analysis

2.4.1 RNA extraction and quantification

Cells were washed in PBS and scraped into 500 µL of Tri-Reagent (Sigma-Aldrich). One-hundred and twenty five µL of chloroform (Sigma-Aldrich) was added to each lysate and tubes were incubated on ice for 10 minutes. Samples were centrifuged at 18,800 *x g* for 20 minutes at 4˚ C to isolate RNA from the content of the cell. The upper clear aqueous phase of RNA was added to 400 µL of isopropanol and samples were incubated on ice for 10 minutes. The samples were centrifuged at 18,800 *x g* for 30 minutes at 4˚C to yield an RNA pellet. The pellet was washed in 75% EtOH and the samples were once again centrifuged at 18,800 *x g* for 10 minutes at 4˚C. All residual EtOH was removed and the pellets were allowed to air dry for 15 minutes, before resuspending in a volume of nuclease-free water (Promega, WI, USA). A NanoDrop UV-Vis spectrophotometer (Thermo Fisher Scientific) was used to quantify RNA, according to manufacturer's instructions.

2.4.2 cDNA synthesis

RNA samples were diluted in nuclease-free water up to 7 µL to yield 1 µg per sample. One µL of DNase I (Invitrogen), combined with 1 µL of 10X reaction buffer (Invitrogen), was added to each sample and incubated at room temperature for 15 minutes. One µL of EDTA (25 mM) was added to each sample and all samples were subsequently heated at 65˚C for 10 minutes to denature the DNase I. cDNA was synthesised using the high capacity cDNA reverse transcription kit (Invitrogen) as per manufacturer's instructions. Samples were incubated in the Bio-Rad T100 Thermal Cycler (BioRad) at 25˚C for 10 minutes, followed by 37˚C for 60 minutes and 85˚C for 5 minutes. Sixty µL nuclease-free water was added to the 20 µL cDNA once synthesised in order to dilute reaction products.

2.4.3 Quantitative real time polymerase chain reaction (qRT-PCR)

A primer master mix was prepared for each primer set (see appendix 1 for sequences) to yield 10 µM of each forward and reverse primer (Eurofins MWG, Kraainem, Belgium). For one well in a 96-well plate, 5 µL SYBR green (Promega) was added to 0.6 µL primer master mix (300 nM each primer total) and 0.4 µL nuclease-free water. A master mix was prepared for each primer set accordingly, and 6 µL of the mix was added into the appropriate number of wells in a 96-well plate, followed by 4 µL of cDNA in duplicate. The plate was sealed, centrifuged briefly in a benchtop centrifuge to spin down the contents of the well, and placed into an Applied Biosystems 7500 real time PCR system set to the following temperature cycles: 2 minutes at 50˚C, 10 minutes at 95˚C, followed by 40 cycles oscillating between 15 seconds at 95˚C and 1 minute at 60˚C. A melting curve was generated after each run in order to ensure primer specificity: 15 seconds at 95˚C, 15 seconds at 60˚C and 15 seconds at 95˚C.

2.4.4 RNA sequencing (RNA-seq)

2.4.4.1 Preparation of samples

LCC1 and LCC9 cells were seeded at 7 x 10^5 cells per well in a 6-well plate. The next day, both cell lines were transfected with two independent siRNAs targeted to USP11 and an siRNA non-targeting control (NTC) using lipofectamine 2000, as described above. Cells were incubated for 72 hours before extraction of RNA. Samples were prepared in biological triplicate.

2.4.4.2 Library preparation

All RNA samples were diluted one in ten in nuclease-free water to reduce high concentrations. The quality of the RNA was determined using the 2100 Bioanalyser (Agilent technologies, Santa Clara, CA, USA). To prime the RNA chip, 9 µL of gel was added to the well labelled with a highlighted 'G'. A syringe was used to disperse the gel across the entire chip. Nine µL of gel was added to all wells labelled 'G'. Five µL of the marker was added to all other wells. One µL of ladder was added to the well labelled with an image of a ladder. One µL of each RNA sample was added to individual wells. The entire chip was vortexed for one minute. The chip was run and data was analysed using 2100 Expert Software (Agilent technologies).

All samples were diluted to 100 ng RNA in 12.5 µL resuspension buffer (RSB) (Illumina, San Diego, CA, USA) in a 96-well plate. RNA purification beads (Illumina) were added to each sample, 12.5 µL per well. mRNA denaturation was carried out at 65 ˚C for 5 minutes. Illumina's neoprep library card was set up as per manufacturer's instructions. cDNA libraries were prepared overnight and final libraries were automatically normalised to 10 nM.

2.4.4.3 RNA sequencing (RNA-seq)

All samples were diluted to 4 nM in 10 µL RSB. The samples were pooled together by adding 5 µL of each sample in to a 1.5 mL microcentrifuge tube (ligated adaptors distinguish each individual sample). The sample was denatured using 0.2 N NaOH. Five µL 0.2 N NaOH was added to 5 µL of the sample pool in a fresh tube. Samples were vortexed and subsequently centrifuged at 280 *x g* for 1 minute. Following 5 minutes incubation at RT, 5 µL RSB was added to the sample to quench the reaction. HT1 buffer was added to the sample at a volume of 985 µL, to give a final concentration of 20 pM DNA. The sample was vortexed and centrifuged briefly on a benchtop centrifuge. One-hundred and seventeen µL of the sample was added to 1183 µL HT1 buffer to give a final concentration of 1.8 pM DNA. PhiX was used as a positive control; 117 µL of 20 pM phiX was added to 1183 µL HT1 buffer. Thirteen µL was added to the working sample. The entire sample was transferred to the sequence cartridge and the NextSeq 500 (Illumina) was prepared as per manufacturer's instructions. Two x 75 bp paired-end reading was performed.

Bioinformatic analysis of sequencing reads was carried out by Dr. Bruce Moran, University College Dublin. Fastq files were downloaded from Illumina BaseSpace using the BaseSpace download tool:
(https://github.com/ReddyLab/BaseSpaceFastqDownload).
The quality of Fastq files was determined using FastQC: (https://www.bioinformatics.babraham.ac.uk/projects/fastqc/).
Reads were trimmed to remove poor quality base calls (Phred score < 20) and sequencing adaptors, using BBDuk tool in the BBMap package (https://jgi.doe.gov/data-and-tools/bbtools/bb-tools-user-guide/bbmap-guide/).

Sequencing reads were aligned to the human hg19/GRCh37 genome reference using the STAR alignment algorithm, version 2.5.2a (Dobin et al., 2013). This produced a BAM file which was sorted by coordinate. Duplicate reads were marked in the BAM using Picard-Tools 'MarkDuplicates' call (https://broadinstitute.github.io/picard/). Read counts were produced by the featureCounts tool from the SubRead package (Liao et al., 2014). These counts were combined for all samples and used as input for differential gene expression analysis.

2.4.4.4 Differential Expression

Differential expression (DE) analysis of genes was carried out using the DESeq2 package (Love et al., 2014) in the R statistical environment (R Development Core Team, 2012). The data.frame of counts had all genes with a sum of zero across all samples removed. A 'conditions' data.frame was created based on the sample names, their group (i.e. LCC1_control, LCC1_si7, LCC1_si8, LCC9_control, LCC9_si7 or LCC9_si8) and their biological replicate number. The counts and conditions data.frames were loaded into a DESeq2DataSet class object using the DESeqDataSetFromMatrix() call, with the design variable set as '~ group'. The DESeq() call produced two sets of results, based on LCC1 or LCC9 cells, comparing the two individual siRNA knockdowns to the control for each cell line. Four text files resulted, containing each gene expressed, the $\log_2$FoldChange value and the FDR adjusted p-value. Principal component analysis plots were produced for the full dataset to determine the quality of the count data and similarity of samples from the 6 conditions. These followed the standard protocol from the DESeq2 guide (https://bioconductor.org/packages/release/bioc/vignettes/DESeq2/inst/doc/DESeq2.

html). Fragments-per-kilobase per million reads (FPKMs) were produced using the edgeR package (McCarthy et al., 2012) rpkm() call.

RNA-seq was validated using qRT-PCR as described above, using the same sequenced RNA samples.

2.4.4.5 Enrichment analysis

DE genes were subjected to gene ontology (GO) enrichment analysis in order to detect altered cellular pathways following USP11 knockdown. The Database for Annotation, Visualisation and Integrated Discovery (DAVID) (http://david.abcc.ncifcrf.gov/) was used for GO and Kyoto Encyclopaedia of Genes and Genomes (KEGG) pathway enrichment (Huang da et al., 2009). Significantly DE genes, grouped in to up- and downregulated with USP11 knockdown, were entered in to DAVID for enrichment analysis. An FDR (False Discovery Rate) <5% was considered statistically significant.

Gene Set Enrichment Analysis (GSEA) is an improved method of analysis to define the biological functions of gene sets (Subramanian et al., 2005). The method uses weighted genes according to their correlation with phenotype rather than equal weights for each gene. GSEA 3.0 and gene sets were downloaded from the Molecular Signatures Database (MsigDBv3.1) website: (http://www.broadinstitute.org/gsea/msigdb/index.jsp). Phenotypes were assigned to both knockdown and control samples, and enrichment analysis was carried out against a defined gene set. The GSEA procedure was performed as follows; an enrichment score (ES) was calculated ranking genes according to their differential expression and a nominal P value was obtained as an estimate of the significance level of the enrichment score. Subsequently, the enrichment score was normalised (NES) and FDR was calculated to adjust for multiple hypothesis testing.

2.5 Phenotypic assays

2.5.1 Dual luciferase reporter assay

2.5.1.1 Sample preparation

ZR-75-1 USP11 knockdown and non-targeting control cells were seeded in a 24-well plate at 75,000 cells per well. The following day the dual luciferase reporters were cotransfected. Five hundred ng ERE-luciferase reporter and 50 ng CMV-renilla were added to serum-free media (SFM) to a final volume of 25 µL. An appropriate volume

of lipofectamine 3000 (0.75 µL) was diluted in SFM to a total of 25 µL, and both mixtures were left to incubate at room temperature for 5 minutes. Next, both mixtures were combined and incubated for 15 minutes at room temperature to allow DNA transfection complexes to form. During this time, media was removed from each well and replaced with 350 µL of fresh antibiotic-free media. Fifty µL of the lipofectamine 3000:DNA complex was gently added in droplets to each well and the plate was rocked back and forth to mix. The next day, cells were transferred to phenol-red free DMEM for 48 hours. Cells were then stimulated with 1 nM E2 for 24 hours or remained in hormone-depleted conditions.

HEK293T cells were seeded at 75 x 10^3 cells per well in a 24-well plate. The next day, reporters were transfected as described above, including 100 ng of an ERα overexpression vector. One-hundred ng of USP11 wild-type or mutant overexpression vector was also included in rescue experiments. The next day following transfection, cells were transferred to phenol-red free DMEM for 24 hours. Cells were then stimulated with 1 nM E2 for 24 hours or remained in hormone-depleted conditions.

2.5.1.2 Detection of luciferase activity

Luciferase activity was detected in the cells using the Dual Luciferase Reporter assay system (Promega). Cells were lysed by agitation in 1X passive lysis buffer for 15 minutes at room temperature. Twenty µL of the lysate was then added in triplicate to a 96-well white-walled plate, avoiding the cellular debris. Luciferase activity was then detected using a Fluoroskan Ascent FL (Thermo Scientific) as per manufacturer's instructions, and activity calculated by normalisation to the transfection control.

2.5.2 Cell viability assay

Cell viability was assessed using the colorimetric MTT cell viability assay, which determines the number of viable cells based on their metabolic activity. ZR-75-1 cells were seeded in sextuplicate at a density of 3000 cells per well in a 96-well plate. On the final day, 15 µL of thiazolyl blue tetrazolium bromide (MTT, 20 mg/mL) was added to each well containing 150 µL culture medium to yield a final concentration of 0.5 mg/mL. The plate was covered in tin foil and incubated at 37˚C for 3 hours. The supernatant was removed and crystals were dissolved in 200 µL

DMSO. The plate was placed on a plate shaker for 20 minutes at RT to allow the crystals to dissolve. Absorbance at 570 nm was measured using the Victor Wallac plate reader.

2.5.3 Colony formation assay

ZR-75-1 USP11 knockdown and non-targeting control cells were seeded in technical duplicate at 3,000 cells per well in a 6-well plate. The cells were left to incubate for 2 weeks; the media was changed twice a week. The cells were washed with PBS and fixed for 10 minutes with 10% neutral buffered formalin. The cells were left to air dry for one hour before staining with 0.25% crystal violet for 10 minutes to visualise colonies.

2.5.4 Drug treatments

For tamoxifen and fulvestrant treatments, ZR-75-1 cell were seeded in a 96-well plates at a density of 6000 cells per well. The next day, media was replaced with 150 µL of drug-containing media at a range of concentrations (0.001 - 10 µM tamoxifen, 0.08 – 10 µM fulvestrant. Untreated and vehicle (DMSO) controls were also included. After 72 hours, an MTT viability assay was carried out, as described above.

2.5.5 Flow cytometry and propidium iodide (PI) staining

Cells were washed, trypsinised and centrifuged at 244 *x g* for 5 minutes. Cells were then resuspended in 1 mL PBS. To fix the cells, the PBS suspension was supplemented with ethanol to a final concentration of 70%. Ethanol was added dropwise while the sample was gently vortexed continuously. Samples were either stored in the fridge or stained with PI immediately.

Cells were centrifuged at 244 *x g* for 5 minutes. The supernatant was removed and cells were resuspended in 500 µL PI solution (25 µL PI 1 mg/mL, 50 µL triton-X 0.5%, 20 µL RNase A 2.5 mg/mL, PBS up to 500 µL). Samples were incubated at 37˚C for 40 minutes. Three mL PBS was added to each sample and tubes were centrifuged at 244 *x g* for 5 minutes. The supernatant was removed and the cells were resuspended in 500 µL PBS and transferred to flow cytometry test tubes. Flow cytometry was carried out using the BD FASC (Becton Dickinson,

Franklin Lakes, NJ, USA). Gates were applied to include viable, single cells in the final analysis.

2.5.6 Immunocytochemistry (ICC)

2.5.6.1 Sample preparation

Ten mm circular coverslips were cleaned with 70% v/v ethanol and placed in a 24-well plate. The plate and cover slips were exposed to UV light in the laminar flow hood to sterilize before use. ZR-75-1 cells were seeded on to the coverslips in hormone-depleted media at a density of 100,000 cells per well. After 48 hours, cells were stimulated with 1 nM E2 for either 4 or 24 hours, or left in hormone-depleted conditions.

Media was aspirated, cells were washed in PBS and subsequently fixed in 100% methanol for 20 minutes. The cells were washed 2 x 5 minutes in PBS before blocking in 10% goat serum in 5% w/v BSA/PBS for 60 minutes. The cells were washed in PBS for 5 minutes before a 90 minute incubation in the primary antibody (USP11 1:250) diluted in 10% human serum in 5% w/v BSA/PBS. The cells were washed 2 x 5 minutes in PBS to remove excess primary antibody. The cells were then incubated in secondary antibody (Alex Fluor® 594, 1:200) diluted in 10% human serum in 5% w/v BSA/PBS, for 60 minutes, and the plate was covered in tin foil to protect from light. The cells were washed 2 x 5 minutes in PBS before mounting the cover slip on to a microscope slide. A small volume of Vectashield mounting medium containing DAPI (Vector Laboratories, CA, USA) was placed on the microscope slide and the coverslip was gently lowered on to the slide. The coverslip was sealed using clear nail polish.

2.5.6.2 Imaging and analysis

Widefield fluorescent microscopy was carried out using a Nikon Eclipse 90i equipped with a DS-Ri1 camera and Plan Fluor 20x (N.A 0.5) objective paired with DAPI and TRITC filtersets. NIS-Elements BR 3.10 was used to capture images with fixed acquisition settings.

A Carl Zeiss LSM 710 equipped with a W Plan-Apochromat 20x objective (N.A 1.0) was used to capture confocal images with fixed acquisition settings. Samples were simultaneously excited with 405 and 594 nm lasers and the resulting emissions captured using spectral detectors over the range of 409 – 495 and 598 –

726nm respectively. 4x averaging and a spacing of 0.806 µm was used when capturing z stacks in the Zen 2008 software.

FIJI (Schindelin et al., 2012) was used for the preparation of both widefield and confocal images. All z stacks are presented as maximum image projections.

2.6 Immunohistochemistry

2.6.1 Cell pellet preparation

Cell pellets were used to confirm the quality of the antibody and to determine optimal staining concentrations before the staining of patient samples. Cells were grown to approximately 75% confluency in T175 cm^2 flasks. Cells were enzymatically detached with a volume of trypsin, pelleted and resuspended in 10% (v/v) neutral-buffered formalin (Sigma-Aldrich) for 4 hours at room temperature. The fixed cells were centrifuged at 500 *x g* for 10 minutes, resuspended in 10 mL PBS to wash and centrifuged again to pellet. The fixed cell pellet was resuspended in 200 µL 1% agarose and subsequently transferred to the lid of a 1.5 mL microcentrifuge tube. Once solidified, the pellet was transferred to a cassette, and then processed using the Sakura Tissue-Tek VIP E300 floor tissue processor (Sakura, The Netherlands). Cells were then embedded in paraffin for the preparation of slides.

2.6.2 Deparaffinisation, rehydration and antigen retrieval

Formalin-fixed paraffin-embedded (FFPE) cell pellet or TMA slides were deparaffinised and rehydrated through a series of graded ethanol solutions. Briefly, slides were incubated at 60˚C for 10 minutes and immediately deparaffinised in xylene (2 X 5 minutes; Sigma-Aldrich). Slides were then rehydrated in descending concentrations of ethanol (Sigma-Aldrich) in coplin jars as follows: briefly washed in 100% ethanol to remove excess xylene, 2 x 5 minutes in 100% ethanol, 5 minutes in 95% v/v ethanol, 5 minutes in 80% v/v ethanol and 5 minutes in dH_2O. Antigen retrieval was achieved by incubating slides at 95 ˚C for 15 minutes in 1X citrate buffer pH 6.0 (Thermo Fischer Scientific) in a PT module (LabVision, UK).

2.6.3 Immunohistochemistry

Immunohistochemistry was performed using the Ultravision LP Large Volume Detection System HPR polymer (Labvision) and DAB Plus Substrate System (Labvision). Slides were incubated for 10 minutes in 3% H_2O_2 to block endogenous

peroxidases and then rinsed with PBS, 0.1% v/v Tween (PBS-T; Sigma-Aldrich). Protein block was then applied for 5 minutes, excess block removed and slides were incubated in USP11 primary antibody (Bethyl Laboratories, Texas, USA) for 60 minutes. Slides were then rinsed with PBS-T x 3, incubated with secondary antibody solution (primary antibody enhancer) for 10 minutes and rinsed again with PBS-T x 3. Finally, slides were incubated in HRP-polymer for 15 minutes, washed with PBS-T x 3 and incubated in 3, 3'-diaminobenzidinetrahydrochloride (DAB) for 10 minutes. Following development of the positive signal, sections were rinsed with dH_2O x 4. Slides were then counterstained by a 3 minute exposure to haematoxylin (Sigma-Aldrich) and subsequent agitation in tepid dH_2O until a blue colour was observed. Slides were dehydrated in ascending concentrations of ethanol in coplin jars as follows: 3 minutes in 80% v/v ethanol, 3 minutes in 95% v/v ethanol, 2 x 3 minutes in 100% v/v ethanol and 2 x 3 minutes in xylene. Slides were then mounted in Permount mounting medium (Thermo Fisher Scientific) using an automated coverslipper (Leica Microsystems). Lastly, slides were scanned using a ScanScope XT Digital Slide Scanner (Aperio Technologies, CA, USA) and analysed using ImageScope software (Aperio Technoloiges).

2.6.4 Tissue microarray (TMA) cohorts

The screening TMA cohort used in this study was generated from 144 patients diagnosed with invasive BC in Malmo University Hospital, Sweden, in 2001 and 2002. These patients did not receive any neoadjuvant treatment prior to surgery. 72% of total tumours were ER+ with complete anti-endocrine data available for 95 patients; 77 of whom received tamoxifen, 3 an aromatase inhibitor and 25 a combination of both. Thirty patients received adjuvant chemotherapy while 83 received radiotherapy. At the time of the last follow up 41 patients had passed away, 22 of which were a direct result of breast cancer.

2.7 Mass spectrometry (UbiScan®)

2.7.1 Preparation of samples

ZR-75-1 USP11 knockdown (x2) and non-targeting control (NTC) cells were seeded at a density of 10×10^6 in a T175 cm^2 culture flask in duplicate. Cells were incubated under normal growth conditions for 48 hours until 70-80% confluent and subsequently transferred to hormone-depleted media for a further 48 hours. One set

of three cell lines were transferred to hormone-depleted media containing 1 nM E2, while the other set were incubated under hormone-free conditions, both for a further 24 hours. The cells were then harvested, snap-frozen in liquid nitrogen, and taken to the lab of Prof. Benedikt Kessler, Nuffield Department of Medicine, University of Oxford for further sample preparation and mass spectrometry.

2.7.2 Cell lysis and protein digestion

The frozen cells were left to thaw on ice for 1 hour before lysing in urea lysis buffer (9M urea, 20 mM HEPES pH 8.0, 1 mM sodium orthovanadate, 2.5 M sodium pyrophosphate, 1 mM beta-glycerophosphate). To further lyse the cells, samples were sonicated using a microtip. The samples were exposed to three 15 W outputs at 15 seconds each, cooling on ice for 1 minute between each burst. The lysate was cleared by centrifugation at 20,000 *x g* for 15 minutes at room temperature.

2.7.3 Reduction and alkylation

To reduce the samples, 37 µL of 1.25 M DTT was added to each 10 mL sample. All tubes were incubated at 55°C for 30 minutes. The samples were placed on ice following incubation to allow them to cool to room temperature. To alkylate the samples, 1 mL iodoacetamide (Sigma-Aldrich) was added to each tube and the samples were incubated in the dark for 15 minutes.

2.7.4 Trypsin digestion

All samples were made up to 40 mL with 20 mM HEPES pH 8.0 to give a final concentration of 2 mM urea and 20 mM HEPES. Trypsin-TPCK was prepared at 1 mg/mL in 1 mM HCl, and a 1/100 volume (400 µL) was added to each sample. All samples were placed on the end-over-end shaker and incubated overnight at room temperature.

To ensure sufficient digestion, all samples were analysed by Western blotting. Fifteen µL of lysate was combined with 5 µL loading buffer and samples were loaded on the gel. The gel was run at 200 V for 30 minutes before removal and staining with InstantBlue™ (Sigma-Aldrich), a comassie-based stain that binds to protein bands. All samples were sufficiently digested (Figure 2.1).

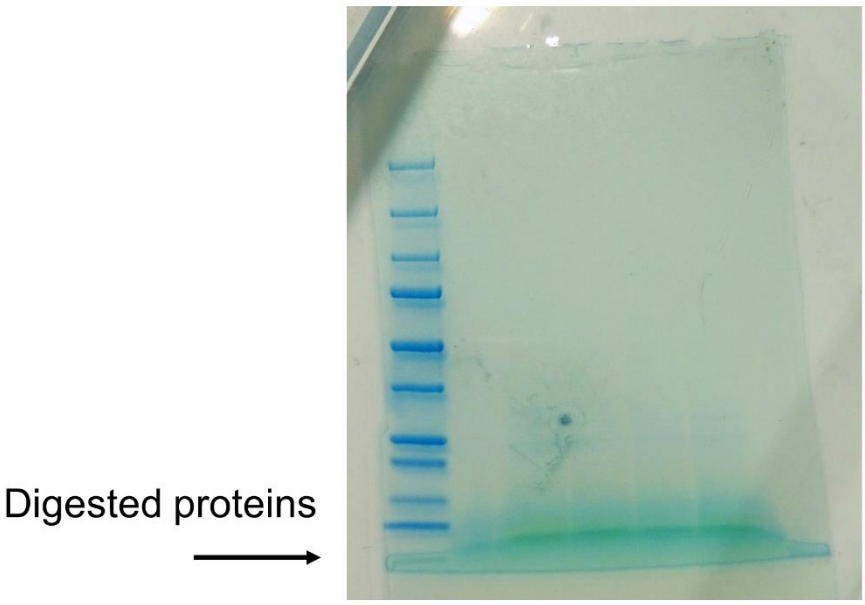

Figure 2.1: Western blot stained with InstantBlue™ for visualisation of digested proteins

2.7.5 Acidification

Acidification is used to remove fatty acids from the digested peptide solution. Twenty % trifluoroacetic acid (TFA) was prepared and this was added to the sample at give a final concentration of 1% (2 mL to 40 mL). The samples were placed on ice for 15 minutes to allow precipitation of fatty acids to form. The samples were centrifuged at 1,780 *x g* for 15 minutes at room temperature. The supernatant was placed in a fresh 50 mL falcon, without disturbing the precipitate.

2.7.6 Sep-Pak® C18 purification of proteins

Six 10 mL syringes were each attached to a Sep-Pak column and attached to a vacuum manifold. To equilibrate the column, 5 mL of solution B (65% CH_3CN, 35% MilliQ-H_20, 0.1% TFA) was added. The syringe was washed with 10 mL solution A (98% MilliQ-H_20, 2% CH_3CN, 0.1% TFA) before the addition of the peptide solution, avoiding bubbles at all times. The peptide solution was cleared through the Sep-Pak column, with the peptide collecting within the column. The peptide was washed with 10 mL solution A. Finally, the peptide was eluted in to a fresh 50 mL falcon, using 2 x 3 mL solution B. The samples were frozen at -80°C overnight. The next morning, tubes were place in the GeneVac® for lyophilization for 72 hours.

2.7.7 Immunoaffinity purification (IAP)

The lyophilized peptide was centrifuged at 2000 *x g* at room temperature for 5 minutes. All samples were resuspended in 1.4 mL (immunoaffinity purification) IAP buffer and transferred to a 1.7 mL reaction tube. The pH of each sample was recorded to ensure all samples were at a neutral pH. Samples were centrifuged at 10,000 *x g* for 15 minutes at 4°C. In the meantime, UbiScan® beads were washed four times with PBS, centrifuged at 2000 *x g* for 30 seconds between each wash. The beads were resuspended in 40 µL PBS following the final wash. The supernatant from the peptide solution was added to the beads and all samples were incubated at 4°C for 2 hours with constant agitation.

The flow-through was transferred to a new reaction tube and stored. The beads were washed with 1X IAP buffer two times, centrifuged at 2000 *x g* for 30 seconds at 4°C between each wash. The beads were then washed with water three times, centrifuged at 2000 *x g* for 30 seconds at 4°C between each wash. After the last wash step, tubes were centrifuged at 2000 *x g* for 5 seconds at 4°C to spin down any remaining water on the walls of the tubes. The remaining water was removed from the beads using a gel-loading tip. Fifty-five µL of 0.15 % TFA was added to each tube of beads and mixed gently. Samples were left to incubate at room temperature for 10 minutes, mixing gently every two minutes. The samples were centrifuged at 2000 *x g* for 30 seconds and the supernatant was collected in a new tube. This elution step was repeated.

2.7.8: Concentration and purification of peptides on StageTip

The C18 tip was equilibrated by passing 50 µL of solution B, followed by 50 µL solution A, twice. The sample was passed through the C18 tip twice in order to collect the peptide. The C18 tip was washed twice with 55 µL solution A. The peptide was eluted by passing 10 µL solution B through the C18 tip twice. This was repeated for every sample. All samples were lyophilized for one hour and placed in the -80°C.

2.7.9 Preparation of samples for liquid chromatography mass spectrometry (LC-MS) analysis

The peptides were resuspended in 20 µL buffer A (2% acetonitrile, 0.1% TFA, 97.9% H_20) and vortexed for 20 minutes at room temperature. Samples were sonicated gently for 5 minutes before centrifugation at 20,000 *x g* for 10 minutes at room

temperature to pellet any aggregates. Samples were transferred to LC-MS vials for mass spectrometry.

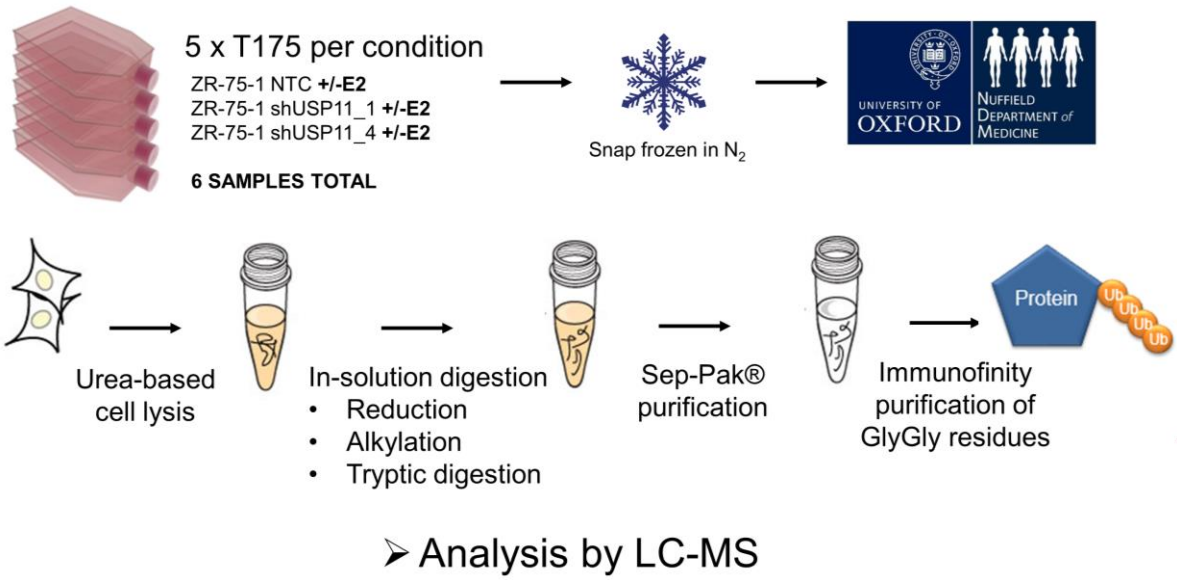

Figure 2.2: Workflow of sample preparation for LC-MS.

2.7.10 LC-MC Analysis

The MaxQuant (Tyanova et al., 2016a) computational platform was used to convert spectra generated from the Q Exactive Hybrid Quadrupole-Orbitrap Mass Spectrometer (Thermo Scientific) to peptides. First, the *Homo sapiens* proteome data was downloaded from Uniprot to MaxQuant, and the spectra were converted to peptides using the Andromeda search engine (Cox et al., 2011). The parameters for the MaxQuant run are listed in Table 2.4:

Table 2.4: MaxQuant parameters

Parameter	Value
Variable modifications	Oxidation (M), Deamination (NQ) and/or GlyGly (K)
Fixed modifications	Carbamidomethyl (C)
Maximum missed cleavages	2 or 3 (ubiquitome)
Match between runs?	YES
Include contaminants?	YES
Second peptides?	YES
Peptides for quantitation	1 and unique
LFQ quantitation?	YES

The “protein groups” file generated by MaxQuant was used for future statistical analysis (detailed below).

Statistical analysis of identified peptides was handled using the Perseus computational platform (Tyanova et al., 2016b). Label-free quantification (LFQ) values were extracted from the protein groups file previously generated by MaxQuant, and uploaded to the Perseus suite. Peptides only identified by site, reverse peptides, and potential contaminants were excluded from analysis. LFQ intensities were subject to a log2(x) transformation, and technical replicates were categorically annotated into individual groups. Proteins that had less than 3 valid values in at least one group were excluded from analysis. Missing values were imputed from a normal distribution (width 0.3, down shift 1.8) of the total matrix (Hein et al., 2015). A histogram showing counts vs LFQ intensity was generated for each sample to highlight the distribution of counts, and the imputation performed previously. Principle component analysis (PCA) was performed on samples in order to demonstrate how each sample grouped respective to all other samples. To highlight differentially expressed proteins between any two groups, a volcano plot was generated using a two-sided t-test (unpaired). The false discovery rate for all volcano plots was set to 5% (0.05), and the s0 LFQ difference value was kept at the default 0.1.

2.8 Statistical Analysis

In silico analysis was carried out using Gene Expression Based Outcome (GOBO), where differences were outlined in overall survival (OS), distant metastasis-free survival (DMFS) and recurrence-free survival (RFS) according to USP11 expression. A p-value <0.05 was considered statistically significant.

For TMA analysis, biopsy cores were manually scored (0-3) based on the degree of DAB positive staining. Kaplan-Meier and Cox regression analysis was then used to determine differences in OS, RFS and breast cancer-specific survival (BCSS) according to USP11 expression. Pearson's chi-squared test was used to evaluate associations between USP11 expression and clinicopathological characteristics. SPSS version 20.0 (SPSS Inc, Chicago, IL, USA) was used to carry out TMA statistical analysis, and a p-value <0.05 was considered statistically significant.

GraphPad Prism 5 was used to carry out statistical analysis on all *in vitro* work. Student's t-test/one-way ANOVA statistical tests were used, with a p-value <0.05 considered statistically significant.

Chapter 3: The functional and prognostic role of USP11 in estrogen receptor- positive (ERα+) breast cancer

3.1 Introduction

As described in Chapter 1, the role of DUBs in the oncology arena has come to light in recent years, with many of these enzymes recognized as key oncogenes or tumour suppressors. To investigate the functional role of DUBs in ERα driven breast cancer, we performed an RNAi loss-of-function screen, targeting all 108 known or putative DUBs in the human genome. This was carried out using an in-house shRNA DUB library in the lab of Prof. Rene Bernards at the Netherlands Cancer Institute, Amsterdam. shRNA screening is a common and reliable method to assess the function of a family of proteins and has proved to be a useful tool in cancer genomics (Bernards et al., 2006). The DUB library utilised in this study has contributed towards several fruitful studies from the Bernards laboratory. The library has been used to determine a role for USP1 in the Fanconi anaemia (FA) DNA-damage pathway (Nijman et al., 2005), as well as a role for CYLD in NF-κB activation (Brummelkamp et al., 2003).

The DUB library consists of pools of four non-overlapping shRNAs targeted to each DUB, 432 in total. These pools were transiently co-transfected in to the ZR-75-1 ERα+ BC cell line, along with ERE-luciferase and CMV-renilla reporters. The cells were hormone-starved for 48 hours before stimulation with 1 nM estradiol (E2). Promega's Dual luciferase reporter assay system was then used to assess activity at each reporter. This assay allows for detection of firefly (ERE-luciferase) and renilla (CMV-renilla) luciferases in each cell. ERα-bound ERE-luciferase reporter will emit light when the luciferase assay reagent (LAR) is added to the sample. This reaction is quenched by the addition of Stop & Glo® reagent, which then stimulates the renilla luciferase reaction which is used as an internal control. ERE-luciferase activity is directly proportional to ERα activation in these cells. Although an artificial method of detecting ERE-binding in ERα+ cancer cells, the dual luciferase reporter system has proved to be a fruitful tool in steroid hormone receptor research.

As demonstrated in Figure 3.1, DUB knockdown either repressed, enhanced or unchanged activity at an ERE. DUBs that repress ERα activity following knockdown were of particular interest to this study, as they may possess an oncogenic role and could be targetable in the clinic as an indirect means of abrogating ERα activity. The two samples with the most repressed ERE activity followed knockdown of OTUB1 and the BRCA-associated DUB, USP11. OTUB1 has been previously reported to directly deubiquitinate ERα and prevent degradation of

the receptor (Stanisic et al., 2009). It was therefore concluded in this case that knockdown of OTUB1 increased ERα ubiquitination and receptor degradation, thus reducing its activity in the cell. However, at the time of writing, no link between USP11 and ERα has been made.

3.2 USP11

Ubiquitin-specific protease 11 (USP11) was first cloned in 1996, when Swanson *et al.* suggested the enzyme may be linked to X-linked retinal disorders due to its X chromosomal location and high expression in retinal tissue (Swanson et al., 1996). This was later dismissed when an evaluation of patients with X-linked retinal disease revealed no mutations in USP11 (Brandau et al., 1998). Swanson *et al.* also made the first link between USP11 and cancer, highlighting the presence of a gene locus implicated in ovarian cancer in close proximity to USP11 on the short arm of chromosome X, although this was never investigated (Swanson et al., 1996).

Several studies highlight a role for USP11 in viral regulation. Of particular interest, USP11 deubiquitinates HPV-16E7, a transforming protein implicated in cervical abnormalities and cancer development. This results in stabilisation of HPV-16E7 and its ability to transform cervical cells, suggesting an oncogenic role for USP11 (Lin et al., 2008). In non-oncogenic viral pathways, USP11 can positively regulate influenza A by deubiquitinating influenza nucleoprotein (Liao et al., 2010). Furthermore, functional genomic screening identified a role for USP11 in hepatitis C replication and translation (Li et al., 2014). These studies combined highlight the importance of USP11 in viral pathways and the therapeutic potential of the enzyme in viral infection.

USP11 has an important role in the stabilisation and function of inhibitor of apoptosis (IAP) proteins. USP11 deubiquitinates cellular IAP2 (cIAP2), stabilising the protein and therefore suppressing apoptosis in tumour cells. The authors of this study showed that cancer cell lines with high levels of USP11 exhibited Smac-mimetic drug resistance, suggesting that USP11 may stand as a molecular barrier against IAP-targeting agents in the clinic (Lee et al., 2015). Later, mass spectrometry identified X-linked IAP (XIAP) as a USP11 target, with USP11 knockdown in MCF10A cells increased their colony forming ability through XIAP stabilisation. This study also showed that USP11 expression is higher in breast

tumours than in matched normal tissue, with increased expression in more differentiated, lymph node-positive tumours (n= 65).

Although USP11 has been described as an oncogene for the most part, some evidence in the literature suggests a tumour suppressing role. Promyelocytic leukaemia (PML) protein, a tumour suppressor downregulated in several cancer types, is deubiquitinated and stabilised by USP11. In human glioma, Hey1 represses USP11 function, leading to PML downregulation and high-grade malignancy (Wu et al., 2014). USP11 can also deubiquitinate and stabilise vestigial-like protein 4, (VGLL4), a YAP transcriptional repressor downregulated in several cancer types (Zhang et al., 2016a).

Perhaps the best known function of USP11 is its role in the DNA damage response (DDR). This first came to light when immunopurification mass spectrometry revealed an association with USP11 and breast cancer susceptibility gene 2 (BRCA2), a key DNA damage repair protein that when mutated leads to an increased risk of the development of breast and ovarian cancers. USP11 deubiquitinated BRCA2 in an overexpression system, and when silenced, increased cellular sensitivity to the DNA-damaging agent mitomycin-c (MM-C) in a BRCA-dependant manner. This was the first suggestion that USP11 plays a role in the BRCA DDR pathway (Schoenfeld et al., 2004).

Wiltshire *et al.* elucidated this role further and confirmed a role for USP11 in homologous recombination (HR). In order to identify genes that when silenced, result in synthetic lethality with PARP inhibition, an RNAi synthetic lethality screen was carried out. Seventy-three genes thought to play a role in HR were silenced and cells were exposed to the PARP inhibitor olaparib. Synthetic lethality occurred in cells with USP11 knockdown, supporting a role for USP11 in DNA repair. The authors demonstrated that USP11 knockdown hypersensitises cells to PARP inhibition and ionizing radiation, and that the enzymatic activity of USP11 is required for RAD51 and 53BP1 recruitment (Wiltshire et al., 2010). Later, USP11 was shown to deubiquitinate yH2AX, allowing for ubiquitination by RNF8/RNF168 and recruitment of these DDR factors at double-strand break sites (Yu et al., 2016).

Potentially the most important breakthrough study in this field was the identification of a role for USP11 in HR control during the cell cycle, published in 2015 in *Nature*. In the absence of sister chromatids, HR does not occur in the G1 phase of the cell cycle. Orthwein *et al.* demonstrate that PALB2 ubiquitination

supresses its interaction with BRCA1, suppressing the HR during the G1 phase. Deubiquitination of PALB2 by USP11 counteracts this, restoring PALB2-BRCA1 binding and as a result, HR (Orthwein et al., 2015).

The inability of a cancer cell to correctly repair damaged DNA via the DDR induces genomic instability during tumour development and is an enabling characteristic of cancer (Hanahan and Weinberg, 2011). Not only this, DNA repair inhibitors hold great promise as anti-cancer agents, highlighting the interest in studying the DDR regulatory components. The role of USP11 in cancer pathways has been relatively understudied, with no current information available on its molecular role in BC and/or ERα function. We therefore chose to further explore the function of this protein in ERα+ breast cancer, hypothesising that USP11 is a novel regulator of ERα activity and represents a novel therapeutic target in ERα+ breast cancer.

Table 3.1: Identified USP11 substrates

Substrate	Gene name	Function	Reference
RanBPM	Ran binding protein in the microtubule-organizing center	Scaffolding protein required for correct nucleation of microtubules; nuclear translocation	(Ideguchi et al., 2002)
BRCA2	Breast cancer type 2 susceptibility protein	DNA-damage protein associated with breast and ovarian cancer risk	(Schoenfeld et al., 2004)
HPV-16E7	Human papillomavirus type 16 - E7	Transforming protein involved in cervical cancer development	(Lin et al., 2008)
IκBα	Inhibitor of kappa B	Anchoring molecule, inhibitor of NFKB	(Sun et al., 2010)
MEL18	Polycomb group ring finger 2	Polycomb group protein	(Maertens et al., 2010)
BMI1	Polycomb group ring finger 2	Polycomb group protein	(Maertens et al., 2010)
RING1	Really interesting new gene 1	Polycomb group protein, E3 ligase	(Maertens et al., 2010)
NP	Influenza virus nucleoprotein	Protects viral RNA from nucleases by encapsulating the negative strand	(Liao et al., 2010)
Alk5	Tranforming growth factor beta receptor 1	Enhances TGFβ1-induced gene transcription	(Al-Salihi et al., 2012)
PML	Promyelocytic leukaemia	Tumour suppressor, component of PML nuclear bodies and regulator of several cellular pathways altered in cancer	(Wu et al., 2014)
p53	Tumour protein p53	Tumour suppressor, regulates the cell cycle	(Ke et al., 2014)
cIAP2	Cellular inhibitor of apoptosis 2	Inhibitor of apoptosis, E3 ligase which regulates TNFR signalling	(Lee et al., 2015)
SUMO-Ub chains	Small Ubiquitin-like Modifier ubiquitin chains	Removes Ub polymers on SUMO chains to counteract RNF4	(Hendriks et al., 2015)
γH2AX	Gamma histone 2AX	Scaffolding protein for DNA-damage proteins at DSB	(Yu et al., 2016)
PALB2	Partner and localizer of BRCA2	DNA-damage protein, interacts with BRCA to direct recruitment of BRCA2 and RAD51 to DNA breaks	(Orthwein et al., 2015)
Mgl-1	Mammalian homologue of Drosophila tumor suppressor protein Lgl	Tumour suppressor	(Lim et al., 2016)
LPA1	Lysophosphatidic acid receptor 1	G protein-coupled receptor with a pro-inflammatory function	(Zhao et al., 2016)
TβRII	Tranforming growth factor beta receptor 2	Enhances TGFB1-induced gene transcription	(Jacko et al., 2016)
XIAP	X-linked inhibitor of apoptosis	Inhibitor of apoptosis	(Zhou et al., 2017)
VGLL4	Vestigial-like protein 4	Transcription coactivator, negative regulator of YAP-TEAD	(Zhang et al., 2016a)

		transcriptional complex	
E2F1	Retinoblastoma-Associated Protein 1	Transcription factor, regulates the cell cycle	(Wang et al., 2017a)
XPC	Xeroderma pigmentosum	Recognises DNA adducts in nucleotide excision repair	(Shah et al., 2017)
RAE1	Ribonucleic acid export 1	Regulator of bipolar spindle formation in mitosis	(Stockum et al., 2018)
eIF4B	Eukaryotic initiation factor 4B	Transcription initiation complex, promotes oncogenic translation	(Kapadia et al., 2018)

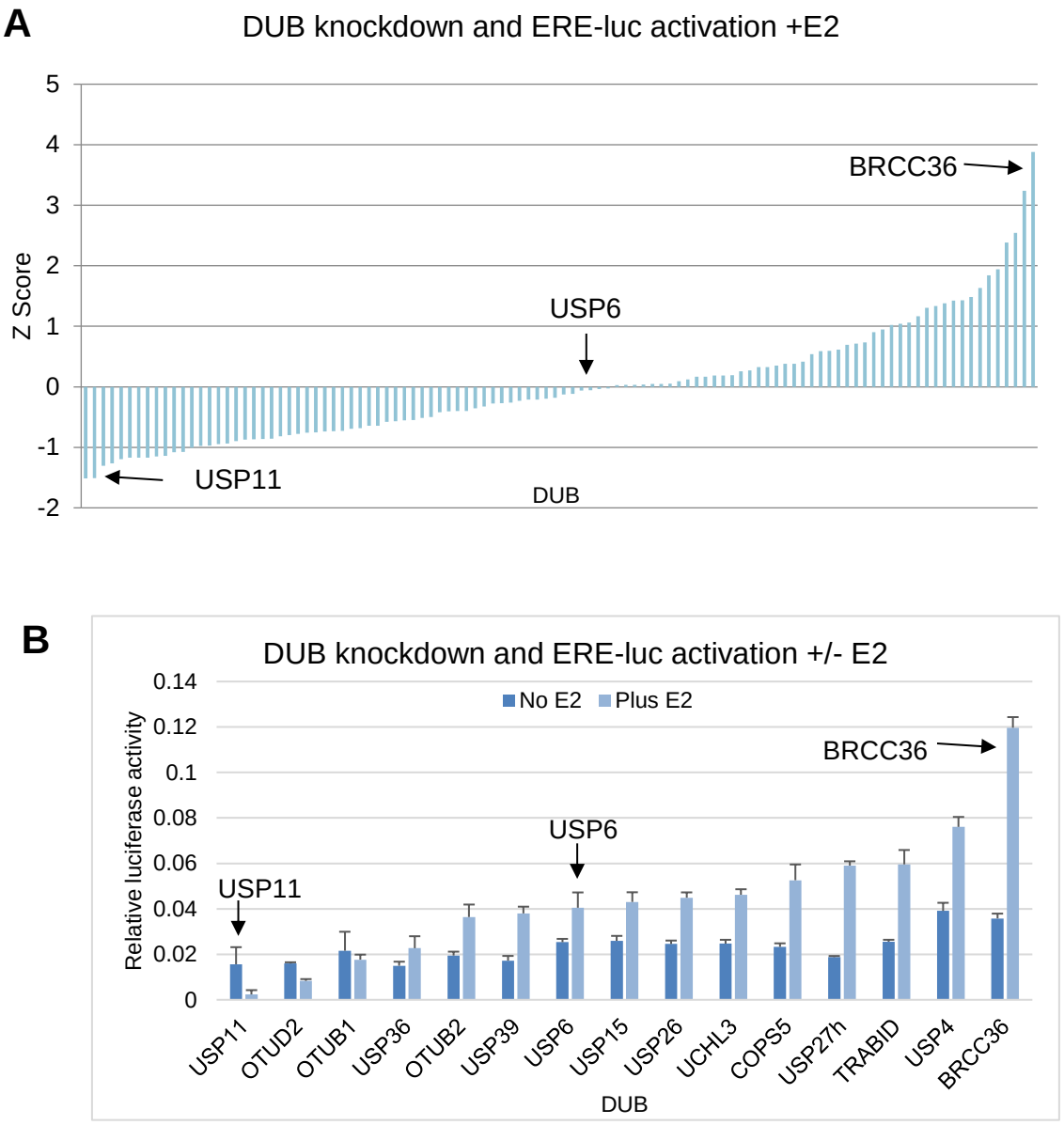

Figure 3.1: RNAi loss-of-function screen using a library of shRNA vectors targeting all human DUB genes identifies a role for USP11 in the ERα regulatory mechanism. *(A) ERE-luciferase reporter assay depicting the effects of DUB knockdown on the transcriptional activity of ERα. ZR-75-1 cells were co-transfected with pools of four non-overlapping shRNAs targeted to each DUB, as well as ERE-luciferase and CMV-renilla reporters. Cells were hormone starved for 48 hours before stimulation with 1 nM E2 for 24 hours. Cells were harvested and luciferase activity was detected. (B) Triplicate ERE-luciferase reporter assay demonstrating the effect of DUB knockdown on the transcriptional activity of ERα in the presence or absence of E2 stimulation. Error bars represent SEM. Data courtesy of Prof. Darran O'Connor, RCSI Dublin.*

3.3 Aims of this chapter

- Validate the RNAi loss-of-function screen and investigate the functional and prognostic relevance of USP11 in ERα+ breast cancer.
- Develop a robust model for studying the effect of USP11 silencing
- Examine the phenotypic effects of USP11 silencing and investigate how USP11 responds to E2
- Investigate the clinical relevance of USP11 by examining BC patient cohorts

3.4 Results

3.4.1 Knockdown of USP11 in ZR-75-1 cells and the role of USP11 in ERα transcriptional activity

In order to investigate the role of USP11 in ERα function, a stable USP11 knockdown BC model was developed using RNAi. Five individual shRNAs targeted to USP11 were used to knockdown the enzyme in the ZR-75-1 cell line. A non-targeting control (NTC) cell line was also generated to ensure RNAi activation had no off-target effects on the cells. Dr. Aisling O'Connor generated these cell lines by viral transduction in the Conway Institute of Biomolecular and Biomedical Sciences, UCD.

Protein knockdown was validated by western blotting (Figure 3.2) and the two cell lines with the most efficient knockdown (shUSP11_1 and shUSP11_4) were selected for ongoing studies. USP11 knockdown was validated in triplicate at both the protein and mRNA level before commencement of phenotypic studies.

In order to validate the results that were obtained from the RNAi loss-of-function screen, a dual luciferase reporter assay was carried out in ZR-75-1 USP11 knockdown cells, in the same manner as the screen. USP11 knockdown resulted in decreased activity at an ERE (Figure 3.3, A), therefore supporting earlier findings. Significance was achieved in one knockdown cell line (shUSP11_1). To further determine the role of USP11 in ERα transcriptional activity, progesterone receptor (PgR) expression was examined. *PgR* is a well-defined ERα target gene. With an ERE in its promotor, *PgR* is directly upregulated by ERα so both receptors can co-localise in female reproductive tissues. Together, they play a key role in both normal breast physiology and malignancy (Carroll et al., 2017). Again, one of two knockdown cell lines (shUSP11_1) significantly decreased PgR expression at both the protein (Figure B, i) and the mRNA level (Figure B, ii). Western blot analysis indicated that PgR isoform B is downregulated in both knockdown cell lines, while isoform A is downregulated in shUSP11_1 only (Figure B, i).

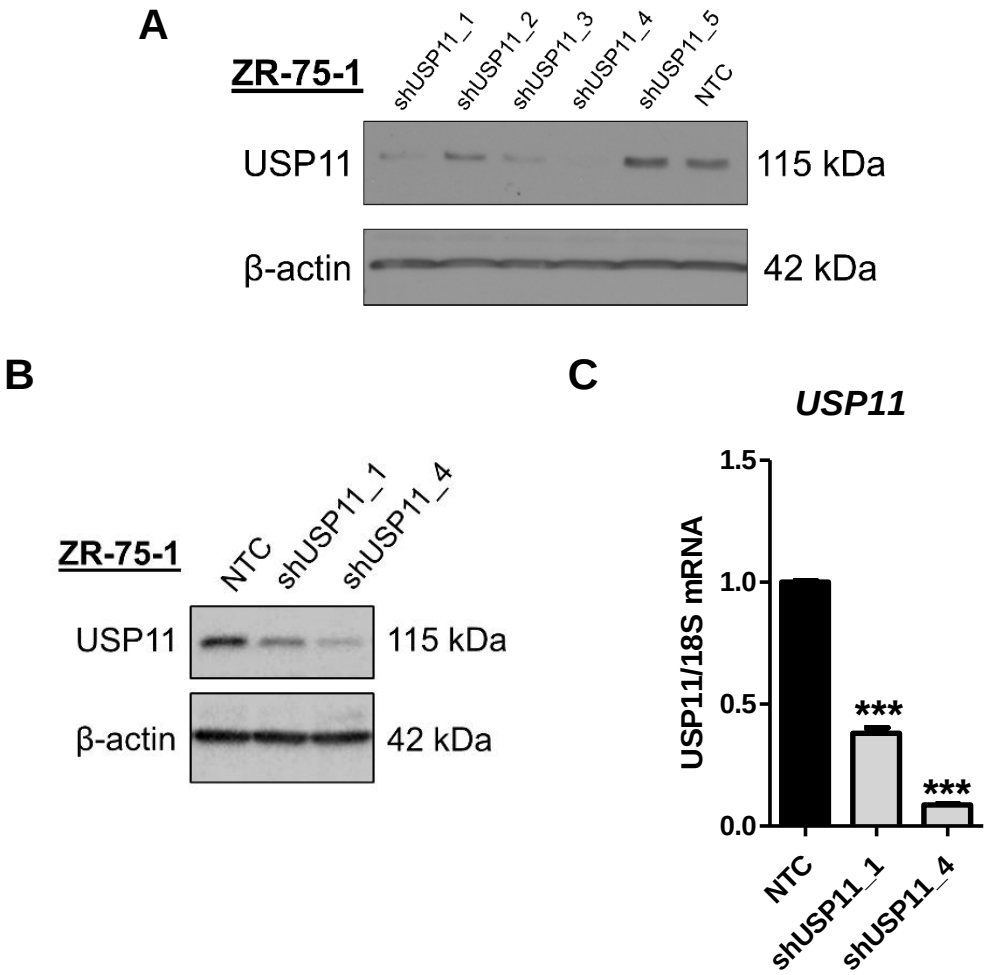

Figure 3.2: USP11 levels are diminished in the ZR-75-1 BC cell line following shRNA viral transduction and is a sufficient model for the study of its functional role. *(A) Five shRNAs targeted to USP11 and a non-targeting control (NTC) vector were virally transduced in to the ZR-75-1 cell line. (B) Triplicate validation of USP11 knockdown on chosen knockdown cell lines. Knockdown was validated at the (i) protein level by Western blotting and the (ii) mRNA level by qRT-PCR. Western blot images are representative of three biological replicates;* β*-actin was used as a loading control. qRT-PCR data was normalized to 18S expression, with samples normalised to siControl. Error bars represent standard error of the mean (SEM); *** p<0.001, student's t-test, unpaired.*

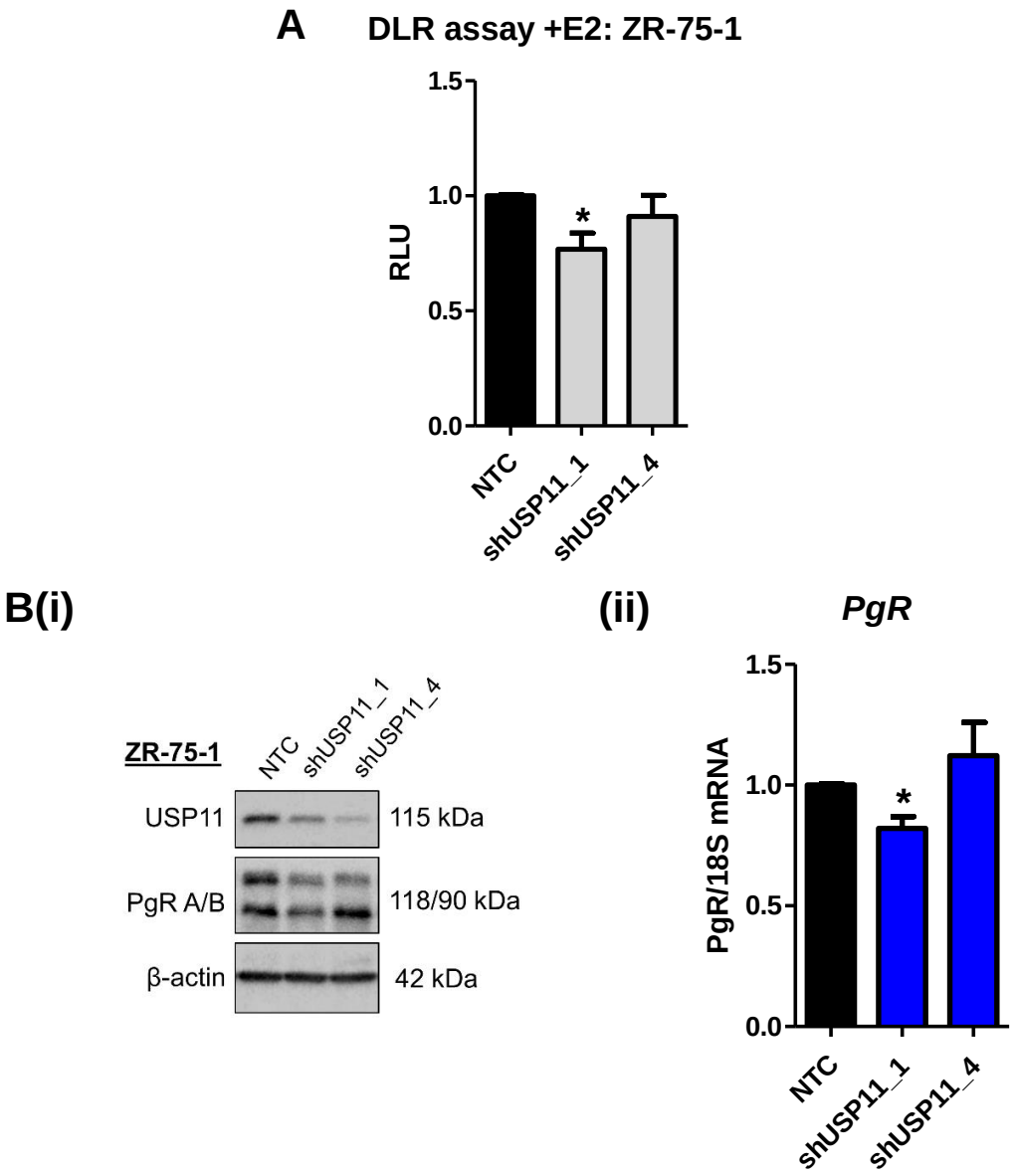

Figure 3.3: USP11 knockdown decreased ERα transcriptional activity in one of two knockdown cell lines. *(A) Dual luciferase reporter assay in USP11 knockdown and control ZR-75-1 cells. Cells were transfected with ERE-luc and CMV-renilla reporters, hormone-starved for 48 hours before subsequent stimulation with 1 nM E2 for 24 hours. Results are presented as a percentage of the control (NTC); error bars represent SEM. (B) Matching PgR expression at (i) the protein and (ii) the mRNA level, as determined by Western blotting and qRT-PCR, respectively. Cells were hormone starved for 48 hours before subsequent stimulation with 1 nM E2 for 24 hours. Western blot is representative of three biological replicates;* β*-actin was used as a loading control. mRNA expression was normalized to 18S expression and knockdown samples were normalised to NTC. * p<0.005, student's t-test, unpaired.*

shRNA knockdown cells are selected and potential compensatory mechanisms to detrimental growth effects could be activated. In addition, the expression of ERα target genes were examined in ZR-75-1 cells, using two independent siRNAs targeted to USP11. After 72 hours both *PgR* and *TFF1* were downregulated in USP11 knockdown cells, when compared to an siRNA control (Figure 3.4). Only one siRNA reached significance (siUSP11_1).

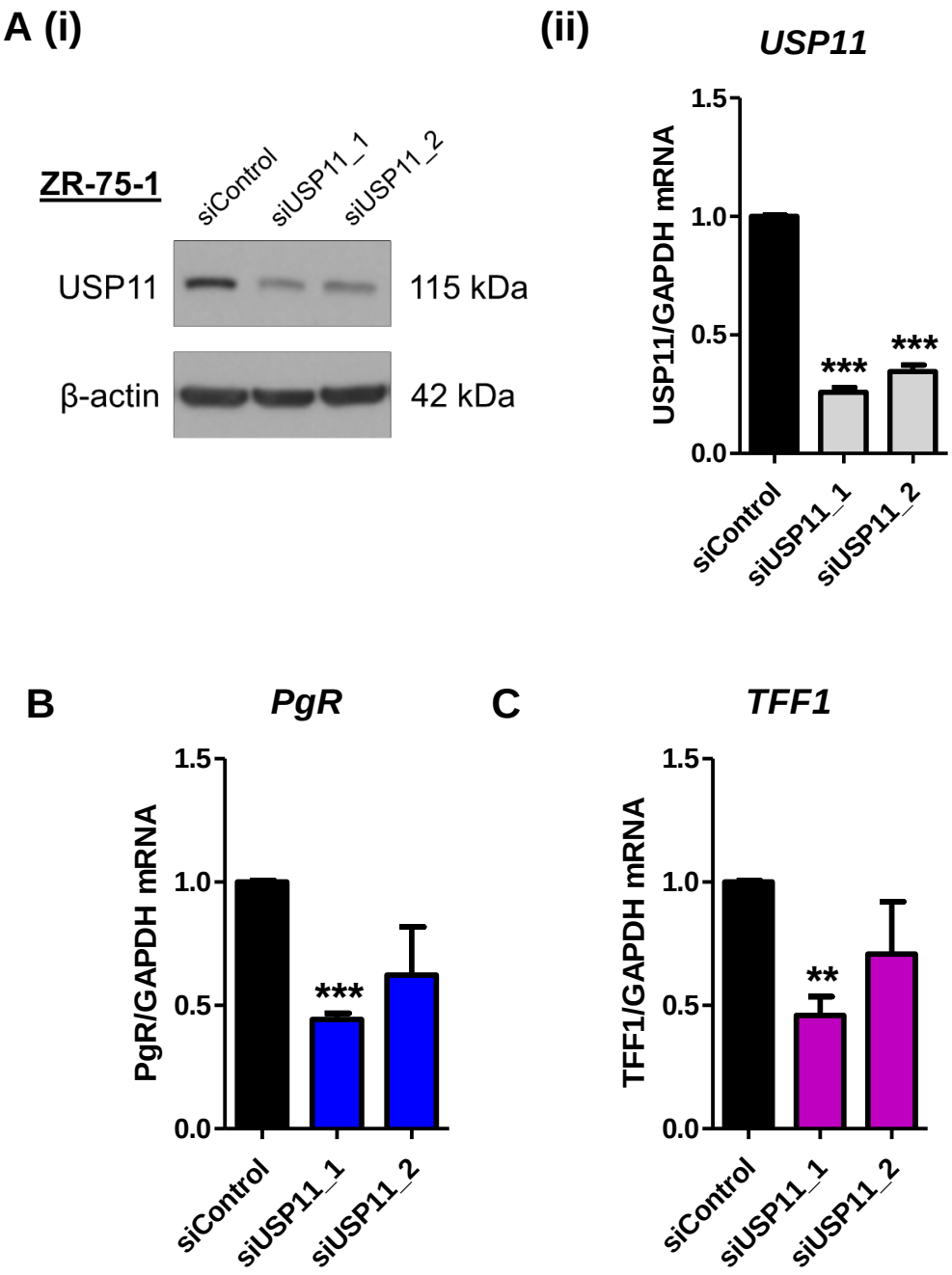

Figure 3.4: USP11 knockdown using two individual siRNAs reduced the mRNA expression of PgR and TFF1. *(A) USP11 knockdown was confirmed at (i) the protein level and (ii) the mRNA level, 72 hours following transfection. (B) mRNA expression of PgR and TFF1, 72 hours following transfection of USP11 siRNAs. All experiments were performed in biological triplicate. β-actin was used as a loading control. mRNA expression was normalised to 18S expression and all samples were normalised to unstimulated cells. Error bars represent SEM; ** p<0.01; *** p<0.001, student's t-test, unpaired.*

3.4.2 USP11 expression in response to estradiol (E2)

As a potential ERα interactor, it was hypothesised that USP11 may respond to estrogen in the cell and could potentially be an ERα target gene itself. To investigate this, ZR-75-1 cells were treated with 1 nM E2 for 4 and 24 hours respectively and USP11 expression was examined. After 24 hours E2 treatment, USP11 was upregulated at both the protein and mRNA level (Figure 3.5, A), although these results were not statistically significant. ERα protein expression was also examined; downregulation can be observed at 4 hours E2 treatment, with re-expression occurring at 24 hours (Figure 3.5, A). ERα mRNA expression was increased following 24 hours E2 exposure while no change was observed at the 4 hour time point. *PgR* was used as a positive control; expression was increased at both 4 and 24 hours E2 treatment, indicating ERα activation at these chosen time points.

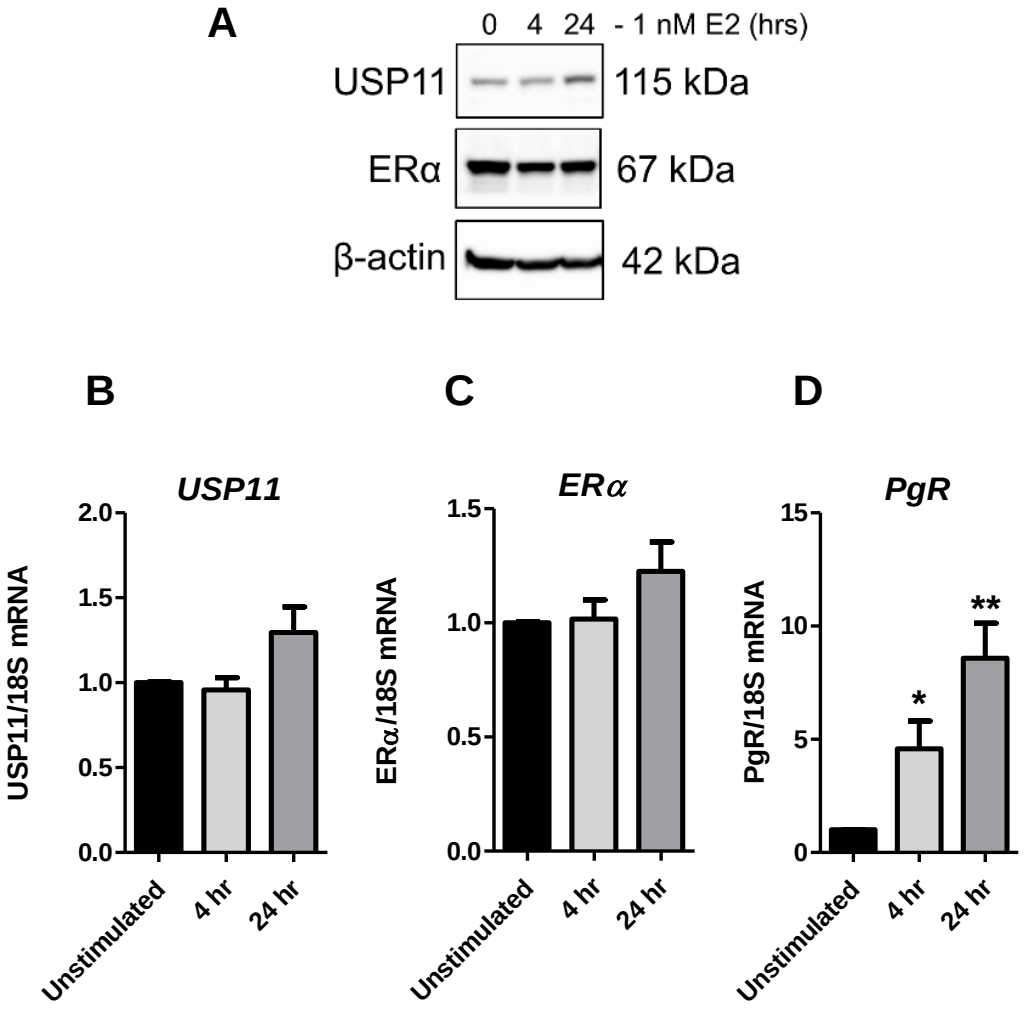

Figure 3.5: USP11 was upregulated in breast cancer cells following E2 stimulation. *ZR-75-1 cells were hormone starved for 48 hours before stimulation with 1 nM E2 for either 4 or 24 hours. (A) Representative Western blot showing USP11 and ERα protein expression following E2 stimulation.* β*-actin was used as a loading control. (B) mRNA expression of (i) USP11, (ii) ERα and (iii) PgR, as determined by qRT-PCR, n=3. PgR expression was used as a positive control for ERα activation. mRNA expression was normalised to 18S expression and all samples were normalised to unstimulated cells. Error bars represent SEM; * p<0.05; ** p<0.01, student's t-test, paired.*

The above results indicated that USP11 is upregulated following 24 hours exposure to E2, however the location of upregulated USP11 within the cell is unknown. Reports indicate that USP11 is expressed in both the cell nucleus and cytoplasm, with main expression localised to the nucleoplasm (HPA, 2018). It was

hypothesised that USP11 expression was increased in the nucleus following E2 treatment, as ERα transcriptional activity is occurring here. To investigate this, protein cellular fractions were generated. This allowed for individual analysis of the nuclear, cytoplasmic, and membrane proteins. As hypothesised, USP11 expression was increased in the nucleus of the cell following E2 stimulation in a time dependent manner (Figure 3.6). Cytoplasmic expression was unchanged but interestingly, a second, smaller band of protein was also present in the cytoplasmic fraction. USP11 membrane expression appears unchanged in response to E2. ERα protein expression was used as a positive control; it was absent in the cytoplasm and moved away from the membrane in a time-dependent manner following E2 treatment. Tubulin, trimethyl histone H3 and cytochrome-C were used as cytoplasm, nuclear and membrane markers, respectively.

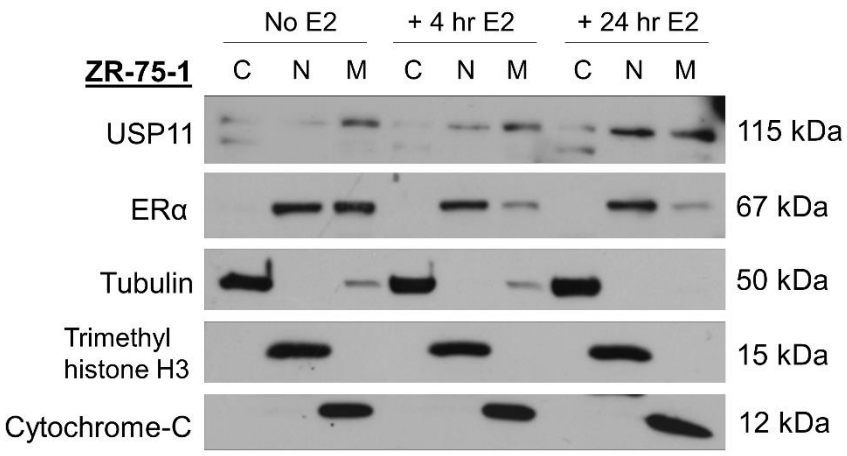

Figure 3.6: USP11 was upregulated in the nucleus of ZR-75-1 cells in a time dependent manner following E2 stimulation. *Cells were deprived of hormone stimulation for 48 hours before treatment for either 4 or 24 hours with E2. Protein fractions were isolated and protein levels were determined by western blotting. Tubulin, trimethyl histone H3 and cytochrome-C were used as cytoplasmic (C), nuclear (N) and membrane (M) markers, respectively. Western blot image is representative of two biological replicates.*

To confirm the finding of increased expression of USP11 in the nucleus, immunocytochemistry (ICC) was performed on E2 treated ZR-75-1 cells. Cells were exposed to the same conditions, fixed in methanol and probed with a USP11

antibody. A red florescent secondary (Alexa Flour® 594) was used and the cells were imaged by florescent microscopy. Interestingly, USP11 foci appeared in the nucleus following E2 treatment (Figure 3.7, A). The experiment was repeated and cells were imaged using confocal microscopy with Dr. Brenton Cavanagh, RCSI. In unstimulated ZR-75-1 cells there was no obvious detection of USP11 foci in the nuclei. Following 4 hours E2 stimulation, foci were bright and widespread throughout the nuclei. After 24 hours E2 exposure, foci were still detected, with increased overall USP11 expression in the nuclei (Figure 3.7, B).

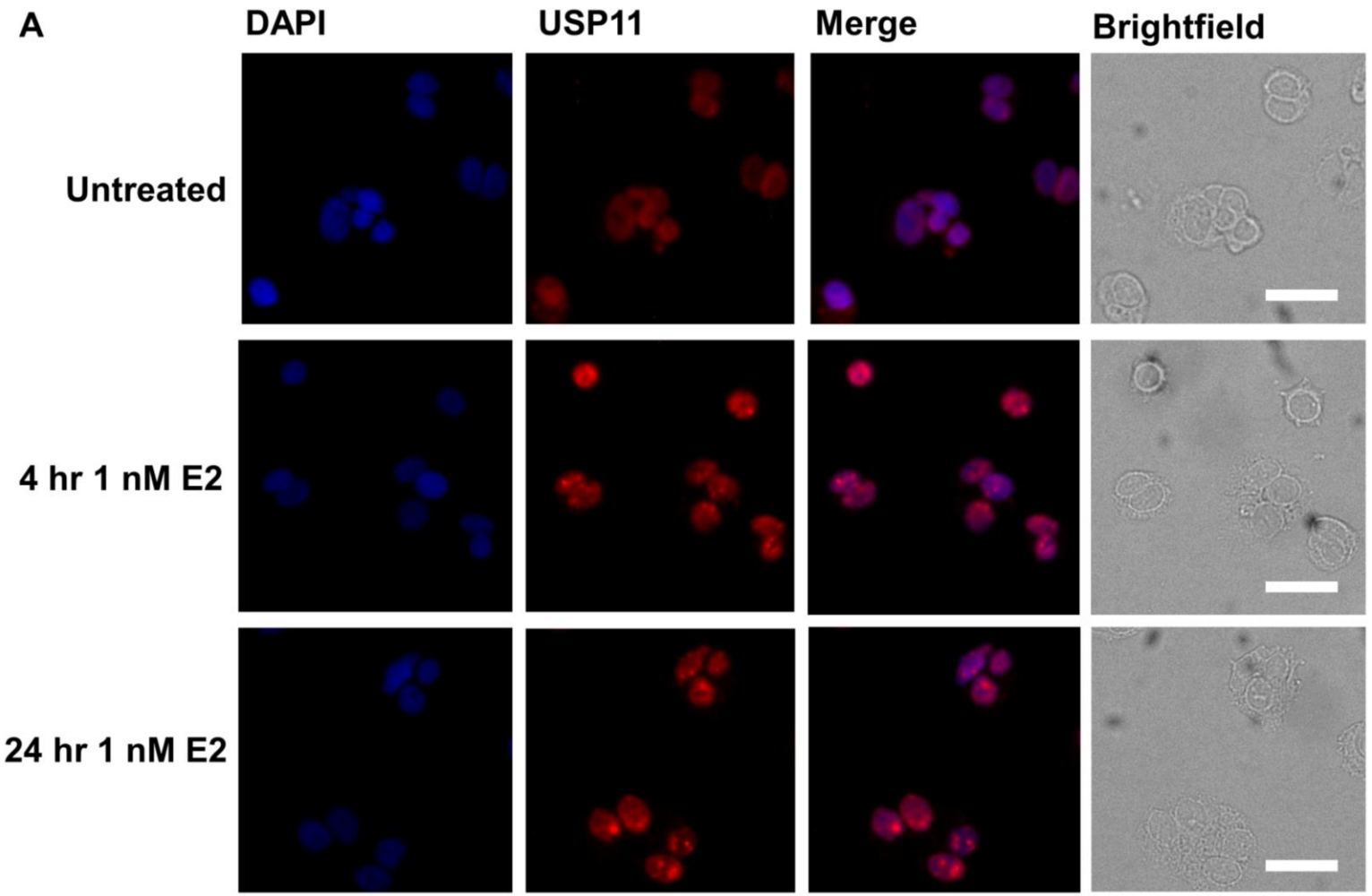
A
DAPI
USP11
Merge
Brightfield
Untreated
4 hr 1 nM E2
24 hr 1 nM E2

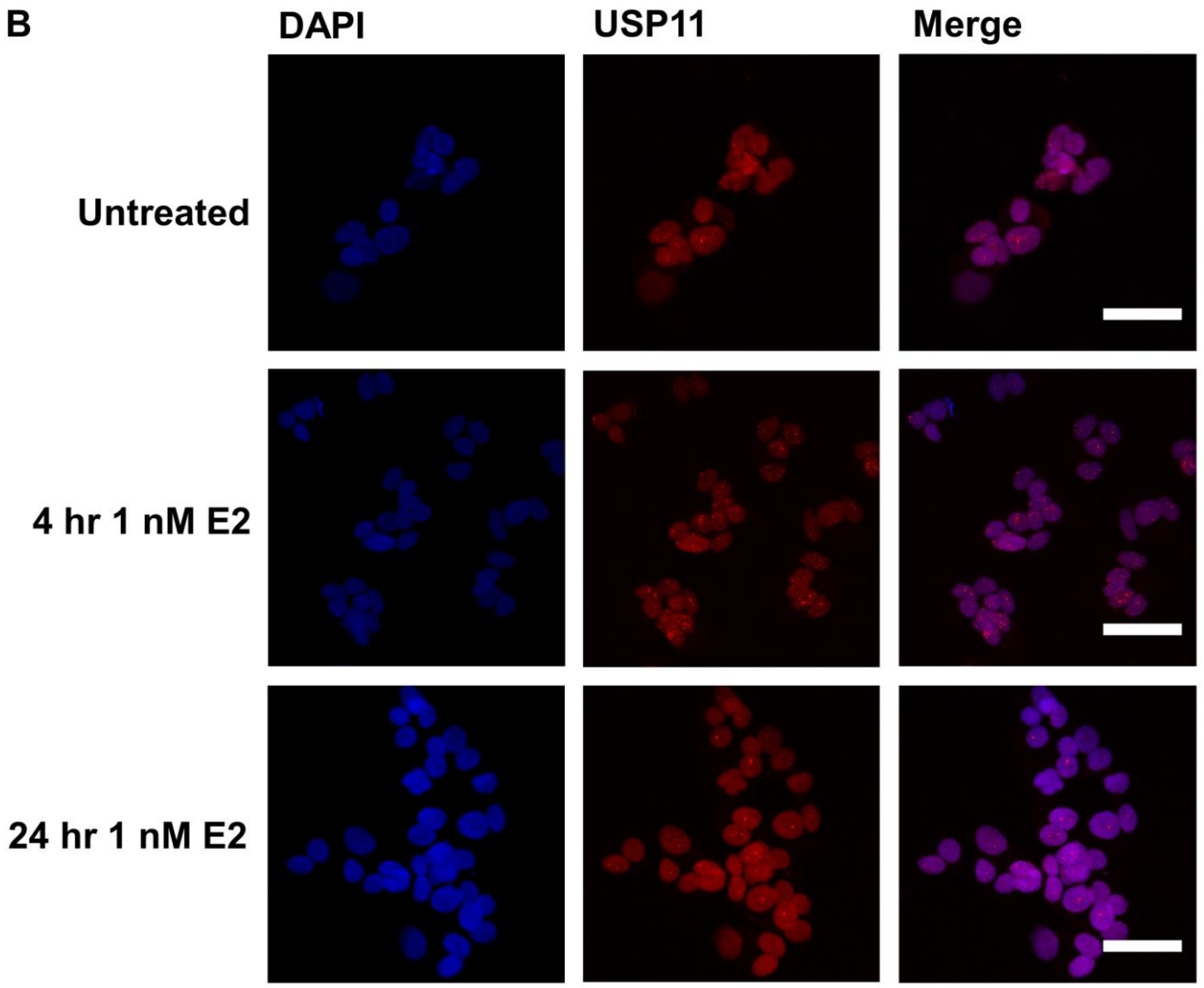
B
DAPI
USP11
Merge
Untreated
4 hr 1 nM E2
24 hr 1 nM E2

Figure 3.7: USP11 foci appeared in ZR-75-1 nuclei following E2 stimulation. *(A) Florescent microscopy examining USP11 expression. Cells were seeded on to coverslips in a 24-well plate, hormone starved for 48 hours and subsequently treated with E2 for 4 or 24 hours. Cells were fixed and permeabilised in methanol, blocked in goat serum and probed with USP11 primary antibody (1:250, optimised). Alexa Flour® 594 anti-rabbit secondary was used to detect USP11 antigens by florescence. Mounting medium containing DAPI (blue) for nuclear staining was used to mount the coverslip on to a microscope slide. (B) Confocal microscopy examining USP11 expression. Conditions were similar to (A). Edits to each image were consistent. Scale bars: 50 µM.*

The above results are preliminary and whether USP11 is shuttled in to the nucleus following E2 exposure is currently unknown. If this was the case, USP11 would contain a nuclear localisation signal/sequence (NLS), an amino acid sequence which is recognised by importin for transport through the nuclear pore (Lange et al., 2007). To check if USP11 contains a NLS, the FASTA sequence was obtained from Uniprot and uploaded on to cNLS Mapper, an online tool used to predict the presence of a NLS within an amino acid sequence. As expected, USP11 contained both a monopartile and bipartile NLS (Figure 3.8). These are classic NLS, defined by one or two (mono- or bipartile) amino acid stretches (Lange et al., 2007).

Predicted NLSs in query sequence

```
MAVAPRLFGGLCFRFRDQNPEVAVEGRLPISHSCVGCRRERTAMATVAAN 50
PAAAAAAVAAAAAVTEDREPQHEELPGLDSQWRQIENGESGRERPLRAGE 100
SWFLVEKHWYKQWEAYVQGGDQDSSTFPGCINNATLFQDEINWRLKEGLV 150
EGEDYVLLPAAAWHYLVSWYGLEHGQPPIERKVIELPNIQKVEVYPVELL 200
LVRHNDLGKSHTVQFSHTDSIGLVLRTARERFLVEPQEDTRLWAKNSEGS 250
LDRLYDTHITVLDAALETGQLIIMETRKKDGTWPSAQLHVMNNNMSEEDE 300
DFKGQPGICGLTNLGNTCFMNSALQCLSNVPQLTEYFLNNCYLEELNFRN 350
PLGMKGEIAEAYADLVKQAWSGHHRSIVPHVFKNKVGHFASQFLGYQQHD 400
SQELLSFLLDGLHEDLNRVKKKEYVELCDAAGRPDQEVAQEAWQNHKRRN 450
DSVIVDTFHGLFKSTLVCPDCGNVSVTFDPFCYLSVPLPISHKRVLEVFF 500
IPMDPRRKPEQHRLVVPKKGKISDLCVALSKHTGISPERMMVADVFSHRF 550
YKLYQLEEPLSSILDRDDIFVYEVSGRIEAIEGSREDIVVPVYLRERTPA 600
RDYNNSYYGLMLFGHPLLVSVPRDRFTWEGLYNVLMYRLSRYVTKPNSDD 650
EDDGDEKEDDEEDKDDVPGPSTGGSLRDPEPEQAGPSSGVTNRCPFLLDN 700
CLGTSQWPPRRRRKQLFTLQTVNSNGTSDRTTSPEEVHAQPYIAIDWEPE 750
MKKRYYDEVEAEGYVKHDCVGYVMKKAPVRLQECIELFTTVETLEKENPW 800
YCPSCKQHQLATKKLDLWMLPEILIIHLKRFSYTKFSREKLDTLVEFPIR 850
DLDFSEFVIQPQNESNPELYKYDLIAVSNHYGGMRDGHYTTFACNKDSGQ 900
WHYFDDNSVSPVNENQIESKAAYVLFYQRQDVARRLLSPAGSSGAPASPA 950
CSSPPSSEFMDVN                                       963
```

Predicted monopartite NLS		
Pos.	Sequence	Score
444	QNHKRRNDSV	6.5

Predicted bipartite NLS		
Pos.	Sequence	Score
748	EPEMKKRYYDEVEAEGYVKHDCVGYVMKKAPV	6

Figure 3.8: USP11 contains both a monopartile and bipartile NLS. *The amino acid sequence of USP11 was obtained on Uniprot and uploaded on to cNLS Mapper to predict NLS (cut off score 5.0).*

3.4.3 The effect of USP11 knockdown on ZR-75-1 growth and response to anti-endocrine agents

The ZR-75-1 is an ERα+ BC cell line that is highly dependent on the receptor for growth and differentiation. The above data suggests that USP11 affects ERα transcriptional activity and as a result it was hypothesised that silencing of USP11 may slow the growth of these cells. An MTT viability assay was used to assess this. After 4 days under normal growth conditions, one of the USP11 knockdown cell lines (shUSP11_4) was significantly less viable compared to NTC cells ($p=0.004$). The second knockdown cell line (shUSP11_1) was also less viable when compared to control cells, but this result was not significant (Figure 3.9, A). A colony formation assay was carried out on the same cell lines to examine the effect of USP11 on anchorage independent growth. Surprisingly, USP11 knockdown supressed colony forming ability in one of two knockdown cell lines. Surprisingly, shUSP11_4 appeared to have more, larger colonies than NTC cells (Figure 3.9, B).

To further explore the effect of USP11 silencing on cell growth, cell cycle analysis was performed by propidium iodide (PI) staining and flow cytometry. PI is a florescent DNA intercalating agents that can be used to determine at what stage in the cell cycle each cell is at. There were no significant changes to the cell cycle in USP11 knockdown cells when compared to NTC cells. In both knockdown cell lines, there were a higher percentage of cells in the G1 phase, but these results were not significant. Very few cells were present in the Sub-G1 phase in both control and knockdown cell lines (Figure 3.9, C). The average percentage of cells in each phase of the cell cycle can be examined in Table 1.2.

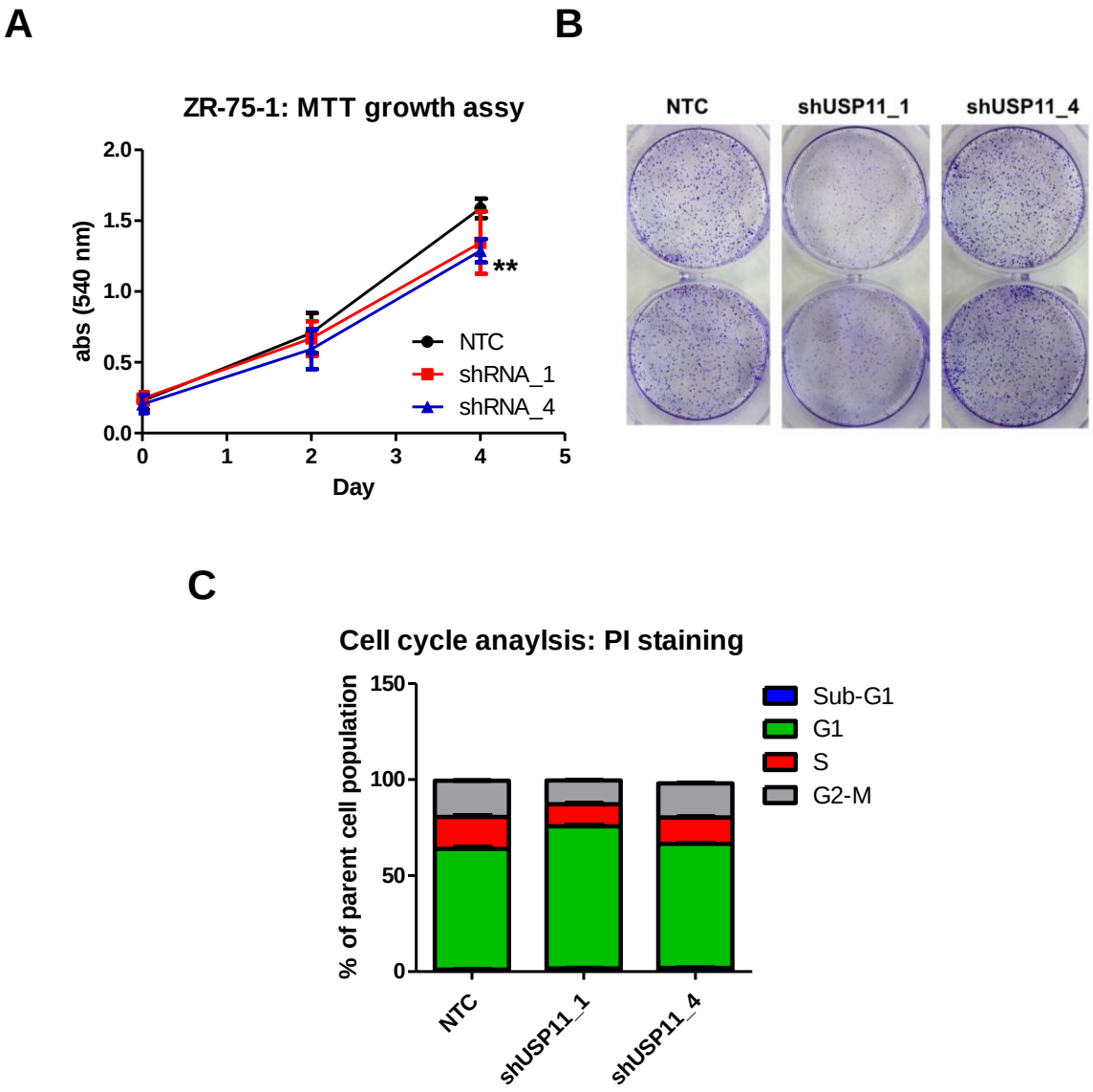

Figure 3.9: USP11 knockdown slowed the proliferation of ZR-75-1 breast cancer cells, however no significant changes to the cell cycle were observed. *(A) MTT viability assay depicting the effect of USP11 knockdown on ZR-75-1 cell growth. Cells were incubated under normal growth conditions for the days stated before cell viability was assessed by the MTT assay. Error bars represent SEM; ** p<0.01, student's t-test comparing siControl and shUSP11_4 day 4 only. (B) Colony formation assay depicting the effect of USP11 knockdown on ZR-75-1 colony forming ability. Cells were seeded at a low viability and incubated for 2 weeks; n= 2. (C) Cell cycle analysis by PI staining and flow cytometry. Cells were incubated under normal growth conditions for 48 hours before staining. One-way ANOVA, Tukey post-test was performed and no significant changes were detected in knockdown cell lines.*

Table 3.2: Average percentage of cells in each phase of the cell cycle (n= 3)

	NTC	***shUSP11_1***	***shUSP11_4***
Sub-G1	1.1	1.6	1.9
G1	62.8	74.1	64.7
S	16.6	11.5	13.7
G2-M	18.9	12.3	17.8

As mentioned in Chapter 1, both tamoxifen and fulvestrant are used to treat patients with endocrine-driven breast cancer. To recap, tamoxifen is an ERα antagonist in breast tissue while fulvestrant induces receptor degradation. ZR-75-1 cells are quite responsive to both anti-endocrine agents, with IC50s in the low μM range for both drugs. As such, it was hypothesised that knockdown of USP11 would have little effect on the sensitivity of these cells to either drug; if USP11 is interacting with ERα and receptor function/expression is affected by an anti-endocrine agent, it would leave little functioning ERα to interact with.

To test this, ZR-75-1 USP11 knockdown and NTC cells were treated with a range of either 4-hydroxytamoxifen (4-HT) or fulvestrant for 72 hours. As hypothesised, USP11 knockdown had no significant effect on the sensitivity of ZR-75-1 cells to either drug (Figure 3.10).

A

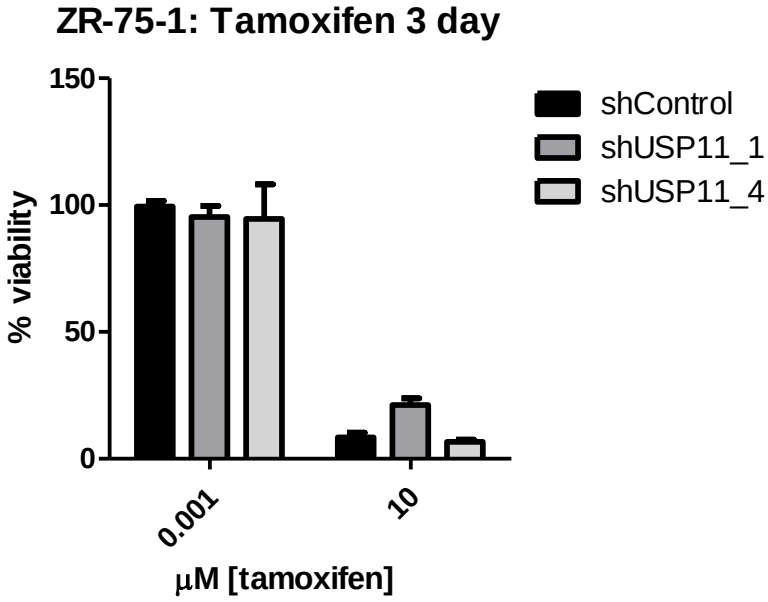

B

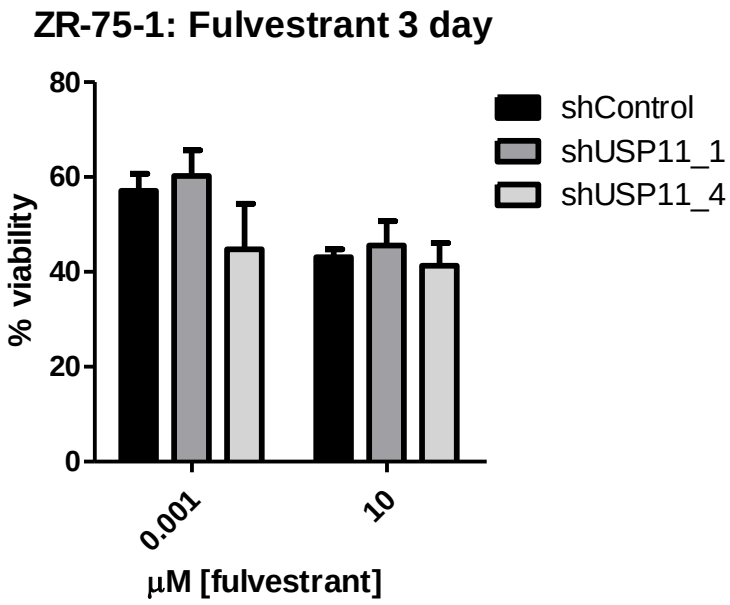

Figure 3.10: Knockdown of USP11 in ZR-75-1 cells had no significant effect on the sensitivity to either tamoxifen or fulvestrant. *ZR-75-1 cells were seeded in a 96-well plate and treated with a range of concentrations of either tamoxifen or fulvestrant. After 72 hours, cell viability was assessed by an MTT viability assay. The above graphs demonstrate cell viability at the lowest and highest drug concentrations used. Error bars represent SEM.*

3.4.4 The role of USP11 in ERα function in a HEK293T CRISPR knockout cell line

Due to the unfortunate time restrictions of this project, generating a USP11 knockout BC cell line was not achievable. Furthermore, the ZR-75-1 BC cell line is highly genomically unstable, posing a challenge in the generation of a CRISPR knockout cell line model. In 2015, Orthwein and colleagues published their mechanism for the suppression of homologous recombination (HR) in G1 cells in *Nature,* as discussed in section 3.2. *(Orthwein et al., 2015)*. The group used a HEK293T USP11 knockout cell line to elucidate this mechanism and were happy to share these cells for this project.

Human embryonic kidneys (HEK) cells are widely used in molecular biology research due to their fast, reliable growth and easily transfectable nature (DuBridge et al., 1987). Although immortalised, these cells are not malignant and are not suitable for the study of malignant phenotypes. They are however, very suitable for mechanistic studies and although they are negative for the expression of ERα, ectopic expression was easily achieved.

USP11 knockout in these cells was first confirmed in the laboratory before proceeding. Knockout was assessed at both the protein and mRNA level and was found to be sufficient for further studies (Figure 3.11).

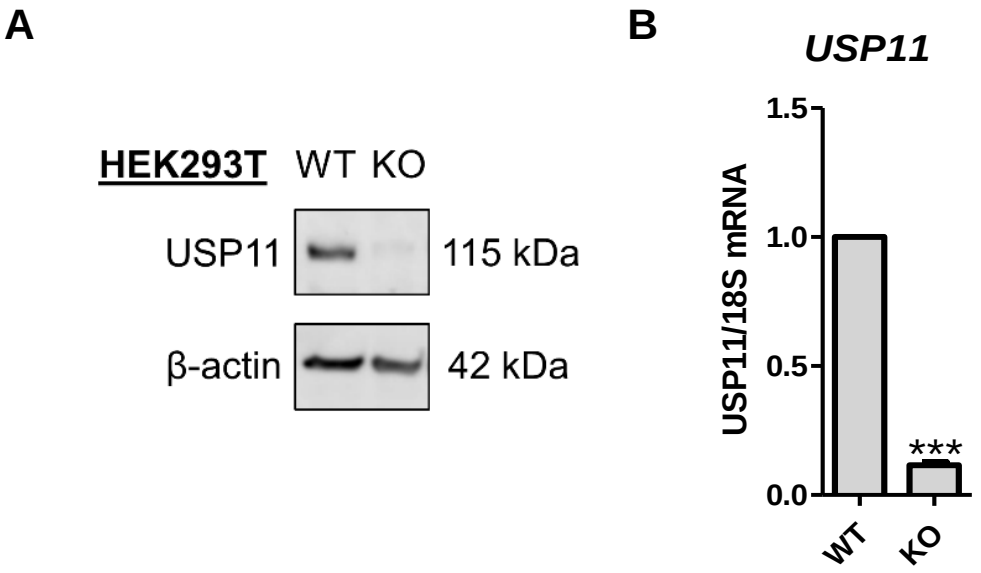

Figure 3.11: HEK293T cells have no expression of USP11 following CRISPR knockout. *(A) Representative western blot image detecting USP11 protein levels in wild-type (WT) and USP11 knockout (KO) cells. β-actin was used as a loading control. (B) qRT-PCR detecting USP11 mRNA expression in WT and KO cells. Both protein and mRNA validation was performed in biological triplicate; error bars represent SEM. *** p<0.001, student's t-test, unpaired.*

As mentioned, HEK293T cells are ERα-negative and require ectopic expression to study the role of USP11 in receptor function. ERα was transiently transfected in to the cells using lipofectamine. In order to then study ERα function, a dual luciferase reporter assay was carried out. ERα was co-transfected with an ERE-luciferase and CMV-renilla reporter, as described previously. Knockout of USP11 resulted in a significant decrease in activity at an ERE in response to E2. Activity was also decreased in the absence of estradiol, however this result was non-significant (Figure 3.12, A).

To further assess ERα function in USP11 knockout cells, the induction of ERα-target genes was examined following ERα transfection and E2 stimulation. As expected, both *PgR* and *TFF1* mRNA expression was induced following E2 stimulation, however this induction was repressed in USP11 knockout cells (Figure 3.12, B, C).

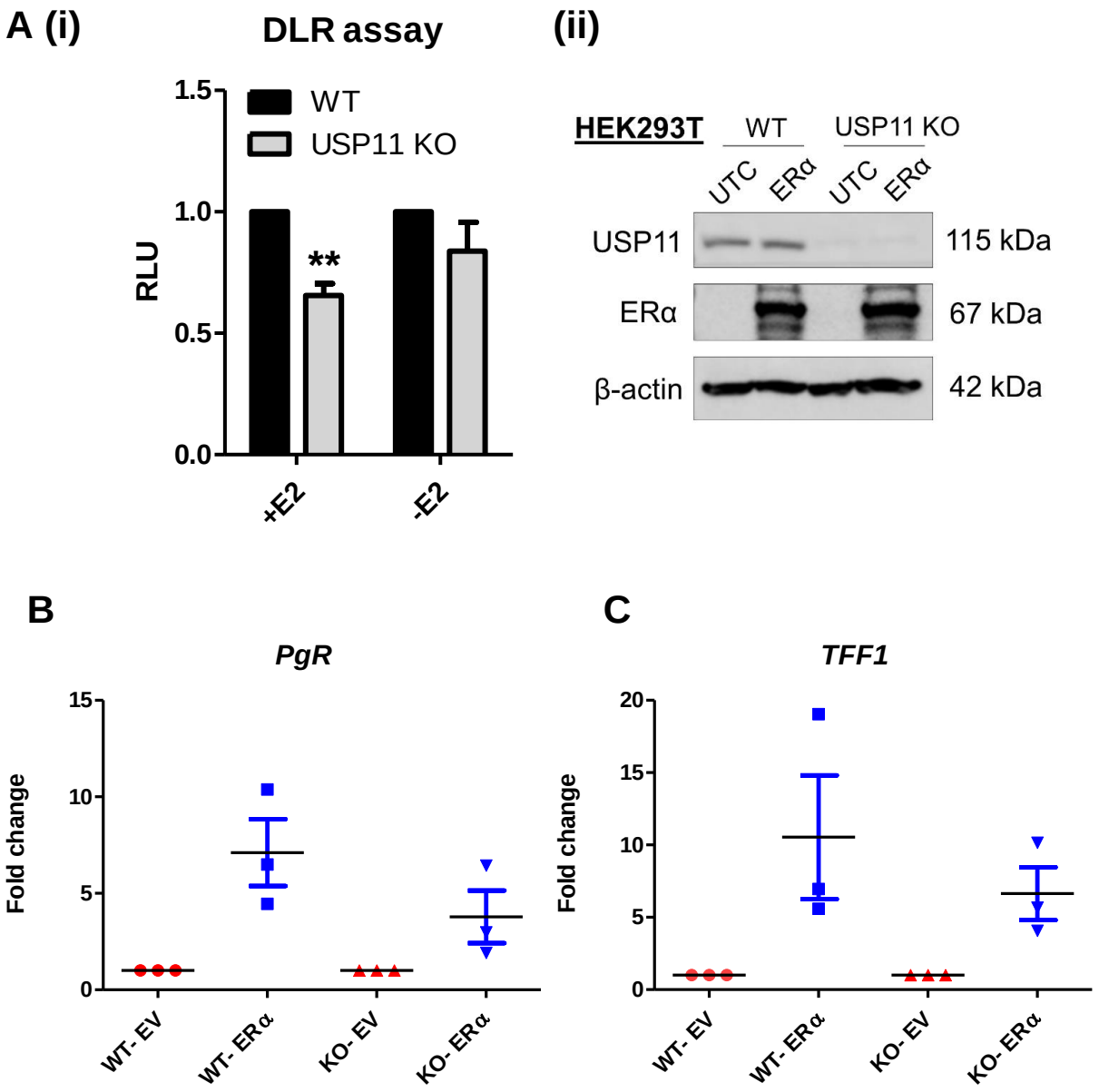

Figure 3.12: Knockout of USP11 represses ERα transcriptional activity in HEK293T cells ectopically expressing ERα. *(A) Dual luciferase reporter (DLR) assay in HEK293T in wild-type (WT) and USP11 knockout (USP11 KO) cells transiently overexpressing ERα. Cells were transfected with ERα and reporters (ii), hormone-deprived for 24 hours and subsequently stimulated with E2 for 24 hours. Experiment was performed in biological triplicate, error bars represent SEM. ** p<0.01, student's t-test, unpaired. (B & C) qRT-PCR detecting the induction of ERα-target genes, PgR and TFF1, following E2 stimulation. HEK293T WT and KO cells were transfected with either ERα or pcDNA empty vector (EV), hormone deprived for 48 hours and stimulated with E2 for 4 hours. Error bars represent SEM.*

3.4.5 The role of USP11 DUB activity on ERα transcriptional activity

Initial data suggests that USP11 plays a role in ERα transcriptional activity, but how this effect is exerted is unknown. It was hypothesised, that as a DUB, the enzymatic activity of USP11 is required for its regulation of ERα. In order to investigate this, a USP11 DUB-null mutant was obtained from Prof. David Cortez, Vanderbilt University Medical School in Nashville, TN. The Cortez group were the first to describe the role of USP11 in HR double-strand DNA repair (Wiltshire et al., 2010) and generated this mutant plasmid for their studies. The USP11 sequence contains a cysteine to serine substitution within the enzymatic active site, suppressing its deubiquitinating activity.

Before proceeding with the experiment, both wild type and mutant vectors were sent for Sanger sequencing to confirm the presence of the amino acid substitution (Figure 3.13).

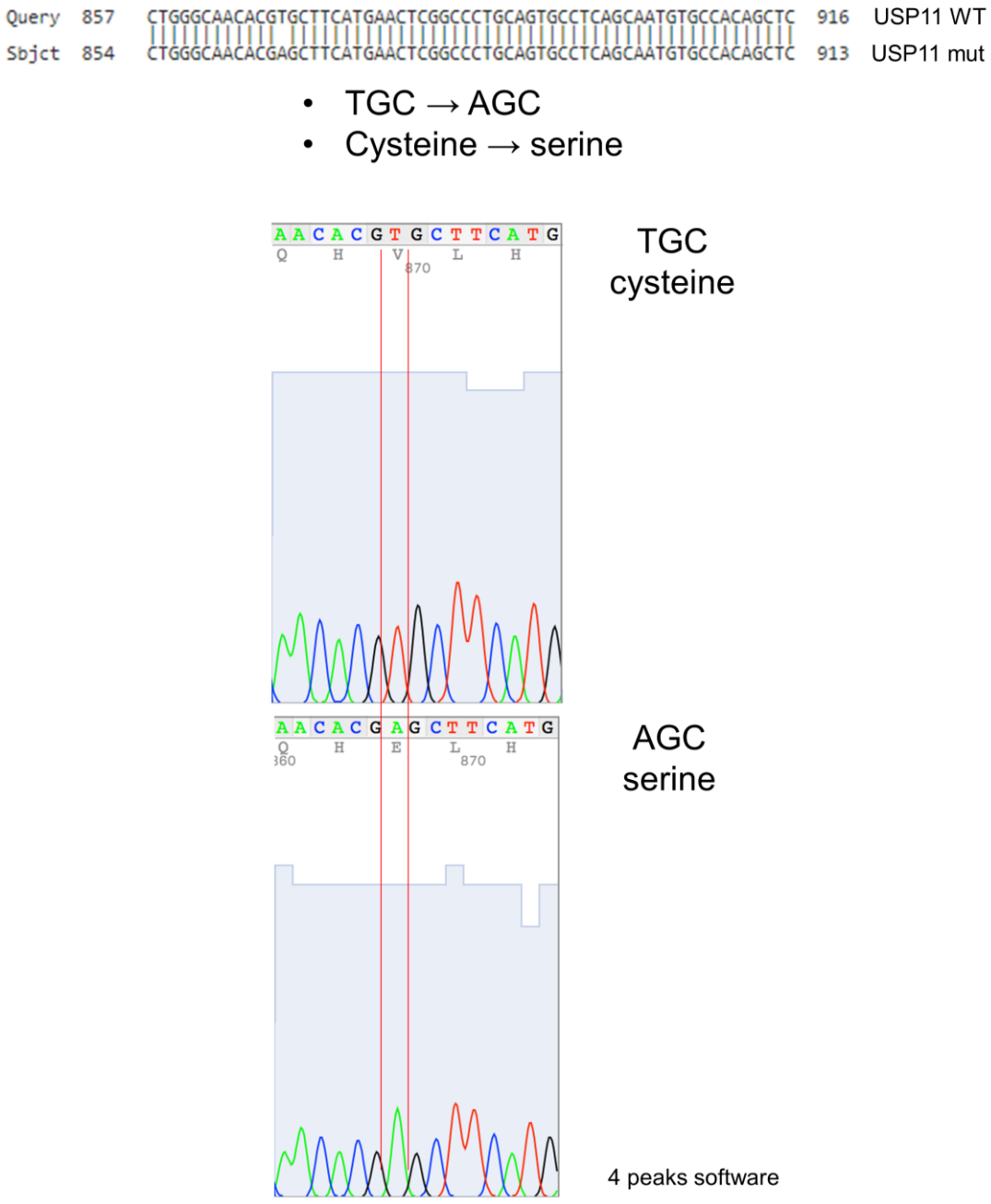

Figure 3.13: Sanger sequencing confirms the presence of a cysteine to serine substitution within the USP11 catalytic domain. *Plasmids were sent to Source Biosciences for Sanger sequencing. Raw reads were analysed using BLAST and 4Peaks software.*

In order to investigate if the enzymatic activity of USP11 was required for its role in ERα transcriptional activity, the DUB-null mutant vector was co-transfected in to the HEK293T USP11 knockout cells, along with ERα and luciferase reporters. The HEK293T cell line was chosen for this experiment, as USP11 is absent from these cells. Some residual protein expression remains in the ZR-75-1 USP11 knockdown cell lines that may have affected the final results of this experiment and was therefore not used. Matching protein samples were analysed by Western blotting and confirmed the overexpression of USP11 in both wild type and mutant transfected cells (Figure 3.14, A).

A dual luciferase assay was performed in the presence and absence of E2. With E2 stimulation, knockout of USP11 significantly decreased ERα transcriptional activity. Overexpression of wild type USP11 (USP11_wt) in HEK293T wild type cells significantly enhanced ERα transcriptional activity. Overexpression of wild type USP11 (USP11_wt) in HEK293T USP11 knockout cells restored a phenotype similar to that of wild type cells. Transfection of mutant USP11 (USP11_mut) in to HEK293T USP11 knockout cells had no significant effect on ERα transcriptional activity (Figure 3.14, B). A similar phenotype was observed in the absence of E2 (Figure 3.14, C).

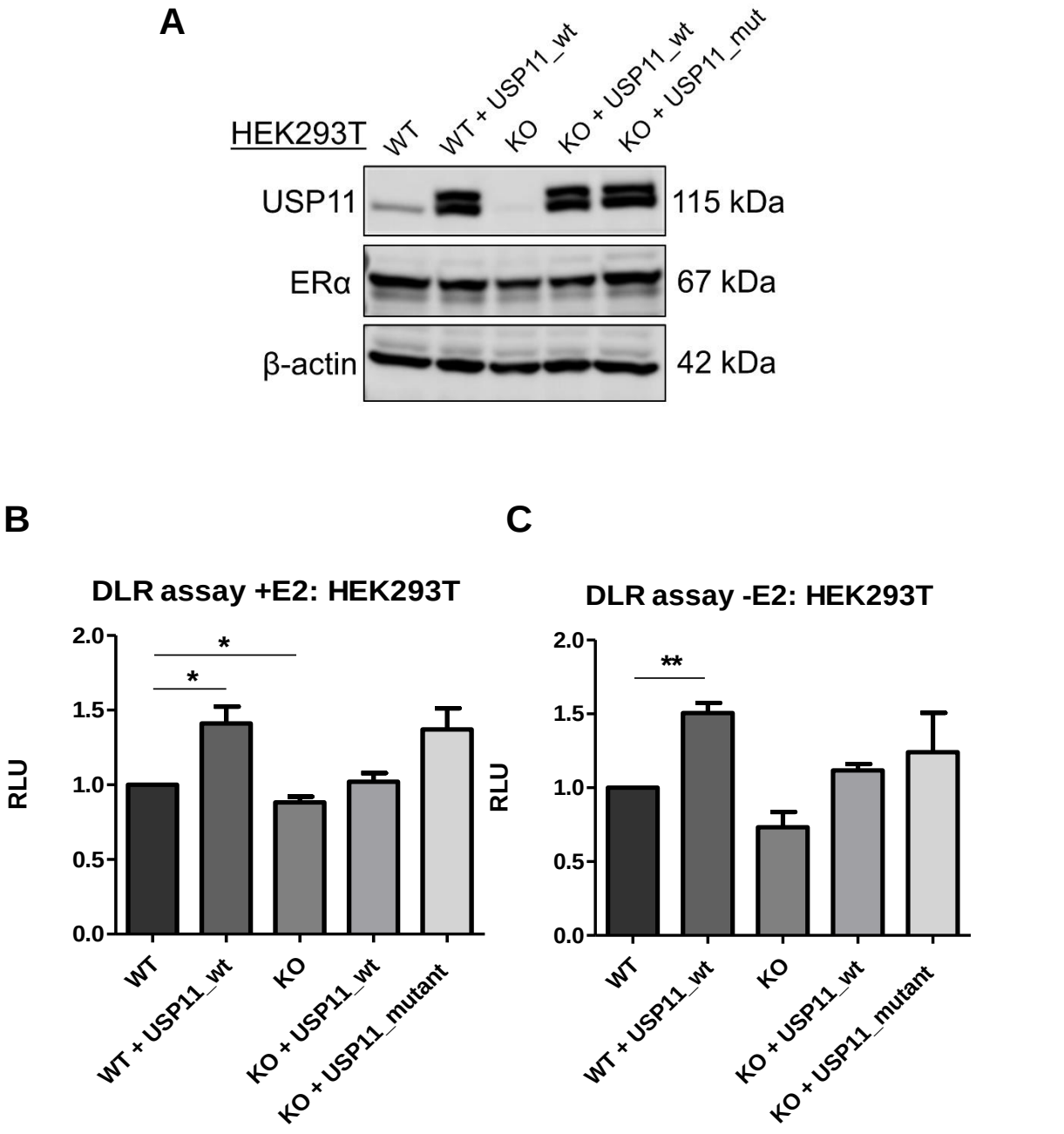

Figure 3.14: Introduction of a DUB-null USP11 vector in to USP11 knockout cells has no significant effect on ERα transcriptional activity, as determined by DLR assay. *(A) DLR assay in HEK293T in wild-type (WT) and USP11 knockout (KO) cells. Cells were transfected with ERα and reporters and either a wild-type (USP11_wt) or mutant (USP11_mut) USP11 vector. Cells were hormone-deprived for 24 hours and subsequently stimulated with E2 for 24 hours. Experiment was performed in biological triplicate, error bars represent SEM. * p<0.05; ** p<0.01, student's t-test, unpaired.*

3.4.5 The prognostic relevance of USP11 in ERα+ breast cancer

In order to investigate the clinical relevance of USP11 in ERα+ breast cancer, an *in silico* analysis was performed using a publicly available BC dataset, gene expression-based outcome (GOBO) (http://co.bmc.lu.se/gobo/gsa.pl) (Ringner et al., 2011). It is common practice to first perform *in silico* analysis of publicly available datasets before immunohistochemical staining of valuable patient tissue microarrays. GOBO, Developed at Lund University, Sweden, is a user-friendly online tool used for assessing the prognostic relevance of single or multiple genes. The database consists of 1881 cases pooled from 11 public microarray datasets analysed using Affymetrix U133A. The clinical characteristics of each dataset are outlined in Table 3.3.

Table 3.3: Clinical characteristics of each BC dataset combined for the GOBO tool. (Ringner et al., 2011)

GEO ID	Number of samples	ER: −/+[A]	LN: −/+[B]	DMFS (0/1)[C]	Average DMFS (years)	OS (0/1)[D]	Average OS (years)	RFS[E] (0/1)	Average RFS (years)	Grade: 1/2/3	Median age (years)	Average size (mm)	Reference
GSE7390	198	64/134	198/0	136/62	10.8±5.4	142/56	11.4±3.7	107/91	9.3±5.6	30/83/83	46±7	22±8	[50]
GSE3494	251	34/213	158/84	NA	NA	132/119	7.9±4.1	155/96	5.5±3.4	67/128/54	64±14	22±13	[51]
GSE1456	159	29/130	94/60	NA	NA	119/40	6.4±1.9	119/40	6.2±2.3	28/58/61	56±14	22±12	[52]
GSE2034	286	77/209	286/0	179/107	6.5±3.5	NA	NA	NA	NA	6/42/139*	53±12*	10±6*	[6]
GSE2603	99	42/57	34/65	55/27	5.2±2.3	NA	NA	NA	NA	NA	56±14	36±17	[53]
GSE6532	327	45/262	221/85	225/68	6.3±3.7	NA	NA	195/111	6.3±3.7	65/145/60	60.5±12	23±12	[27]
GSE4922	40	NA	NA	NA	NA	NA	NA	NA	NA	0/40/0	NA	NA	[36]
GSE12093	136	0/136	136/0	116/20	7.7±3.2	NA	NA	NA	NA	NA	NA	NA	[28]
GSE5327	58	58/0	NA	47/11	6.8±3.1	NA	NA	NA	NA	NA	NA	NA	[54]
GSE11121	197	NA	197/0	153/44	7.8±4.2	NA	NA	NA	NA	29/135/33	NA	21±10	[55]
Chin	130	46/84	59/71	102/27	5.7±4	84/45	6.4±3.7	NA	NA	14/46/65	51±15	27±14	[41]
Total	1881	395/1225	1383/365	1013/366	7.2±4.2	477/260	8.2±4.4	576/338	6.7±4.2	239/677/495	55±13	20±12	

[A]ER: Estrogen receptor.
[B]LN: Lymph node.
[C]DMFS: Distant metastasis-free survival.
[D]OS: Overall survival.
[E]RFS: Relapse-free survival.
*Collected from publications.
doi:10.1371/journal.pone.0017911.t001

To investigate the prognostic relevance of USP11 within these combined datasets, GOBO was used to define the expression of USP11 within each tumour. Analysis of Log_2fold expression in each cohort indicates differential USP11 across all patients (Figure 3.15, A). For survival analysis, two groups were selected; those with high expression of USP11 (red) and those with low expression (grey). Full censoring was applied and OS was selected as the end point. Interestingly, high expression of USP11 was significantly associated with poor OS in ERα+ patients (p= 0.032), and not ERα- patients (p= 0.51). Moreover, the association between high USP11 expression and poor survival in luminal B patients was trending towards significance (p= 0.052), a more aggressive ERα+ tumour type than luminal A, where no significant association between USP11 expression and survival was made (p= 0.11) (Figure 3.15). Multivariate analysis indicated that high USP11 expression was associated with tumour size, grade, and patients over 50 years of age. Again, this association was made in ERα+ patients only (Figure 3.16).

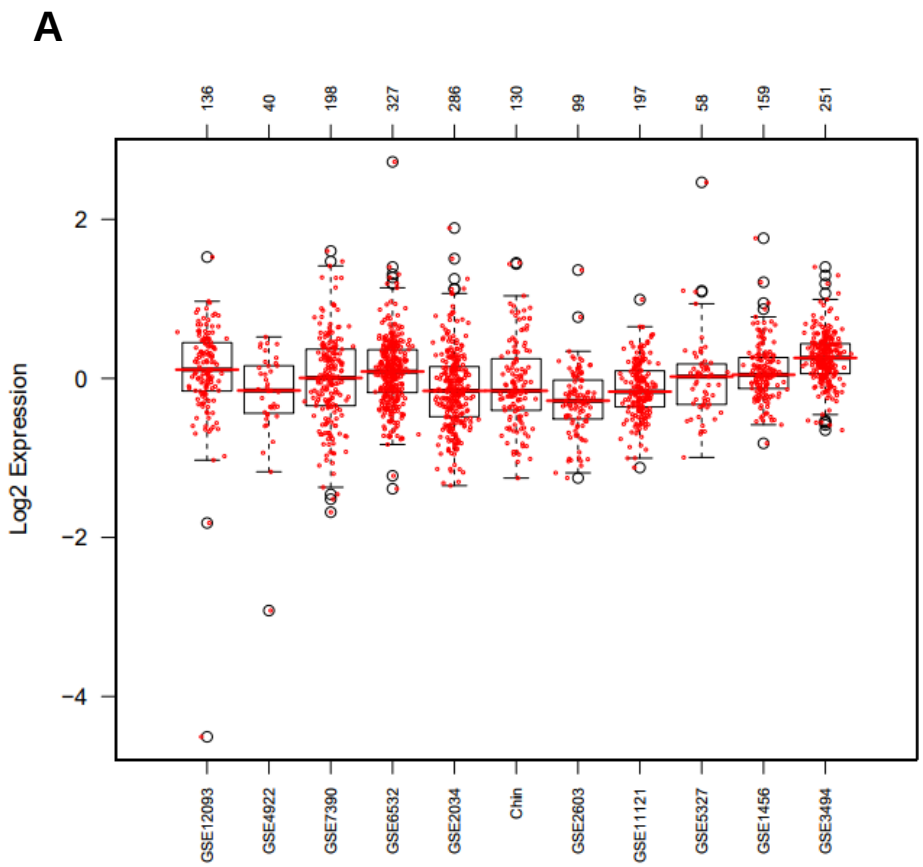

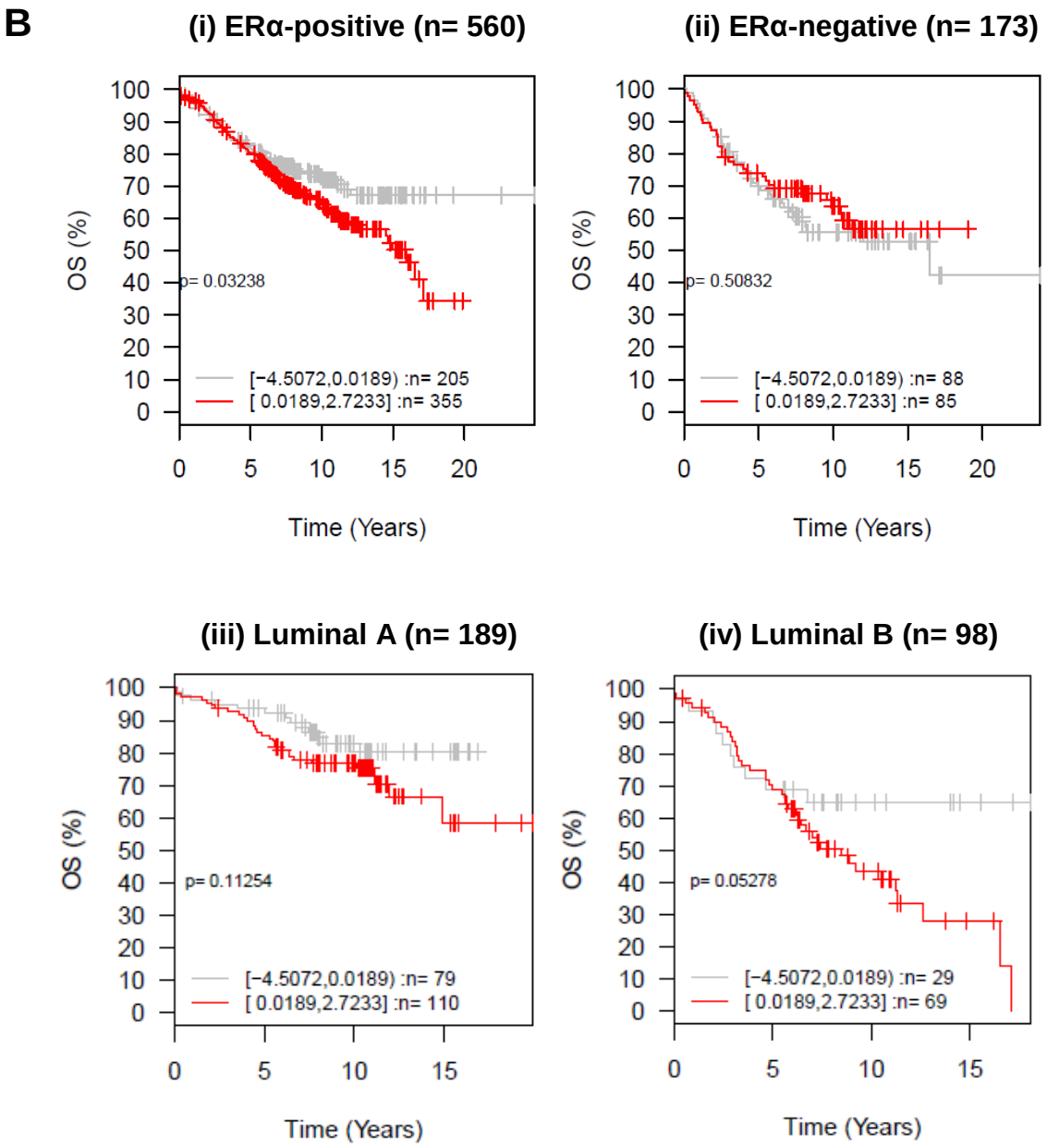

Figure 3.15: High expression of USP11 is significantly associated with poor OS in ERα+ patients. *(A) Scatter plot demonstrating differential USP11 expression within each dataset available on GOBO. (B) Kaplan- Meier analysis of USP11 expression in (i) ERα+, (ii) ERα-, (iii) luminal A and (iv) luminal B datasets. Two groups were analysed (grey= low; red= high) with full patient follow-up (indicated on y-axis).*

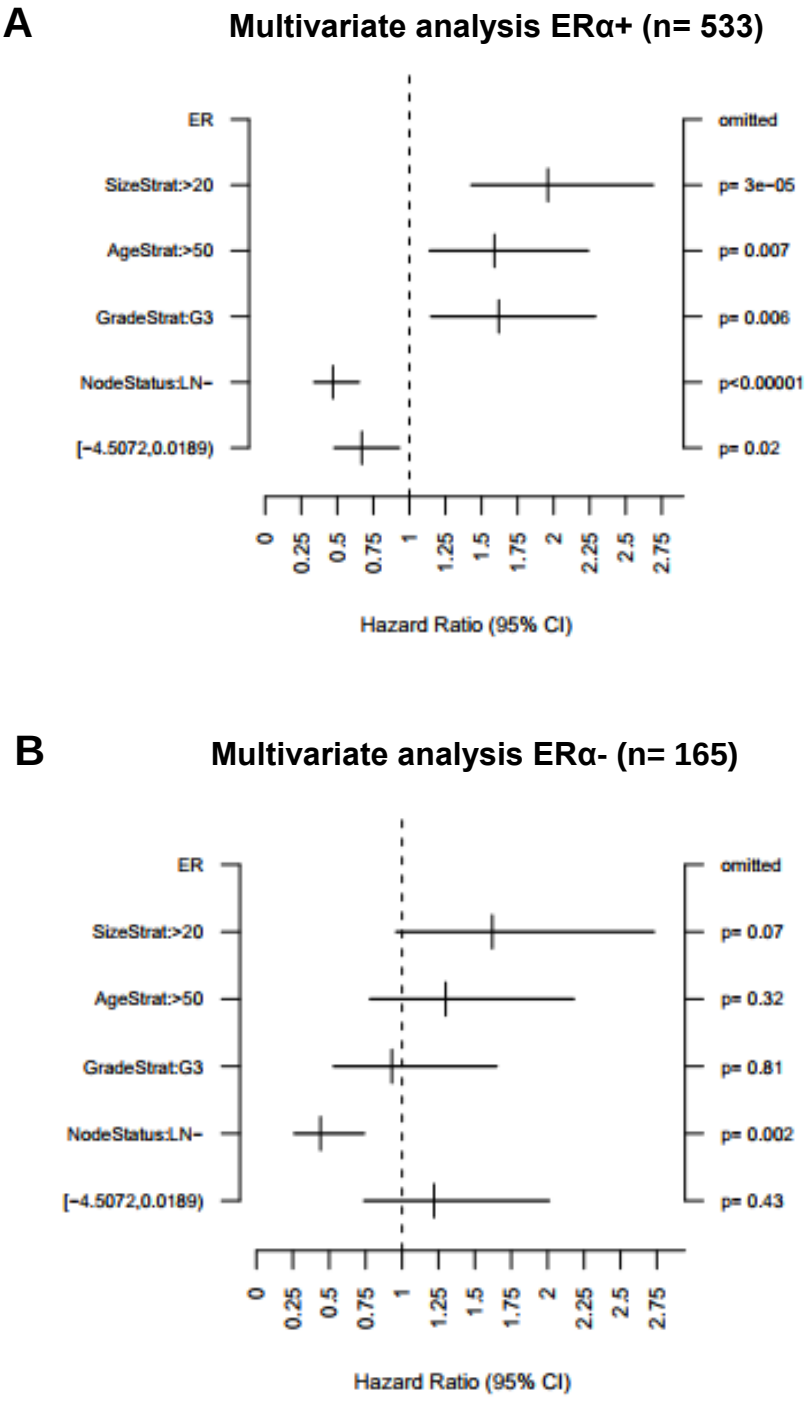

Figure 3.16: High expression of USP11 is significantly associated with tumour size, grade and patients over 50 years of ages in ERα-positive patients only, as determined using GOBO (Ringner et al., 2011).

Based on the above *in silico* observation, immunohistochemical staining of a 144-patient TMA was carried out. The TMA, described previously in the literature (Brennan et al., 2008, DeNardo et al., 2011), consists of core samples from 144 cases of invasive breast cancer, diagnosed in Lund University hospital between 2001 and 2002. The TMA consisted of 103 ERα+ patients for final analysis. Prior to staining, antibody optimisation was carried out by Dr. Aisling O'Connor, UCD (data not shown). TMA staining was carried out by Dr. Aisling O'Connor and full analysis was carried out by the author with assistance from Dr. Laoighse Mulrane, UCD.

Manual scoring was carried out by two individual researchers to ensure accuracy, using the images in Figure 3.17 as guidance. USP11 expression was grouped in to low (score 0 and 1) and high (score 2 and 3) expression and outcome based on each group was determined using SPSS statistics. Kaplan-Meier analysis revealed a significant association between high USP11 expression and poor OS (p= 0.003) and BCSS (p= 0.041). A similar trend was observed between high USP11 expression and RFS (p= 0.066) (Figure 3.18). Cross tabulation (cross-tab) univariate analysis was also carried out in order to correlate USP11 staining with clinicopathological features such as tumour grade, histopathological subtype and nuclear receptor status (Table 3.4). High USP11 staining was significantly associated with positive lymph node status (p= 0.009). No other clinicopathological features were significantly associated with high or low USP11 staining. Multivariate analysis was not carried out due to low patient number.

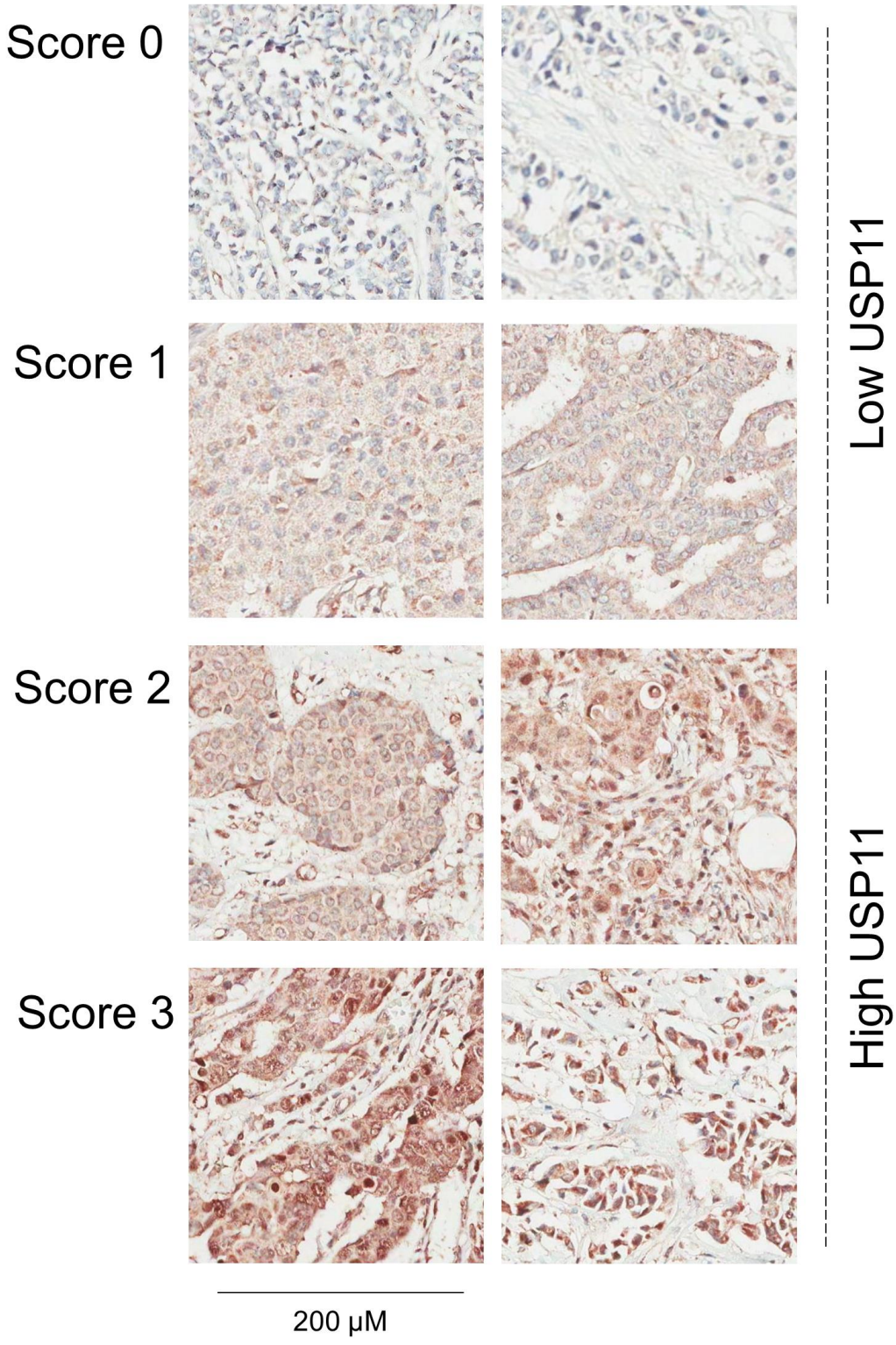

Figure 3.17: Representative images of each USP11 expression score from TMA cores were used as a guideline for full scoring of the 144-patient TMA. *Two images assigned to each score were selected as a guideline.*

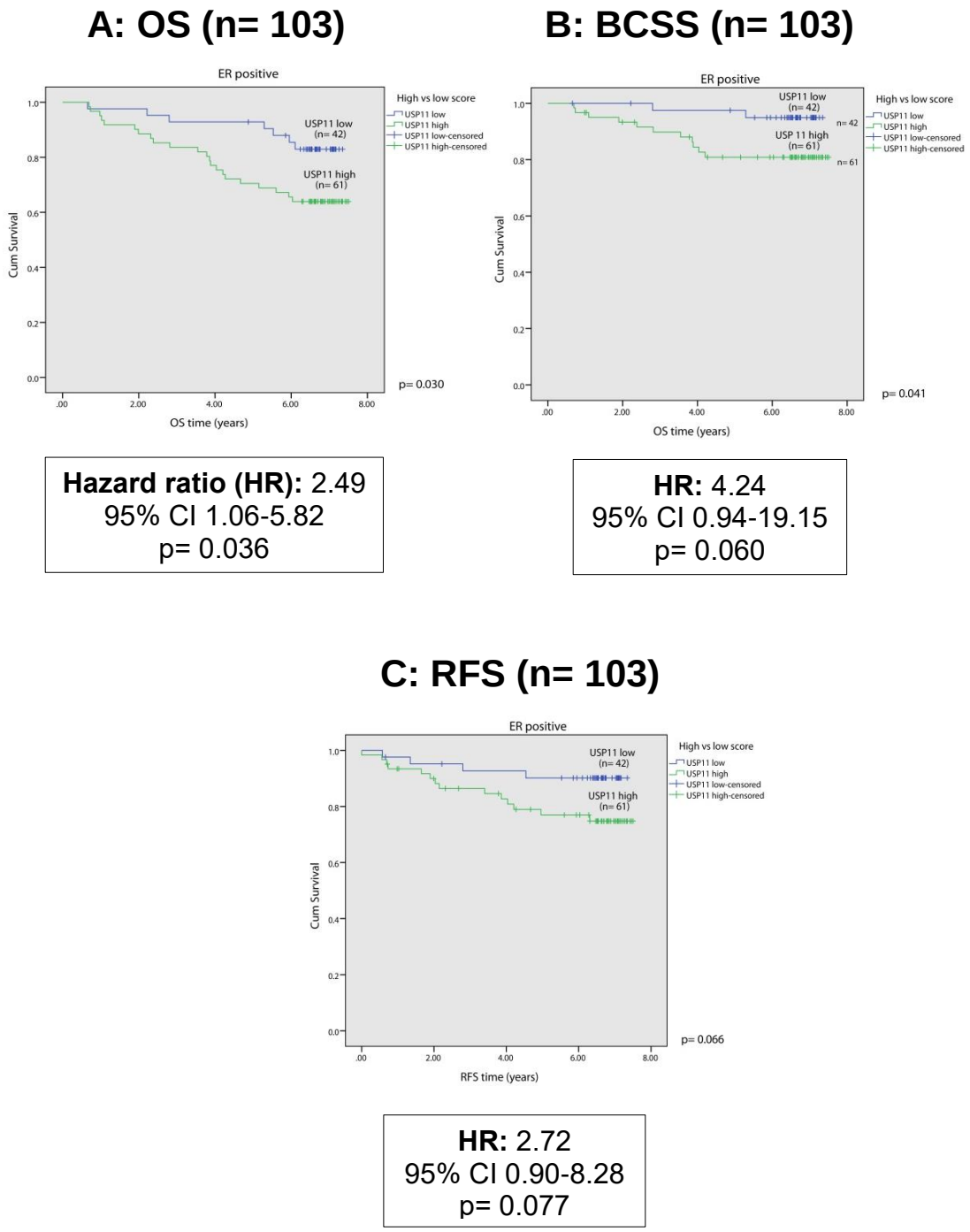

Figure 3.18: High expression of USP11 is significantly associated with poor OS and BCSS in a TMA cohort of 103 patients. *Kaplan Meier survival analysis relating USP11 expression to (A) overall, (B) breast cancer-specific and (C) recurrence-free survival in ERα+ patients. A dichotomised score of high USP11 expression (green line) and low USP11 expression (blue line) was applied.*

Table 3.4: Cross-tab univariate analysis correlates USP11 staining with clinicopathological features.

	LOW USP11 n(%)	*HIGH USP11 n(%)*	*p-value*
Age (years)			
<=50	9 (17.3%)	8 (11.8%)	0.388
>50	43 (82.7%)	60 (88.2%)	
Tumour size (mm)			
<=20	23 (44.2%)	32 (47.1%)	0.758
>20	29 (55.8%)	36 (52.9)	
Grade			
I	4 (7.7%)	12 (17.6%)	0.261
II	23 (44.2%)	29 (42.6%)	
III	25 (48.1%)	27 (39.7%)	
Histological Subtype			
Mixed	1 (1.9%)	1 (1.5%)	0.941
Ductal	38 (73.1%)	51 (75.0%)	
Lobular	10 (19.2%)	14 (20.6%)	
Tubular	1 (1.9%)	1 (1.5%)	
Medullary	2 (3.8%)	1 (1.5%)	
Nodal Status			
Negative	32 (72.7%)	31 (47.7%)	**0.009**
Positive	12 (27.3%)	34 (52.3%)	
HER2 IHC			
0-2+	51 (98.1%)	60 (89.6%)	0.065
3+	1 (1.9%)	7 (10.4%)	
ER Status			
ER-	10 (19.2%)	7 (10.3%)	0.164
ER+	42 (80.8%)	61 (89.7%)	
PR Status			
PR-	18 (34.6%)	23 (33.8%)	0.928
PR+	34 (65.4%)	45 (66.2%)	
Ki67			
0-10%	1 (2.1%)	3 (5.0%)	0.693
11-25%	20 (41.7%)	26 (43.3%)	
>25%	27 (56.2%)	31 (51.7%)	

3.5 Discussion

Using unbiased functional genomic screening, it was demonstrated for the first time that suppression of the deubiquitinase USP11 decreased ERα transcriptional activity in BC cells. As the principal driver of oncogenesis, elucidation of novel mechanisms that regulate ERα can extend our understanding of BC progression and offer attractive new therapeutic opportunities. This chapter provides significant evidence for the role of USP11 in the ERα regulatory network and for the use of USP11 as prognostic marker in the clinic.

In order to validate the results obtained from the screen and investigate the role of USP11 in ERα function, stable knockdown BC cell lines and a HEK293T knockout cell line were used. In BC cells, USP11 knockdown resulted in suppression of ERα transcriptional activity, as determined by ERE-luciferase activity and expression of ERα-target genes. While both knockdown cell lines reduced ERα activity, only one cell line reached significance (shUSP11_1). It was hypothesised that the robust knockdown of USP11 in shUSP11_4 (>90%) lead to the initiation of compensatory mechanisms, a common issue with stable knockdown cell lines in growth over time (Clift et al., 2017). To overcome this, USP11 was knocked down in ZR-75-1 using two independent siRNAs. ERα-target gene expression was analysed after 3 days, with both siRNAs yielding reduced mRNA expression of ERα target genes.

It was hypothesised that as a novel ERα interactor, USP11 may be regulated by a positive feedback loop from the receptor. To test this, USP11 expression was examined in response to E2. After 24 hours E2 treatment, USP11 was upregulated at the protein and mRNA level. These results were not significant, however, ERα activity is quite variable due to rapid receptor cycling and the influence of other mechanisms and pathways on receptor activity (Romano et al., 2010). Western blot analysis of cellular fractions revealed that this upregulation was occurring in the cell nucleus, suggesting an E2-driven ERα-USP11 interaction. To support this further, ICC revealed an upregulation of USP11 in the nucleus following E2 treatment, as well as the increased formation of USP11 foci. Further investigation is required to reveal if these foci are co-localising with ERα or dependant on ERα activation. It has been previously shown that USP11 foci form in the nuclei of HeLa cells following γ-irradiation and the formation of DNA double strand breaks (DSB) (Yu et al., 2016). E2 induces DSB and genomic instability and is a potential mechanism by which

prolonged exposure to estrogen confers BC risk and progression (Caldon, 2014). Furthermore, E2-induced DSB, recruit Rad51 to the point of damage, suggesting these breaks are repaired by HR (Williamson and Lees-Miller, 2011). As USP11 is a key player in HR it is hypothesised that the enzyme has a significant role in DBS repair induced by E2, however further investigation is warranted.

It is unknown if E2 induces USP11 transport from the cytoplasm in to the nucleus. Using cNLS Mapper, a monopartile and bipartile NLS was predicted within the USP11 amino acid sequence. To test if E2 effects USP11 shuttling, it would be possible to inactivate these NLS by site-directed mutagenesis and test the effect of E2 on USP11 localisation.

USP11 knockdown slowed the growth of ZR-75-1 cells, however surprising results were obtained from a colony formation assay. shUSP11_1 cells decreased colony forming ability, while shUSP11_4 cells appeared to increase the number and size of colonies when compared to NTC cells. This may also be a result of compensatory mechanisms being initiated, as discussed above. No significant changes to the cell cycle were observed. Interestingly, there appears to be some cell arrest in the G1 phase in knockdown cell lines, highlighting an interesting point for further investigation. The effect of USP11 silencing alone has not been studied previously, however USP11 knockdown in combination with a DNA-damaging agent significantly slowed the growth of cells (Wiltshire et al., 2010, Orthwein et al., 2015).

USP11 knockdown had no effect on the response to anti-endocrine agents tamoxifen and fulvestrant. It was hypothesised that as ZR-75-1 cells are highly sensitive to these drugs, ERα activity was sufficiently depleted and USP11 knockdown had no further effect. How cells respond to USP11 knockdown combined with aromatase inhibition would be a more valuable route to explore, as these therapeutic agents deplete estradiol levels as oppose to acting directly on the receptor.

USP11 knockout in HEK293T cells resulted in suppression of ERα transcriptional activity, as illustrated by reduced ERE-luciferase activity and repressed ERα-target gene induction in knockout cells. Due to long term stable knockout of USP11, initial concerns over the induction of compensatory mechanisms were raised, however as these cells are ERα-negative and ectopic expression was introduced over a short period this was not an issue. This was not the first study to use HEK293T cells to investigate the role of a DUB in ERα function. Stanisic and

colleagues elucidated the role of OTUB1 in ERα transcriptional activity using HEK293T cells ectopically expressing ERα. This study performed mass spectrometry on these cells and also identified USP11 as an ERα interactor (Stanisic et al., 2009), as mentioned.

The USP11 DUB-null mutant vector had no significant effect on ERα transcriptional activity when transfected in to knockout cells. As a DUB, it was hypothesised that the enzymatic activity of USP11 was required for regulation of ERα, however these results would suggest otherwise. While overexpression of wild-type USP11 rescued the phenotype observed with knockdown, mutant USP11 yielded a similar, yet non-significant result. It must be considered that the formation of a specific USP11 protein complex may positively enhance ERα transcriptional activity and the phenotype observed is not dependent on direct DUB activity. However, some concerns were raised over the validity of these results which warrant further investigation. First, USP11 overexpression, in both the wild-type and mutant cells, was far higher than that of endogenous USP11 expression in HEK293T cells, this may have caused off-target effects. In order to overcome this, the experiment must be repeated using reduced USP11 overexpression vector (<100 ng). Second, the transfection of both luciferase reporters, ERα and USP11 at the same time may have interfered with DNA vector uptake, raising further concerns. As a result, further investigation in to how the enzymatic activity affects ERα function is necessitated.

The clinical relevance of a protein is of utmost importance when investigating the validity of a potential novel drug target in cancer. Proteins associated with a poor prognosis may represent attractive therapeutic targets in the oncology clinic. Before proceeding with this investigation, the role of USP11 in ERα+ BC patients was investigated. *In silico* analysis indicated that USP11 is associated with poor OS in ERα+ patients, with no significant association made in ERα- patients. Furthermore, high expression was associated with poor OS in luminal B patients, a more aggressive ERα+ subtype. GOBO was chosen for this preliminary investigation due to the availability of multivariate analysis. Interestingly, high expression of USP11 was significantly associated with tumour size, grade, and patients over 50 years old in ERα+ cases only. Based on this *in silico* search, staining of a BC TMA was carried out. High expression of USP11 was associated with poor overall and breast cancer-specific survival in ERα+ patients. This study represents the first association

between USP11 and poor prognosis in BC in the clinic and will be further validated by staining of a 498-patient TMA.

This chapter presents preliminary evidence for the role of USP11 in regulation ERα transcriptional activity, although the precise mechanism of action remains unknown. Despite the current knowledge of USP11 activity there has been no research into the association of the enzyme with ERα; therefore this study represents the first investigation of this topic. Elucidating the role of USP11, both physiologically in the cell, as well as its precise mechanism of controlling ERα transcriptional activity, will give a better insight into the function of this DUB in breast cancer. Specifically, the prognostic implications of USP11 in specific subtypes of breast cancer, as well as the role for USP11 as a potential drug target, warrants further investigation.

Chapter 4: The role of USP11 in an estrogen-independent, anti-endocrine resistant setting

4.1 Introduction

Estrogen-independent ERα activity is associated with several aspects of BC pathogenesis, including metastasis and anti-endocrine resistance. ERα can be activated by other cellular components including epidermal growth factor (EGF), insulin-like growth factor 1 (IGF-1) and cyclic adenosine monophosphate (cAMP), which recruit alternative cofactors to the receptor (Carascossa et al., 2010). Post-translational modifications of ERα, phosphorylation in particular, play a large role in estrogen-independent ERα function (Maggi, 2011). Furthermore, ERα mutations, which recurrently occur in the ligand-binding domain (LBD) of the receptor, stimulate ERα activation in the absence of estradiol (Jeselsohn et al., 2018). Understanding how ERα functions in the absence of estradiol is crucial to our understanding of BC progression and may offer attractive therapeutic opportunities in anti-endocrine resistant cancer. To date, information on the role of DUBs in ERα activity is limited, with no reference to a role for these enzymes in estrogen-independent function.

4.1.1 The LCC cell line series

In order to study the role of USP11 in an estrogen-independent setting, the LCC cell line series was used, an isogenic model obtained from the lab of Prof. Robert Clarke, Georgetown University, Washington DC. These cells were derived from the commonly used estrogen-dependent BC cell line MCF-7, isolated in the 1970s from the pleural effusion of a patient with adenocarcinoma of the breast (Soule et al., 1973). MCF-7 cells are ERα+, PgR+ and HER2-, and are tumourigenic in mice in the presence of estrogen. In order to derive a hormone-independent model from these cells, MCF-7s were implanted into the mammary fat pad of an ovariectomised athymic NCr *nu\nu* nude mouse. After 6 months, when the tumour established in the absence of endogenous estradiol, the tumour was isolated and cultured *ex vivo.* This process was repeated in full to yield the estrogen-independent cell line LCC1 (Brunner et al., 1993). Although these cells grow in culture in the absence of estradiol supplementation, they continue to express ERα, respond to estradiol stimulation and are sensitive to anti-endocrine agents such as tamoxifen and fulvestrant. LCC1 cells represent a viable model for the study of hormone autonomy.

In order to yield an anti-endocrine resistant model for the study of therapy resistance *in vitro*, LCC1 cells were exposed to increasing concentrations of fulvestrant. Selection was initiated with 10 pM, with drug concentration increasing

after three successful passages at each dose. The highest dose the cells were exposed to was 1 μM. This yielded the LCC9 cell line which are cross-resistant to fulvestrant and tamoxifen, although never exposed to the latter (Figure 4.1, 4.2) (Brunner et al., 1997). LCC1 and LCC9 cells therefore represent the ideal model to study both hormone-independence and anti-endocrine resistance.

4.2 Aims of this chapter

- Study the role of USP11 in an estrogen independent setting
- Investigate the effect of USP11 silencing on ERα activity and compare this phenotype between LCC1 and LCC9 cells
- Use state-of-the-art RNA sequencing (RNA-seq) technology to reveal transcriptomic changes in USP11 knockdown LCC1 and LCC9 cells
- Investigate the functional significance of these changes and compare both cells lines

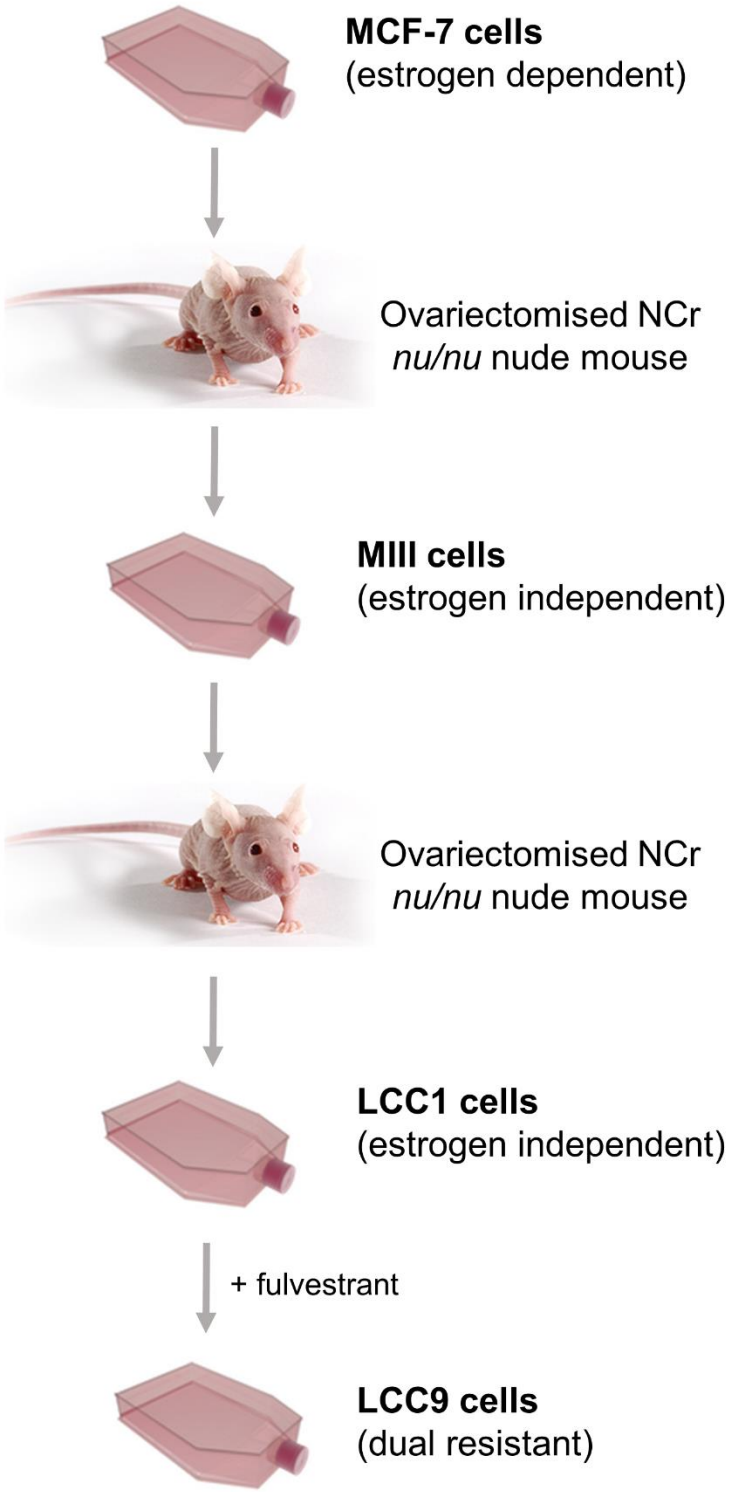

Figure 4.1: Development of the LCC cell line series in the laboratory of Prof. Robert Clarke, Georgetown University, Washington DC. *Adapted from Brunner et al. 1997, 'MCF7/LCC9: an anti-estrogen-resistant MCF-7 variant in which acquired resistance to the steroidal anti-estrogen ICI 182,780 confers an early cross-resistance to the nonsteroidal anti-estrogen tamoxifen' (Brunner et al., 1997).*

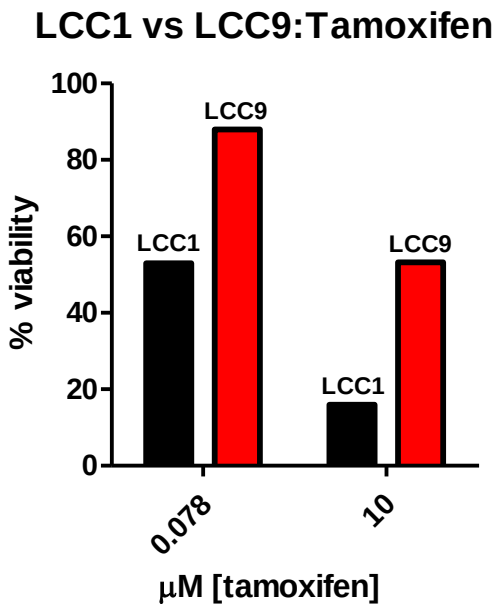

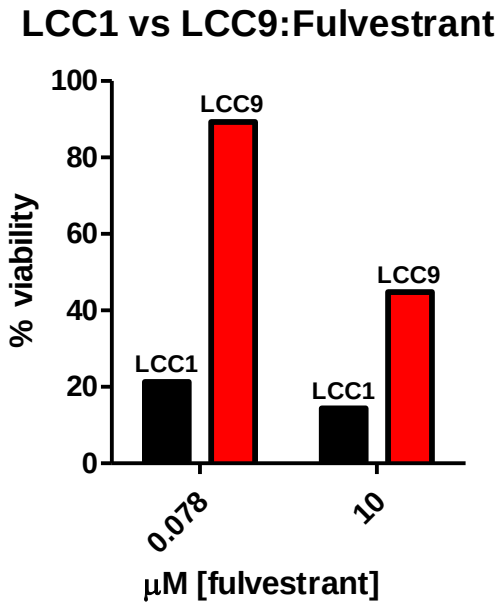

Figure 4.2: LCC9 cells are resistant to both tamoxifen and fulvestrant. *Cells were incubated for 8 days under varying drug concentrations, drugs were replenished on day 4. Viability was assessed using the MTT viability assay. The above graphs demonstrate cell viability at the lowest and highest drug concentrations used.*

4.3 Results

4.3.1 USP11 expression in the LCC isogenic cell line model

The completion of chapter 3 presented new avenues for the study of USP11 in ERα+ breast cancer. At this point, the role of USP11 in ERα transcriptional activity in other cell line models was unknown. First, protein expression was examined across all ERα+ cell lines available in the laboratory. To do so, protein was harvested from all cells and USP11 expression was examined by Western blotting. Differential USP11 expression was observed across all cell lines. ERα positivity was confirmed in all cell lines. (Figure 4.3, A).

Interestingly, USP11 expression correlated with ERα expression. This was confirmed by the generation of a correlation plot (Pearson r: 0.76; p-value: 0.027). Notably, USP11 appeared to be upregulated in ILC cell lines, MDA-MB-134VI and SUM44, when compared to ERα+ IDC cells. Of particular interest to this study, USP11 expression was higher in LCC1 and LCC9 cells when compared to their parental MCF-7 cells. Based on these findings, a further understanding as to how USP11 functions in these cell lines was sought after.

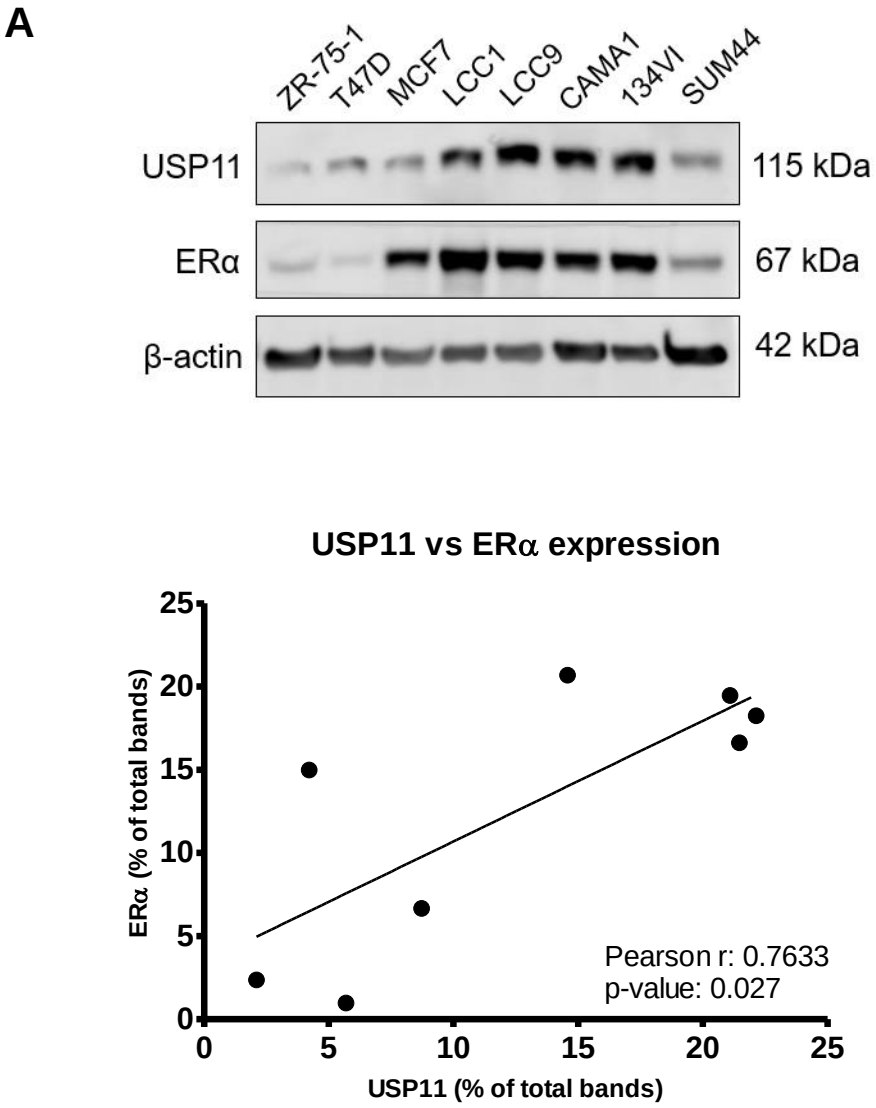

Figure 4.3: USP11 is differentially expressed across a panel of ERα+ breast cancer cell lines. *(A) Protein from 8 cell lines was harvested and analysed by Western blotting. ERα expression was also examined. β-actin was used as a loading control. (B) Correlation plot based on densitometric analysis of USP11 and ERα Western blot. Results are expressed as a percentage of the total area of all bands.*

Before proceeding with the investigation in to the role of USP11 in these cells, expression was validated at the protein and mRNA level in biological triplicate. USP11 was significantly upregulated in both LCC1 and LCC9 cells compared to MCF-7 cells (Figure 4.4, A & B). ERα expression was also examined and was found to be significantly upregulated in LCC1 cells and significantly downregulated in LCC9 cells when compared to MCF-7 cells (Figure 4.4, C).

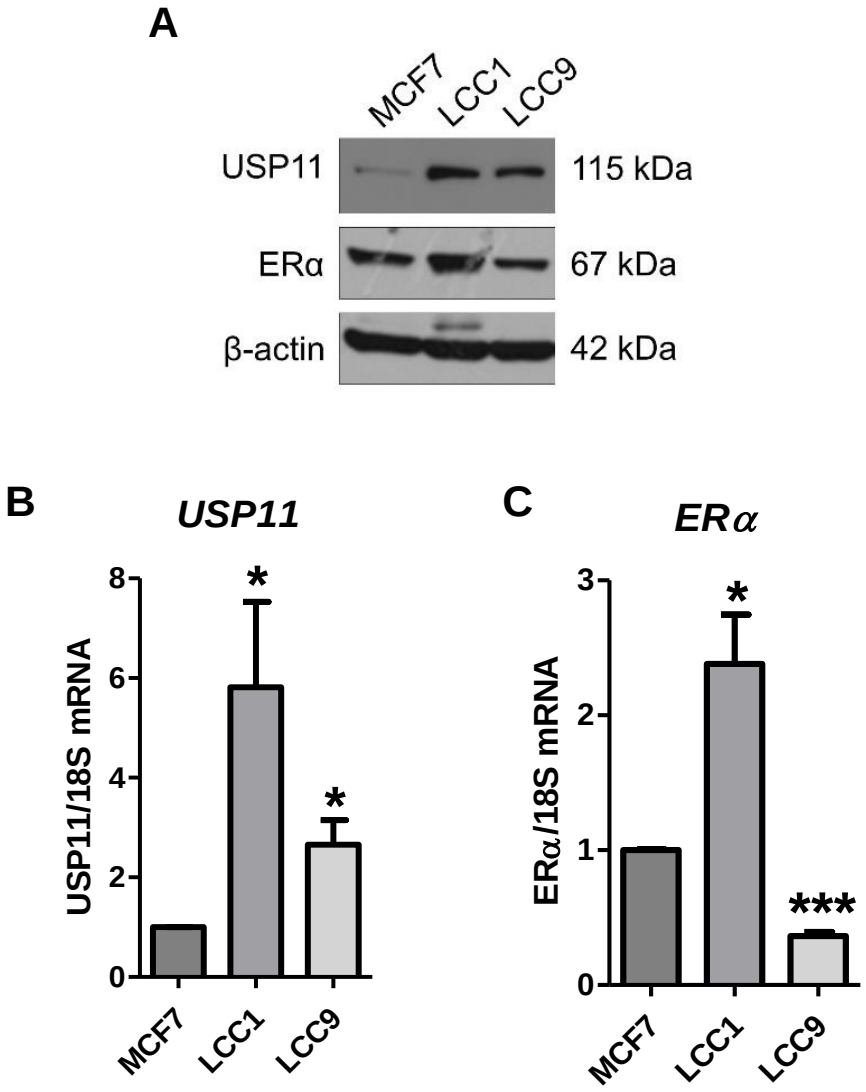

Figure 4.4: Triplicate validation confirmed the upregulation of USP11 in LCC1 and LCC9 cells at both the protein and mRNA level. *(A) Western blot displaying protein expression of USP11 and ERα in the LCC isogenic cell line model. Image is representative of three biological replicates; β-actin was used as a loading control. (B & C) qRT-PCR examining the mRNA expression of (B) USP11 and (C) ERα in the LCC isogenic cell line model. mRNA expression was normalized to 18S expression and LCC1 and LCC9 values were normalised to MCF-7 values. n= 3, error bars represent SEM. * p< 0.05; *** p< 0.001, student's t-test, unpaired.*

To study the function of USP11 in LCC1 and LCC9 cells, two individual siRNAs targeted to USP11 were used to silence expression of the enzyme. As shown in figure 4.5, knockdown of USP11 was confirmed at both the protein and mRNA level prior to assessing the impact on phenotype.

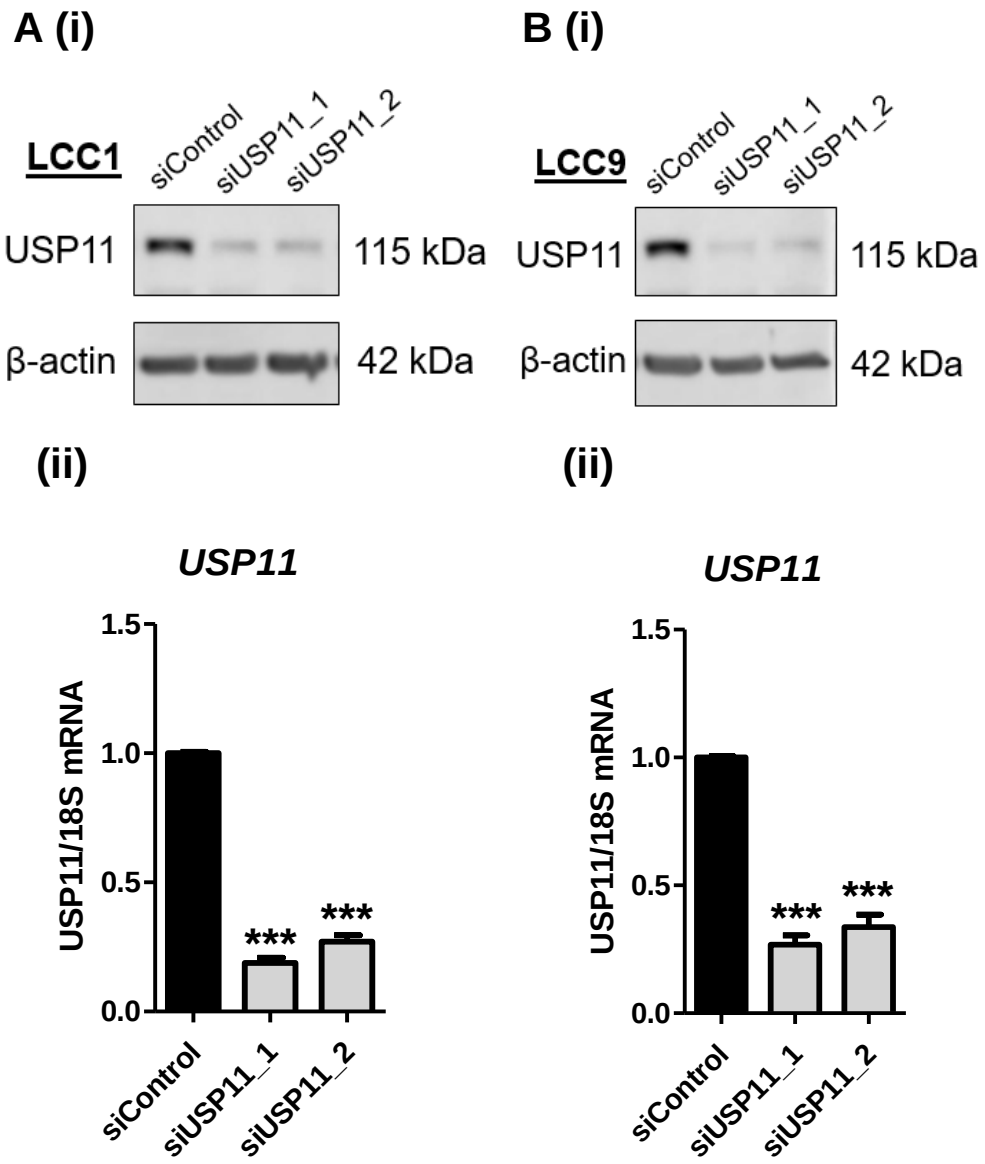

Figure 4.5: USP11 silencing using RNAi was used as a model for studying protein function in LCC1 and LCC9 cells. *Confirmation of USP11 knockdown in (A) LCC1 and (B) LCC9 cell lines using two individual siRNAs. Both cell lines were transfected with 30 nM siRNA using lipofectamine 2000 and incubated for 72 hours before assessing knockdown. (i) Representative Western blot confirming USP11 knockdown in both cell lines; β-actin was used as a protein loading control. (ii) qRT-PCR confirming USP11 knockdown at the mRNA level; mRNA expression was normalized to 18S expression and knockdown values were normalised to siControl. n= 3, error bars represent SEM. *** p< 0.001, student's t-test, unpaired.*

4.3.2 USP11 and ERα function in LCC1 and LCC9 cells

As mentioned, LCC1 cells are viable in culture in the absence of E2, however, they remain sensitive to anti-endocrine therapies similar to the parental MCF-7 cell line, indicating they are still reliant on ERα for growth and survival. LCC9 cells however, are anti-endocrine resistant, suggesting they have evolved to depend on other growth pathways independent of ERα signaling (Figure 4.2). As a result it was hypothesised that USP11 silencing in LCC1 cells would suppress ERα function, while silencing in LCC9 cells would have no effect on the function of the receptor.

In chapter 3, the role of USP11 in ligand-activated ERα was elucidated, with preliminary evidence suggesting that USP11 can positively regulate ERα in a ligand-independent manner. In order to investigate if USP11 affects ERα transcriptional activity in LCC1 and LCC9 cells, the mRNA expression of ERα-target genes was examined in both cell lines. qRT-PCR revealed a significant reduction in the expression of a panel of ERα-target genes in LCC1 USP11 knockdown cells (Figure 4.6). Silencing of USP11 in LCC9 cells had no significant effect on the mRNA expression of ERα-target genes (Figure 4.7), as hypothesised. Interestingly, Cyclin D1 levels remain unchanged in LCC1 USP11 knockdown cells, while mRNA levels were significantly reduced in LCC9 USP11 knockdowns.

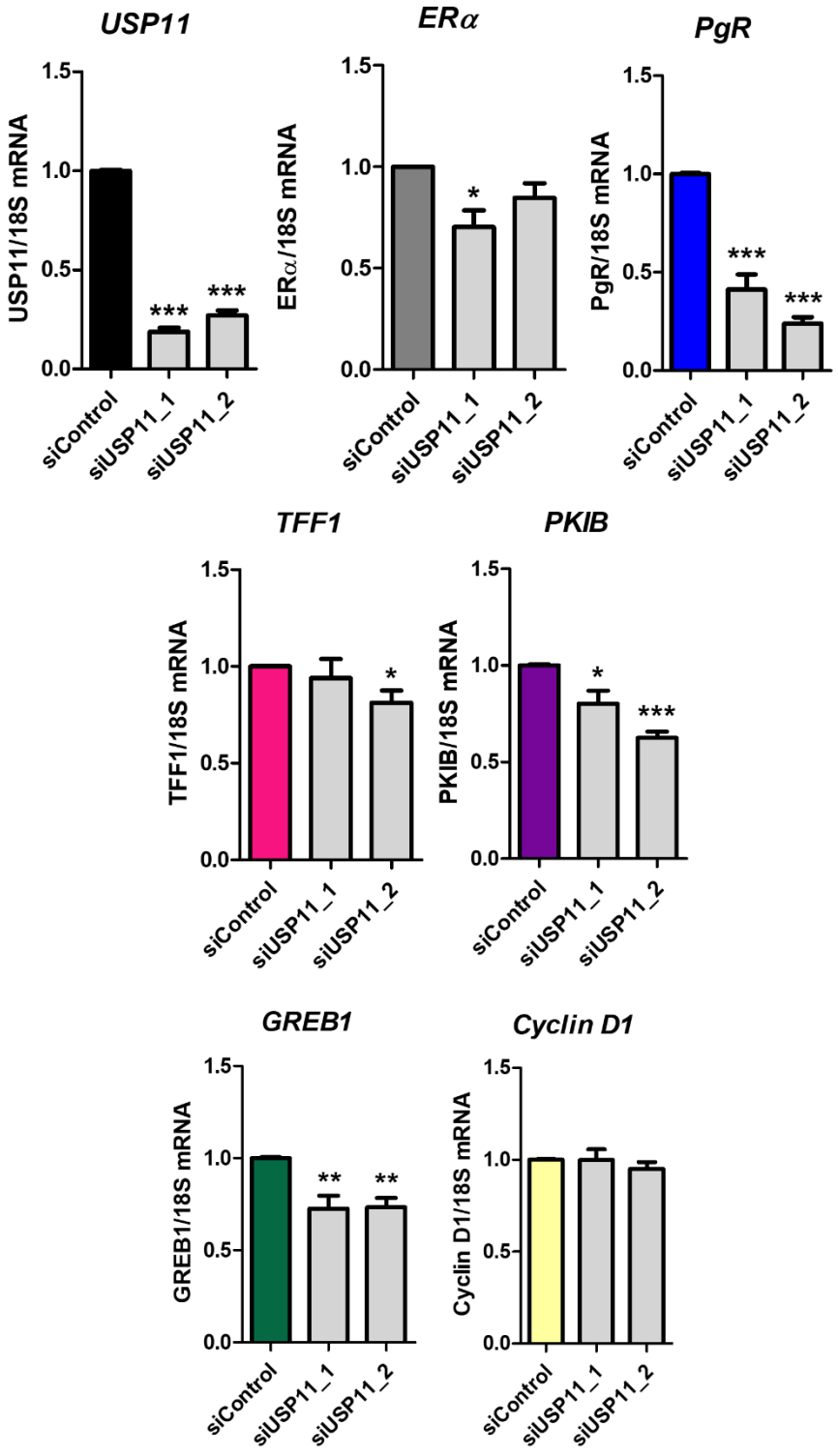

Figure 4.6: USP11 knockdown significantly reduced the mRNA expression of a panel of ERα-target genes in LCC1 cells. *Cells were transfected with 30 nM siRNA using lipofectamine 2000 and incubated for 72 hours before examining the mRNA expression of ERα-target genes. mRNA expression was normalized to 18S expression and knockdown values were normalised to siControl. n= 3, error bars represent SEM. * p< 0.05; ** p<0.01; *** p< 0.001, student's t-test, unpaired.*

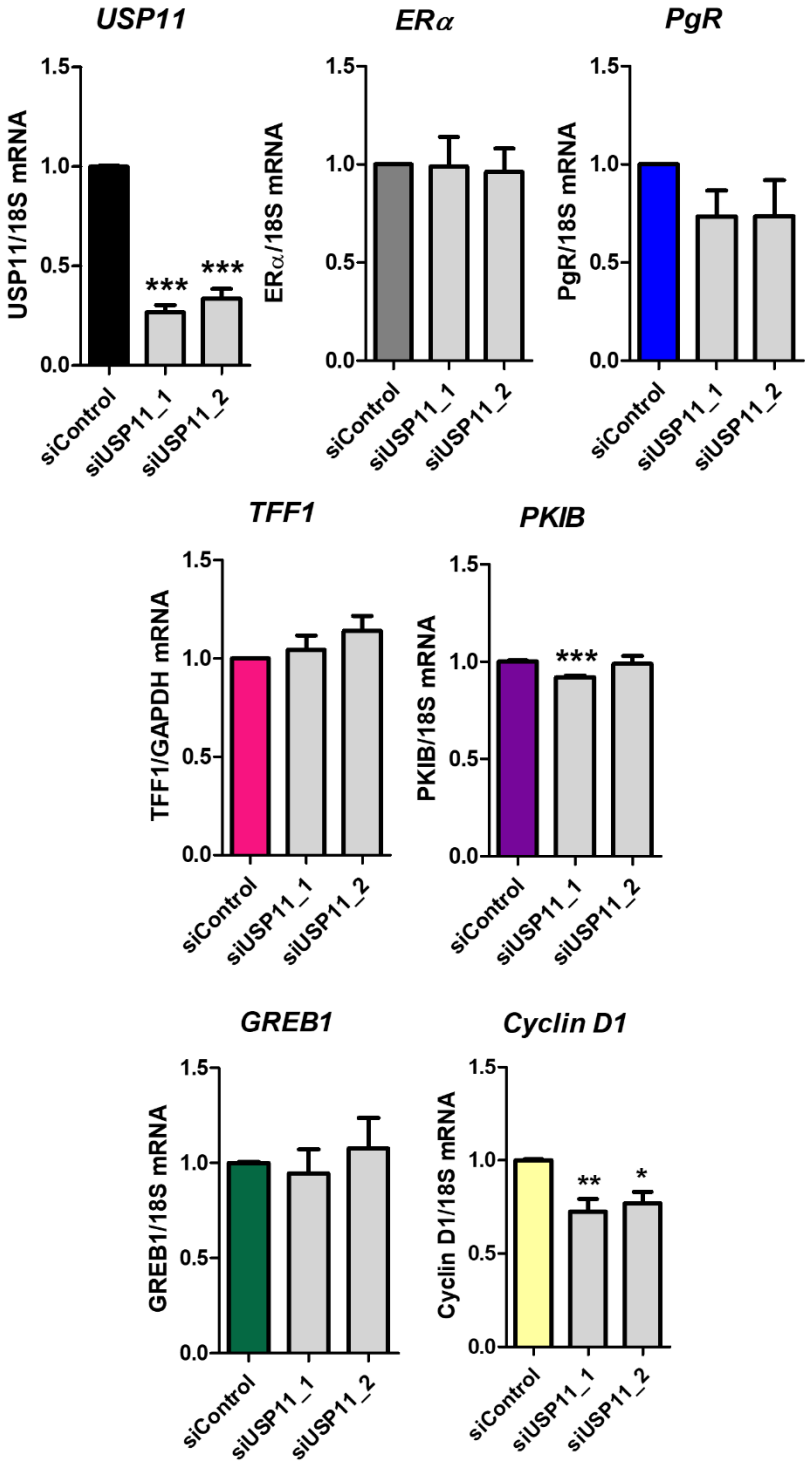

Figure 4.7: USP11 knockdown had no significant effect on the expression of ERα-target genes in LCC9 cells. *Cells were transfected with 30 nM siRNA using lipofectamine 2000 and incubated for 72 hours before examining the mRNA expression of ERα-target genes. mRNA expression was normalized to 18S expression and knockdown values were normalised to siControl. n= 3, error bars represent SEM. * p< 0.05; ** p<0.01; *** p< 0.001, student's t-test, unpaired.*

4.3.3 RNA-seq on LCC1 and LCC9 USP11 knockdown cells

To further elucidate the effects of USP11 knockdown and to identify both differences and similarities of USP11 function in both cell lines, RNA-seq was carried out on USP11 knockdown and control cells in collaboration with Dr. Sudipto Das, RCSI and Dr. Bruce Moran, UCD. RNA-seq is a well-established high-throughput sequencing approach that allows for assessment of global gene expression profiles in a given sample. In order to maintain consistency, the same RNA used to determine ERα-target gene expression above was used for RNA-seq. Prior to sequencing, RNA quality was tested on the Agilent Bioanalyzer System, which confirmed a high-quality yield for all samples (RIN > 8 across all samples). RNA-seq was carried out in biological triplicate with six samples per replicate (18 in total). Both cell lines included an siControl (CONTROL) and two individual siRNAs targeted to USP11 (SI7 and SI8). The first two replicates were run together on the same flow cell, while the third replicate was run on a second flow cell. For this reason, reads were corrected for batch effect. Following the completion of RNA-seq, data was kindly analysed by Dr. Bruce Moran, UCD.

First, principle component analysis (PCA) was carried out, a method which uses linear combinations of the original gene expression values to obtain a set of unrelated variables, or principal components. These values were plotted in order to visualise the variance between groups and replicates and to detect any outliers. PCA score plots were generated using principle components uncorrected (Figure 4.8, A & C) and corrected (Figure 4.8, B & D) for batch effect. Following correction, group clustering can be observed with some unexpected variance detected.

A: LCC1

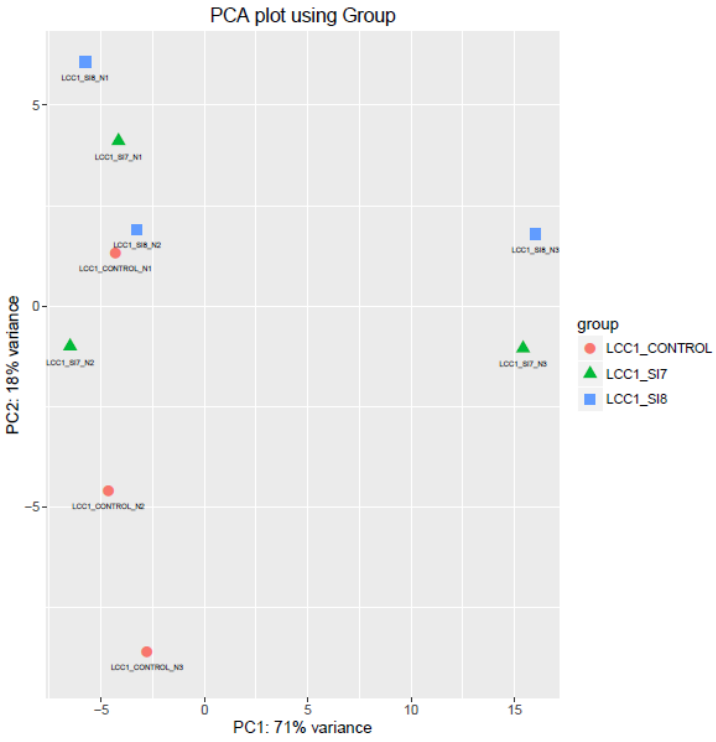

B: LCC1 (correct for batch effect)

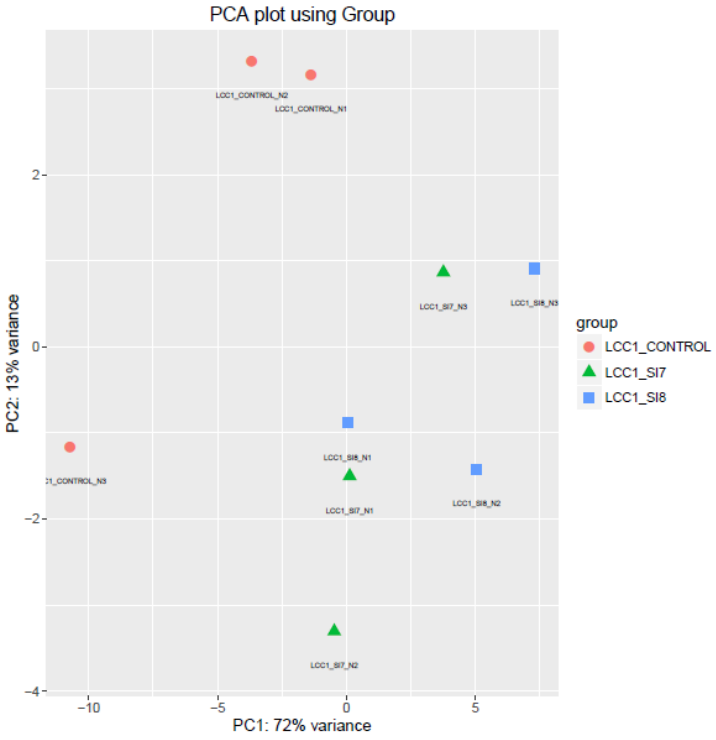

C: LCC9

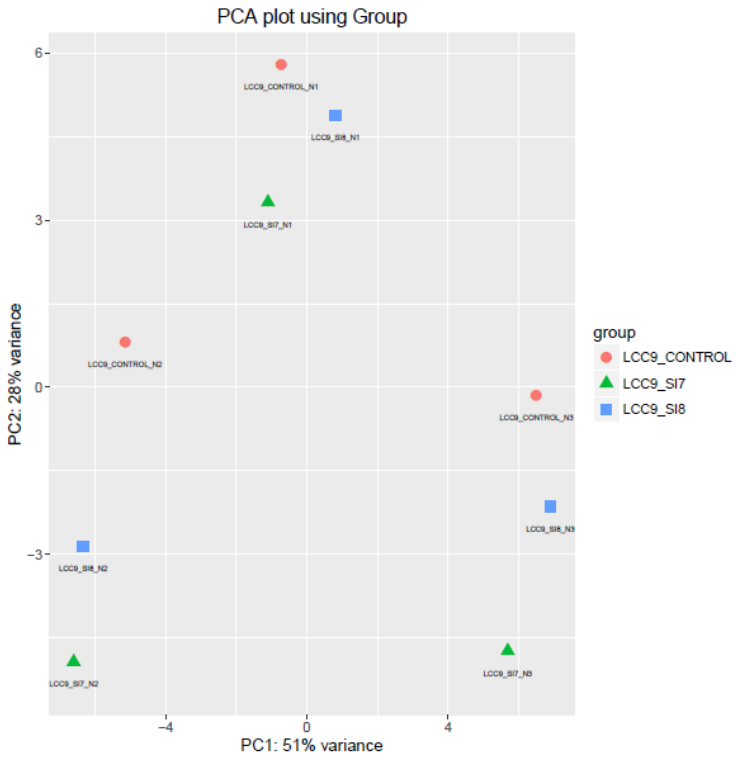

D: LCC9 (corrected for batch effect)

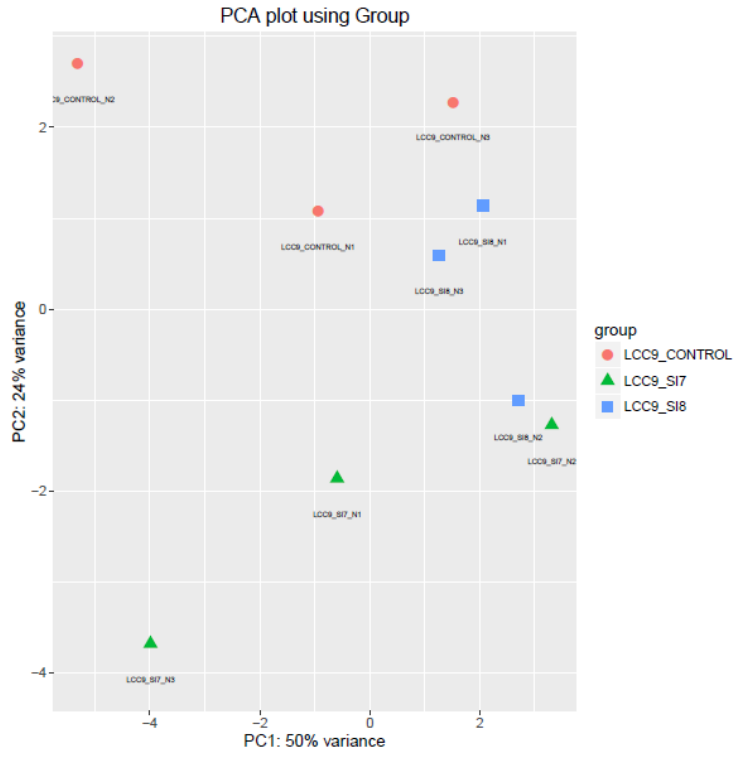

Figure 4.8: PCA plots demonstrating variance between each group and replicate. *PCA was carried out before (A & C) and after (B & D) reads were corrected for batch effect. 'SI7' refers to siUSP11_1, and 'SI8' refers to siUSP11_2. Plots were generated by Dr. Bruce Moran, UCD.*

Next, log_2fold values of siControl samples were compared to each individual siUSP11 sample in order to determine genes which were differentially expressed (DE) following USP11 silencing. Both siRNA lists were compared and the common DE genes were subjected to further analysis, in order to minimise any non-specific errors. In LCC1 cells, 278 DE genes were common to both siRNAs; in LCC9 cells only 29 DE genes were common to both siRNAs (Figure 4.9). DE genes in both cell lines were then compared. only 9 genes were common to both cell lines (Figure 4.9; Table 4.1). Two oligoadenylate synthase genes (OAS1, OAS2) and oligoadenylate synthase-like (OASL) gene appeared in the LCC1/LCC9 overlap, which encode enzymes involved in innate immune response to viral infection. A full list of significant DE genes can be found in Appendix 3.

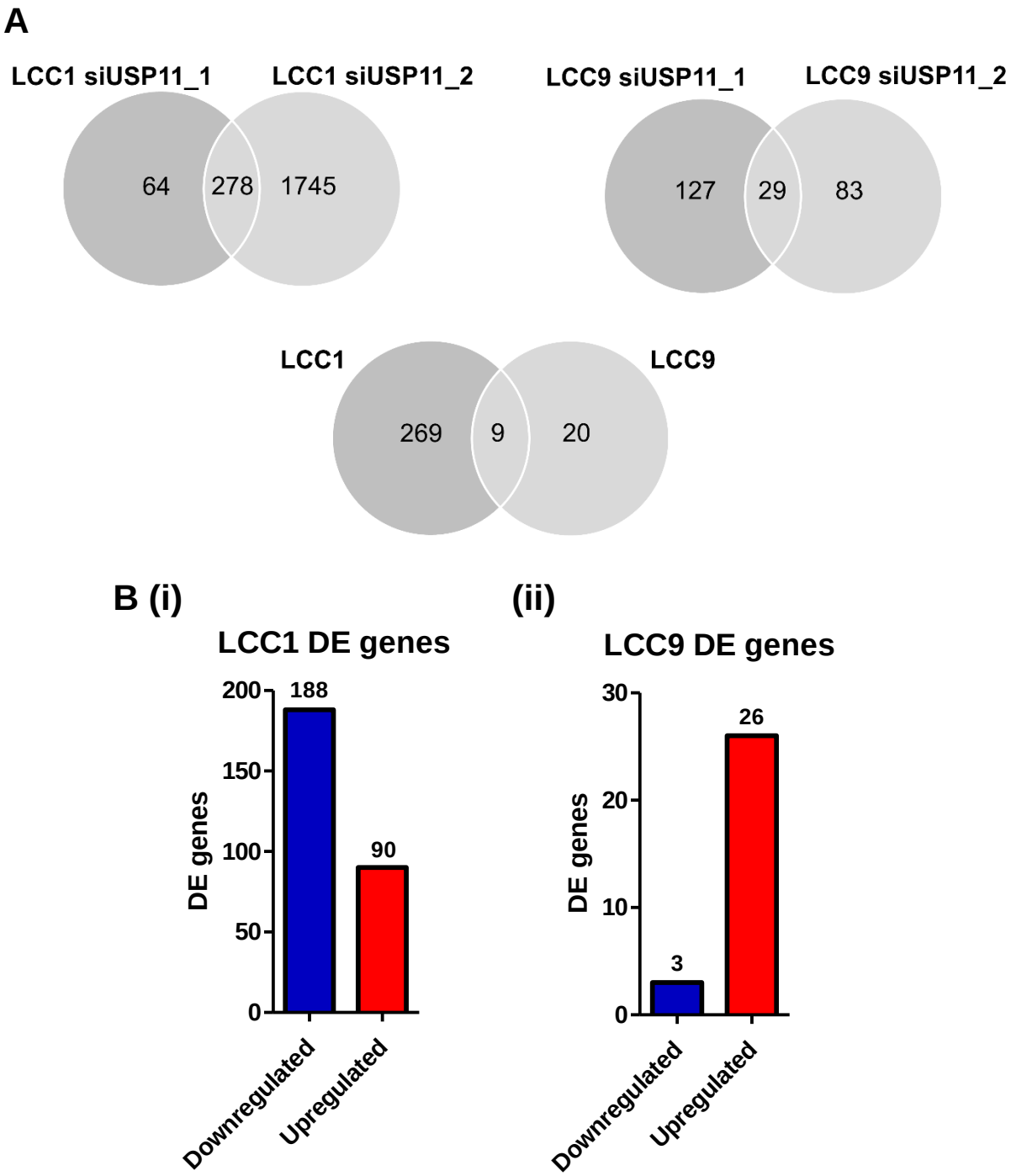

Figure 4.9: RNA-seq on LCC1 and LCC9 USP11 knockdown cells revealed a number of significantly DE genes. *(A) Venn diagrams illustrating the number of DE genes with USP11 knockdown, identified by RNA-seq. DE genes were first compared between each individual siRNA in both cell lines. Common DE genes between both siRNAs were then compared between both cell lines. (B) Bar graphs depicting the number of significantly down- (blue) and upregulated (red) genes in (i) LCC1 and (ii) LCC9 knockdown cells.*

Table 4.1: DE genes with USP11 knockdown common to both cell lines

Gene	Gene name	Function
USP11	Ubiquitin specific protease 11	Deubiquitinating enzyme
OAS1	Oligoadenylate synthase 1	Involved in innate immune response to viral infection
OAS2	Oligoadenylate synthase 2	Involved in innate immune response to viral infection
OASL	Oligoadenylate synthase-like	Involved in innate immune response to viral infection
HIST1H2BD	Histone Cluster 1 H2B Family Member D	Protein component of chromatin, involved in gene expression
CMPK2	Cytidine/Uridine Monophosphate Kinase 2	Nucleotide synthesis
IFIT3	Interferon Induced Protein With Tetratricopeptide Repeats 3	Immune cytokine signalling
RSAD2	Radical S-Adenosyl Methionine Domain Containing 2	Immune cytokine signalling, antiviral
TRIM22	Tripartite Motif Containing 22	E3 ligase

Before proceeding with further analysis RNA-seq was validated using qRT-PCR. A number of genes which are of interest to this study were selected for validation. *TOP2A* was downregulated with USP11 knockdown. A previous study identified Mitoxantrone, a chemotherapeutic in the oncology clinic, as a non-specific USP11 inhibitor (Burkhart et al., 2013). This publication along with this current study indicates that USP11 and TOP2A interact with each other in the cell, however the nature of this interaction is currently unknown. It is already widely accepted that USP11 plays a role in the BRCA DDR pathway (Orthwein et al., 2015), therefore *BRCA1* was chosen for RNA-seq validation. *DIAPH3* was previously identified as a candidate driver genes in BC (Johansson et al., 2013), while *CKAP2L* was identified as a poor prognostic marker of RFS in BC (Kim et al., 2014). Both *NCAPG* and *NCAPH*, members of the chromosome condensin complex, are both ERα target

genes, as identified by MCF-7 ChIP-seq (Deblois et al., 2009). *BLM* is also an ERα target gene (Iso et al., 2007) and is highly associated with BC risk due to its role in the DDR (Sassi et al., 2013). *TRIM22* upregulation was validated in both cell lines; this E3 ligase is a p53 target gene and with a tumour suppressing role in cancer, including breast (Sun et al., 2013).

qRT-PCR confirmed both down (blue) and upregulated (red) genes identified by RNA-seq (Figure 4.10, 4.11). RAD51B was downregulated in LCC9 knockdown cell lines, however qRT-PCR did not confirm this (Figure 4.11).

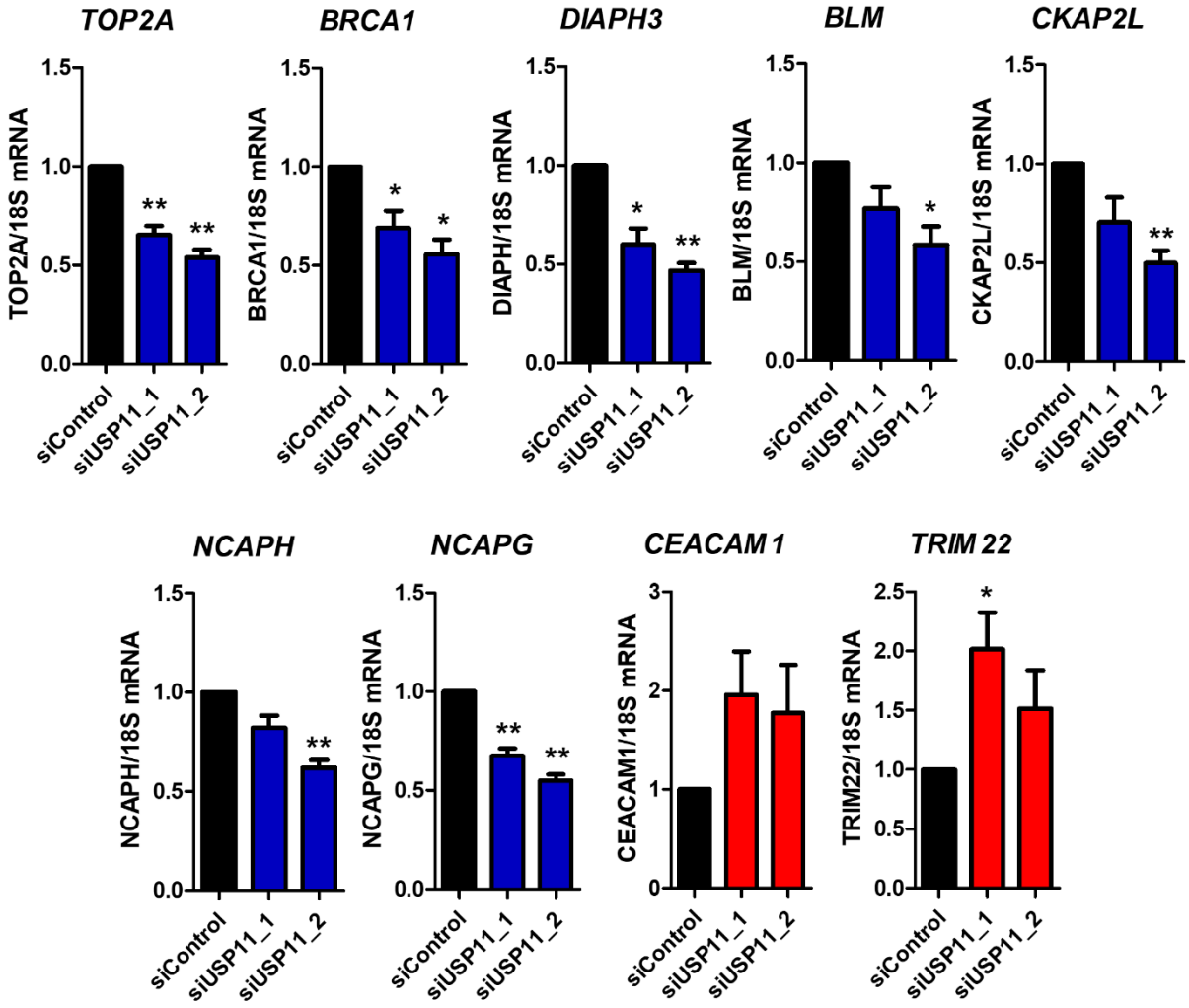

Figure 4.10: qRT-PCR was used to validate RNA-seq results and confirmed DE of a selected panel of genes in LCC1 USP11 knockdown cells. *Blue graphs represent genes downregulated with USP11 knockdown while red graphs represent genes upregulated with USP11 knockdown. mRNA expression was normalized to 18S expression and knockdown values were normalised to siControl. n= 3, error bars represent SEM. * p<0.05; ** p<0.01; student's t-test, unpaired.*

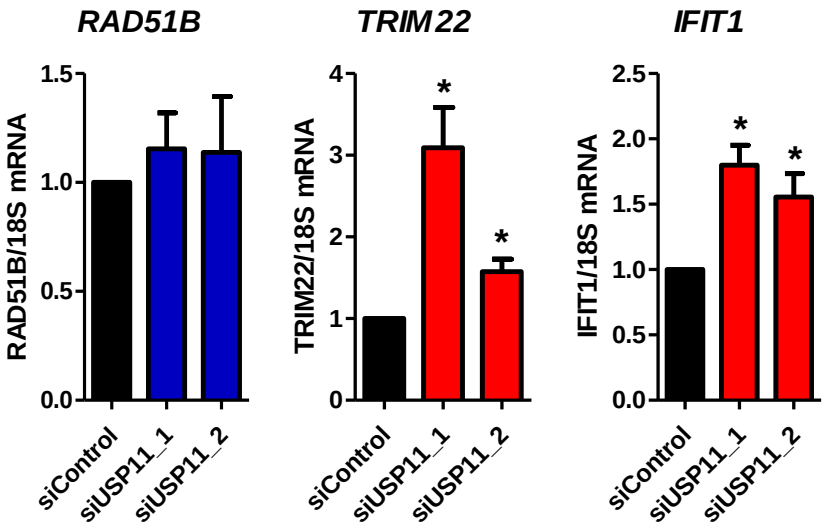

Figure 4.11: qRT-PCR was used to validate RNA-seq results and confirmed upregulation of TRIM22 and IFIT1 in LCC9 USP11 knockdown cells. *Blue graphs represent genes downregulated with USP11 knockdown while red graphs represent genes upregulated with USP11 knockdown. mRNA expression was normalized to 18S expression and knockdown values were normalised to siControl. n= 3, error bars represent SEM. * p< 0.05; student's t-test, unpaired.*

In order to further understand the effect of USP11 silencing on cellular function, DE genes were subject to gene ontology (GO) analysis, a method which allows for the query of genes based on their shared biology (Ashburner et al., 2000). GO analysis allowed for the identification of key cellular pathways which are altered with USP11 silencing in LCC1 and LCC9 cells.

Both DAVID v6.8 (Huang da et al., 2009) and GSEA 3.0 (Subramanian et al., 2005) bioinformatical tools were used for GO and analysis. Upregulated and downregulated genes in each cell line were grouped for GO pathway analysis. ENSEMBLE gene IDs were uploaded and all GO biological concepts were analysed, including biological processes (BP), molecular function (MF) and cellular component (CC). The Kyoto Encyclopaedia of Genes and Genomes (KEGG) pathway was selected and a functional annotation chart was generated from the input. Interestingly, knockdown of USP11 in LCC1 cells resulted in a significant decrease in cell cycle-associated genes. Key cellular processes such as mitosis, chromosome segregation and organelle fission were all significantly downregulated with USP11

knockdown (Figure 4.12, B; Table 4.2). This phenotype was unique to LCC1 cells and was of primary interest going forward with this study.

Knockdown of USP11 resulted in a significant increase in inflammatory-associated genes in both cell lines, identifying a common attribute of USP11 silencing in both LCC1 and LCC9 cells (Figure 4.12, C & D). In LCC1 knockdown cells, upregulated genes were associated with an innate immune response and interferon (INF) signaling, while the genes upregulated in LCC9 knockdown cells were primarily associated with a viral response pathways. Tables 4.2, 4.3 and 4.4 highlight the 20 most significant cellular pathways associated with each group, as defined using DAVID.

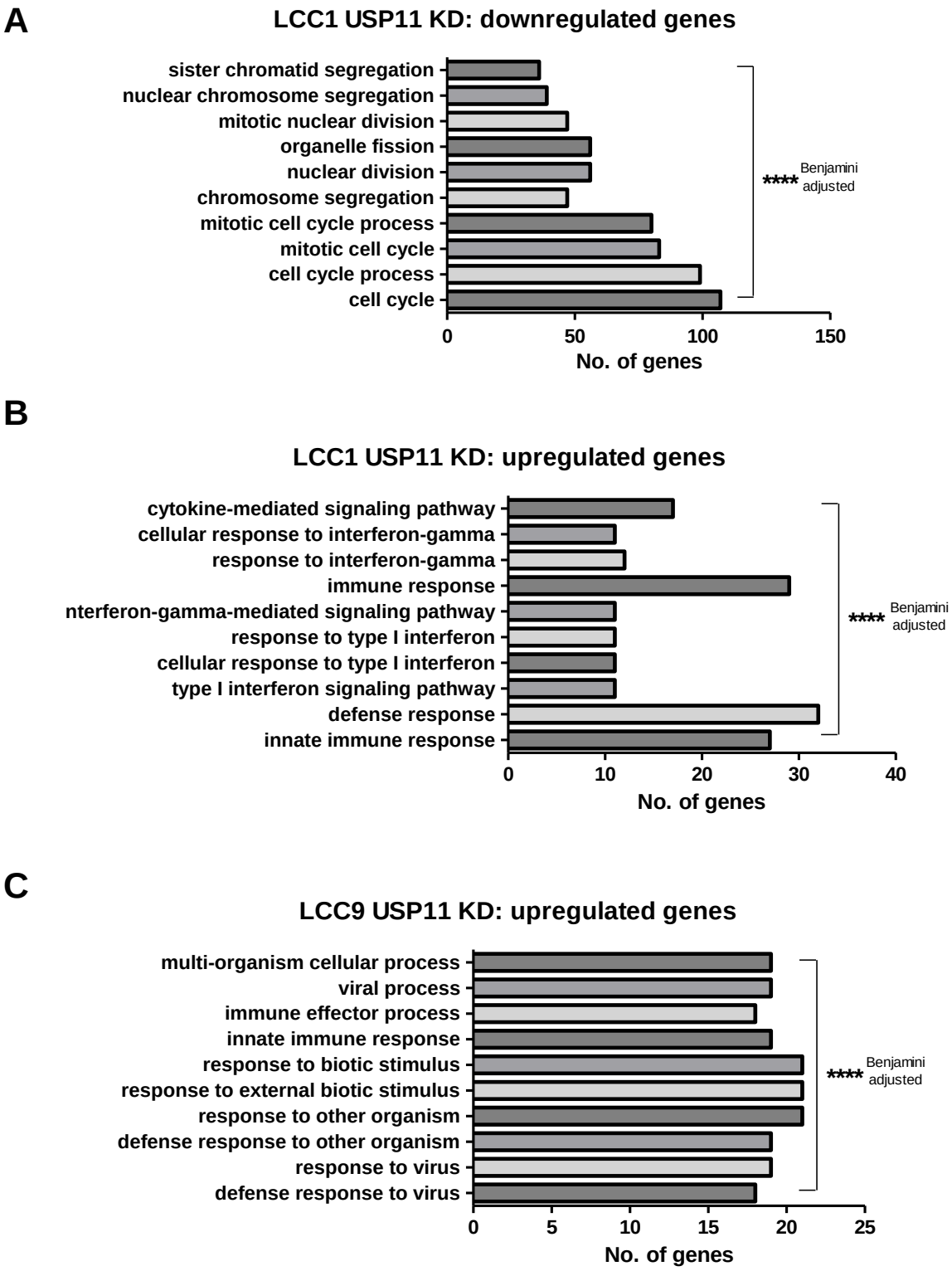

Figure 4.12: Knockdown of USP11 significantly decreased the expression of cell cycle-associated genes in LCC1 cells and increased the expression of inflammatory-associated genes in LCC1 and LCC9 cells, as determined by GO enrichment analysis. *(B, C, D) Bar graphs portraying the 10 most significant GO pathways associated with each group. **** p< 0.0001, Benjamini adjusted (FDR).*

Table 4.2: GO analysis of downregulated genes in LCC1 USP11 knockdown cells

Cellular process	No. of genes overlapping	Benjamini p-value
Cell cycle	107	1.00E-62
Cell cycle process	99	5.50E-62
Mitotic cell cycle	83	5.60E-55
Mitotic cell cycle process	80	3.20E-54
Chromosome segregation	47	1.20E-37
Nuclear division	56	5.80E-37
Organelle fission	56	1.60E-35
Mitotic nuclear division	47	1.00E-32
Nuclear chromosome segregation	39	4.30E-30
Sister chromatid segregation	36	3.90E-30
Microtubule cytoskeleton	60	3.40E-27
Cell division	47	2.80E-27
Chromosome	56	2.70E-27
Chromosome organization	61	6.50E-26
Mitotic cell cycle phase transition	43	4.50E-25
Cell cycle phase transition	44	4.40E-25
Intracellular non-membrane-bounded organelle	103	9.00E-25
Non-membrane-bounded organelle	103	9.00E-25
Spindle	34	5.40E-24
Microtubule cytoskeleton organization	38	1.00E-22

Table 4.3: GO analysis of upregulated genes in LCC1 USP11 knockdown cells

Cellular process	No. of genes overlapping	Benjamini p-value
Innate immune response	27	2.80E-12
Defence response	32	1.20E-10
Type I interferon signalling pathway	11	7.90E-10
Cellular response to type I interferon	11	7.90E-10
Response to type I interferon	11	1.00E-09
Interferon-gamma-mediated signalling pathway	11	1.10E-09
Immune response	29	1.90E-08
Response to interferon-gamma	12	4.50E-08
Cellular response to interferon-gamma	11	1.30E-07
Cytokine-mediated signalling pathway	17	6.50E-07
Defence response to other organism	16	1.00E-06
Response to biotic stimulus	20	1.50E-06
Response to cytokine	19	2.20E-06
Response to other organism	19	3.50E-06
Response to external biotic stimulus	19	3.50E-06
Immune system process	32	4.00E-06
Cellular response to cytokine stimulus	17	1.20E-05
MHC class I protein complex	5	2.90E-05
Immune effector process	17	2.20E-05
MHC protein complex	6	2.40E-05

Table 4.4: GO analysis of upregulated genes in LCC9 USP11 knockdown cells

Cellular process	No. of genes overlapping	Benjamini p-value
Defence response to virus	18	3.60E-24
Response to virus	19	2.60E-24
Defence response to other organism	19	8.00E-21
Response to other organism	21	1.40E-20
Response to external biotic stimulus	21	1.40E-20
Response to biotic stimulus	21	3.10E-20
Innate immune response	19	5.20E-17
Immune effector process	18	3.00E-16
Viral process	19	5.10E-16
Multi-organism cellular process	19	5.20E-16
Symbiosis	19	7.30E-16
Interspecies interaction between organisms	19	7.30E-16
Defence response	21	8.30E-16
Immune system process	22	3.30E-13
Response to external stimulus	21	3.20E-13
Immune response	19	1.30E-12
Multi-organism process	21	3.00E-12
Type I interferon signalling pathway	8	5.20E-10
Cellular response to type I interferon	8	5.20E-10
Response to cytokine	14	5.80E-10

GSEA, developed at the Broad Institute of Massachusetts of Technology and Harvard, is a freely available bioinformatical tool comprised of 1,325 gene sets (Subramanian et al., 2005). GSEA was used to further interpret RNA-seq data, providing an in-depth analyses of GO pathways, as well as other gene sets obtained from the literature available on GSEA software. Here, Fragments Per Kilobase of transcript per Million mapped reads (FPKM) values for each DE gene were used, in order to give a better representation of the changes between each biological replicate. All DE genes for each cell line were uploaded on to the GSEA software, along with the GO pathway files downloaded from the GSEA website. Enrichment plots and heatmaps were generated for pathways which were found to be significantly associated with DE genes.

As previously highlighted, knockdown of USP11 in LCC1 cells significantly decreased the expression of genes associated with the cell cycle. Figure 4.13 illustrates these differences in the form of an enrichment plot and heatmap. An enrichment score (ES) was determined from the enrichment plot, which reflects the degree to which the gene set being examined is overrepresented in a given set of genes (e.g. cell cycle). The enrichment plot in Figure 4.13 highlights the under-representation of cell cycle genes in USP11 knockdown cells, with an ES of 0.52 in control samples. The heatmap, which represents FPKM values of control cells and two individual knockdown cell lines in biological triplicate, also reflects this, with blue squares in knockdown samples indicating lower FPKM scores. From this heatmap it is apparent that cell cycle-associated genes are further downregulated in siUSP11_2. Very few genes are upregulated in knockdown cells and associated with the cell cycle, as seen at the bottom of the heat map.

Forty downregulated genes in LCC1 USP11 knockdown cells were associated with chromosome segregation, the formation of two sister chromatids during mitosis. Figure 4.14 represents these changes in the form of an enrichment plot and heatmap, concluding that knockdown of USP11 in LCC1 cells negatively regulates this key step in cell division. As before, genes are further downregulated in siUSP11_2. As highlighted earlier following GO enrichment analysis using DAVID, USP11 knockdown negatively regulates several cellular processes associated with the cell cycle and cell division. The enrichment plots in Figure 4.15 illustrate the underrepresentation of these genes in USP11 knockdown cells, with overrepresentation in control cells. ES are highlighted in table 4.5.

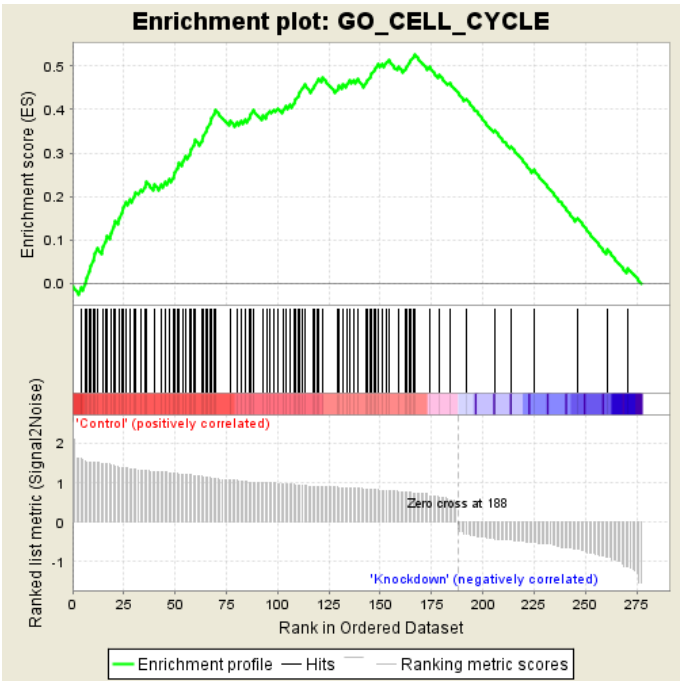

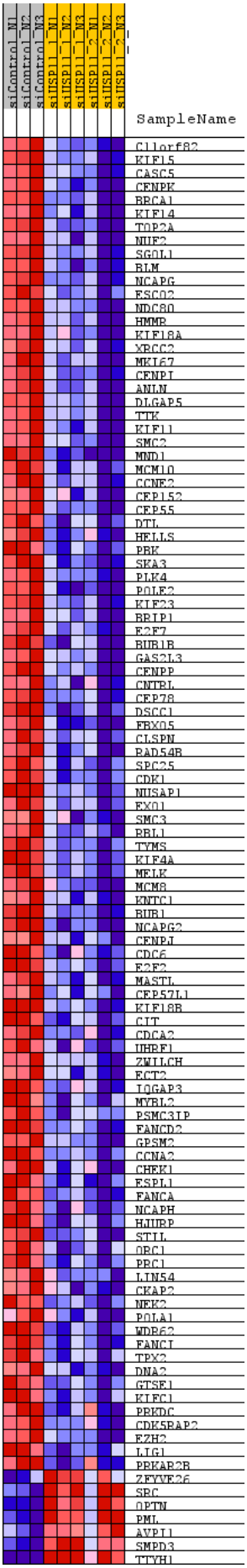

Figure 4.13: Cell cycle-associated genes were underrepresented in LCC1 USP11 knockdown cells, with enrichment observed in control samples, as determined by GSEA. *(A) Enrichment plot depicting the enrichment of cell cycle genes in LCC1 USP11 knockdown and control cells. The green line, representing the enrichment profile, shows the running ES for the gene set. The black bars (or 'hits') indicate where the members of the cell cycle gene set appear in the ranked list of genes. The ranking metric at the bottom of the plot measures each gene's correlation with the phenotype. Positive values indicate a correlation with control samples, while negative values indicate a correlation with knockdown samples. ES= 0.525; normalised ES= 2.79; nominal p-value= 0; FDR q-value= 0; FWER p-value= 0. (B) Heatmap representing FPKM values of DE genes in LCC1 knockdown cells associated with the cell cycle. Coloured squares represent FPKM intensity, where the colour range (red, pink, light blue, dark blue) represents the gene expression range (high, moderate, low, very low, respectively).*

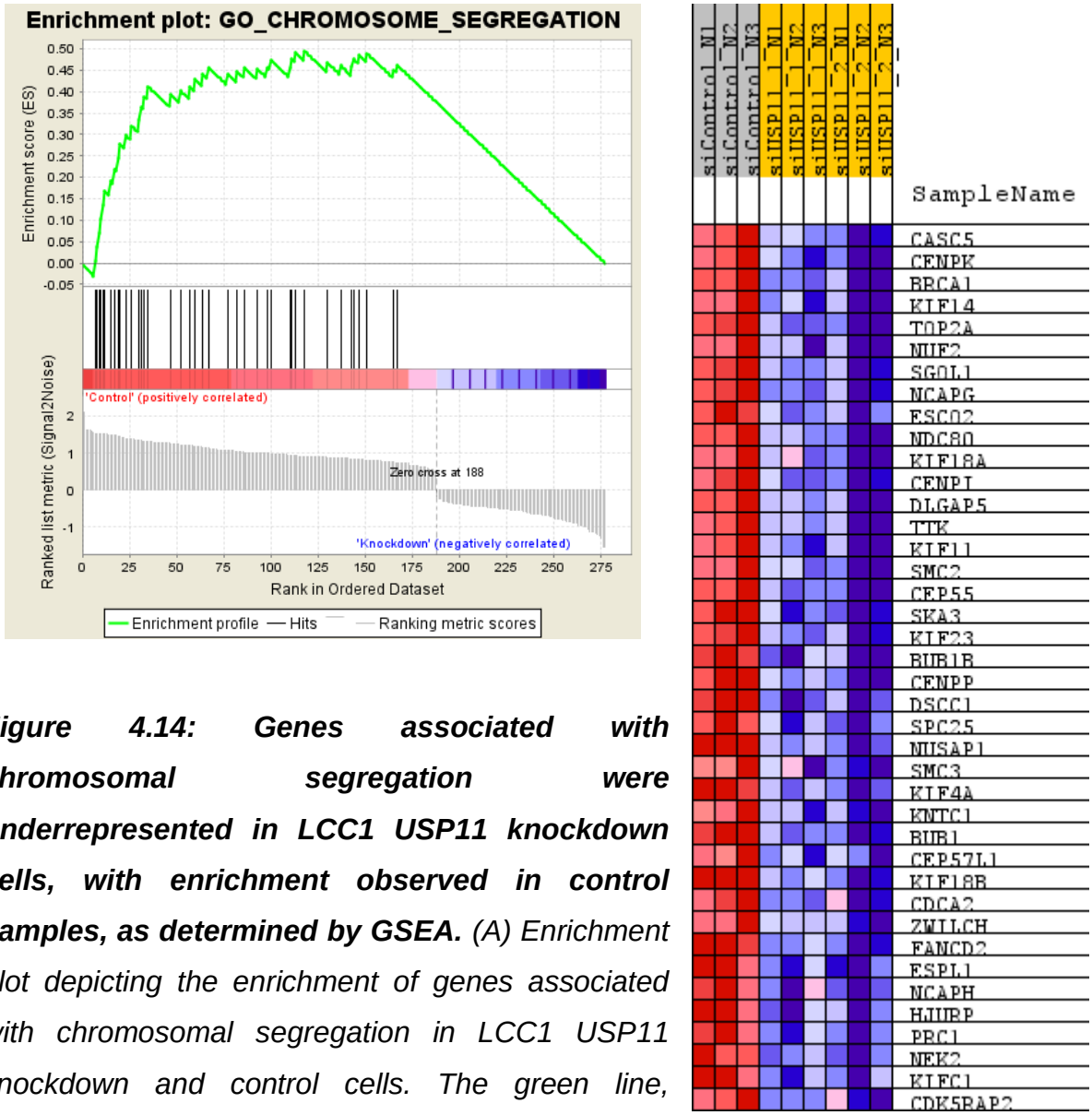

Figure 4.14: Genes associated with chromosomal segregation were underrepresented in LCC1 USP11 knockdown cells, with enrichment observed in control samples, as determined by GSEA. *(A) Enrichment plot depicting the enrichment of genes associated with chromosomal segregation in LCC1 USP11 knockdown and control cells. The green line, representing the enrichment profile, shows the running ES for the gene set. The black bars (or 'hits') indicate where the members of the gene set appear in the ranked list of genes. The ranking metric at the bottom of the plot measures each gene's correlation with the phenotype. Positive values indicate a correlation with control samples, while negative values indicate a correlation with knockdown samples. ES= 0.49; normalised ES= 2.25; nominal p-value= 0; FDR q-value= 0.001; FWER p-value= 0.008. (B) Heatmap representing FPKM values of DE genes in LCC1 knockdown cells associated with chromosomal segregation. Coloured squares represent FPKM intensity, where the colour range (red, pink, light blue, dark blue) represents the gene expression range (high, moderate, low, very low, respectively).*

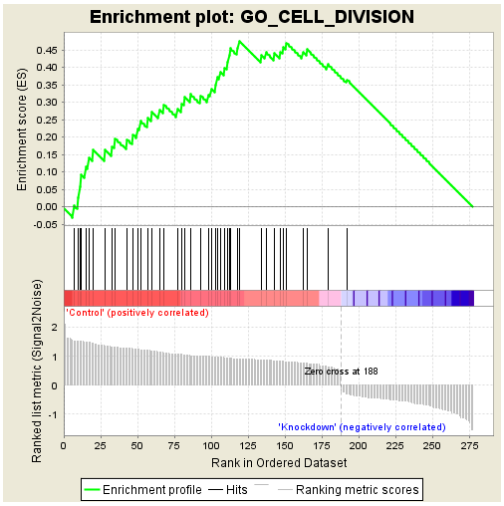
Enrichment plot: GO_CELL_DIVISION
Enrichment score (ES)
Ranked list metric (Signal2Noise)
'Control' (positively correlated)
Zero cross at 188
'Knockdown' (negatively correlated)
Rank in Ordered Dataset
Enrichment profile
Hits
Ranking metric scores

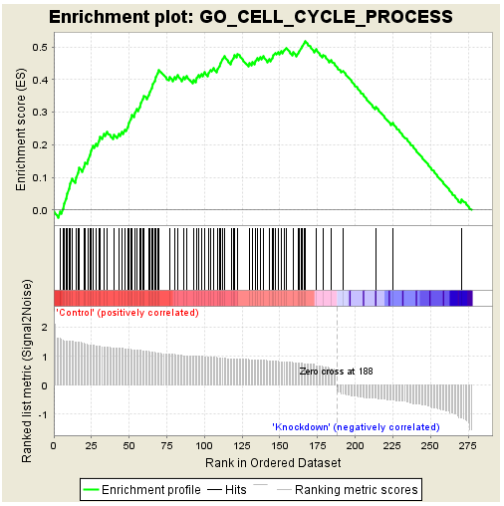
Enrichment plot: GO_CELL_CYCLE_PROCESS
Enrichment score (ES)
Ranked list metric (Signal2Noise)
'Control' (positively correlated)
Zero cross at 188
'Knockdown' (negatively correlated)
Rank in Ordered Dataset
Enrichment profile
Hits
Ranking metric scores

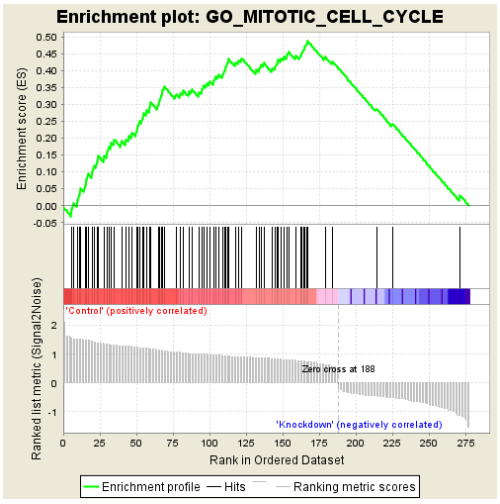
Enrichment plot: GO_MITOTIC_CELL_CYCLE
Enrichment score (ES)
Ranked list metric (Signal2Noise)
'Control' (positively correlated)
Zero cross at 188
'Knockdown' (negatively correlated)
Rank in Ordered Dataset
Enrichment profile
Hits
Ranking metric scores

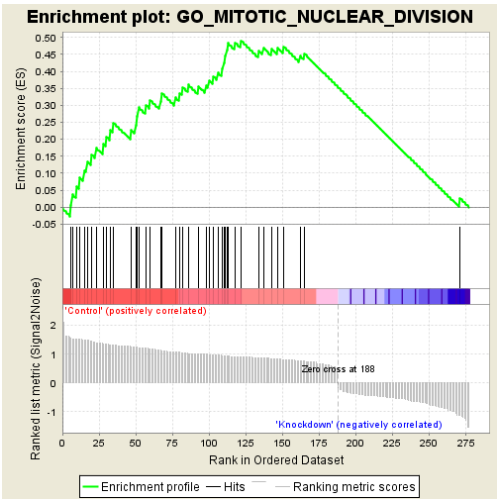
Enrichment plot: GO_MITOTIC_NUCLEAR_DIVISION
Enrichment score (ES)
Ranked list metric (Signal2Noise)
'Control' (positively correlated)
Zero cross at 188
'Knockdown' (negatively correlated)
Rank in Ordered Dataset
Enrichment profile
Hits
Ranking metric scores

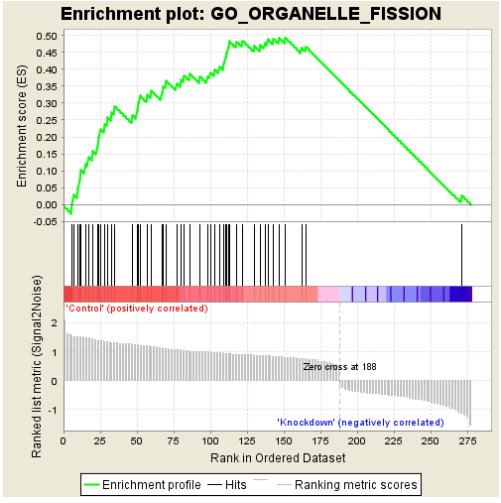
Enrichment plot: GO_ORGANELLE_FISSION
Enrichment score (ES)
Ranked list metric (Signal2Noise)
'Control' (positively correlated)
Zero cross at 188
'Knockdown' (negatively correlated)
Rank in Ordered Dataset
Enrichment profile
Hits
Ranking metric scores

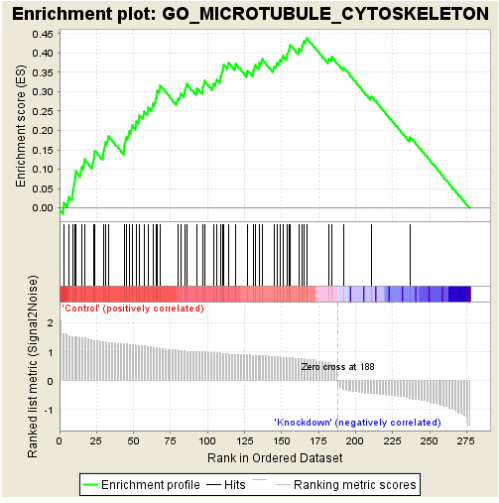
Enrichment plot: GO_MICROTUBULE_CYTOSKELETON
Enrichment score (ES)
Ranked list metric (Signal2Noise)
'Control' (positively correlated)
Zero cross at 188
'Knockdown' (negatively correlated)
Rank in Ordered Dataset
Enrichment profile
Hits
Ranking metric scores

Figure 4.15: GO pathways associated with the cell cycle and cell division were significantly associated with USP11 knockdown in LCC1 cells, as determined by GSEA. *(A-F) Enrichment plot depicting the enrichment of genes in each stated GO pathway in LCC1 USP11 knockdown and control cells. The green line, representing the enrichment profile, shows the running ES for the gene set. The black bars (or 'hits') indicate where the members of the cell cycle gene set appear in the ranked list of genes. The ranking metric at the bottom of the plot measures each gene's correlation with the phenotype. Positive values indicate a correlation with control samples, while negative values indicate a correlation with knockdown samples.*

Table 4.5: Statistics associated with enrichment plots in Figure 4.15

GO pathway	ES	NES	Nominal p-value	FDR q-value	FWER p-value
A: Cell division	0.47	2.21	0	0.0015	0.012
B: Cell cycle process	0.51	2.72	0	0	0
C: Mitotic cell cycle	0.48	2.51	0	0	0
D: Mitotic nuclear division	0.49	2.29	0	5.66 E-4	0.003
E: Organelle fission	0.49	2.38	0.00108	2.36 E-4	0.001
F: Microtubule cytoskeleton	0.44	2.17	0	0.0017	0.016

Figure 4.6 demonstrated that USP11 silencing in LCC1 cells significantly reduced the mRNA expression of ERα target genes, suggesting that USP11 plays a role in ERα transcription in LCC1 cells in a ligand-independent manner. In order to further investigate this, RNA-seq results were analysed for the downregulation of known or putative ERα target genes. The panel of genes analysed in Figure 4.5 were not significantly downregulated LCC1 USP11 knockdown cells when analysed by RNA-seq, however analysis of FPKM values confirmed downregulation of these genes in knockdown cells.

The LCC1 knockdown list of downregulated genes were analysed by GSEA. These genes were compared against the GSEA curated genes sets, which were

obtained from various sources such as the scientific literature and online pathway databases. The availability of these gene sets represents one of the main advantages of GSEA software when compared to other methods of RNA-seq analysis. Remarkably, one of the most significant overlapping genes sets was that published by Dutertre and colleagues, which is composed of 324 genes upregulated in MCF-7 cells treated with E2 for 24 hours. This study was conducted to investigate gene and alternative promotor (AP) regulation in response to estradiol and as a result the authors identified several novel ERα target genes. (Dutertre et al., 2010). Of the 188 downregulated genes in the LCC1 USP11 knockdown list, 95 overlapped with the Dutertre dataset (p-value: 8.69 e-162; FDR q-value: 2.06 e-158), suggesting that these are ERα target genes downregulated by USP11 silencing. A 6-hour E2 gene set was also available from this study, with 26 genes from the downregulated genes list overlapping with this dataset. These overlapping sets can be visualised in the heatmaps in Figure 4.16, where differences between FPKM values of knockdown and control samples are represented.

A: 6 hours E2 **B: 24 hours E2**

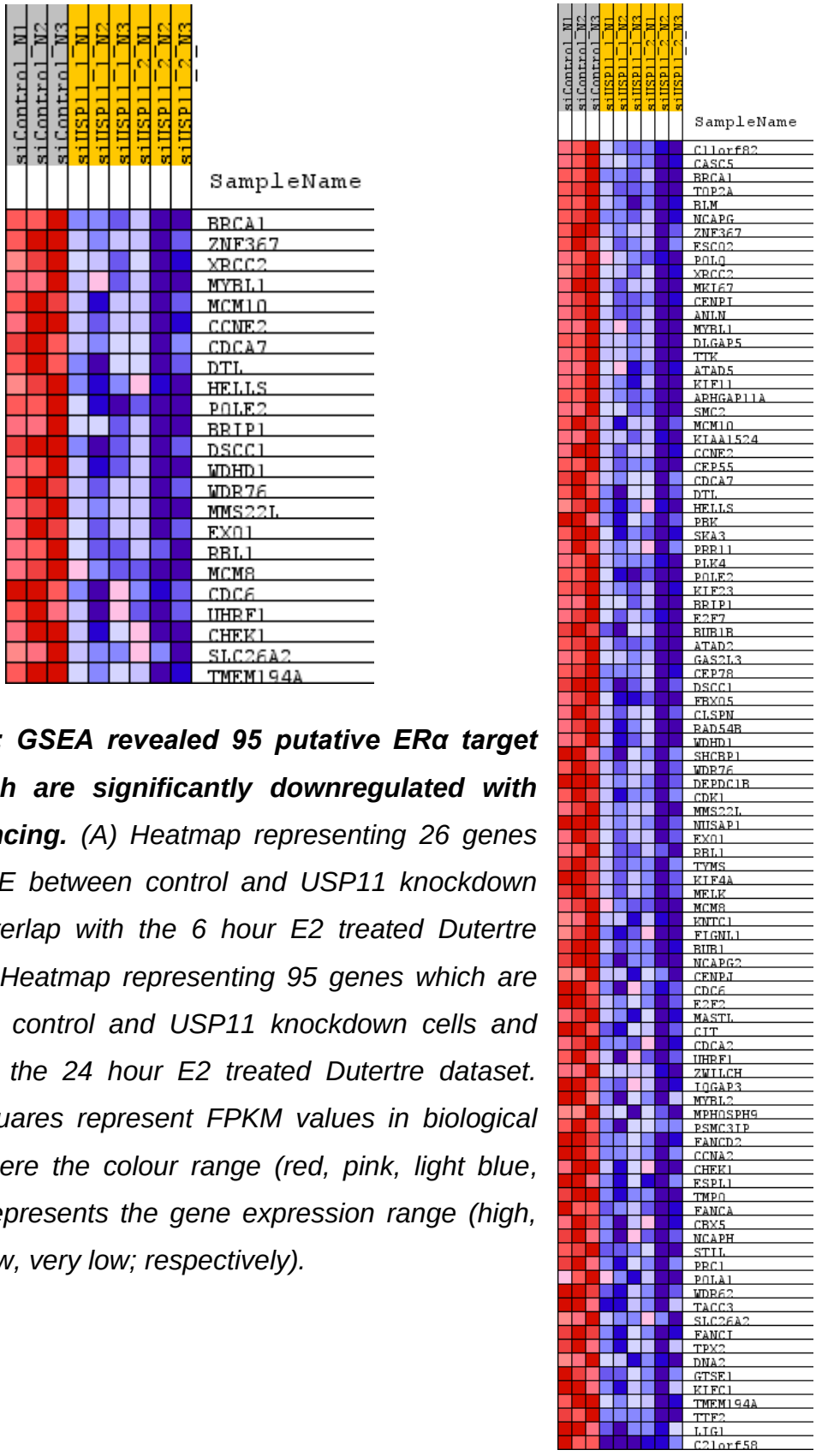

Figure 4:16: GSEA revealed 95 putative ERα target genes which are significantly downregulated with USP11 silencing. *(A) Heatmap representing 26 genes which are DE between control and USP11 knockdown cells and overlap with the 6 hour E2 treated Dutertre dataset. (B) Heatmap representing 95 genes which are DE between control and USP11 knockdown cells and overlap with the 24 hour E2 treated Dutertre dataset. Coloured squares represent FPKM values in biological triplicate, where the colour range (red, pink, light blue, dark blue) represents the gene expression range (high, moderate, low, very low; respectively).*

As highlighted, the Dutertre gene sets are defined as genes upregulated with E2 stimulation in MCF-7 cells. As LCC1 cells are derived from MCF-7 cells it was hypothesised that these genes would also be regulated by E2 in LCC1 cells, but due to the differential nature of ERα activation in this cell line an investigation was warranted. Cells were treated with 1 nM E2 for 4 and 24 hours and the mRNA expression of a selected panel of genes was determined. *BRCA1*, *BLM*, *NCAPH* and *NCAPG*, which were all downregulated in LCC1 USP11 knockdown cells and overlapped with the 24 hour E2 Dutertre gene set, were upregulated after 24 hours in response to E2.

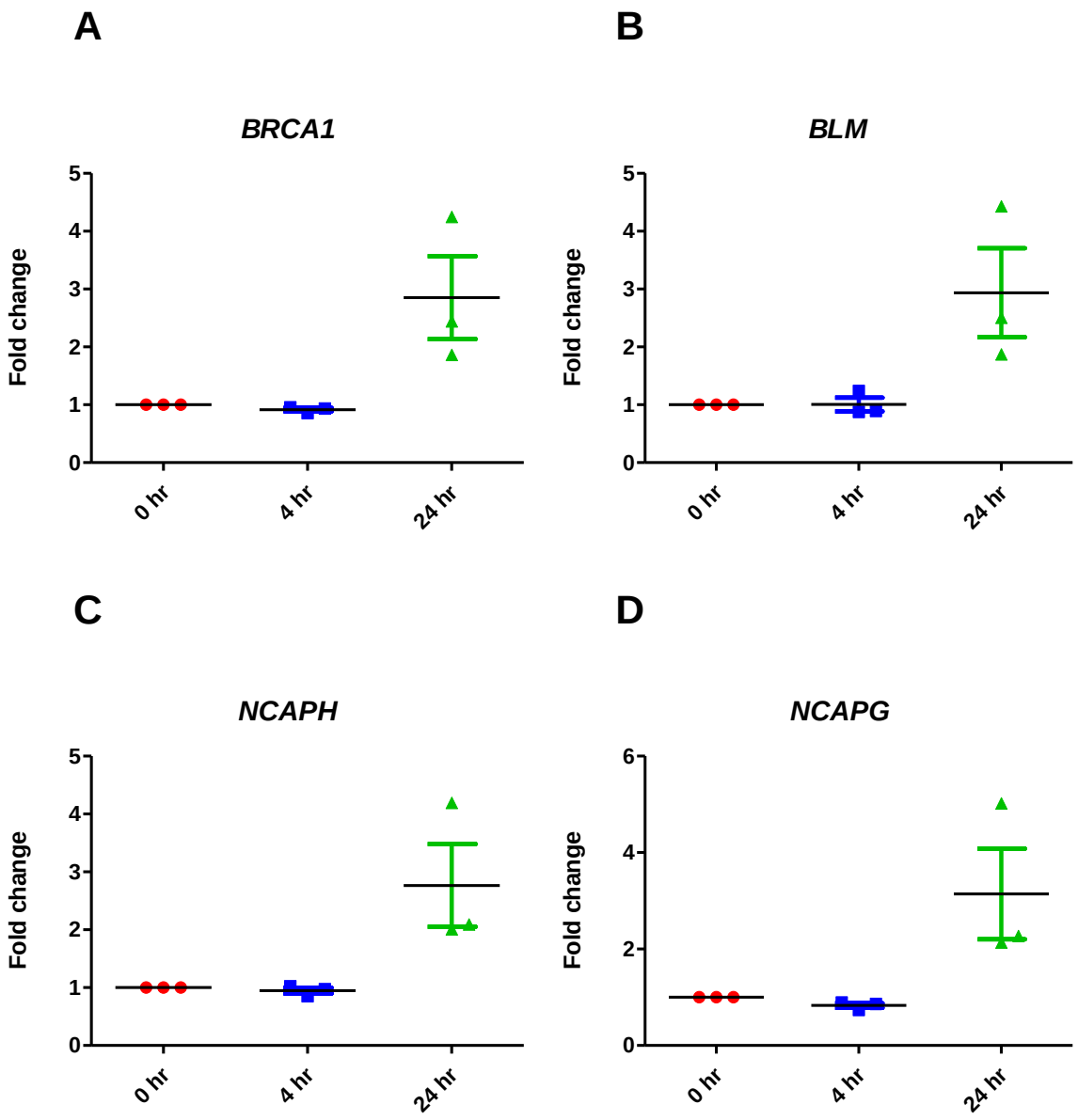

Figure 4.17: Treatment with E2 for 24 hours increased the mRNA expression of BRCA1, BLM, NCAPH and NCAPG in LCC1 cells. *Cells were seeded and incubated for 24 hours in hormone-starved conditions before subsequent stimulation with 1 nM E2 for 4 and 24 hours. All samples were normalised to 0 hour treatment; gene expression was normalised to 18S expression. Error bars represent SEM.*

4.4 Discussion

Using state-of-the-art RNA-seq technology, USP11 was identified as an important player in both ERα function and the cell cycle in LCC1 cells. LCC1 cells, derived from the estrogen-dependent MCF-7 cell line, display estrogen independence following passage through an ovariectomised mouse. LCC1 cells remain sensitive to tamoxifen and fulvestrant while displaying resistance to AIs, indicating their dependence on ERα in an estrogen independent manner.

Analysis of USP11 protein expression in a full panel of ERα+ cell lines available in the laboratory indicated increased expression in both LCC1 and LCC9 cells when compared to their parental MCF-7 cells. Triplicate validation confirmed a significant upregulation of USP11 in both cell lines. ERα expression was significantly down in LCC9 cells, perhaps due to their E2 independent growth, anti-endocrine resistance and as a result, less dependence on the receptor. ERα expression was significantly upregulated in LCC1 cells when compared to MCF-7 cells, an observation that was not surprising to this study due to their continued ERα dependence. The first report of the LCC1 cell line however, states that ERα levels are uniform in both LCC1 and MCF-7 cells and suggests that estrogen-independence can occur without gene amplification (Brunner et al., 1993). As with any *in vitro* model, it is likely LCC1 cells have readapted during their time in growth and their mechanisms of estrogen independent growth may have evolved. Recently, Zhang *et al*. identified a 46-gene signature that is required for survival of LCC1 cells and is dispensable in MCF-7 cells (Zhang et al., 2016b). USP11 was not included in the authors' original 'Estrogen Response Network' set of 631 genes, however, the results obtained from this current study suggest a pivotal role for USP11 in LCC1 cell growth.

First, to investigate the role of USP11 in both LCC1 and LCC9 cells, two independent siRNAs targeted to USP11 were used to silence the enzyme in both cells lines. Following knockdown validation, the mRNA expression of a panel of ERα target genes was examined in each cell line. For this study, the ERα target gene panel was expanded from chapter 3. Interestingly mRNA target gene expression was significantly downregulated in LCC1 cells only. Despite the significant increase in USP11 expression in LCC9 cells, knockdown had no effect on ERα target gene expression, suggesting an ERα independent role of USP11 in these cells. Interestingly, Cyclin D1 expression was unchanged in LCC1 USP11 knockdown

cells, while expression was significantly supressed in LCC9 knockdowns. Cyclin D1 regulates CDK4 and CDK6 for progression though the cell cycle. It is a well-described ERα target gene and is upregulated in over half of breast cancers (Neuman et al., 1997). In Chapter 5, analysis of the USP11 ubiquitinome by mass spectrometry identified USP11 as a regulator of Cyclin D1, with protein expression increased in USP11 knockdown cells. Although further validation and investigation in to these results has yet to be carried out, this maybe explain the surprising result obtained in LCC1 and LCC9 USP11 knockdown cells.

To further investigate the role of USP11 in these cells, RNA-seq was carried out on LCC1 and LCC9 knockdown cells lines in collaboration with Dr. Sudipto Das, RCSI and Dr. Bruce Moran, UCD. As expected, a large number of genes (278) were DE in LCC1 cells, while 29 genes were DE in LCC9 cells. Despite the high expression of USP11 in LCC9 cells, the protein appears to be redundant. This represents a key piece of evidence for the role of USP11 in ERα function; in an isogenic cell line model, the cells which are dependent on ERα are also highly dependent on USP11.

Unsurprisingly, very few DE genes were common to both LCC1 and LCC9 cells. Perhaps the overlap of most interest are the oligoadenylate synthase family of proteins, which are involved in the innate immune response to viral infection. Three out of the four enzymes in the OAS family (OAS1, OAS2, OAS3, OASL) were upregulated with USP11 knockdown in both LCC1 and LCC9 cells. Interferon-regulated, OAS proteins can sense viral cytosolic nucleic acids and impede translation (Hornung et al., 2014). This represents an interesting point of further exploration in the role of USP11 in viral pathways, as discussed in chapter 3.

In both cell lines, USP11 silencing enhances inflammatory-associated gene expression. It was hypothesised that as a negative regulator of NF-κB (Sun et al., 2010), USP11 knockdown can enhance NF-κB activity and as a result, the inflammatory response. Based on this result, it may be useful to examine the presence of immune cells in the USP11 stained TMA (referred to in chapter 3) and if this correlates with USP11 expression.

Of particular interest to this study were the genes downregulated with USP11 knockdown in LCC1 cells. Following GO enrichment analysis, a significant amount of genes were found to be associated with the cell cycle. This would indicate that USP11 silencing slows the progression of the cell cycle in an ERα-dependant, E2-

independent setting. Recent evidence in the literature identified RAE1, a key player in mitotic spindle assembly checkpoint, as a novel USP11 substrate. Knockdown of USP11 in this particular study decreased U2OS cell proliferation and increased multipolar spindle formation (Stockum et al., 2018). Of the downregulated proteins with USP11 knockdown, 34 are significantly associated with the cell spindle. Taking this in to account, it was hypothesised that USP11 could be downregulating the cell cycle via this mechanism in LCC1 cells. Whether ERα transcriptional repression in these cells is correlated or causative to this phenotype warrants further investigation.

As mentioned, a 46-gene signature has been identified that are selectively required for survival of LCC1 cells and not MCF-7 cells. Kinesin-like protein 1A (*KIF1A*) is included in this signature. Kinesins are motor proteins which move along microfilaments and support mitosis. Eight members of the kinesin family (*KIF15, KIF11, KIF14, KIF23, KIF18A, KIF4A, KIF18B and KIFC1*) are significantly downregulated with USP11 knockdown in LCC1 cells. This suggests USP11 positively regulates kinesin function, which LCC1 cells depend on for survival. TFF1, a well-known ERα target gene, is also included in this signature, suggesting ERα dependence in the absence of E2. Further experimentation is required to link USP11 to this gene signature, however. Additionally, it is vital to correlate these RNA-seq results with an *in vitro* phenotype. Cell cycle analysis by flow cytometry in LCC1 and LCC9 USP11 knockdown cells will be performed to confirm that USP11 affects the cell cycle in LCC1 cells only.

Multiple ERα target genes were downregulated with USP11 knockdown, as determined by RNA-seq and GSEA. GSEA associated the LCC1 downregulated gene set with a study by Dutertre *et al*., investing the role of alternative promotor (AP) regulation by estradiol in MCF-7 cells. As most ERα binding sites are downstream of the promotor the likelihood of AP regulation by E2 is high. The authors identified several novel ERα target genes as a result of this study (Dutertre et al., 2010). Several genes significantly overlapped with genes that were upregulated by E2 at 24 hours, while many also overlapped at the 6 hour time point. Analyses of publicly available ChIP-seq datasets detected further overlaps with the LCC1 downregulated gene set (Mohammed et al., 2015, Deblois et al., 2009). These aforementioned studies were conducted on MCF-7 cells; at present no such ChIP-seq or gene array studies on LCC1 cells are publicly available. LCC1 cells were treated with E2 and the expression of a small selection of identified genes were

analysed. All selected genes were upregulated in response to E2, indicating that the use of MCF-7 datasets are reliable when comparing analysing LCC1 and LCC9 data.

In conclusion, this data suggests that USP11 silencing represses ERα transcriptional activity in LCC1 cells and not LCC9 cells, as determined by qRT-PCR and RNA-seq technologies. Although the precise mechanism(s) of estrogen independent growth in these cells is unknown, the data presented defines a key role for USP11 in this mechanism. While this initial analysis provides a reasonable insight into the USP11-mediated transcriptomic alterations, further investigation is required to elucidate the precise mechanism involved in these processes.

Chapter 5: Investigation in to the nature of the USP11-ERα interaction and identification of novel USP11 substrates

5.1 Introduction

Previous data suggests that USP11 plays a key role in ERα transcriptional activity and may represent a prognostic marker in ERα+ BC. Despite this information, the mechanism by which USP11 exerts a positive role on ERα function is unknown. A previous study by Stanišić *et al*., investigating the role of DUBs on ERα transcriptional activity, identified USP11 as an ERα interactor. HEK293T cells ectopically expressing ERα were treated with E2 and ERα was immunoprecipitated. Mass spectrometry analysis of these cells revealed an association with three DUBs: OTUB1, USP9X and USP11. (Stanisic et al., 2009). The roles of both OTUB1 and USP9X in ERα function have been elucidated in previous studies (Stanisic et al., 2009, Oosterkamp et al., 2014), however, the role of USP11 in ERα function has yet to be determined. Whether USP11 deubiquitinates ERα, interacts with a cofactor, or forms part of the transcription complex is currently unknown.

To discover novel substrates of USP11, which may provide evidence as to how USP11 controls ERα function, label-free quantification (LFQ) of the proteome and analysis by mass spectrometry (MS) was carried out. Unlike classic MS techniques, label-free MS does not involve the chemical attachment of a stable isotope to proteins. This poses a number of advantages, including reduced sample preparation and analysis time, elimination of variability between samples, reduced costs and higher sequence coverage (Patel et al., 2009). Importantly, due to the low amount of protein required for label-free analysis (~50 µg), proteome and ubiquitinome analysis can be performed in parallel. It was hypothesised that knockdown of USP11 would induce significant changes to the proteome and reveal novel substrates of this DUB.

To follow this, immunoaffinity purification (IAP) of Ub glycine-glycine (Gly-Gly) residues, followed by LC-MS analysis was carried out. In the past, the detection of ubiquitinated peptides via mass spectrometry proved a challenge. Ubiquitinated proteins have low stoichiometry and are structurally diverse (Udeshi et al., 2013). Moreover, Ub itself is large (8 kDa), resulting in a large modification that is turned over rapidly in the cell (Peng et al., 2003). Ub itself is cleaved during trypsin digestion, and while this initially posed a challenge for detection of ubiquitinated peptides, modern technologies now use this to an advantage. Trypsin digestion cleaves Ub at the C-terminus, leaving a Gly-Gly residue that is still attached to a lysine on the target protein. The presence of this Gly-Gly residue prevents further

cleavage by trypsin (Udeshi et al., 2013), and so remains evidence of a ubiquitinated protein following digestion of the sample.

The development of antibodies targeted to this Gly-Gly residue has been a dramatic step forward in ubiquitination proteomics. UbiScan®, developed by Cell Signalling Technologies, uses a Ub remnant motif (K-ε-GG) antibody-bead conjugate to isolate ubiquitinated peptides. This kit has been previous used for a number of high impact studies (Onizawa et al., 2015, Kronke et al., 2014). A schematic of the IAP process is outlined in Figure 5.1.

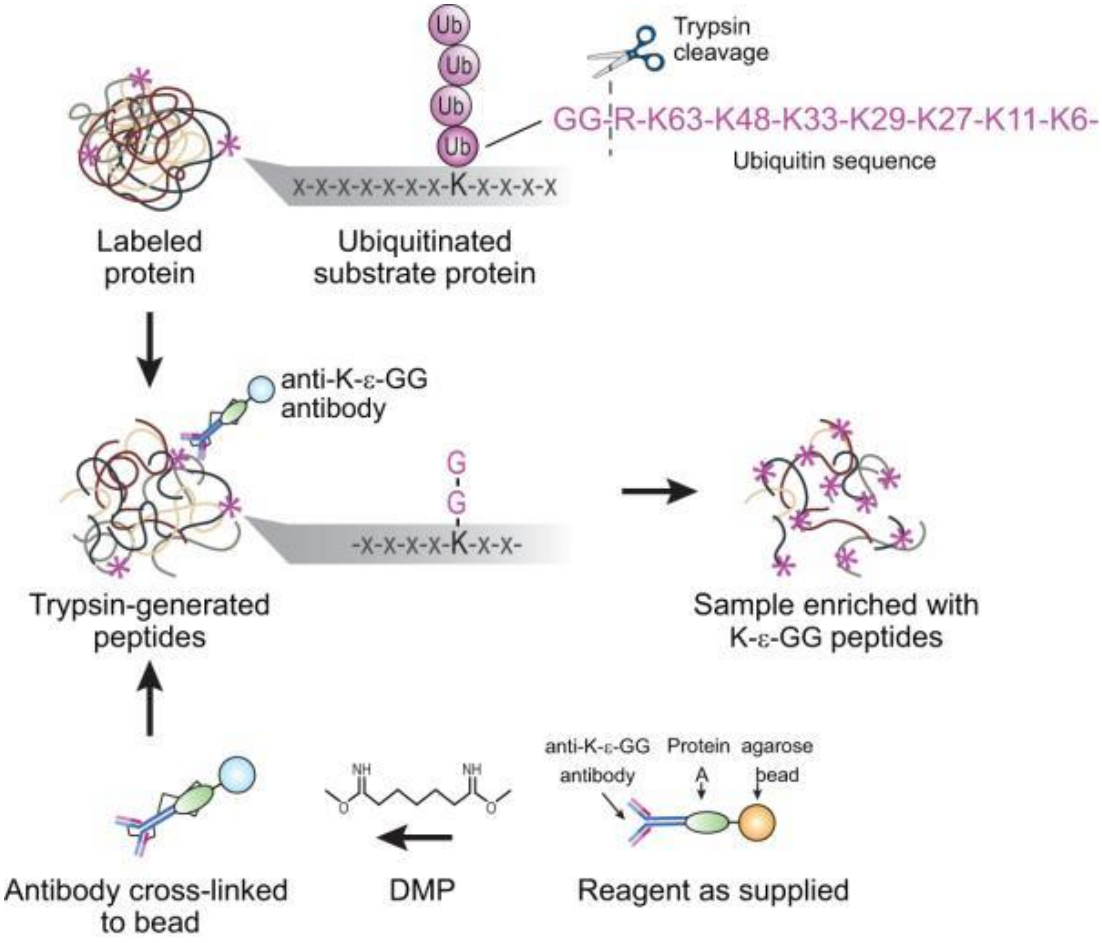

Figure 5.1: A K-ε-GG antibody-bead conjugate recognises Ub remnants on ubiquitinated proteins, which are later analysed by LC-MS (Udeshi et al., 2013).

5.2 Aims of this chapter

- Investigate if USP11 associates with ERα and/or if it affects ERα ubiquitination status using immunoprecipitation (IP) techniques
- Study the effects of USP11 knockdown on the full ZR-75-1 proteome using LC-MS
- Elucidate, for the first time, the effect of USP11 knockdown on the ZR-75-1 ubiquitinome and identify novel USP11 substrates

5.3 Results

5.3.1 Immunoprecipitation of ERα

Based on previous data, both here and in the literature, it was hypothesised that USP11 directly interacts with ERα and plays a role in transcriptional function. To investigate this, IP techniques were implied. As the name suggests, IP involves the purification of an antigen on a target protein using a specific antibody to that antigen. The protein of interest, as well as its binding partners, will be isolated for analysis by Western blotting.

First, endogenous ERα was immunoprecipitated from ZR-75-1 BC cells in the presence and absence of E2. Under both conditions, USP11 was not co-immunoprecipitated with ERα (Figure 5.2). ERα was also not co-immunoprecipitated with USP11 (data not shown).

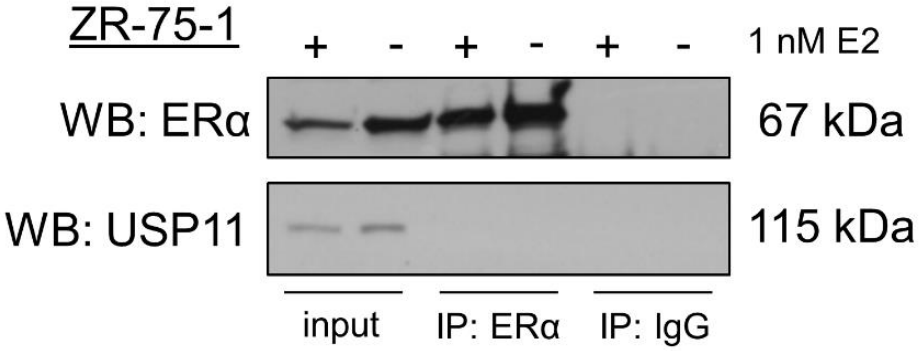

Figure 5.2: ***USP11 was not co-immunoprecipitated with endogenous ERα in a breast cancer cell line.*** *Representative Western blot image depicting IP of ERα. ZR-75-1 cells were hormone starved for 48 hours and subsequently stimulated with E2 for 24 hours. Cells were harvested and ERα was immunoprecipitated with an ERα (F10) antibody, immobilised to sepharose A beads. Image is representative of three biological replicates; anti-IgG (mouse) was used as an IP control.*

In the event that endogenous ERα levels were too low to detect a binding partner, an ERα overexpression system was implied. ERα was ectopically expressed in HEK293T wild-type (WT) and USP11 knockout (KO). Again, USP11 was not co-immunoprecipitated with ERα, either in the presence or absence of E2 (Figure 5.3).

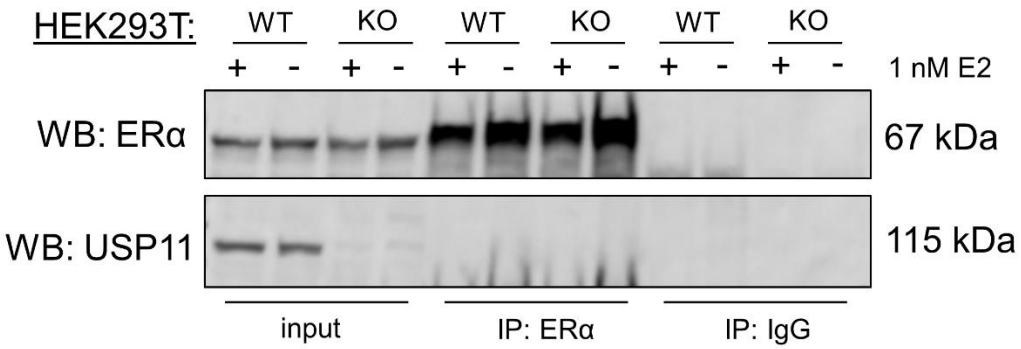

Figure 5.3: USP11 was not co-immunoprecipitated with ERα in an ERα overexpression system. *Representative Western blot image depicting IP of ERα. HEK293T cells were transfected with ERα, hormone starved for 48 hours and either stimulated with E2 or not. Cells were harvested and ERα was immunoprecipitated with an ERα (F10) antibody, immobilised to sepharose A beads. Image is representative of three biological replicates; anti-IgG (mouse) was used as an IP control.*

The above results suggest that USP11 does not bind ERα under the conditions tested, however, a transient interaction may have been missed and deubiquitination of ERα by USP11 remained a possibility. The effect of USP11 expression on ERα ubiquitination was examined using IP techniques in both USP11 wild-type and knockout cell lines. First, co-transfection of VP16 ERα and HA-Ub overexpression vectors (vector maps can be found in Appendix 2) was optimised and confirmed by Western blotting (Figure 5.4).

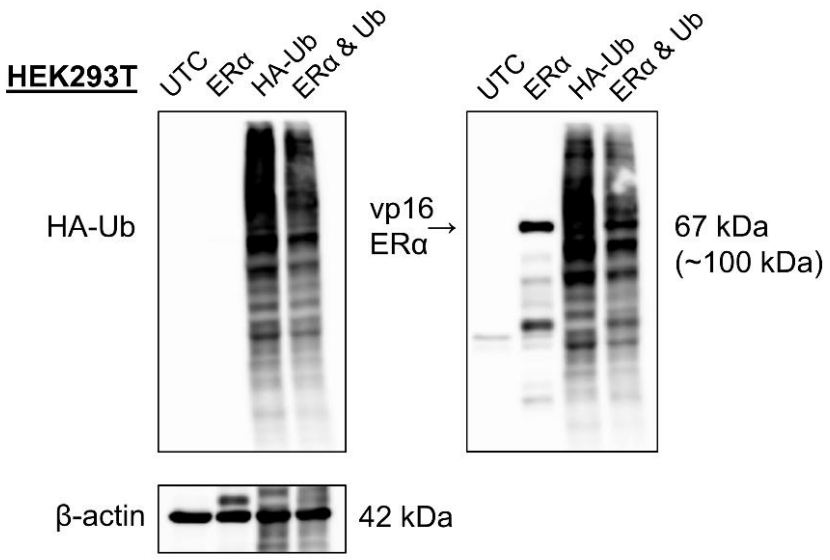

Figure 5.4: Western blotting confirmed the co-expression of VP16-ERα and HA-Ub following co-transfection of both vectors. *HEK293T cells were transfected, incubated under normal growth conditions for 48 hours, then harvested and analysed. β-actin was used as a loading control.*

In order to detect ubiquitinated ERα and to investigate if USP11 has an effect on this modification, HEK293T WT and KO cells were co-transfected with VP16 ERα and HA-Ub. As Ub is a small protein, overexpression is often required to detect co-IP levels. ERα was immunoprecipitated using two individual ERα antibodies, (Santa Cruz D12 and F10), in the event previous IPs using F10 alone were inaccurate. Interestingly, knockdown of USP11 had no effect on ERα ubiquitinated levels, which were only detected following IP with ERα D12 antibody (Figure 5.5). Due to time restrictions, this experiment was not repeated, therefore further validation is required to make a valid conclusion.

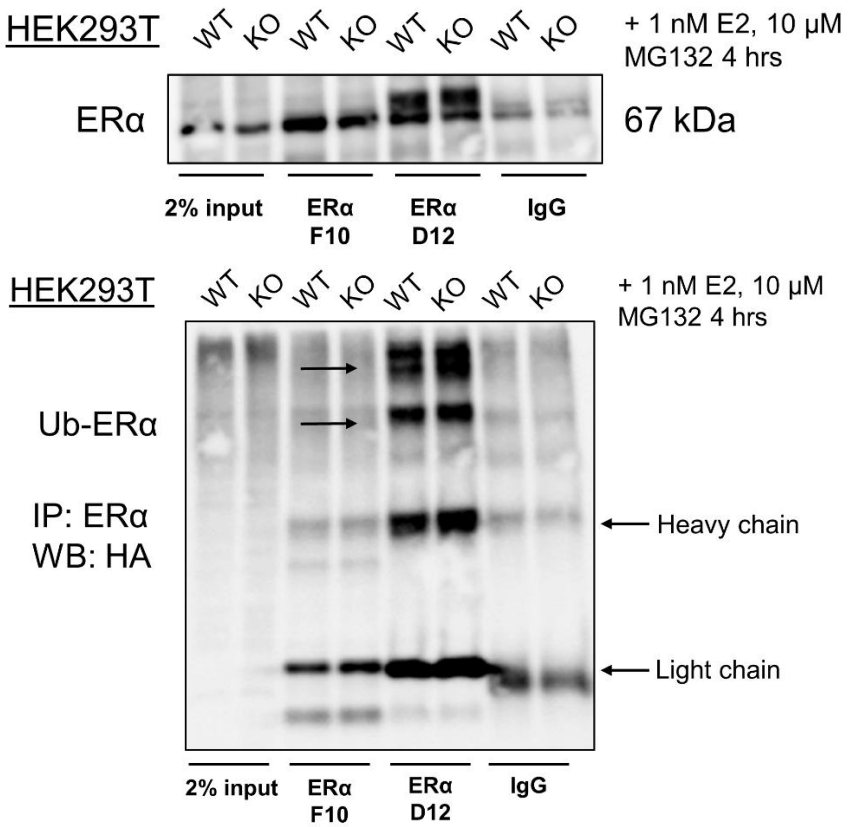

Figure 5.5: USP11 did not affect ubiquitination of ERα, although further validation is required. *Western blot image depicting IP of ERα. HEK293T cells were co-transfected with VP16 ERα and HA-Ub, hormone starved for 48 hours and subsequently treated with E2 and MG132. Cells were harvested and ERα was immunoprecipitated with an ERα (F10) antibody, immobilised to sepharose A beads. Image is representative of one biological replicate; anti-IgG (mouse) was used as an IP control.*

5.3.2 Proteomic analysis of USP11 knockdown cell lines

Preliminary evidence suggests that USP11 does not directly deubiquitinate ERα. In order to further investigate this, the full proteome of USP11 knockdown and control BC cells, both in the presence and absence of E2, was analysed by LC-MS. First, a histogram was generated for each sample to examine the distribution of counts. As observed in Figure 5.6, the counts for each sample are normally distributed. For analysis, missing values were imputed by values simulating noise around the detection limit, as highlighted by red bars on each histogram (Hein et al., 2015).

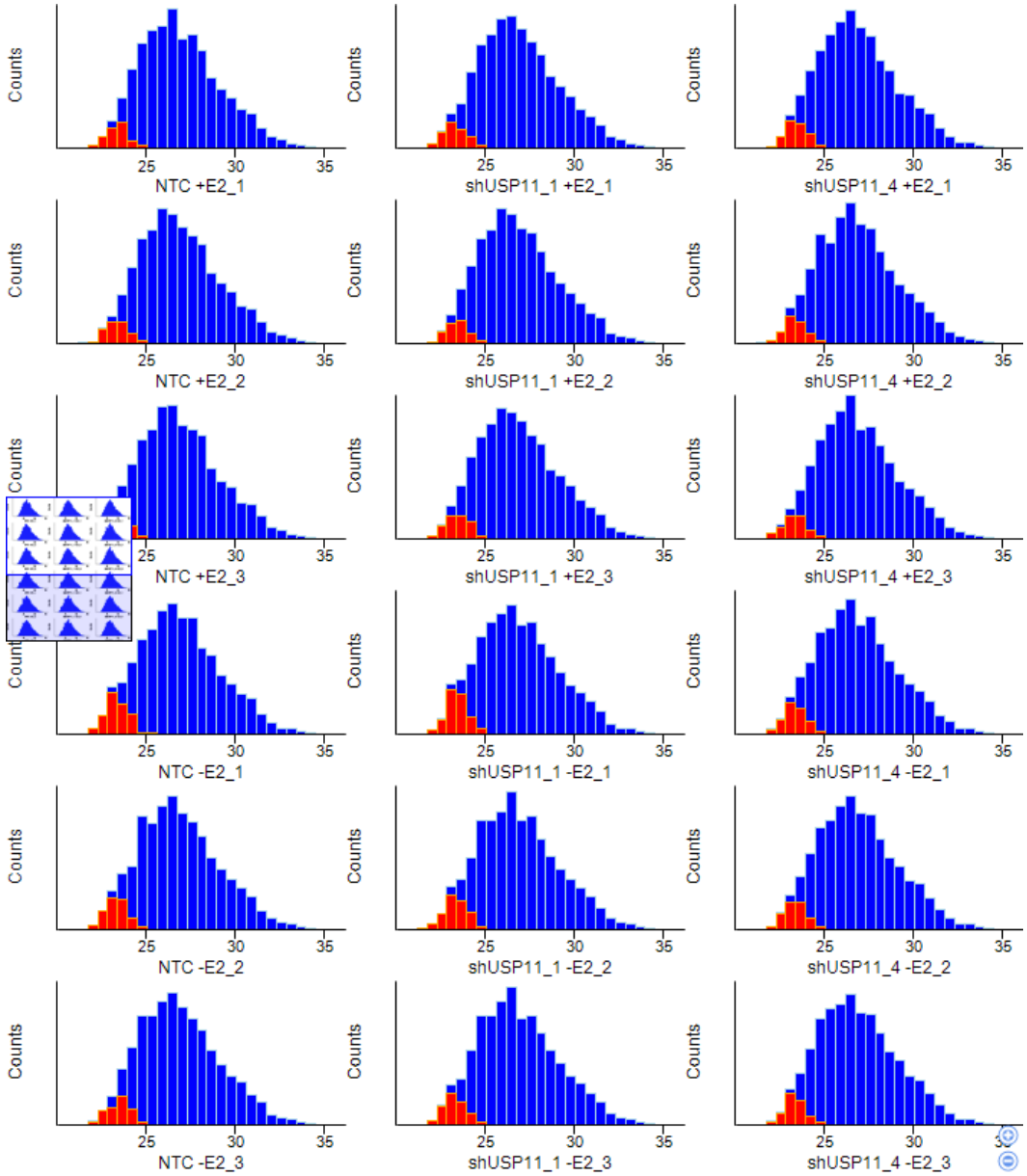

Figure 5.6: Proteome MS counts were normally distributed for each sample. *Imputed values are highlighted in red.*

For the current study, mass spectrometry samples were ran in technical triplicate to reduce the influence of noise on statistical testing. To ensure the grouping of technical replicates, hierarchical clustering and PCA analysis was carried out on Z score values generated from label-free quantification (LFQ) values. Both the intensity map (Figure 5.7, A) and PCA plot (Figure 5.7, B) demonstrate clustering of each group. Interestingly, grouping of E2 stimulated and unstimulated samples was also observed, highlighting the significant proteomic changes induced by E2.

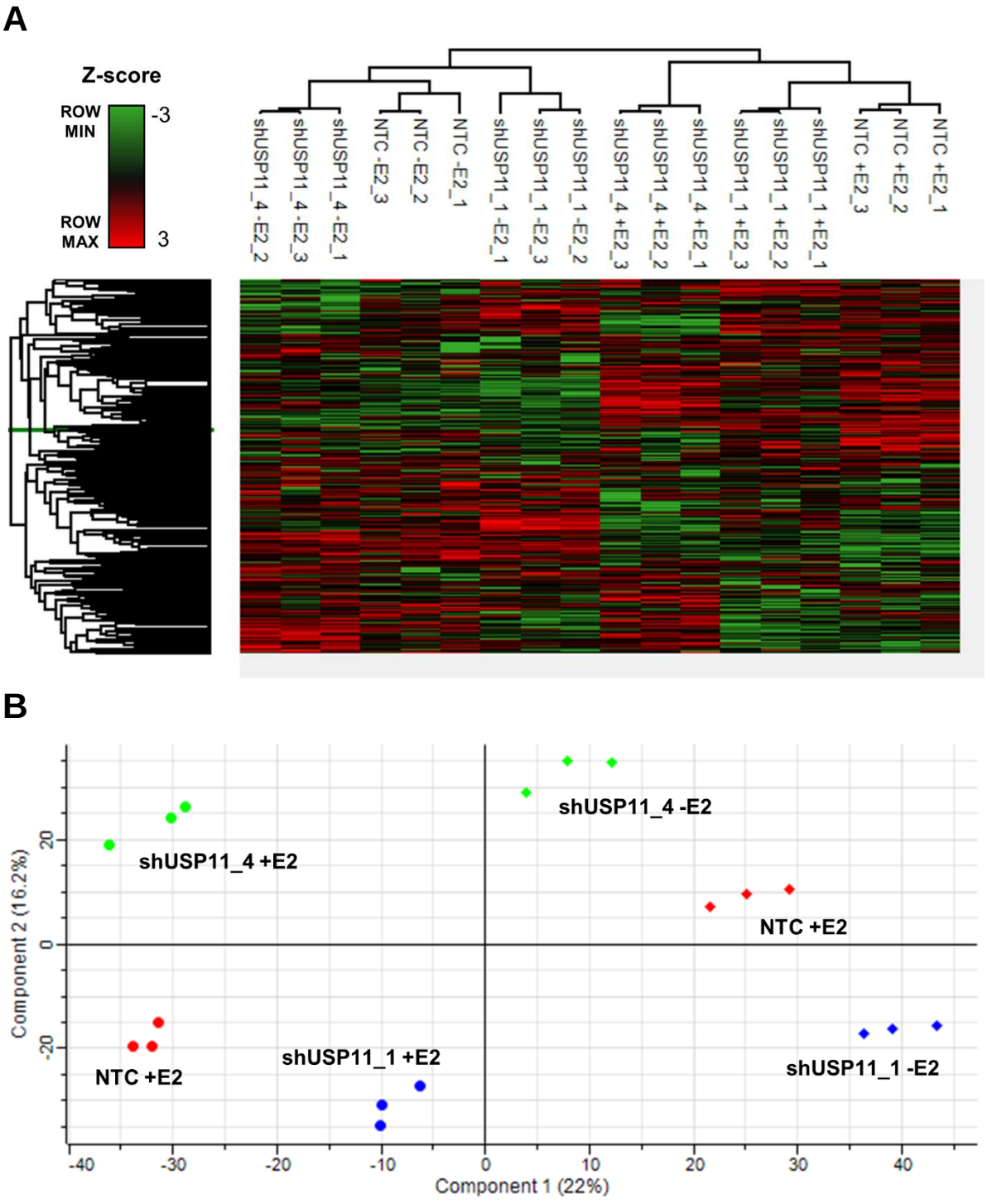

Figure 5.7: Mass spectrometry technical replicates were grouped together, as determined by intensity mapping and PCA. *(A) Heatmap representing the intensity of each detected protein (3572 in total) in each sample and technical replicate. Coloured squares represent Z-score intensity values, where the colour range (red, black green) represents the intensity range (high, moderate, low, respectively). (B) PCA plot demonstrating variance between each group and replicate.*

It was hypothesised that knockdown of a deubiquitinating enzyme would result in significant changes to the proteome. Furthermore, comparing the proteome of USP11 knockdown to control cells may reveal proteins regulated or deubiquitinated by USP11. To investigate this, volcano plots were generated, comparing the proteome of each knockdown cell line to the control (NTC), both in the presence and absence of E2. A volcano plot is a graphical method for visualising significant fold-changes in a data set. Fold change is plotted on the x-axis and significance on the y-axis.

As expected, a number of significant changes occurred in the proteome of USP11 knockdown cells in the presence of E2 (Figure 5.8, A). In unstimulated cells, changes were observed between knockdown and control cells, but only one of these changes were statistically significant (Figure 5.8, B).

A

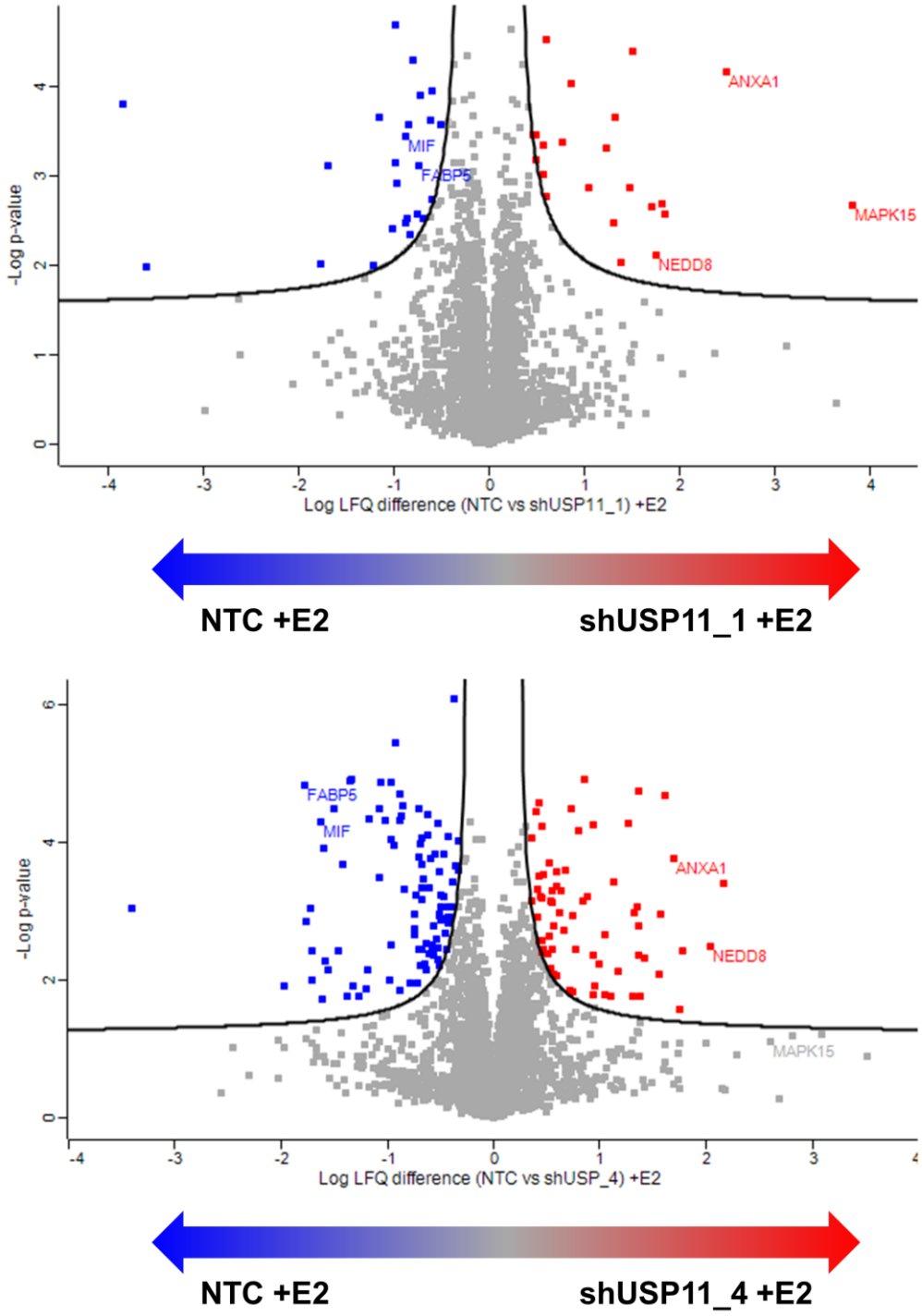

Figure 5.8: Knockdown of USP11 induced significant changes in the proteome in the presence of E2. *Red dots represent proteins upregulated in knockdown cells; blue dots represent proteins upregulated in NTC cells. Proteins of interest discussed below are labelled. Statistical analysis was performed using a two-sided t-test (unpaired), FDR was set to 5% (0.05).*

B

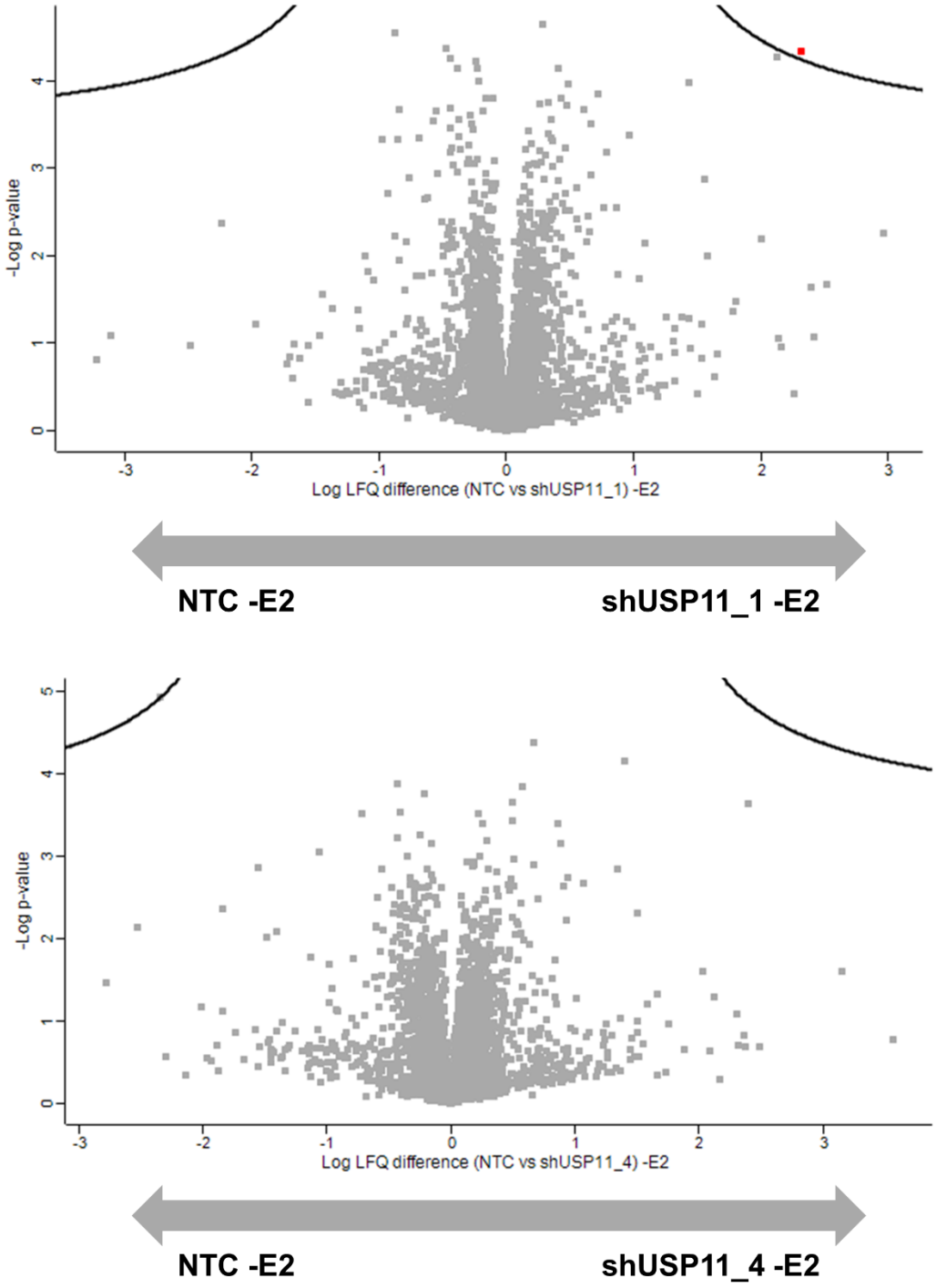

Figure 5.9: Knockdown of USP11 induced no significant changes in the proteome in the absence of E2. *The single red dot in NTC vs. shUSP11_1 represents the only protein significantly upregulated in shUSP11_1 cells (ANXA1). Statistical analysis was performed using a two-sided t-test (unpaired), FDR was set to 5% (0.05).*

First, proteins common to both shRNAs were analysed in order to eliminate any non-specific changes that may have occurred (Table 5.1). Annexin A1 (ANXA1) was significantly upregulated in both shUSP11_1 and shUSP11_4 in the presence of E2, and intriguingly, was the only significantly upregulated protein in shUSP11_1 in the absence of E2. ANXA1 is important in both the innate and adaptive immune response and is regulated by glucocorticoids (Perretti and D'Acquisto, 2009). Neural Precursor Cell Expressed, Developmentally Down-Regulated 8 (NEDD8), a ubiquitin like protein (60% sequence homology) involved in DNA-damage repair was also upregulated in both shRNAs.

Proteins upregulated in NTC cells, when compared to USP11 knockdown cells, could potentially be substrates of USP11. Of these proteins include macrophage migration inhibitory factor (MIF), a protein involved in the inflammatory pathway and cancer pathogenesis (O'Reilly et al., 2016) and fatty acid binding protein 5 (FABP5), which has been implicated in several cancer types, including breast (Powell et al., 2015). Validation is required to fully confirm if these proteins are direct USP11 substrates, however. A fill list of significantly upregulated proteins in all samples can be found in Appendix 4.

Table 5.1: Proteins significantly altered in both NTC vs. shUSP11_1 and NTC vs. shUSP11_4 +E2

Upregulated in NTC samples	Protein name	Upregulated in shUSP11 samples	Protein name
SERPINB6	Serpin Family B Member 6	**POLR1D**	RNA Polymerase I Subunit D
MUC6	Mucin 6	**APOD**	Apolipoprotein D
GGCT	Gamma-Glutamylcyclotransferase	**ANXA1**	Annexin A1
OAT	Ornithine Aminotransferase	**NEDD8**	Neural Precursor Cell Expressed, Developmentally Down-Regulated 8
HNRNPA1	Heterogeneous Nuclear Ribonucleoprotein A1	**AGR3**	Activity-regulated cytoskeleton-associated protein
MIF	Macrophage Migration Inhibitory Factor	**CORO2A**	Coronin, actin binding protein, 2A
HNRNPH3	Heterogeneous Nuclear Ribonucleoprotein H3	**GTPBP3**	GTP Binding Protein 3, Mitochondrial
TAGLN2	Transgelin 2	**TBC1D23**	TBC1 Domain Family Member 23
ERH	Enhancer of rudimentary homolog		
FABP5	Fatty acid-binding protein, epidermal		
DNAJC9	DnaJ homolog subfamily C member 9		
ABRACL	Costars family protein ABRACL		

Next, NTC samples were compared, both in the presence and absence of E2. As expected, a number of classic ERα target proteins were upregulated in E2 treated cells, such as TFF1, PgR and GREB1. Interestingly, many genes which were downregulated with USP11 knockdown in LCC1 cells, as determined by RNA-seq (Chapter 4), were upregulated at the protein level in E2 treated ZR-75-1 cells. These included UHRF1, NCAPH, NCAPG, a number of kinesin proteins, and importantly, TOP2A, which was the most significantly upregulated protein with E2 treatment (Figure 5.10).

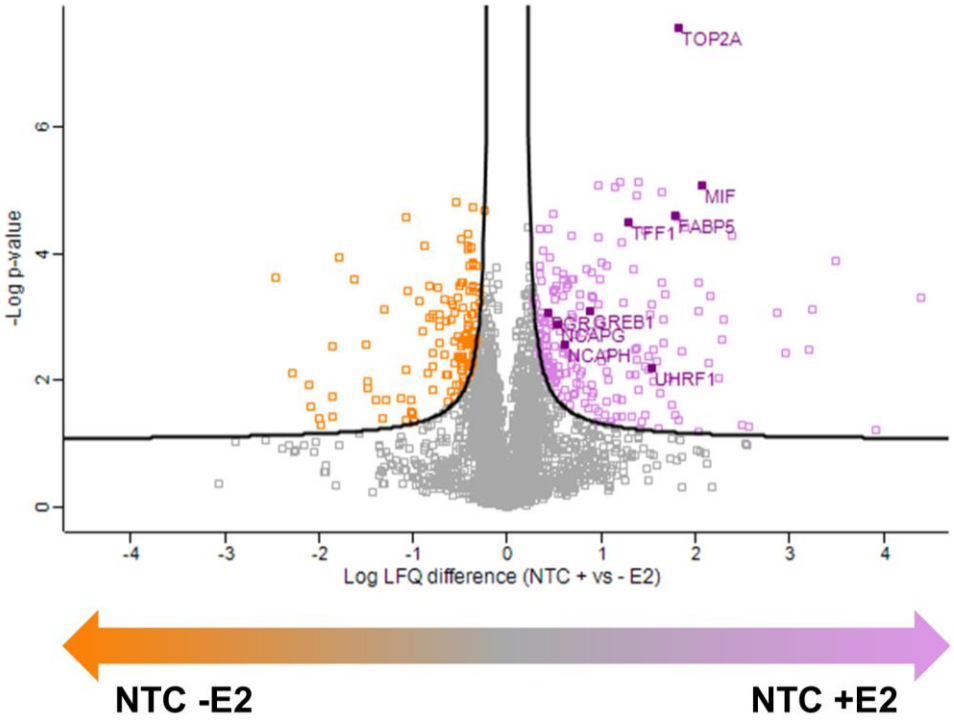

Figure 5.10: E2 induced significant changes in the proteome. *Purple dots represent proteins upregulated in ZR-75-1 NTC cells treated with E2; orange dots represent proteins upregulated in ZR-75-1 NTC untreated cells. Proteins of interest discussed below are labelled. Statistical analysis was performed using a two-sided t-test (unpaired), FDR was set to 5% (0.05).*

5.3.3 UbiScan®: USP11 ubiquitinome

IAP of ubiquitinated peptides, followed by LC-MS analysis was carried out in both USP11 knockdown and control BC cells. Unlike the proteome results, there were some initial issues with the MS run, with inconsistency among replicates and samples. First, two samples had a mayor outlier among technical replicates, possibly due to an error during the MS run. For this reason, technical duplicates instead of triplicates were considered. Second, the two individual shUSP11 samples clustered drastically different to each other, with shUSP11_4 showing a closer resemblance to NTC both in the presence and absence of E2 (data now shown). This was determined by hierarchical clustering. For ongoing analysis, shUSP11_1 was selected, because (i) the proteins clustered significantly different to the NTC, as expected and (ii) the known USP11 substrate, yH2AX, was ubiquitinated in USP11 knockdown cells.

First, a histogram was generated for each sample to examine the distribution of counts, as before. As observed in Figure 5.11, the counts for each sample are normally distributed. For analysis, missing values were imputed by values simulating noise around the detection limit, as highlighted by red bars on each histogram (Hein et al., 2015).

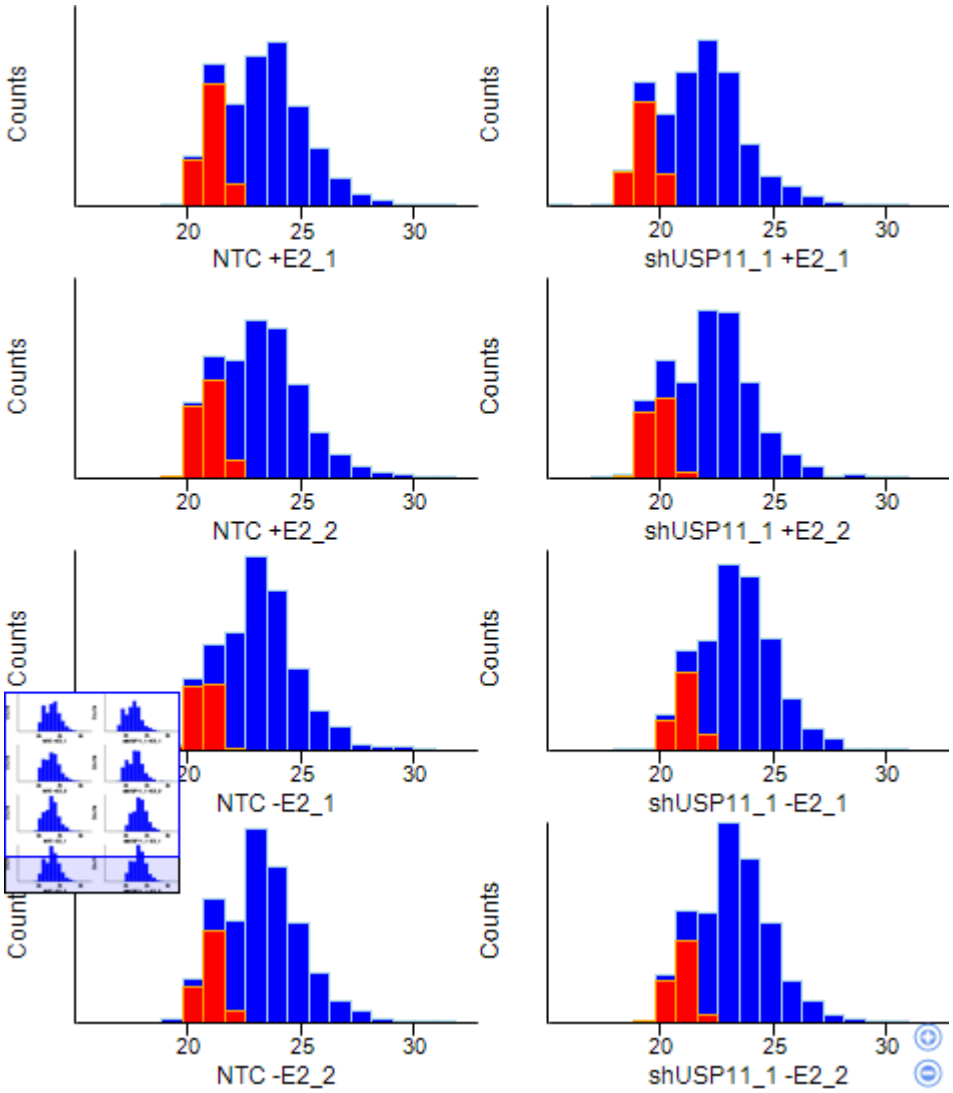

Figure 5.11: Ubiquitinome mass spectrometry counts were normally distributed for each sample. *Imputed values are highlighted in red.*

Hierarchical clustering of technical duplicates was carried out using Z score values generated from label-free quantification (LFQ) values (Figure 5.12). Again, grouping of E2 stimulated and unstimulated samples was also observed, highlighting the significant changes in ubiquitinated proteins induced by E2.

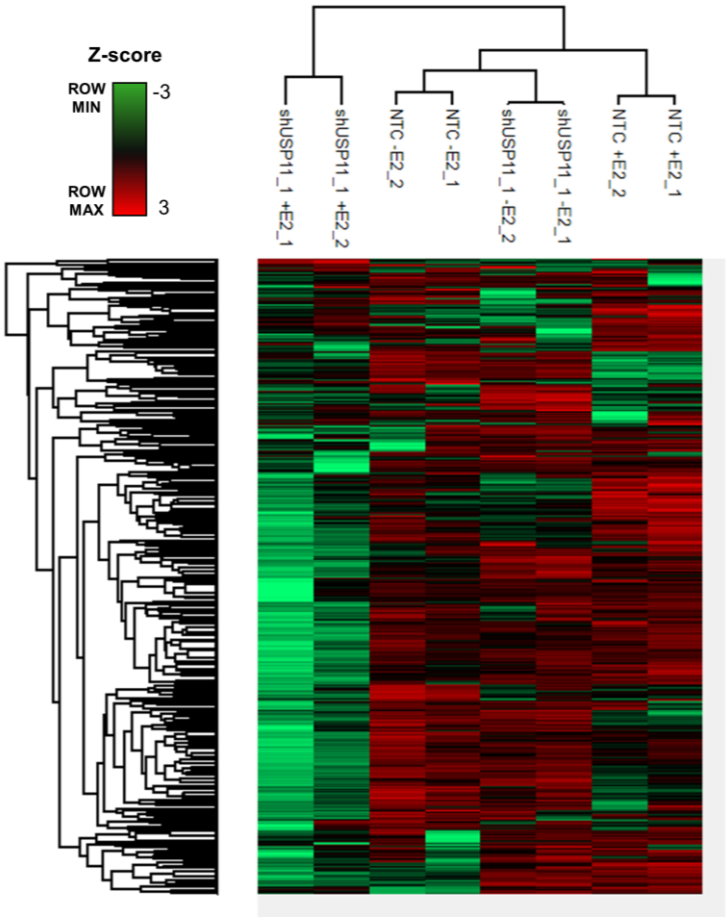

Figure 5.12: Mass spectrometry technical replicates were grouped together, as determined by intensity mapping. *Heatmap representing the intensity of each detected protein (1539 in total) in each sample and technical duplicate. Coloured squares represent Z-score intensity values, where the colour range (red, black green) represents the intensity range (high, moderate, low, respectively).*

Ubiquitinated proteins unique to USP11 knockdown cells could potentially represent novel substrates. To investigate this, volcano plots were generated, comparing the ubiquitinome of shUSP11_1 cells to the NTC cells, both in the presence and absence of E2. As with the proteome, the majority of significant changes occurred in the presence of E2. Reassuring, a known USP11 substrate, γH2AX (Yu et al., 2016) was detected in knockdown cells (Figure 5.13). The full USP11 ubiquitinome can be found in Appendix 6.

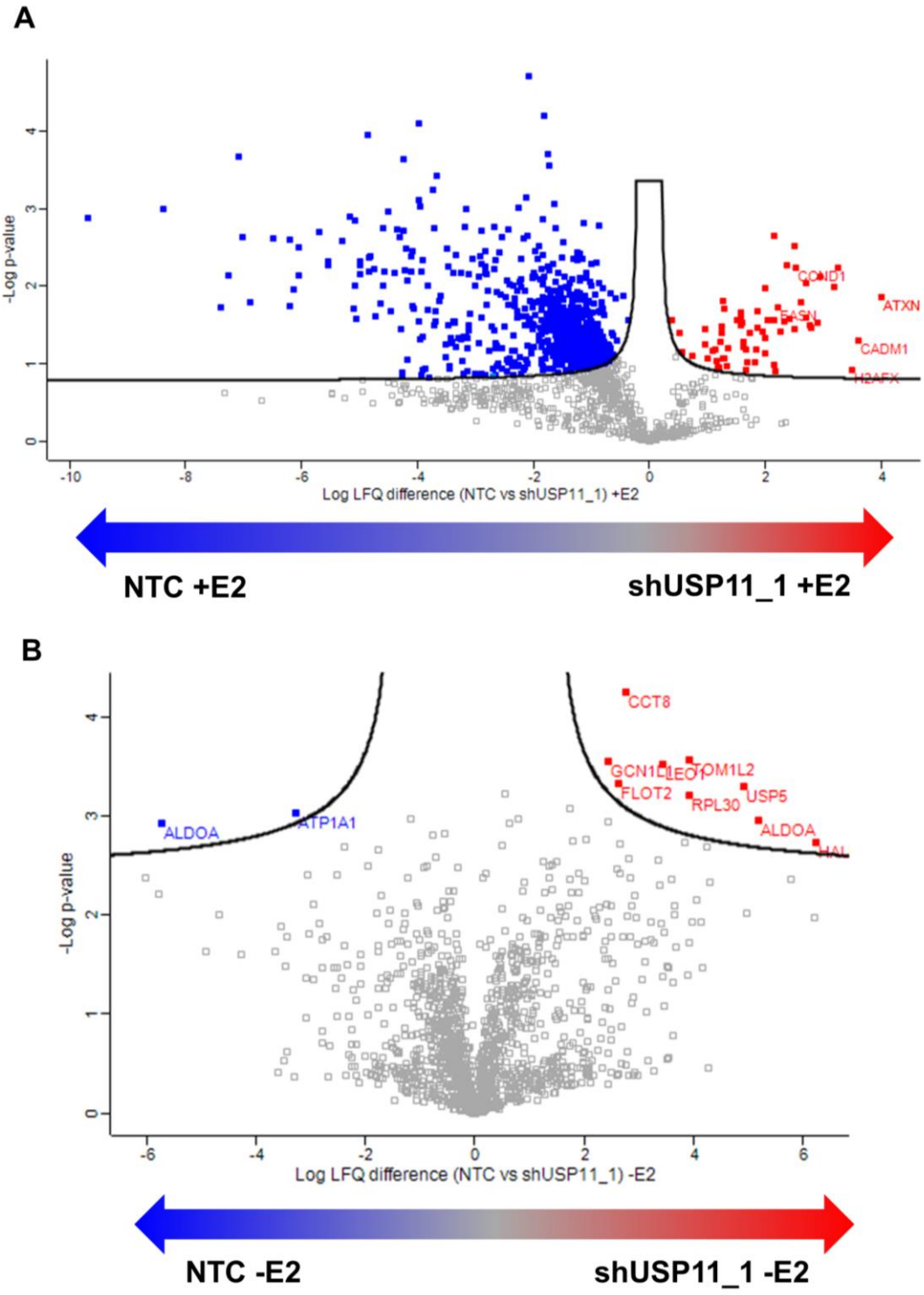

Figure 5.13: Knockdown of USP11 induced significant changes in the ubiquitinome. *Analysis was carried out in both (A) the presence and (B) the absence of E2. Red dots represent proteins upregulated in shUSP11_1 cells; blue dots represent proteins upregulated in NTC cells. Proteins of interest are labelled. Statistical analysis was performed using a two-sided t-test (unpaired), FDR was set to 5% (0.05).*

One of the main purposes of this experiment was to further elucidate the role of USP11 in ERα function by examining the USP11 ubiquitinome. In order to decipher a link between USP11 and the receptor, the proteins significantly upregulated in USP11 knockdown cells when compared to control cells (USP11 ubiquitinome) were uploaded to STRING (version 10.5), an online database used to detect known and putative protein-protein interactions. These proteins were uploaded along with ESR1 (ERα) to reveal any interactions. The STRING search revealed several known, putative, direct and indirect ERα interactors (Figure 5.14).

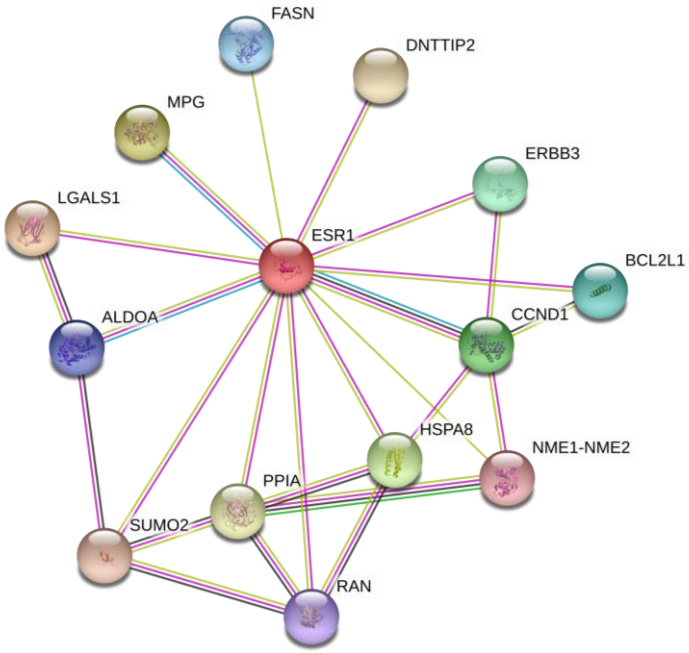

Figure 5.14: A search for protein-protein interactions using the online database STRING revealed several putative and known interactions between ERα and the USP11 ubiquitome.

Finally, using LFQ values from ZR-75-1 NTC cells, analysis of proteins ubiquitinated following E2 exposure was carried out. Interestingly, OTUB1, a known ERα DUB, was ubiquitinated in response to E2 (Figure 5.15).

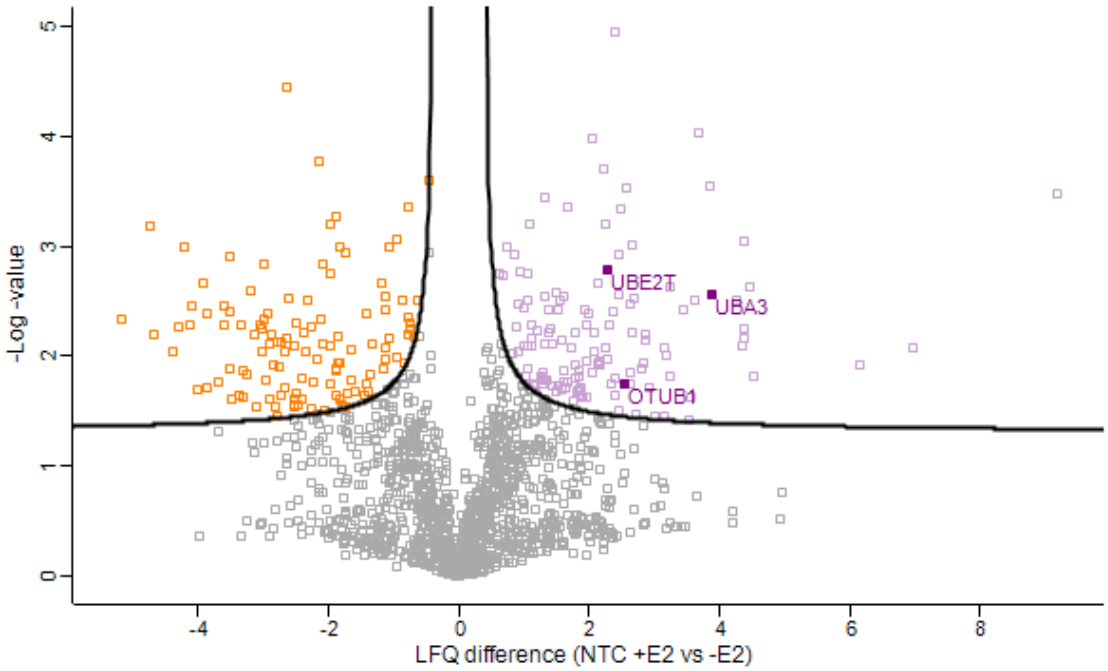

Figure 5.15: Both E2 treatment and E2 deprivation induced the ubiquitination of multiple proteins. *Purple dots represent proteins upregulated in ZR-75-1 NTC cells treated with E2; orange dots represent proteins upregulated in ZR-75-1 NTC untreated cells. Proteins of interest are labelled. Statistical analysis was performed using a two-sided t-test (unpaired), FDR was set to 5% (0.05).*

UbiScan® followed by LC-MS has revealed a number of interesting avenues to be explored regarding the role of USP11 in ERα function. With further investigation in to the proteins revealed by MS analysis of USP11 knockdown cells, it is anticipated the mechanism by which USP11 regulates ERα will be unveiled.

5.4 Discussion

Results Chapters 3 and 4 of this study provide evidence, never previously demonstrated, for a role for the DUB USP11 in ERα function in BC. Despite these key findings however, the nature of this role has yet to be elucidated. This chapter aimed to first explore and interaction between USP11 and ERα and second, investigate changes in the proteome and ubiquitinome induced by USP11 silencing.

Using IP techniques, the USP11 and ERα interaction was tested and under the conditions investigated, no direct interaction was detected. As a previous study had identified a USP11-ERα interaction (Stanisic et al., 2009), and the results presented in Chapter 3 and 4 highlighted a key role for USP11 in ERα function, these results were surprising. The aforementioned experiments were carried out under 24 hour E2 treatments. This time point was chosen as experiments in Chapter 3 confirmed an upregulation of USP11 in the nucleus of the cell at this time point. A transient interaction between USP11 and ERα may have been missed, however, and repetition of this experiment under different E2 time points is warranted as a result. Furthermore, the final experiment carried out, investigating the effect of USP11 knockout on ERα ubiquitination status, confirmed the advantage of using anti-ERα (D12) over anti-ERα (F10) antibody. Future IP experiments will carried out using the anti-ERα (D12) antibody, as well as investigating the use of a protein tag, such as HA or Myc, for immunoprecipitation.

Nevertheless, this chapter highlighted the significant changes that occur in the proteome and ubiquitinome in USP11 knockdown cells. The most intriguing finding perhaps, was that the majority of these significant changes only occur in the presence of E2, suggesting that USP11 function in ZR-75-1 cells is mainly estrogen-driven. While downstream validation of this large-scale proteomic experiment is required, a number of interesting proteins, potentially directly regulated by USP11, were significantly altered following USP11 knockdown.

First, the proteome of USP11 knockdown and control breast cancer cells was examined, both in the presence and absence of E2. Proteins common to both NTC vs. shUSP11_1 and NTC vs. shUSP11_4 were examined in order to eliminate any proteins that were non-specifically altered. ANXA1, a protein important in the immune response, was upregulated in the presence of E2 and was the only protein significantly upregulated in shUSP11_1 in the absence of E2. ANXA1 may have an oncogenic or tumour suppressing role, depending on the type of cancer cells and

tissues (Guo et al., 2013). Its role in BC is controversial, however, with conflicting evidence presented in the literature. A number of studies present differential ANXA1 localisation and expression in both histological and molecular subtypes of BC (Tu et al., 2017). The role of ANXA1 in the ZR-75-1 BC cell line model and its regulation by USP11 however, has yet to be defined. NEDD8, a Ub-like molecule, was upregulated in both knockdown cell lines in the presence of E2 and is a key protein in the DDR. The main NEDD8 substrates are the cullins, which act as molecular scaffolds for cullin RING Ub ligases (CRLs) and are involved in nucleotide excision repair and DNA damage cell checkpoint responses (Brown and Jackson, 2015). Both NEDD8 and neddylation have been associated with a number of different cancers (Wang et al., 2017b). It is unknown whether suppression of USP11, a key DNA-damage repair protein, has initiated upregulation of NEDD8 to repair DNA damage.

Mitogen-activated protein kinase 15 (MAPK15) was significantly upregulated in shUSP11_1 when compared to NTC, with a log LFQ difference of almost four-fold. A similar trend was also observed in shUSP11_4 cells, although upregulation of MAPK15 was not significant. Interestingly, a previous study by Chia *et al.* suggests that MAPK15 downregulation activates cell motility. The same study suggests that MAPK15 expression is reduced in both breast and lung cancer, when compared to normal tissue (Chia et al., 2014). If downregulation of MAPK15 is oncogenic, upregulation of MAPK15 as a result of USP11 silencing would be valuable in a clinical setting. More research is required to confirm this, however.

Proteins upregulated in NTC cells when compared to knockdown cells are potential novel USP11 substrates, and will be confirmed with downstream validation. The presence of these proteins in NTC cells and not shUSP11 cells suggests that they may have been deubiquitinated and stabilised in NTC cells. A number of interesting proteins were detected, one of which was MIF. MIF is a cytokine involved in the innate and adaptive immune response (O'Reilly et al., 2016) and is involved in BC pathways. Previously, MIF was found to be upregulated in BC tissue and induce angiogenesis. (Xu et al., 2008). Furthermore, MIF is stabilised by HSP90 in cancer cells and may be targeted with inhibition of this chaperone protein. This is of great relevance to this study, as ERα function is also regulated by HSP90 (O'Reilly et al., 2016). This provides support for the investigation in to the role of USP11 in HSP90 function, which could be a mechanism by which USP11 regulates ERα.

FABP5 was also upregulated in NTC samples. FABP5 binds and stores long chain fatty acids and is overexpressed in multiple tumour types (Levi et al., 2013). FABP5 is important in PPARβ/δ activation in BC and promotes proliferation in BC cells by induction of EGFR (Levi et al., 2013). Importantly, FABP5 is strongly associated with TNBC and was found to be associated with high grade cancers and worse survival following staining of a 423-patient TMA. Furthermore, FABP5 promotes metastasis in TNBC cells through EGFR stabilisation (Powell et al., 2015). During the study presented here in this thesis, USP11 was found to be upregulated in TNBC cell lines, but as this was beyond the scope of this project, no further analysis was carried out. Investigating the role of USP11 in FABP5 function in TNBC may be in interesting avenue to explore.

Perhaps the most interesting observation regarding MIF and FABP5 it that both proteins are significantly upregulated following E2 treatment in ZR-75-1 NTC cells, suggesting regulation by ERα. Downregulation of these proteins in USP11 knockdown cells may be a result of supressed ERα activity in these cells, supporting the role of USP11 in ERα transcriptional activity.

Proteins significantly altered in the presence of E2 were also examined in ZR-75-1 NTC cells. Reassuringly, a number of classic ERα target proteins were upregulated in the presence of E2, such as PgR, GREB1 and TFF1. Interestingly, a number of proteins, which were found to be downregulated at the mRNA level with USP11 knockdown in Chapter 4, were upregulated with E2 treatment in ZR-75-1 cells (29 in total). These included NCAPH and NCAPG, members of the condensin complex; UHRF1, a multifunctional methytransferase and E3 ligase implemented in BC progression (Gao et al., 2017); a number of kinesin motor proteins and importantly to this study, TOP2A . TOP2A, as mentioned previously, encodes topoisomerase II which is a key part of transcriptional machinery. TOP2A mRNA was downregulated with USP11 knockdown in LCC1 cells, as confirmed by RNA-seq and qRT-PCR in Chapter 4. Intriguingly, it was the third most significantly downregulated gene in LCC1 cells following RNA-seq analysis, suggesting a key role for USP11 in TOP2A function. Furthermore, mitoxantrone, a chemotherapeutic and TOP2A inhibitor, inhibits USP11 enzymatic function, further supporting a role for USP11 in TOP2A function. TOP2A expression is significantly associated with poor survival in ERα+ BC patients (Sparano et al., 2012) and USP11 is likely to be a significant player in its oncogenic function.

Using PTMScan® the ubiquitinome of USP11 knockdown and control cells was analysed. As discussed, preliminary issues with the MS run resulted in only one USP11 knockdown cell line, shUSP11_1, being used in further analysis. Reassuringly, a known USP11 substrate, γH2AX (Yu et al., 2016), was ubiquitinated in these knockdown cells and represents a reliable positive control.

Once again, the majority of significant changes occurred in presence of E2. This suggests the DUB function of USP11 in ZR-75-1 BC cells is largely dependent on E2 and ERα function. Unlike the proteome however, there are several proteins significantly ubiquitinated in USP11 in the absence of E2. USP5 ubiquitination is significantly upregulated in knockdown cells in both the presence and absence of E2. USP5 has been recognised as an oncogene in both hepatocellular carcinoma (Liu et al., 2017) and pancreatic cancer (Kaistha et al., 2017) and may be an interesting avenue to explore in BC.

Of particular interest to this study are the proteins ubiquitinated in knockdown cells in the presence in E2. These proteins, which are ubiquitinated in the absence of USP11, may represent novel USP11 substrates and may provide a link between USP11 and ERα. Fascinatingly, Cyclin D1 (CCND1) is ubiquitinated in knockdown cells. As mentioned in Chapter 4, Cyclin D1 is a well-described ERα target gene and is upregulated in over half of BCs. Suppression of USP11 and as a result, Cyclin D1 expression by ubiquitination, may be favourable in the treatment of ERα+ BC.

Perhaps the most interesting protein found to be ubiquitinated in USP11 knockdown cells is fatty acid synthase (FASN). FASN is an enzymatic system which catalyses the synthesis of palmitate into long-chain fatty acids and is upregulated in many human cancers (Menendez and Lupu, 2017). Recently, FASN was found to regulate USP11 by inducing PI3K-S6Kinase signalling, which in turn phosphorylates USP11 and augments its interaction with eukaryotic initiation factor 4B (eIF4B). This pathway promotes oncogenesis in large B-cell lymphoma (Kapadia et al., 2018) and whether this translates to BC has yet to be investigated. USP11 may deubiquitinate FASN to support its oncogenic role in BC. Interestingly, FASN can regulate ERα signalling. Previously, FASN inhibition has been shown to decrease the amount of E2 needed for optimal ERα activation, suppress BC cell proliferation and colony formation and reduce the protein expression of ERα (Menendez and Lupu, 2017). A FASN/ERα fusion transcript is also present in many cancer cell lines, including breast MCF7 cells. Further investigation is required to confirm the interplay between

USP11, ERα and FASN, however evidence in the literature points towards a strong interaction.

This chapter has provided many new avenues to explore the role of USP11 in BC. Ultimately, it is anticipated that further analysis and validation of the presented MS data will reveal some clue as to how USP11 positively regulates ERα function. The aforementioned proteins of interest may represent novel regulators of E2-driven pathways in BC cells and these will be explored as this project progresses.

Chapter 6: General Discussion

6.1 Overview

While our understanding and management of BC is now better than ever, over half a million women worldwide lose their lives to this disease every year (WHO). Despite improvements in treatment options, resistance to chemotherapeutics and targeted agents remains a clinically significant problem. To overcome this, a better understanding of the molecular drivers behind BC pathogenesis and treatment resistance is urgently required. Our knowledge of ERα function in BC has vastly improved in recent years, however, translating this knowledge in to the clinical setting has proved challenging. For this reason, further elucidation of the molecular mechanisms that control ERα activation in breast, and other cancers, may provide exciting new therapeutic opportunities.

With the success of proteasome inhibition in the clinic (Bold, 2004, Fostier et al., 2012), the Ub-proteasome system is becoming an attractive area of therapeutic intervention, and as DUBs are often differentially expressed or activated in tumours, much of the focus has shifted in this direction (Pal et al., 2014). As most DUBs are cysteine proteases (Shi and Grossman, 2010), a well-researched class of pharmacological targets, it may be feasible to construct specific inhibitors of these enzymes. In this context, there are a number of pre-clinical DUB inhibitors in development, for example WP1130, a non-specific inhibitor of USP9x, USP5 and USP14 which induces apoptosis and enhances response to chemotherapy (Chauhan et al., 2012) and FT671, a newly developed, specific inhibitor of USP7 which results in stabilisation of p53 and induction of apoptosis (Turnbull et al., 2017). As we further interpret the role of DUBs in both physiological and oncogenic pathways, the coming years may see rise some exciting advances in DUB drug discovery (Harrigan et al., 2018). It is anticipated, with further evidence to support this current study, that USP11 will be considered in the DUB drug discovery pipeline.

6.2 Summary of key findings

This project outlines, for the first time, the role of the deubiquitinase USP11 in ERα function. Functional genomic screening, examining the effect of DUB knockdown on ERα transcriptional activity, identified a role for the key DNA-damage DUB USP11 in ERα regulation. This study sought to determine the role of USP11 in ERα+ BC cells, the mechanism behind this role, and importantly, the prognostic relevance of USP11 in the oncology clinic.

In Chapter 3, validation of the loss-of-function screen was carried out using RNAi-mediated silencing of USP11 in ZR-75-1 BC cells, where repressed ERα activity was confirmed by the downregulation of *PgR* and reduced activity at an ERE reporter. E2 stimulation led to an increase in USP11 expression in the cell nucleus, as well as the formation of distinct USP11 nuclear foci. USP11 knockdown slowed the growth of ZR-75-1 cells, however no significant changes to the cell cycle occurred. These results were further validated in HEK293T USP11 CRISPR knockout cells ectopically expressing ERα.

In silico analysis of a publicly available BC dataset revealed a significant association between high USP11 expression and poor prognosis in ERα+ patients. This was further supported in the laboratory by IHC staining of a BC patient TMA, where high expression of USP11 was significantly associated with poor OS and BCSS. This suggests that USP11 is a poor prognostic marker in ERα+ BC, although validation in a larger cohort is required to fully conclude this.

Chapter 4 revealed an intriguing role for USP11 in a ligand-independent setting. USP11 expression was increased in both LCC1 and LCC9 cell lines, when compared to parental MCF7 cells. USP11 knockdown resulted in decreased mRNA expression of a panel of ERα target genes in LCC1 cells only, which are estrogen-independent but remain dependant on ERα for growth. Furthermore, USP11 knockdown in LCC1 cells resulted in suppression of cell cycle-associated genes, such as those involved in mitosis and chromosome segregation. A significant number of genes downregulated with USP11 knockdown in LCC1 cells were also identified as ERα-target genes, as determined by comparison to publicly available datasets. Importantly, this phenotype was not observed in USP11 knockdown LCC9 cells, which do not depend on ERα as demonstrated by their anti-endocrine resistance.

Finally in Chapter 5, IP of ERα revealed no interaction with USP11, suggesting the role USP11 plays in ERα activity is either transient or indirect. USP11 knockout in HEK293T cells had no effect on ERα ubiquitination status, suggesting USP11 does not directly deubiquitinate the receptor; however, further validation is required to determine this. In order to reveal novel substrates of USP11, the full proteome and ubiquitinome of both USP11 knockdown and control ZR-75-1 cells was analysed by LC-MS. Knockdown of USP11 resulted in significant changes to the proteome, and intriguingly, this only occurred in the presence of E2. Analysis of the

USP11 ubiquitinome has revealed a number of interesting proteins which will be investigated and validated during the completion of this project, with the hope of elucidating the mechanism by which USP11 regulates ERα.

6.3 Current hypotheses and future work

This study provides preliminary evidence for the role of USP11 in ERα transcriptional activity, however, there are a number of future experiments warranted to fully define the role of USP11 in this setting. Here, a number of different hypotheses will be discussed, which will address the potential mechanistic, prognostic, and therapeutic roles of USP11 in ERα+ BC.

6.3.1 Mechanistic

First, the mechanism by which USP11 positively regulates ERα has yet to be discovered. It is hoped, through the validation and interpretation of the USP11 ubiquitinome, an indication as to how USP11 affects receptor function will be revealed. At present, a number of different hypotheses have been considered.

Perhaps the most straightforward hypothesis is that USP11 deubiquitinates ERα, prevents degradation and as a result, enhances activation. Although preliminary results presented here would not suggest this, a transient interaction may have been missed, and as activated ERα cycles rapidly this occurrence is likely. To investigate this, ERα-USP11 co-IPs will be repeated under different E2 time points, using the proteasome inhibitor MG132 to prevent degradation of ubiquitinated proteins. If USP11 deubiquitinates ERα, ERα-Ub will be higher in knockout cells. Additionally, knockdown of USP11 had no effect on ERα expression in BC cells. However, ERα can be rapidly re-translated following receptor degradation. To prevent this, knockdown and control cells will be simultaneously treated at different time points with E2 and cycloheximide, a protein synthesis inhibitor produced by *S. griseus*. If USP11 deubiquitinates ERα, ERα expression will be lower in USP11 silenced cells.

A second hypothesis to be considered is that USP11 affects the acetylation/ubiquitination balance of ERα. As mentioned in Chapter 1, BRCA1 can repress ERα acetylation via the coactivator p300, while BRCA1/BARD1 represses ERα activity via monoubiquitination at K302 (Ma et al., 2010). It is hypothesised that USP11 removes this monoubiquitin from ERα, allowing the receptor to be acetylated

and activated. To test this, ERα will be immunoprecipitated and acetylated lysine will be detected by Western blotting in both USP11 silenced and control cells. Detecting the exact site of any PTM can be challenging, however.

To date, the best described function of USP11 is its role in the HR DNA-damage repair pathway. Previous studies have confirmed the role of USP11 in both BRCA1 and BRCA2 function (Orthwein et al., 2015, Schoenfeld et al., 2004). Mutations in BRCA tumour suppressing proteins result in impaired DNA damage repair and genomic instability, however, why this leads to increased risk of cancer in estrogen-responsive tissues only remains elusive. Both oophorectomy and tamoxifen treatment reduce the risk of cancer in BRCA mutation carriers, highlighting the importance of estrogen and ERα in the initiation of BC in a BRCA mutant setting (Wang and Di, 2014). Estrogen induces DNA damage breaks and may be one of the primary mechanisms by which it contributes to BC initiation and progression (Caldon, 2014). This estrogen-induced DNA damage, combined with impaired BRCA function, may be a likely explanation as to why BRCA mutant carriers have an increased risk of breast and ovarian cancers. It is now thought that DSBs are essential for transcriptional activation of ERα and the initiation of transcriptional programs require the generation of these breaks and the recruitment of DDR proteins (Haffner et al., 2011). The interplay of USP11 here is worth consideration as it is likely USP11 is recruited to DSB sites and contributes towards the initiation of ERα transcription, as a result. To test this, the ICC experiments presented in this thesis will be repeated to include ERα and γH2AX localisation. It is hypothesised that USP11 and ERα will colocalise at sites of DNA damage.

Finally, results obtained from the DUB-null mutant study suggest that the role USP11 plays in ERα function is not dependent on DUB enzymatic activity, although further investigation is warranted. If this be the case, the formation of a USP11 protein-protein complex may positively regulate ERα function. In Chapter 4, USP11 was shown to positively regulate TOP2A, with knockdown suppressing mRNA expression. Interestingly in Chapter 5, TOP2A protein expression was significantly upregulated in E2 treated ZR-75-1 cells. TOP2A is also a poor prognostic marker in ERα+ BC, further highlighting the regulation of this gene by ERα (Sparano et al., 2012). Mitoxantrone, like other chemotherapeutics, targets topoisomerase II, and was also found to inhibit USP11 enzymatic function (Burkhart et al., 2013). From this evidence, one can speculate that USP11 may form a complex with topoisomerase II

α and engage in a positive feedback loop to regulate ERα. Topoisomerase II may also be involved in inducing DNA damage to initiate ERα transcriptional activity.

6.3.2 Prognostic

Clinical data presented in Chapter 3 suggests that USP11 is a poor prognostic marker in ERα+ BC, however validation in a larger cohort of patients is required to fully conclude this statement. To address this, a 498 patient consecutive TMA, consisting of invasive BC patients diagnosed at Malmö University Hospital, Sweden, was stained. In order to improve staining quality and eliminate background, the USP11 antibody and IHC protocol was re-optimised at the Department of Pathology, Beaumont Hospital. In the coming weeks, this array will be scored and USP11 expression will be analysed in the 378 ERα+ patients. It is hypothesised that these results will further support the clinical data presented in this thesis, recognising USP11 as a poor prognostic marker in ERα+ BC.

6.3.3 Therapeutic

At present, a specific inhibitor to USP11 is not available. A study by Burkhart *et al*. screened 2000 FDA-approved compounds for USP11 inhibition and identified six active compounds, including mitoxantrone. Mitoxantrone is a chemotherapeutic used to treat leukaemia, non-Hodgkin's lymphoma, prostate cancer unresponsive to endocrine therapy and metastatic BC (CRUK, 2017b). Mitoxantrone functions by inhibition of type II topoisomerase and DNA synthesis. In the aforementioned study, mitoxantrone impacted the growth of pancreatic ductal adenocarcinoma (PDA) cell lines in a USP11 dependant manner. As mentioned, the results presented in Chapter 4 indicate that USP11 regulates TOP2A in a positive manner. It is hypothesised that USP11 expression is a predictive marker of mitoxantrone response and may be a useful tool in the management of BC. To test this, BC cell lines will be treated with mitoxantrone to test if response is correlated with USP11 expression.

Additionally, USP11 inhibition combined with PARP inhibition in BRCA wild type BC may be an exciting therapeutic approach. In January 2018, the PARP inhibitor olaparib was FDA approved for the treatment of BRCA-mutant, HER2-metastatic BC (AstraZeneca, 2018). It is already known that the efficacy of PARP inhibition is enhanced with USP11 silencing (Wiltshire et al., 2010, Orthwein et al., 2015). To test this, USP11 knockdown in combination with olaparib will be tested in

both BRCA mutant and wild type BC cell lines. The effect of ERα dependence on the outcome of this experiment will also be considered. It is hypothesised that USP11 silencing and PARP inhibition will be synthetically lethal in BRCA wild type cells (where response to olaparib alone is poor), and that ERα+ cell lines will demonstrate a better response.

6.3 Conclusion

This study highlights, for the first time, the role of USP11 in ERα transcriptional activity in BC. It is hoped, with further research to support these findings, that USP11 may be considered as a biomarker and therapeutic target in endocrine-driven BC. Ultimately, USP11 inhibition may enhance response to currently available anti-cancer agents and may open new avenues for the management and treatment of this complex disease.

References

ABDUL REHMAN, S. A., KRISTARIYANTO, Y. A., CHOI, S. Y., NKOSI, P. J., WEIDLICH, S., LABIB, K., HOFMANN, K. & KULATHU, Y. 2016. MINDY-1 Is a Member of an Evolutionarily Conserved and Structurally Distinct New Family of Deubiquitinating Enzymes. *Mol Cell,* 63**,** 146-55.

AL-HAKIM, A. K., ZAGORSKA, A., CHAPMAN, L., DEAK, M., PEGGIE, M. & ALESSI, D. R. 2008. Control of AMPK-related kinases by USP9X and atypical Lys(29)/Lys(33)-linked polyubiquitin chains. *Biochem J,* 411**,** 249-60.

AL-SALIHI, M. A., HERHAUS, L., MACARTNEY, T. & SAPKOTA, G. P. 2012. USP11 augments TGFbeta signalling by deubiquitylating ALK5. *Open Biol.* England.

AMERIK, A. Y. & HOCHSTRASSER, M. 2004. Mechanism and function of deubiquitinating enzymes. *Biochim Biophys Acta,* 1695**,** 189-207.

ANBALAGAN, M. & ROWAN, B. G. 2015. Estrogen receptor alpha phosphorylation and its functional impact in human breast cancer. *Mol Cell Endocrinol,* 418 Pt 3**,** 264-72.

ANZICK, S. L., KONONEN, J., WALKER, R. L., AZORSA, D. O., TANNER, M. M., GUAN, X. Y., SAUTER, G., KALLIONIEMI, O. P., TRENT, J. M. & MELTZER, P. S. 1997. AIB1, a steroid receptor coactivator amplified in breast and ovarian cancer. *Science,* 277**,** 965-8.

ASHBURNER, M., BALL, C. A., BLAKE, J. A., BOTSTEIN, D., BUTLER, H., CHERRY, J. M., DAVIS, A. P., DOLINSKI, K., DWIGHT, S. S., EPPIG, J. T., HARRIS, M. A., HILL, D. P., ISSEL-TARVER, L., KASARSKIS, A., LEWIS, S., MATESE, J. C., RICHARDSON, J. E., RINGWALD, M., RUBIN, G. M. & SHERLOCK, G. 2000. Gene ontology: tool for the unification of biology. The Gene Ontology Consortium. *Nat Genet,* 25**,** 25-9.

ASTRAZENECA. 2017. *Faslodex receives US FDA approval as monotherapy for expanded use in breast cancer* [Online]. [Accessed 3rd March 2018].

ASTRAZENECA. 2018. *Lynparza approved by US FDA in germline BRCA-mutated metastatic breast cancer* [Online]. [Accessed 21st March 2018].

BADVE, S., DABBS, D. J., SCHNITT, S. J., BAEHNER, F. L., DECKER, T., EUSEBI, V., FOX, S. B., ICHIHARA, S., JACQUEMIER, J., LAKHANI, S. R., PALACIOS, J., RAKHA, E. A., RICHARDSON, A. L., SCHMITT, F. C., TAN,

P. H., TSE, G. M., WEIGELT, B., ELLIS, I. O. & REIS-FILHO, J. S. 2011. Basal-like and triple-negative breast cancers: a critical review with an emphasis on the implications for pathologists and oncologists. *Mod Pathol,* 24**,** 157-67.

BAIRD, R. D. & CARROLL, J. S. 2016. Understanding Oestrogen Receptor Function in Breast Cancer and its Interaction with the Progesterone Receptor. New Preclinical Findings and their Clinical Implications. *Clin Oncol (R Coll Radiol),* 28**,** 1-3.

BASELGA, J., CORTES, J., KIM, S. B., IM, S. A., HEGG, R., IM, Y. H., ROMAN, L., PEDRINI, J. L., PIENKOWSKI, T., KNOTT, A., CLARK, E., BENYUNES, M. C., ROSS, G. & SWAIN, S. M. 2012. Pertuzumab plus trastuzumab plus docetaxel for metastatic breast cancer. *N Engl J Med,* 366**,** 109-19.

BERG, J. M., TYMOCZKO, J. L. & STRYER, L. 2007. *Biochemistry,* New York, W. H. Freeman and Company.

BERNARDS, R., BRUMMELKAMP, T. R. & BEIJERSBERGEN, R. L. 2006. shRNA libraries and their use in cancer genetics. *Nat Methods,* 3**,** 701-6.

BJORNSTROM, L. & SJOBERG, M. 2005. Mechanisms of estrogen receptor signaling: convergence of genomic and nongenomic actions on target genes. *Mol Endocrinol,* 19**,** 833-42.

BLACKWELL, K. L., BURSTEIN, H. J., STORNIOLO, A. M., RUGO, H. S., SLEDGE, G., AKTAN, G., ELLIS, C., FLORANCE, A., VUKELJA, S., BISCHOFF, J., BASELGA, J. & O'SHAUGHNESSY, J. 2012. Overall survival benefit with lapatinib in combination with trastuzumab for patients with human epidermal growth factor receptor 2-positive metastatic breast cancer: final results from the EGF104900 Study. *J Clin Oncol,* 30**,** 2585-92.

BOLD, R. 2004. "Development of the proteasome inhibitor Velcade (Bortezomib)" by Julian Adams, Ph.D., and Michael Kauffman, M.D., Ph.D. *Cancer Invest,* 22**,** 328-9.

BRANDAU, O., NYAKATURA, G., JEDELE, K. B., PLATZER, M., ACHATZ, H., ROSS, M., MURKEN, J., ROSENTHAL, A. & MEINDL, A. 1998. UHX1 and PCTK1: precise characterisation and localisation within a gene-rich region in Xp11.23 and evaluation as candidate genes for retinal diseases mapped to Xp21.1-p11.2. *Eur J Hum Genet,* 6**,** 459-66.

BREASTCANCER.ORG. 2017. *Treatment and side effects* [Online]. [Accessed 1st March 2018].

BREASTCHECK. 2018. *Breast screening* [Online]. [Accessed 13th March 2018].

BRENNAN, D. J., REXHEPAJ, E., O'BRIEN, S. L., MCSHERRY, E., O'CONNOR, D. P., FAGAN, A., CULHANE, A. C., HIGGINS, D. G., JIRSTROM, K., MILLIKAN, R. C., LANDBERG, G., DUFFY, M. J., HEWITT, S. M. & GALLAGHER, W. M. 2008. Altered cytoplasmic-to-nuclear ratio of survivin is a prognostic indicator in breast cancer. *Clin Cancer Res,* 14**,** 2681-9.

BROWN, J. S. & JACKSON, S. P. 2015. Ubiquitylation, neddylation and the DNA damage response. *Open Biol,* 5**,** 150018.

BROWNE, A. L., CHARMSAZ, S., VARESLIJA, D., FAGAN, A., COSGROVE, N., COCCHIGLIA, S., PURCELL, S., WARD, E., BANE, F., HUDSON, L., HILL, A. D., CARROLL, J. S., REDMOND, A. M. & YOUNG, L. S. 2018. Network analysis of SRC-1 reveals a novel transcription factor hub which regulates endocrine resistant breast cancer. *Oncogene*.

BRUMMELKAMP, T. R., NIJMAN, S. M., DIRAC, A. M. & BERNARDS, R. 2003. Loss of the cylindromatosis tumour suppressor inhibits apoptosis by activating NF-kappaB. *Nature,* 424**,** 797-801.

BRUNNER, N., BOULAY, V., FOJO, A., FRETER, C. E., LIPPMAN, M. E. & CLARKE, R. 1993. Acquisition of hormone-independent growth in MCF-7 cells is accompanied by increased expression of estrogen-regulated genes but without detectable DNA amplifications. *Cancer Res,* 53**,** 283-90.

BRUNNER, N., BOYSEN, B., JIRUS, S., SKAAR, T. C., HOLST-HANSEN, C., LIPPMAN, J., FRANDSEN, T., SPANG-THOMSEN, M., FUQUA, S. A. & CLARKE, R. 1997. MCF7/LCC9: an antiestrogen-resistant MCF-7 variant in which acquired resistance to the steroidal antiestrogen ICI 182,780 confers an early cross-resistance to the nonsteroidal antiestrogen tamoxifen. *Cancer Res,* 57**,** 3486-93.

BUNONE, G., BRIAND, P. A., MIKSICEK, R. J. & PICARD, D. 1996. Activation of the unliganded estrogen receptor by EGF involves the MAP kinase pathway and direct phosphorylation. *Embo j,* 15**,** 2174-83.

BURKHART, R. A., PENG, Y., NORRIS, Z. A., THOLEY, R. M., TALBOTT, V. A., LIANG, Q., AI, Y., MILLER, K., LAL, S., COZZITORTO, J. A., WITKIEWICZ, A. K., YEO, C. J., GEHRMANN, M., NAPPER, A., WINTER, J. M., SAWICKI,

J. A., ZHUANG, Z. & BRODY, J. R. 2013. Mitoxantrone targets human ubiquitin-specific peptidase 11 (USP11) and is a potent inhibitor of pancreatic cancer cell survival. *Mol Cancer Res,* 11**,** 901-11.

CALDON, C. E. 2014. Estrogen signaling and the DNA damage response in hormone dependent breast cancers. *Front Oncol,* 4**,** 106.

CARASCOSSA, S., DUDEK, P., CENNI, B., BRIAND, P. A. & PICARD, D. 2010. CARM1 mediates the ligand-independent and tamoxifen-resistant activation of the estrogen receptor alpha by cAMP. *Genes Dev,* 24**,** 708-19.

CARLSON, R. W. 2005. The history and mechanism of action of fulvestrant. *Clin Breast Cancer,* 6 Suppl 1**,** S5-8.

CAROLAN, B. J., HEGUY, A., HARVEY, B. G., LEOPOLD, P. L., FERRIS, B. & CRYSTAL, R. G. 2006. Up-regulation of expression of the ubiquitin carboxyl-terminal hydrolase L1 gene in human airway epithelium of cigarette smokers. *Cancer Res,* 66**,** 10729-40.

CARROLL, J. S., HICKEY, T. E., TARULLI, G. A., WILLIAMS, M. & TILLEY, W. D. 2017. Deciphering the divergent roles of progestogens in breast cancer. *Nat Rev Cancer,* 17**,** 54-64.

CHASTAGNER, P., ISRAEL, A. & BROU, C. 2006. Itch/AIP4 mediates Deltex degradation through the formation of K29-linked polyubiquitin chains. *EMBO Rep,* 7**,** 1147-53.

CHAUHAN, D., TIAN, Z., NICHOLSON, B., KUMAR, K. G., ZHOU, B., CARRASCO, R., MCDERMOTT, J. L., LEACH, C. A., FULCINNITI, M., KODRASOV, M. P., WEINSTOCK, J., KINGSBURY, W. D., HIDESHIMA, T., SHAH, P. K., MINVIELLE, S., ALTUN, M., KESSLER, B. M., ORLOWSKI, R., RICHARDSON, P., MUNSHI, N. & ANDERSON, K. C. 2012. A small molecule inhibitor of ubiquitin-specific protease-7 induces apoptosis in multiple myeloma cells and overcomes bortezomib resistance. *Cancer Cell,* 22**,** 345-58.

CHEN, S. T., OKADA, M., NAKATO, R., IZUMI, K., BANDO, M. & SHIRAHIGE, K. 2015. The Deubiquitinating Enzyme USP7 Regulates Androgen Receptor Activity by Modulating Its Binding to Chromatin. *J Biol Chem,* 290**,** 21713-23.

CHENG, J., ZHANG, C. & SHAPIRO, D. J. 2007. A functional serine 118 phosphorylation site in estrogen receptor-alpha is required for down-

regulation of gene expression by 17beta-estradiol and 4-hydroxytamoxifen. *Endocrinology,* 148**,** 4634-41.

CHIA, J., THAM, K. M., GILL, D. J., BARD-CHAPEAU, E. A. & BARD, F. A. 2014. ERK8 is a negative regulator of O-GalNAc glycosylation and cell migration. *Elife,* 3**,** e01828.

CIECHANOVER, A., ORIAN, A. & SCHWARTZ, A. L. 2000. Ubiquitin-mediated proteolysis: biological regulation via destruction. *Bioessays,* 22**,** 442-51.

CIRUELOS, E., PASCUAL, T., ARROYO VOZMEDIANO, M. L., BLANCO, M., MANSO, L., PARRILLA, L., MUNOZ, C., VEGA, E., CALDERON, M. J., SANCHO, B. & CORTES-FUNES, H. 2014. The therapeutic role of fulvestrant in the management of patients with hormone receptor-positive breast cancer. *Breast,* 23**,** 201-8.

CLARKE, M. J. 1998. Ovarian ablation in breast cancer, 1896 to 1998: milestones along hierarchy of evidence from case report to Cochrane review. *Bmj,* 317**,** 1246-8.

CLARKE, R., TYSON, J. J. & DIXON, J. M. 2015. Endocrine resistance in breast cancer--An overview and update. *Mol Cell Endocrinol,* 418 Pt 3**,** 220-34.

CLEMONS, M., DANSON, S. & HOWELL, A. 2002. Tamoxifen ("Nolvadex"): a review. *Cancer Treat Rev,* 28**,** 165-80.

CLIFT, D., MCEWAN, W. A., LABZIN, L. I., KONIECZNY, V., MOGESSIE, B., JAMES, L. C. & SCHUH, M. 2017. A Method for the Acute and Rapid Degradation of Endogenous Proteins. *Cell,* 171**,** 1692-1706.e18.

COLE, A. J., CLIFTON-BLIGH, R. & MARSH, D. J. 2015. Histone H2B monoubiquitination: roles to play in human malignancy. *Endocr Relat Cancer,* 22**,** T19-33.

COUSSENS, L., YANG-FENG, T. L., LIAO, Y. C., CHEN, E., GRAY, A., MCGRATH, J., SEEBURG, P. H., LIBERMANN, T. A., SCHLESSINGER, J., FRANCKE, U. & ET AL. 1985. Tyrosine kinase receptor with extensive homology to EGF receptor shares chromosomal location with neu oncogene. *Science,* 230**,** 1132-9.

COX, J., NEUHAUSER, N., MICHALSKI, A., SCHELTEMA, R. A., OLSEN, J. V. & MANN, M. 2011. Andromeda: a peptide search engine integrated into the MaxQuant environment. *J Proteome Res,* 10**,** 1794-805.

CRUK. 2017a. *Breast cancer staging, types and grade.* [Online]. [Accessed 1st March 2018].

CRUK. 2017b. *Mitoxantrone (Mitozantrone)* [Online]. [Accessed 22nd March 2018].

CURTIS, C., SHAH, S. P., CHIN, S. F., TURASHVILI, G., RUEDA, O. M., DUNNING, M. J., SPEED, D., LYNCH, A. G., SAMARAJIWA, S., YUAN, Y., GRAF, S., HA, G., HAFFARI, G., BASHASHATI, A., RUSSELL, R., MCKINNEY, S., LANGEROD, A., GREEN, A., PROVENZANO, E., WISHART, G., PINDER, S., WATSON, P., MARKOWETZ, F., MURPHY, L., ELLIS, I., PURUSHOTHAM, A., BORRESEN-DALE, A. L., BRENTON, J. D., TAVARE, S., CALDAS, C. & APARICIO, S. 2012. The genomic and transcriptomic architecture of 2,000 breast tumours reveals novel subgroups. *Nature,* 486**,** 346-52.

DAI, X., LI, T., BAI, Z., YANG, Y., LIU, X., ZHAN, J. & SHI, B. 2015. Breast cancer intrinsic subtype classification, clinical use and future trends. *Am J Cancer Res,* 5**,** 2929-43.

DAVIES, C., PAN, H., GODWIN, J., GRAY, R., ARRIAGADA, R., RAINA, V., ABRAHAM, M., MEDEIROS ALENCAR, V. H., BADRAN, A., BONFILL, X., BRADBURY, J., CLARKE, M., COLLINS, R., DAVIS, S. R., DELMESTRI, A., FORBES, J. F., HADDAD, P., HOU, M. F., INBAR, M., KHALED, H., KIELANOWSKA, J., KWAN, W. H., MATHEW, B. S., MITTRA, I., MULLER, B., NICOLUCCI, A., PERALTA, O., PERNAS, F., PETRUZELKA, L., PIENKOWSKI, T., RADHIKA, R., RAJAN, B., RUBACH, M. T., TORT, S., URRUTIA, G., VALENTINI, M., WANG, Y. & PETO, R. 2013. Long-term effects of continuing adjuvant tamoxifen to 10 years versus stopping at 5 years after diagnosis of oestrogen receptor-positive breast cancer: ATLAS, a randomised trial. *Lancet,* 381**,** 805-16.

DAWSON, S. J., RUEDA, O. M., APARICIO, S. & CALDAS, C. 2013. A new genome-driven integrated classification of breast cancer and its implications. *Embo j,* 32**,** 617-28.

DE LA VEGA, M., KELVIN, A. A., DUNICAN, D. J., MCFARLANE, C., BURROWS, J. F., JAWORSKI, J., STEVENSON, N. J., DIB, K., RAPPOPORT, J. Z., SCOTT, C. J., LONG, A. & JOHNSTON, J. A. 2011. The deubiquitinating enzyme USP17 is essential for GTPase subcellular localization and cell motility. *Nat Commun,* 2**,** 259.

DEBLOIS, G., HALL, J. A., PERRY, M. C., LAGANIERE, J., GHAHREMANI, M., PARK, M., HALLETT, M. & GIGUERE, V. 2009. Genome-wide identification of direct target genes implicates estrogen-related receptor alpha as a determinant of breast cancer heterogeneity. *Cancer Res,* 69**,** 6149-57.

DENARDO, D. G., BRENNAN, D. J., REXHEPAJ, E., RUFFELL, B., SHIAO, S. L., MADDEN, S. F., GALLAGHER, W. M., WADHWANI, N., KEIL, S. D., JUNAID, S. A., RUGO, H. S., HWANG, E. S., JIRSTROM, K., WEST, B. L. & COUSSENS, L. M. 2011. Leukocyte complexity predicts breast cancer survival and functionally regulates response to chemotherapy. *Cancer Discov,* 1**,** 54-67.

DIRAC, A. M. & BERNARDS, R. 2010. The deubiquitinating enzyme USP26 is a regulator of androgen receptor signaling. *Mol Cancer Res.* United States.

DOBIN, A., DAVIS, C. A., SCHLESINGER, F., DRENKOW, J., ZALESKI, C., JHA, S., BATUT, P., CHAISSON, M. & GINGERAS, T. R. 2013. STAR: ultrafast universal RNA-seq aligner. *Bioinformatics,* 29**,** 15-21.

DONG, Y., HAKIMI, M. A., CHEN, X., KUMARASWAMY, E., COOCH, N. S., GODWIN, A. K. & SHIEKHATTAR, R. 2003. Regulation of BRCC, a holoenzyme complex containing BRCA1 and BRCA2, by a signalosome-like subunit and its role in DNA repair. *Mol Cell,* 12**,** 1087-99.

DUBRIDGE, R. B., TANG, P., HSIA, H. C., LEONG, P. M., MILLER, J. H. & CALOS, M. P. 1987. Analysis of mutation in human cells by using an Epstein-Barr virus shuttle system. *Mol Cell Biol,* 7**,** 379-87.

DUTERTRE, M., GRATADOU, L., DARDENNE, E., GERMANN, S., SAMAAN, S., LIDEREAU, R., DRIOUCH, K., DE LA GRANGE, P. & AUBOEUF, D. 2010. Estrogen regulation and physiopathologic significance of alternative promoters in breast cancer. *Cancer Res,* 70**,** 3760-70.

DUTERTRE, M. & SMITH, C. L. 2000. Molecular mechanisms of selective estrogen receptor modulator (SERM) action. *J Pharmacol Exp Ther,* 295**,** 431-7.

DWANE, L., GALLAGHER, W. M., NI CHONGHAILE, T. & O'CONNOR, D. P. 2017. The Emerging Role of Non-traditional Ubiquitination in Oncogenic Pathways. *J Biol Chem,* 292**,** 3543-3551.

EBCTCG 2005. Effects of chemotherapy and hormonal therapy for early breast cancer on recurrence and 15-year survival: an overview of the randomised trials. *Lancet,* 365**,** 1687-717.

ECCLES, S. A., ABOAGYE, E. O., ALI, S., ANDERSON, A. S., ARMES, J., BERDITCHEVSKI, F., BLAYDES, J. P., BRENNAN, K., BROWN, N. J., BRYANT, H. E., BUNDRED, N. J., BURCHELL, J. M., CAMPBELL, A. M., CARROLL, J. S., CLARKE, R. B., COLES, C. E., COOK, G. J., COX, A., CURTIN, N. J., DEKKER, L. V., SILVA IDOS, S., DUFFY, S. W., EASTON, D. F., ECCLES, D. M., EDWARDS, D. R., EDWARDS, J., EVANS, D., FENLON, D. F., FLANAGAN, J. M., FOSTER, C., GALLAGHER, W. M., GARCIA-CLOSAS, M., GEE, J. M., GESCHER, A. J., GOH, V., GROVES, A. M., HARVEY, A. J., HARVIE, M., HENNESSY, B. T., HISCOX, S., HOLEN, I., HOWELL, S. J., HOWELL, A., HUBBARD, G., HULBERT-WILLIAMS, N., HUNTER, M. S., JASANI, B., JONES, L. J., KEY, T. J., KIRWAN, C. C., KONG, A., KUNKLER, I. H., LANGDON, S. P., LEACH, M. O., MANN, D. J., MARSHALL, J. F., MARTIN, L., MARTIN, S. G., MACDOUGALL, J. E., MILES, D. W., MILLER, W. R., MORRIS, J. R., MOSS, S. M., MULLAN, P., NATRAJAN, R., O'CONNOR, J. P., O'CONNOR, R., PALMIERI, C., PHAROAH, P. D., RAKHA, E. A., REED, E., ROBINSON, S. P., SAHAI, E., SAXTON, J. M., SCHMID, P., SMALLEY, M. J., SPEIRS, V., STEIN, R., STINGL, J., STREULI, C. H., TUTT, A. N., VELIKOVA, G., WALKER, R. A., WATSON, C. J., WILLIAMS, K. J., YOUNG, L. S. & THOMPSON, A. M. 2013. Critical research gaps and translational priorities for the successful prevention and treatment of breast cancer. *Breast Cancer Res,* 15**,** R92.

EICHHORN, P. J., RODON, L., GONZALEZ-JUNCA, A., DIRAC, A., GILI, M., MARTINEZ-SAEZ, E., AURA, C., BARBA, I., PEG, V., PRAT, A., CUARTAS, I., JIMENEZ, J., GARCIA-DORADO, D., SAHUQUILLO, J., BERNARDS, R., BASELGA, J. & SEOANE, J. 2012. USP15 stabilizes TGF-beta receptor I and promotes oncogenesis through the activation of TGF-beta signaling in glioblastoma. *Nat Med.* United States.

ELIA, A. E., BOARDMAN, A. P., WANG, D. C., HUTTLIN, E. L., EVERLEY, R. A., DEPHOURE, N., ZHOU, C., KOREN, I., GYGI, S. P. & ELLEDGE, S. J. 2015. Quantitative Proteomic Atlas of Ubiquitination and Acetylation in the DNA Damage Response. *Mol Cell,* 59**,** 867-81.

ERPAPAZOGLOU, Z., WALKER, O. & HAGUENAUER-TSAPIS, R. 2014. Versatile roles of k63-linked ubiquitin chains in trafficking. *Cells,* 3**,** 1027-88.

FABIAN, C. J. 2007. The what, why and how of aromatase inhibitors: hormonal agents for treatment and prevention of breast cancer. *Int J Clin Pract,* 61**,** 2051-63.

FAN, W., CHANG, J. & FU, P. 2015. Endocrine therapy resistance in breast cancer: current status, possible mechanisms and overcoming strategies. *Future Med Chem,* 7**,** 1511-9.

FOSTIER, K., DE BECKER, A. & SCHOTS, R. 2012. Carfilzomib: a novel treatment in relapsed and refractory multiple myeloma. *Onco Targets Ther,* 5**,** 237-44.

FOX, E. M., ARTEAGA, C. L. & MILLER, T. W. 2012. Abrogating endocrine resistance by targeting ERalpha and PI3K in breast cancer. *Front Oncol,* 2**,** 145.

FRAILE, J. M., MANCHADO, E., LUJAMBIO, A., QUESADA, V., CAMPOS-IGLESIAS, D., WEBB, T. R., LOWE, S. W., LOPEZ-OTIN, C. & FREIJE, J. M. 2017. USP39 Deubiquitinase Is Essential for KRAS Oncogene-driven Cancer. *J Biol Chem,* 292**,** 4164-4175.

FRANCIS, P. A., REGAN, M. M., FLEMING, G. F., LANG, I., CIRUELOS, E., BELLET, M., BONNEFOI, H. R., CLIMENT, M. A., DA PRADA, G. A., BURSTEIN, H. J., MARTINO, S., DAVIDSON, N. E., GEYER, C. E., JR., WALLEY, B. A., COLEMAN, R., KERBRAT, P., BUCHHOLZ, S., INGLE, J. N., WINER, E. P., RABAGLIO-PORETTI, M., MAIBACH, R., RUEPP, B., GIOBBIE-HURDER, A., PRICE, K. N., COLLEONI, M., VIALE, G., COATES, A. S., GOLDHIRSCH, A. & GELBER, R. D. 2015. Adjuvant ovarian suppression in premenopausal breast cancer. *N Engl J Med,* 372**,** 436-46.

GAO, S. P., SUN, H. F., LI, L. D., FU, W. Y. & JIN, W. 2017. UHRF1 promotes breast cancer progression by suppressing KLF17 expression by hypermethylating its promoter. *Am J Cancer Res,* 7**,** 1554-1565.

GARCIA-BECERRA, R., SANTOS, N., DIAZ, L. & CAMACHO, J. 2012. Mechanisms of resistance to endocrine therapy in breast cancer: focus on signaling pathways, miRNAs and genetically based resistance. *Int J Mol Sci,* 14**,** 108-45.

GATTI, M., PINATO, S., MAIOLICA, A., ROCCHIO, F., PRATO, M. G., AEBERSOLD, R. & PENENGO, L. 2015. RNF168 promotes noncanonical K27 ubiquitination to signal DNA damage. *Cell Rep,* 10**,** 226-38.

GEISLER, S., HOLMSTROM, K. M., SKUJAT, D., FIESEL, F. C., ROTHFUSS, O. C., KAHLE, P. J. & SPRINGER, W. 2010. PINK1/Parkin-mediated mitophagy is dependent on VDAC1 and p62/SQSTM1. *Nat Cell Biol,* 12**,** 119-31.

GENENTECH. 1998. *Biotechnology Breakthrough In Breast Cancer Wins FDA Approval* [Online]. [Accessed 2nd March 2018].

GENENTECH. 2013. *FDA Approves Genentech's Kadcyla (Ado-Trastuzumab Emtansine), the First Antibody-Drug Conjugate for Treating Her2-Positive Metastatic Breast Cancer* [Online]. [Accessed 2nd March 2018].

GIACINTI, L., CLAUDIO, P. P., LOPEZ, M. & GIORDANO, A. 2006. Epigenetic information and estrogen receptor alpha expression in breast cancer. *Oncologist,* 11**,** 1-8.

GREGORY, R. C., TANIGUCHI, T. & D'ANDREA, A. D. 2003. Regulation of the Fanconi anemia pathway by monoubiquitination. *Semin Cancer Biol,* 13**,** 77-82.

GUO, C., LIU, S. & SUN, M. Z. 2013. Potential role of Anxa1 in cancer. *Future Oncol,* 9**,** 1773-93.

HAFFNER, M. C., DE MARZO, A. M., MEEKER, A. K., NELSON, W. G. & YEGNASUBRAMANIAN, S. 2011. Transcription-induced DNA double strand breaks: both oncogenic force and potential therapeutic target? *Clin Cancer Res,* 17**,** 3858-64.

HAGLUND, K., DI FIORE, P. P. & DIKIC, I. 2003. Distinct monoubiquitin signals in receptor endocytosis. *Trends Biochem Sci,* 28**,** 598-603.

HANAHAN, D. & WEINBERG, R. A. 2011. Hallmarks of cancer: the next generation. *Cell.* United States: 2011 Elsevier Inc.

HARRIGAN, J. A., JACQ, X., MARTIN, N. M. & JACKSON, S. P. 2018. Deubiquitylating enzymes and drug discovery: emerging opportunities. *Nat Rev Drug Discov,* 17**,** 57-78.

HE, M., ZHOU, Z., SHAH, A. A., ZOU, H., TAO, J., CHEN, Q. & WAN, Y. 2016. The emerging role of deubiquitinating enzymes in genomic integrity, diseases, and therapeutics. *Cell Biosci,* 6**,** 62.

HEIN, M. Y., HUBNER, N. C., POSER, I., COX, J., NAGARAJ, N., TOYODA, Y., GAK, I. A., WEISSWANGE, I., MANSFELD, J., BUCHHOLZ, F., HYMAN, A. A. & MANN, M. 2015. A human interactome in three quantitative dimensions organized by stoichiometries and abundances. *Cell,* 163**,** 712-23.

HELDRING, N., NILSSON, M., BUEHRER, B., TREUTER, E. & GUSTAFSSON, J. A. 2004. Identification of tamoxifen-induced coregulator interaction surfaces within the ligand-binding domain of estrogen receptors. *Mol Cell Biol,* 24**,** 3445-59.

HENDRIKS, I. A., SCHIMMEL, J., EIFLER, K., OLSEN, J. V. & VERTEGAAL, A. C. 2015. USP11 Deubiquitinates Hybrid SUMO-Ubiquitin Chains to Counteract RNF4. *J Biol Chem*.

HERSHKO, A. & CIECHANOVER, A. 1998. The ubiquitin system. *Annu Rev Biochem,* 67**,** 425-79.

HORNUNG, V., HARTMANN, R., ABLASSER, A. & HOPFNER, K. P. 2014. OAS proteins and cGAS: unifying concepts in sensing and responding to cytosolic nucleic acids. *Nat Rev Immunol,* 14**,** 521-8.

HPA. 2018. *The Human Protein Atlas: USP11* [Online]. [Accessed 14th March 2018].

HUANG DA, W., SHERMAN, B. T. & LEMPICKI, R. A. 2009. Systematic and integrative analysis of large gene lists using DAVID bioinformatics resources. *Nat Protoc,* 4**,** 44-57.

ICS. 2015. *Chemotherapy* [Online]. [Accessed 13th March 2018].

IDEGUCHI, H., UEDA, A., TANAKA, M., YANG, J., TSUJI, T., OHNO, S., HAGIWARA, E., AOKI, A. & ISHIGATSUBO, Y. 2002. Structural and functional characterization of the USP11 deubiquitinating enzyme, which interacts with the RanGTP-associated protein RanBPM. *Biochem J.* England.

INCORVATI, J. A., SHAH, S., MU, Y. & LU, J. 2013. Targeted therapy for HER2 positive breast cancer. *J Hematol Oncol,* 6**,** 38.

ISO, T., FUTAMI, K., IWAMOTO, T. & FURUICHI, Y. 2007. Modulation of the expression of bloom helicase by estrogenic agents. *Biol Pharm Bull,* 30**,** 266-71.

JACKO, A. M., NAN, L., LI, S., TAN, J., ZHAO, J., KASS, D. J. & ZHAO, Y. 2016. De-ubiquitinating enzyme, USP11, promotes transforming growth factor beta-1 signaling through stabilization of transforming growth factor beta receptor II. *Cell Death Dis,* 7**,** e2474.

JESELSOHN, R., BERGHOLZ, J. S., PUN, M., CORNWELL, M., LIU, W., NARDONE, A., XIAO, T., LI, W., QIU, X., BUCHWALTER, G., FEIGLIN, A., ABELL-HART, K., FEI, T., RAO, P., LONG, H., KWIATKOWSKI, N., ZHANG,

T., GRAY, N., MELCHERS, D., HOUTMAN, R., LIU, X. S., COHEN, O., WAGLE, N., WINER, E. P., ZHAO, J. & BROWN, M. 2018. Allele-Specific Chromatin Recruitment and Therapeutic Vulnerabilities of ESR1 Activating Mutations. *Cancer Cell,* 33**,** 173-186.e5.

JOHANSSON, I., RINGNER, M. & HEDENFALK, I. 2013. The landscape of candidate driver genes differs between male and female breast cancer. *PLoS One,* 8**,** e78299.

JURA, N., SCOTTO-LAVINO, E., SOBCZYK, A. & BAR-SAGI, D. 2006. Differential modification of Ras proteins by ubiquitination. *Mol Cell,* 21**,** 679-87.

KAISTHA, B. P., KRATTENMACHER, A., FREDEBOHM, J., SCHMIDT, H., BEHRENS, D., WIDDER, M., HACKERT, T., STROBEL, O., HOHEISEL, J. D., GRESS, T. M. & BUCHHOLZ, M. 2017. The deubiquitinating enzyme USP5 promotes pancreatic cancer via modulating cell cycle regulators. *Oncotarget,* 8**,** 66215-66225.

KAPADIA, B., NANAJI, N. M., BHALLA, K., BHANDARY, B., LAPIDUS, R., BEHESHTI, A., EVENS, A. M. & GARTENHAUS, R. B. 2018. Fatty Acid Synthase induced S6Kinase facilitates USP11-eIF4B complex formation for sustained oncogenic translation in DLBCL. *Nat Commun,* 9**,** 829.

KE, J. Y., DAI, C. J., WU, W. L., GAO, J. H., XIA, A. J., LIU, G. P., LV, K. S. & WU, C. L. 2014. USP11 regulates p53 stability by deubiquitinating p53. *J Zhejiang Univ Sci B,* 15**,** 1032-8.

KESSLER, B. M. 2014. Selective and reversible inhibitors of ubiquitin-specific protease 7: a patent evaluation (WO2013030218). *Expert Opin Ther Pat,* 24**,** 597-602.

KIM, H. S., KOH, J. S., CHOI, Y. B., RO, J., KIM, H. K., KIM, M. K., NAM, B. H., KIM, K. T., CHANDRA, V., SEOL, H. S., NOH, W. C., KIM, E. K., PARK, J., BAE, C. D. & HONG, K. M. 2014. Chromatin CKAP2, a new proliferation marker, as independent prognostic indicator in breast cancer. *PLoS One,* 9**,** e98160.

KIM, M. Y., WOO, E. M., CHONG, Y. T., HOMENKO, D. R. & KRAUS, W. L. 2006. Acetylation of estrogen receptor alpha by p300 at lysines 266 and 268 enhances the deoxyribonucleic acid binding and transactivation activities of the receptor. *Mol Endocrinol,* 20**,** 1479-93.

KOVALENKO, A., CHABLE-BESSIA, C., CANTARELLA, G., ISRAEL, A., WALLACH, D. & COURTOIS, G. 2003. The tumour suppressor CYLD

negatively regulates NF-kappaB signalling by deubiquitination. *Nature,* 424**,** 801-5.

KRONKE, J., UDESHI, N. D., NARLA, A., GRAUMAN, P., HURST, S. N., MCCONKEY, M., SVINKINA, T., HECKL, D., COMER, E., LI, X., CIARLO, C., HARTMAN, E., MUNSHI, N., SCHENONE, M., SCHREIBER, S. L., CARR, S. A. & EBERT, B. L. 2014. Lenalidomide causes selective degradation of IKZF1 and IKZF3 in multiple myeloma cells. *Science,* 343**,** 301-5.

LALLOO, F. & EVANS, D. G. 2012. Familial breast cancer. *Clin Genet,* 82**,** 105-14.

LANGE, A., MILLS, R. E., LANGE, C. J., STEWART, M., DEVINE, S. E. & CORBETT, A. H. 2007. Classical nuclear localization signals: definition, function, and interaction with importin alpha. *J Biol Chem,* 282**,** 5101-5.

LAUWERS, E., JACOB, C. & ANDRE, B. 2009. K63-linked ubiquitin chains as a specific signal for protein sorting into the multivesicular body pathway. *J Cell Biol,* 185**,** 493-502.

LE ROMANCER, M., POULARD, C., COHEN, P., SENTIS, S., RENOIR, J. M. & CORBO, L. 2011. Cracking the estrogen receptor's posttranslational code in breast tumors. *Endocr Rev,* 32**,** 597-622.

LE ROMANCER, M., TREILLEUX, I., LECONTE, N., ROBIN-LESPINASSE, Y., SENTIS, S., BOUCHEKIOUA-BOUZAGHOU, K., GODDARD, S., GOBERT-GOSSE, S. & CORBO, L. 2008. Regulation of estrogen rapid signaling through arginine methylation by PRMT1. *Mol Cell,* 31**,** 212-21.

LEE, E. W., SEONG, D., SEO, J., JEONG, M., LEE, H. K. & SONG, J. 2015. USP11-dependent selective cIAP2 deubiquitylation and stabilization determine sensitivity to Smac mimetics. *Cell Death Differ,* 22**,** 1463-76.

LEE, H. R., KIM, T. H. & CHOI, K. C. 2012. Functions and physiological roles of two types of estrogen receptors, ERalpha and ERbeta, identified by estrogen receptor knockout mouse. *Lab Anim Res,* 28**,** 71-6.

LEVI, L., LOBO, G., DOUD, M. K., VON LINTIG, J., SEACHRIST, D., TOCHTROP, G. P. & NOY, N. 2013. Genetic ablation of the fatty acid-binding protein FABP5 suppresses HER2-induced mammary tumorigenesis. *Cancer Res,* 73**,** 4770-80.

LI, Q., ZHANG, Y. Y., CHIU, S., HU, Z., LAN, K. H., CHA, H., SODROSKI, C., ZHANG, F., HSU, C. S., THOMAS, E. & LIANG, T. J. 2014. Integrative

functional genomics of hepatitis C virus infection identifies host dependencies in complete viral replication cycle. *PLoS Pathog,* 10**,** e1004163.

LIAO, T. L., WU, C. Y., SU, W. C., JENG, K. S. & LAI, M. M. 2010. Ubiquitination and deubiquitination of NP protein regulates influenza A virus RNA replication. *Embo j,* 29**,** 3879-90.

LIAO, Y., SMYTH, G. K. & SHI, W. 2014. featureCounts: an efficient general purpose program for assigning sequence reads to genomic features. *Bioinformatics,* 30**,** 923-30.

LIM, K. H., SURESH, B., PARK, J. H., KIM, Y. S., RAMAKRISHNA, S. & BAEK, K. H. 2016. Ubiquitin-specific protease 11 functions as a tumor suppressor by modulating Mgl-1 protein to regulate cancer cell growth. *Oncotarget,* 7**,** 14441-57.

LIN, C. H., CHANG, H. S. & YU, W. C. 2008. USP11 stabilizes HPV-16E7 and further modulates the E7 biological activity. *J Biol Chem,* 283**,** 15681-8.

LING, S., LI, J., SHAN, Q., DAI, H., LU, D., WEN, X., SONG, P., XIE, H., ZHOU, L., LIU, J., XU, X. & ZHENG, S. 2017. USP22 mediates the multidrug resistance of hepatocellular carcinoma via the SIRT1/AKT/MRP1 signaling pathway. *Mol Oncol,* 11**,** 682-695.

LIU, Y., WANG, W. M., LU, Y. F., FENG, L., LI, L., PAN, M. Z., SUN, Y., SUEN, C. W., GUO, W., PANG, J. X., ZHANG, J. F. & FU, W. M. 2017. Usp5 functions as an oncogene for stimulating tumorigenesis in hepatocellular carcinoma. *Oncotarget,* 8**,** 50655-50664.

LOVE, M. I., HUBER, W. & ANDERS, S. 2014. Moderated estimation of fold change and dispersion for RNA-seq data with DESeq2. *Genome Biol,* 15**,** 550.

LU, Y., BEDARD, N., CHEVALIER, S. & WING, S. S. 2011. Identification of distinctive patterns of USP19-mediated growth regulation in normal and malignant cells. *PLoS One,* 6**,** e15936.

LUTZ, S. T., JONES, J. & CHOW, E. 2014. Role of radiation therapy in palliative care of the patient with cancer. *J Clin Oncol,* 32**,** 2913-9.

MA, Y., FAN, S., HU, C., MENG, Q., FUQUA, S. A., PESTELL, R. G., TOMITA, Y. A. & ROSEN, E. M. 2010. BRCA1 regulates acetylation and ubiquitination of estrogen receptor-alpha. *Mol Endocrinol,* 24**,** 76-90.

MAERTENS, G. N., EL MESSAOUDI-AUBERT, S., ELDERKIN, S., HIOM, K. & PETERS, G. 2010. Ubiquitin-specific proteases 7 and 11 modulate Polycomb regulation of the INK4a tumour suppressor. *Embo j,* 29**,** 2553-65.

MAGGI, A. 2011. Liganded and unliganded activation of estrogen receptor and hormone replacement therapies. *Biochim Biophys Acta,* 1812**,** 1054-60.

MALHOTRA, G. K., ZHAO, X., BAND, H. & BAND, V. 2010. Histological, molecular and functional subtypes of breast cancers. *Cancer Biol Ther,* 10**,** 955-60.

MARTIN, L. A., RIBAS, R., SIMIGDALA, N., SCHUSTER, E., PANCHOLI, S., TENEV, T., GELLERT, P., BULUWELA, L., HARROD, A., THORNHILL, A., NIKITOROWICZ-BUNIAK, J., BHAMRA, A., TURGEON, M. O., POULOGIANNIS, G., GAO, Q., MARTINS, V., HILLS, M., GARCIA-MURILLAS, I., FRIBBENS, C., PATANI, N., LI, Z., SIKORA, M. J., TURNER, N., ZWART, W., OESTERREICH, S., CARROLL, J., ALI, S. & DOWSETT, M. 2017. Discovery of naturally occurring ESR1 mutations in breast cancer cell lines modelling endocrine resistance. *Nat Commun,* 8**,** 1865.

MASSARWEH, S., OSBORNE, C. K., JIANG, S., WAKELING, A. E., RIMAWI, M., MOHSIN, S. K., HILSENBECK, S. & SCHIFF, R. 2006. Mechanisms of tumor regression and resistance to estrogen deprivation and fulvestrant in a model of estrogen receptor-positive, HER-2/neu-positive breast cancer. *Cancer Res,* 66**,** 8266-73.

MAXIMOV, P. Y., LEE, T. M. & JORDAN, V. C. 2013. The discovery and development of selective estrogen receptor modulators (SERMs) for clinical practice. *Curr Clin Pharmacol,* 8**,** 135-55.

MCCART REED, A. E., KUTASOVIC, J. R., LAKHANI, S. R. & SIMPSON, P. T. 2015. Invasive lobular carcinoma of the breast: morphology, biomarkers and 'omics. *Breast Cancer Res,* 17**,** 12.

MCCARTHY, D. J., CHEN, Y. & SMYTH, G. K. 2012. Differential expression analysis of multifactor RNA-Seq experiments with respect to biological variation. *Nucleic Acids Res,* 40**,** 4288-97.

MCPHERSON, K., STEEL, C. M. & DIXON, J. M. 2000. ABC of breast diseases. Breast cancer-epidemiology, risk factors, and genetics. *Bmj,* 321**,** 624-8.

MENENDEZ, J. A. & LUPU, R. 2017. Fatty acid synthase regulates estrogen receptor-alpha signaling in breast cancer cells. *Oncogenesis,* 6**,** e299.

MESSICK, T. E. & GREENBERG, R. A. 2009. The ubiquitin landscape at DNA double-strand breaks. *J Cell Biol,* 187**,** 319-26.

MOASSER, M. M. 2007. The oncogene HER2: its signaling and transforming functions and its role in human cancer pathogenesis. *Oncogene,* 26**,** 6469-87.

MOHAMMED, H., RUSSELL, I. A., STARK, R., RUEDA, O. M., HICKEY, T. E., TARULLI, G. A., SERANDOUR, A. A., BIRRELL, S. N., BRUNA, A., SAADI, A., MENON, S., HADFIELD, J., PUGH, M., RAJ, G. V., BROWN, G. D., D'SANTOS, C., ROBINSON, J. L., SILVA, G., LAUNCHBURY, R., PEROU, C. M., STINGL, J., CALDAS, C., TILLEY, W. D. & CARROLL, J. S. 2015. Progesterone receptor modulates ERalpha action in breast cancer. *Nature,* 523**,** 313-7.

MOREAU, P., MASSZI, T., GRZASKO, N., BAHLIS, N. J., HANSSON, M., POUR, L., SANDHU, I., GANLY, P., BAKER, B. W., JACKSON, S. R., STOPPA, A. M., SIMPSON, D. R., GIMSING, P., PALUMBO, A., GARDERET, L., CAVO, M., KUMAR, S., TOUZEAU, C., BUADI, F. K., LAUBACH, J. P., BERG, D. T., LIN, J., DI BACCO, A., HUI, A. M., VAN DE VELDE, H. & RICHARDSON, P. G. 2016. Oral Ixazomib, Lenalidomide, and Dexamethasone for Multiple Myeloma. *N Engl J Med,* 374**,** 1621-34.

MOREAU, P., RICHARDSON, P. G., CAVO, M., ORLOWSKI, R. Z., SAN MIGUEL, J. F., PALUMBO, A. & HAROUSSEAU, J. L. 2012. Proteasome inhibitors in multiple myeloma: 10 years later. *Blood,* 120**,** 947-59.

MORRIS, J. R. & SOLOMON, E. 2004. BRCA1 : BARD1 induces the formation of conjugated ubiquitin structures, dependent on K6 of ubiquitin, in cells during DNA replication and repair. *Hum Mol Genet,* 13**,** 807-17.

NAWAZ, Z., LONARD, D. M., DENNIS, A. P., SMITH, C. L. & O'MALLEY, B. W. 1999. Proteasome-dependent degradation of the human estrogen receptor. *Proc Natl Acad Sci U S A,* 96**,** 1858-62.

NCI. 2012. *FDA Approval for Everolimus* [Online]. [Accessed 5th March 2018].

NCRI 2017. Cancer in Ireland 1994-2015 with estimates for 2015-2017: Annual Report of the National Cancer Registry. NCR, Cork, Ireland.

NEUMAN, E., LADHA, M. H., LIN, N., UPTON, T. M., MILLER, S. J., DIRENZO, J., PESTELL, R. G., HINDS, P. W., DOWDY, S. F., BROWN, M. & EWEN, M. E. 1997. Cyclin D1 stimulation of estrogen receptor transcriptional activity independent of cdk4. *Mol Cell Biol,* 17**,** 5338-47.

NIH. 2007. *FDA Approval for Raloxifene Hydrochloride* [Online]. [Accessed 4th March 2018].

NIJMAN, S. M., HUANG, T. T., DIRAC, A. M., BRUMMELKAMP, T. R., KERKHOVEN, R. M., D'ANDREA, A. D. & BERNARDS, R. 2005. The deubiquitinating enzyme USP1 regulates the Fanconi anemia pathway. *Mol Cell,* 17**,** 331-9.

O'REILLY, C., DOROUDIAN, M., MAWHINNEY, L. & DONNELLY, S. C. 2016. Targeting MIF in Cancer: Therapeutic Strategies, Current Developments, and Future Opportunities. *Med Res Rev,* 36**,** 440-60.

ONIZAWA, M., OSHIMA, S., SCHULZE-TOPPHOFF, U., OSES-PRIETO, J. A., LU, T., TAVARES, R., PRODHOMME, T., DUONG, B., WHANG, M. I., ADVINCULA, R., AGELIDIS, A., BARRERA, J., WU, H., BURLINGAME, A., MALYNN, B. A., ZAMVIL, S. S. & MA, A. 2015. The ubiquitin-modifying enzyme A20 restricts ubiquitination of the kinase RIPK3 and protects cells from necroptosis. *Nat Immunol,* 16**,** 618-27.

OOSTERKAMP, H. M., HIJMANS, E. M., BRUMMELKAMP, T. R., CANISIUS, S., WESSELS, L. F., ZWART, W. & BERNARDS, R. 2014. USP9X downregulation renders breast cancer cells resistant to tamoxifen. *Cancer Res,* 74**,** 3810-20.

ORTHWEIN, A., NOORDERMEER, S. M., WILSON, M. D., LANDRY, S., ENCHEV, R. I., SHERKER, A., MUNRO, M., PINDER, J., SALSMAN, J., DELLAIRE, G., XIA, B., PETER, M. & DUROCHER, D. 2015. A mechanism for the suppression of homologous recombination in G1 cells. *Nature,* 528**,** 422-6.

OSBORNE, C. K. & SCHIFF, R. 2011. Mechanisms of endocrine resistance in breast cancer. *Annu Rev Med,* 62**,** 233-47.

OTTAVIANO, Y. L., ISSA, J. P., PARL, F. F., SMITH, H. S., BAYLIN, S. B. & DAVIDSON, N. E. 1994. Methylation of the estrogen receptor gene CpG island marks loss of estrogen receptor expression in human breast cancer cells. *Cancer Res,* 54**,** 2552-5.

PAL, A., YOUNG, M. A. & DONATO, N. J. 2014. Emerging potential of therapeutic targeting of ubiquitin-specific proteases in the treatment of cancer. *Cancer Res,* 74**,** 4955-66.

PANNER, A., CRANE, C. A., WENG, C., FELETTI, A., FANG, S., PARSA, A. T. & PIEPER, R. O. 2010. Ubiquitin-specific protease 8 links the PTEN-Akt-AIP4

pathway to the control of FLIPS stability and TRAIL sensitivity in glioblastoma multiforme. *Cancer Res,* 70**,** 5046-53.

PATEL, V. J., THALASSINOS, K., SLADE, S. E., CONNOLLY, J. B., CROMBIE, A., MURRELL, J. C. & SCRIVENS, J. H. 2009. A comparison of labeling and label-free mass spectrometry-based proteomics approaches. *J Proteome Res,* 8**,** 3752-9.

PATERNI, I., GRANCHI, C., KATZENELLENBOGEN, J. A. & MINUTOLO, F. 2014. Estrogen receptors alpha (ERalpha) and beta (ERbeta): subtype-selective ligands and clinical potential. *Steroids,* 90**,** 13-29.

PELLOM, S. T., JR. & SHANKER, A. 2012. Development of Proteasome Inhibitors as Therapeutic Drugs. *J Clin Cell Immunol,* S5**,** 5.

PENG, J., SCHWARTZ, D., ELIAS, J. E., THOREEN, C. C., CHENG, D., MARSISCHKY, G., ROELOFS, J., FINLEY, D. & GYGI, S. P. 2003. A proteomics approach to understanding protein ubiquitination. *Nat Biotechnol,* 21**,** 921-6.

PEROU, C. M., SORLIE, T., EISEN, M. B., VAN DE RIJN, M., JEFFREY, S. S., REES, C. A., POLLACK, J. R., ROSS, D. T., JOHNSEN, H., AKSLEN, L. A., FLUGE, O., PERGAMENSCHIKOV, A., WILLIAMS, C., ZHU, S. X., LONNING, P. E., BORRESEN-DALE, A. L., BROWN, P. O. & BOTSTEIN, D. 2000. Molecular portraits of human breast tumours. *Nature,* 406**,** 747-52.

PERRETTI, M. & D'ACQUISTO, F. 2009. Annexin A1 and glucocorticoids as effectors of the resolution of inflammation. *Nat Rev Immunol,* 9**,** 62-70.

PICKART, C. M. 1997. Targeting of substrates to the 26S proteasome. *Faseb j,* 11**,** 1055-66.

PICKART, C. M. 2001. Mechanisms underlying ubiquitination. *Annu Rev Biochem,* 70**,** 503-33.

PICKART, C. M. & EDDINS, M. J. 2004. Ubiquitin: structures, functions, mechanisms. *Biochim Biophys Acta,* 1695**,** 55-72.

PIVA, R., RIMONDI, A. P., HANAU, S., MAESTRI, I., ALVISI, A., KUMAR, V. L. & DEL SENNO, L. 1990. Different methylation of oestrogen receptor DNA in human breast carcinomas with and without oestrogen receptor. *Br J Cancer,* 61**,** 270-5.

POPOV, N., WANZEL, M., MADIREDJO, M., ZHANG, D., BEIJERSBERGEN, R., BERNARDS, R., MOLL, R., ELLEDGE, S. J. & EILERS, M. 2007. The

ubiquitin-specific protease USP28 is required for MYC stability. *Nat Cell Biol,* 9**,** 765-74.

POWELL, C. A., NASSER, M. W., ZHAO, H., WOCHNA, J. C., ZHANG, X., SHAPIRO, C., SHILO, K. & GANJU, R. K. 2015. Fatty acid binding protein 5 promotes metastatic potential of triple negative breast cancer cells through enhancing epidermal growth factor receptor stability. *Oncotarget,* 6**,** 6373-85.

REYES-TURCU, F. E., VENTII, K. H. & WILKINSON, K. D. 2009. Regulation and cellular roles of ubiquitin-specific deubiquitinating enzymes. *Annu Rev Biochem,* 78**,** 363-97.

RINGNER, M., FREDLUND, E., HAKKINEN, J., BORG, A. & STAAF, J. 2011. GOBO: gene expression-based outcome for breast cancer online. *PLoS One,* 6**,** e17911.

ROMANO, A., ADRIAENS, M., KUENEN, S., DELVOUX, B., DUNSELMAN, G., EVELO, C. & GROOTHUIS, P. 2010. Identification of novel ER-alpha target genes in breast cancer cells: gene- and cell-selective co-regulator recruitment at target promoters determines the response to 17beta-estradiol and tamoxifen. *Mol Cell Endocrinol,* 314**,** 90-100.

ROY, R., CHUN, J. & POWELL, S. N. 2011. BRCA1 and BRCA2: different roles in a common pathway of genome protection. *Nat Rev Cancer,* 12**,** 68-78.

SASSI, A., POPIELARSKI, M., SYNOWIEC, E., MORAWIEC, Z. & WOZNIAK, K. 2013. BLM and RAD51 genes polymorphism and susceptibility to breast cancer. *Pathol Oncol Res,* 19**,** 451-9.

SCHINDELIN, J., ARGANDA-CARRERAS, I., FRISE, E., KAYNIG, V., LONGAIR, M., PIETZSCH, T., PREIBISCH, S., RUEDEN, C., SAALFELD, S., SCHMID, B., TINEVEZ, J. Y., WHITE, D. J., HARTENSTEIN, V., ELICEIRI, K., TOMANCAK, P. & CARDONA, A. 2012. Fiji: an open-source platform for biological-image analysis. *Nat Methods,* 9**,** 676-82.

SCHOENFELD, A. R., APGAR, S., DOLIOS, G., WANG, R. & AARONSON, S. A. 2004. BRCA2 is ubiquitinated in vivo and interacts with USP11, a deubiquitinating enzyme that exhibits prosurvival function in the cellular response to DNA damage. *Mol Cell Biol.* United States: 2004 American Society for Microbiology.

SEVER, R. & GLASS, C. K. 2013. Signaling by nuclear receptors. *Cold Spring Harb Perspect Biol,* 5**,** a016709.

SHAH, P., QIANG, L., YANG, S., SOLTANI, K. & HE, Y. Y. 2017. Regulation of XPC deubiquitination by USP11 in repair of UV-induced DNA damage. *Oncotarget,* 8**,** 96522-96535.

SHAH, Y. M. & ROWAN, B. G. 2005. The Src kinase pathway promotes tamoxifen agonist action in Ishikawa endometrial cells through phosphorylation-dependent stabilization of estrogen receptor (alpha) promoter interaction and elevated steroid receptor coactivator 1 activity. *Mol Endocrinol,* 19**,** 732-48.

SHI, D. & GROSSMAN, S. R. 2010. Ubiquitin becomes ubiquitous in cancer: emerging roles of ubiquitin ligases and deubiquitinases in tumorigenesis and as therapeutic targets. *Cancer Biol Ther.* United States.

SILVA, G. M., FINLEY, D. & VOGEL, C. 2015. K63 polyubiquitination is a new modulator of the oxidative stress response. *Nat Struct Mol Biol,* 22**,** 116-23.

SORLIE, T., PEROU, C. M., TIBSHIRANI, R., AAS, T., GEISLER, S., JOHNSEN, H., HASTIE, T., EISEN, M. B., VAN DE RIJN, M., JEFFREY, S. S., THORSEN, T., QUIST, H., MATESE, J. C., BROWN, P. O., BOTSTEIN, D., LONNING, P. E. & BORRESEN-DALE, A. L. 2001. Gene expression patterns of breast carcinomas distinguish tumor subclasses with clinical implications. *Proc Natl Acad Sci U S A,* 98**,** 10869-74.

SOULE, H. D., VAZGUEZ, J., LONG, A., ALBERT, S. & BRENNAN, M. 1973. A human cell line from a pleural effusion derived from a breast carcinoma. *J Natl Cancer Inst,* 51**,** 1409-16.

SPARANO, J. A., GOLDSTEIN, L. J., DAVIDSON, N. E., SLEDGE, G. W., JR. & GRAY, R. 2012. TOP2A RNA expression and recurrence in estrogen receptor-positive breast cancer. *Breast Cancer Res Treat,* 134**,** 751-7.

SPENCE, J., SADIS, S., HAAS, A. L. & FINLEY, D. 1995. A ubiquitin mutant with specific defects in DNA repair and multiubiquitination. *Mol Cell Biol,* 15**,** 1265-73.

STANISIC, V., MALOVANNAYA, A., QIN, J., LONARD, D. M. & O'MALLEY, B. W. 2009. OTU Domain-containing ubiquitin aldehyde-binding protein 1 (OTUB1) deubiquitinates estrogen receptor (ER) alpha and affects ERalpha transcriptional activity. *J Biol Chem.* United States.

STEINER, A. Z., TERPLAN, M. & PAULSON, R. J. 2005. Comparison of tamoxifen and clomiphene citrate for ovulation induction: a meta-analysis. *Hum Reprod,* 20**,** 1511-5.

STOCKUM, A., SNIJDERS, A. P. & MAERTENS, G. N. 2018. USP11 deubiquitinates RAE1 and plays a key role in bipolar spindle formation. *PLoS One,* 13**,** e0190513.

SU, Y. T., GAO, C., LIU, Y., GUO, S., WANG, A., WANG, B., ERDJUMENT-BROMAGE, H., MIYAGI, M., TEMPST, P. & KAO, H. Y. 2013. Monoubiquitination of filamin B regulates vascular endothelial growth factor-mediated trafficking of histone deacetylase 7. *Mol Cell Biol,* 33**,** 1546-60.

SUBRAMANIAN, A., TAMAYO, P., MOOTHA, V. K., MUKHERJEE, S., EBERT, B. L., GILLETTE, M. A., PAULOVICH, A., POMEROY, S. L., GOLUB, T. R., LANDER, E. S. & MESIROV, J. P. 2005. Gene set enrichment analysis: a knowledge-based approach for interpreting genome-wide expression profiles. *Proc Natl Acad Sci U S A,* 102**,** 15545-50.

SUBRAMANIAN, K., JIA, D., KAPOOR-VAZIRANI, P., POWELL, D. R., COLLINS, R. E., SHARMA, D., PENG, J., CHENG, X. & VERTINO, P. M. 2008. Regulation of estrogen receptor alpha by the SET7 lysine methyltransferase. *Mol Cell,* 30**,** 336-47.

SUN, W., TAN, X., SHI, Y., XU, G., MAO, R., GU, X., FAN, Y., YU, Y., BURLINGAME, S., ZHANG, H., REDNAM, S. P., LU, X., ZHANG, T., FU, S., CAO, G., QIN, J. & YANG, J. 2010. USP11 negatively regulates TNFalpha-induced NF-kappaB activation by targeting on IkappaBalpha. *Cell Signal.* England.

SUN, Y., HO, G. H., KOONG, H. N., SIVARAMAKRISHNAN, G., ANG, W. T., KOH, Q. M. & LIN, V. C. 2013. Down-regulation of tripartite-motif containing 22 expression in breast cancer is associated with a lack of p53-mediated induction. *Biochem Biophys Res Commun,* 441**,** 600-6.

SURYADINATA, R., ROESLEY, S. N., YANG, G. & SARCEVIC, B. 2014. Mechanisms of generating polyubiquitin chains of different topology. *Cells,* 3**,** 674-89.

SWANSON, D. A., FREUND, C. L., PLODER, L., MCINNES, R. R. & VALLE, D. 1996. A ubiquitin C-terminal hydrolase gene on the proximal short arm of the X chromosome: implications for X-linked retinal disorders. *Hum Mol Genet,* 5**,** 533-8.

THOMAS, R. S., SARWAR, N., PHOENIX, F., COOMBES, R. C. & ALI, S. 2008. Phosphorylation at serines 104 and 106 by Erk1/2 MAPK is important for estrogen receptor-alpha activity. *J Mol Endocrinol,* 40**,** 173-84.

TU, Y., JOHNSTONE, C. N. & STEWART, A. G. 2017. Annexin A1 influences in breast cancer: Controversies on contributions to tumour, host and immunoediting processes. *Pharmacol Res,* 119**,** 278-288.

TURNBULL, A. P., IOANNIDIS, S., KRAJEWSKI, W. W., PINTO-FERNANDEZ, A., HERIDE, C., MARTIN, A. C. L., TONKIN, L. M., TOWNSEND, E. C., BUKER, S. M., LANCIA, D. R., CARAVELLA, J. A., TOMS, A. V., CHARLTON, T. M., LAHDENRANTA, J., WILKER, E., FOLLOWS, B. C., EVANS, N. J., STEAD, L., ALLI, C., ZARAYSKIY, V. V., TALBOT, A. C., BUCKMELTER, A. J., WANG, M., MCKINNON, C. L., SAAB, F., MCGOURAN, J. F., CENTURY, H., GERSCH, M., PITTMAN, M. S., MARSHALL, C. G., RAYNHAM, T. M., SIMCOX, M., STEWART, L. M. D., MCLOUGHLIN, S. B., ESCOBEDO, J. A., BAIR, K. W., DINSMORE, C. J., HAMMONDS, T. R., KIM, S., URBE, S., CLAGUE, M. J., KESSLER, B. M. & KOMANDER, D. 2017. Molecular basis of USP7 inhibition by selective small-molecule inhibitors. *Nature,* 550**,** 481-486.

TYANOVA, S., TEMU, T. & COX, J. 2016a. The MaxQuant computational platform for mass spectrometry-based shotgun proteomics. *Nat Protoc,* 11**,** 2301-2319.

TYANOVA, S., TEMU, T., SINITCYN, P., CARLSON, A., HEIN, M. Y., GEIGER, T., MANN, M. & COX, J. 2016b. The Perseus computational platform for comprehensive analysis of (prote)omics data. *Nat Methods,* 13**,** 731-40.

UDESHI, N. D., MERTINS, P., SVINKINA, T. & CARR, S. A. 2013. Large-scale identification of ubiquitination sites by mass spectrometry. *Nat Protoc,* 8**,** 1950-60.

VALLABHAPURAPU, S. & KARIN, M. 2009. Regulation and function of NF-kappaB transcription factors in the immune system. *Annu Rev Immunol,* 27**,** 693-733.

VAN WIJK, S. J., DE VRIES, S. J., KEMMEREN, P., HUANG, A., BOELENS, R., BONVIN, A. M. & TIMMERS, H. T. 2009. A comprehensive framework of E2-RING E3 interactions of the human ubiquitin-proteasome system. *Mol Syst Biol,* 5**,** 295.

VARADAN, R., ASSFALG, M., HARIRINIA, A., RAASI, S., PICKART, C. & FUSHMAN, D. 2004. Solution conformation of Lys63-linked di-ubiquitin chain

provides clues to functional diversity of polyubiquitin signaling. *J Biol Chem,* 279**,** 7055-63.

VARADAN, R., WALKER, O., PICKART, C. & FUSHMAN, D. 2002. Structural properties of polyubiquitin chains in solution. *J Mol Biol,* 324**,** 637-47.

VARLAKHANOVA, N., SNYDER, C., JOSE, S., HAHM, J. B. & PRIVALSKY, M. L. 2010. Estrogen receptors recruit SMRT and N-CoR corepressors through newly recognized contacts between the corepressor N terminus and the receptor DNA binding domain. *Mol Cell Biol,* 30**,** 1434-45.

VOGEL, C. L., JOHNSTON, M. A., CAPERS, C. & BRACCIA, D. 2014. Toremifene for breast cancer: a review of 20 years of data. *Clin Breast Cancer,* 14**,** 1-9.

VU, T. & CLARET, F. X. 2012. Trastuzumab: updated mechanisms of action and resistance in breast cancer. *Front Oncol,* 2**,** 62.

WANG, D., ZHAO, J., LI, S., WEI, J., NAN, L., MALLAMPALLI, R. K., WEATHINGTON, N. M., MA, H. & ZHAO, Y. 2017a. Phosphorylated E2F1 is stabilized by nuclear USP11 to drive Peg10 gene expression and activate lung epithelial cells. *J Mol Cell Biol***,** 1-14.

WANG, G., GAO, Y., LI, L., JIN, G., CAI, Z., CHAO, J. I. & LIN, H. K. 2012. K63-linked ubiquitination in kinase activation and cancer. *Front Oncol,* 2**,** 5.

WANG, L. & DI, L. J. 2014. BRCA1 and estrogen/estrogen receptor in breast cancer: where they interact? *Int J Biol Sci,* 10**,** 566-75.

WANG, Y. C., PETERSON, S. E. & LORING, J. F. 2014. Protein post-translational modifications and regulation of pluripotency in human stem cells. *Cell Res,* 24**,** 143-60.

WANG, Z., ZHU, W. G. & XU, X. 2017b. Ubiquitin-like modifications in the DNA damage response. *Mutat Res,* 803-805**,** 56-75.

WEIGEL, M. T. & DOWSETT, M. 2010. Current and emerging biomarkers in breast cancer: prognosis and prediction. *Endocr Relat Cancer,* 17**,** R245-62.

WICKLIFFE, K. E., WILLIAMSON, A., MEYER, H. J., KELLY, A. & RAPE, M. 2011. K11-linked ubiquitin chains as novel regulators of cell division. *Trends Cell Biol,* 21**,** 656-63.

WIJAYARATNE, A. L. & MCDONNELL, D. P. 2001. The human estrogen receptor-alpha is a ubiquitinated protein whose stability is affected differentially by agonists, antagonists, and selective estrogen receptor modulators. *J Biol Chem,* 276**,** 35684-92.

WILLIAMSON, L. M. & LEES-MILLER, S. P. 2011. Estrogen receptor alpha-mediated transcription induces cell cycle-dependent DNA double-strand breaks. *Carcinogenesis,* 32**,** 279-85.

WILTSHIRE, T. D., LOVEJOY, C. A., WANG, T., XIA, F., O'CONNOR, M. J. & CORTEZ, D. 2010. Sensitivity to poly(ADP-ribose) polymerase (PARP) inhibition identifies ubiquitin-specific peptidase 11 (USP11) as a regulator of DNA double-strand break repair. *J Biol Chem.* United States.

WINBORN, B. J., TRAVIS, S. M., TODI, S. V., SCAGLIONE, K. M., XU, P., WILLIAMS, A. J., COHEN, R. E., PENG, J. & PAULSON, H. L. 2008. The deubiquitinating enzyme ataxin-3, a polyglutamine disease protein, edits Lys63 linkages in mixed linkage ubiquitin chains. *J Biol Chem,* 283**,** 26436-43.

WINER, E. P., HUDIS, C., BURSTEIN, H. J., WOLFF, A. C., PRITCHARD, K. I., INGLE, J. N., CHLEBOWSKI, R. T., GELBER, R., EDGE, S. B., GRALOW, J., COBLEIGH, M. A., MAMOUNAS, E. P., GOLDSTEIN, L. J., WHELAN, T. J., POWLES, T. J., BRYANT, J., PERKINS, C., PEROTTI, J., BRAUN, S., LANGER, A. S., BROWMAN, G. P. & SOMERFIELD, M. R. 2005. American Society of Clinical Oncology technology assessment on the use of aromatase inhibitors as adjuvant therapy for postmenopausal women with hormone receptor-positive breast cancer: status report 2004. *J Clin Oncol,* 23**,** 619-29.

WOUTERS, H., VAN GEFFEN, E. C., BAAS-THIJSSEN, M. C., KROL-WARMERDAM, E. M., STIGGELBOUT, A. M., BELITSER, S., BOUVY, M. L. & VAN DIJK, L. 2013. Disentangling breast cancer patients' perceptions and experiences with regard to endocrine therapy: nature and relevance for non-adherence. *Breast,* 22**,** 661-6.

WU, H. C., LIN, Y. C., LIU, C. H., CHUNG, H. C., WANG, Y. T., LIN, Y. W., MA, H. I., TU, P. H., LAWLER, S. E. & CHEN, R. H. 2014. USP11 regulates PML stability to control Notch-induced malignancy in brain tumours. *Nat Commun,* 5**,** 3214.

WU, Y., WANG, Y., YANG, X. H., KANG, T., ZHAO, Y., WANG, C., EVERS, B. M. & ZHOU, B. P. 2013. The deubiquitinase USP28 stabilizes LSD1 and confers stem-cell-like traits to breast cancer cells. *Cell Rep,* 5**,** 224-36.

WU-BAER, F., LAGRAZON, K., YUAN, W. & BAER, R. 2003. The BRCA1/BARD1 heterodimer assembles polyubiquitin chains through an unconventional linkage involving lysine residue K6 of ubiquitin. *J Biol Chem,* 278**,** 34743-6.

XU, J. & LI, Q. 2003. Review of the in vivo functions of the p160 steroid receptor coactivator family. *Mol Endocrinol,* 17**,** 1681-92.

XU, P., DUONG, D. M., SEYFRIED, N. T., CHENG, D., XIE, Y., ROBERT, J., RUSH, J., HOCHSTRASSER, M., FINLEY, D. & PENG, J. 2009. Quantitative proteomics reveals the function of unconventional ubiquitin chains in proteasomal degradation. *Cell,* 137**,** 133-45.

XU, X., WANG, B., YE, C., YAO, C., LIN, Y., HUANG, X., ZHANG, Y. & WANG, S. 2008. Overexpression of macrophage migration inhibitory factor induces angiogenesis in human breast cancer. *Cancer Lett,* 261**,** 147-57.

YU, M., LIU, K., MAO, Z., LUO, J., GU, W. & ZHAO, W. 2016. USP11 Is a Negative Regulator to gammaH2AX Ubiquitylation by RNF8/RNF168. *J Biol Chem,* 291**,** 959-67.

ZHANG, E., SHEN, B., MU, X., QIN, Y., ZHANG, F., LIU, Y., XIAO, J., ZHANG, P., WANG, C., TAN, M. & FAN, Y. 2016a. Ubiquitin-specific protease 11 (USP11) functions as a tumor suppressor through deubiquitinating and stabilizing VGLL4 protein. *Am J Cancer Res,* 6**,** 2901-2909.

ZHANG, Y., VAN DEURSEN, J. & GALARDY, P. J. 2011. Overexpression of ubiquitin specific protease 44 (USP44) induces chromosomal instability and is frequently observed in human T-cell leukemia. *PLoS One,* 6**,** e23389.

ZHANG, Y. W., NASTO, R. E., VARGHESE, R., JABLONSKI, S. A., SEREBRIISKII, I. G., SURANA, R., CALVERT, V. S., BEBU, I., MURRAY, J., JIN, L., JOHNSON, M., RIGGINS, R., RESSOM, H., PETRICOIN, E., CLARKE, R., GOLEMIS, E. A. & WEINER, L. M. 2016b. Acquisition of estrogen independence induces TOB1-related mechanisms supporting breast cancer cell proliferation. *Oncogene,* 35**,** 1643-56.

ZHAO, J., WEI, J., DONG, S., BOWSER, R. K., ZHANG, L., JACKO, A. M. & ZHAO, Y. 2016. Destabilization of Lysophosphatidic Acid Receptor 1 Reduces Cytokine Release and Protects Against Lung Injury. *EBioMedicine,* 10**,** 195-203.

ZHOU, Z., LUO, A., SHRIVASTAVA, I., HE, M., HUANG, Y., BAHAR, I., LIU, Z. & WAN, Y. 2017. Regulation of XIAP Turnover Reveals a Role for USP11 in Promotion of Tumorigenesis. *EBioMedicine,* 15**,** 48-61.

Appendices

Appendix 1: Sequences

1.1 shRNA sequences (5’ -> 3’)

shUSP11_1:

CCCTCCCTTCCGGCCCTCCCTTCTAGTCTTTATTCTCGAGAATAAAGACTAGAA
GGGAGGGTTTTT

shUSP11_2:

CCGTGATGCCGGCCGTGATGATATCTTCGTCTACTCGAGTAGACGAAGATATCA
TCACGGTTTTT

shUSP11_3:

CCGATTCTTCCGGCCGATTCTATTGGCCTAGTATCTCGAGATACTAGGCCAATA
GAATCGGTTTTT

shUSP11_4:

CCGTGACTCCGGCCGTGACTACAACAACTCCTACTCGAGTAGGAGTTGTTGTA
GTCACGGTTTTT

shUSP11_5:

CGGCACAACCGGCGGCACAATGATTTGGGCAAACTCGAGTTTGCCAAATCATT
GTGCCGTTTTT

1.2 USP11 siRNA sequences (5’ -> 3’)

siUSP11_1:

GGACCGUGAUGAUAUCUUC

siUSP11_2:

GAAGAAGCGUUACUAUGAC

1.3 USP11 forward primer for Sanger sequencing

GAATCCGGAAGTGGCTGTT

1.4 Primer sequences used in qRT-PCR analysis (5’ -> 3’):

USP11

Forward: CATTGAACGCAAGGTCATAGAGC

Reverse: AGTTCTACTGGGTACACTTCGAC

PgR

Forward: GACACCTTGCCTGAAGTTTCG

Reverse: CTGCGTCTTTTCGTCGGAG

TFF1

Forward: CCCTCCCAGTGTGCAAATAAG

Reverse: GAACGGTGTCGTCGAAACAG

ERα

Forward: ACAAGGGAAGTATGGCTATGGA

Reverse: GGTCTTTTCGTATCCCACCTTTC

GAPDH

Forward: ATGGGGGAAGGTGAAGGTCG

Reverse: GGGGTCATTGATGGCAACAAT

GREB1

Forward: ACCAGCTTCAGTCACCTTTC

Reverse: GGAAGTTCCCATGGCCTTTA

PKIB

Forward: GGGACAGGAAAGATAGGAGAAAG

Reverse: CAGACTCCACGTCAGTCATTT

TOP2A

Forward: GCTGGATCAGTGGCTGAAAT

Reverse: ATGGGCTGCAAGAGGTTTAG

BRCA1

Forward: CTCGCTGAGACTTCCTGGAC

Reverse: TACCCAGAGCAGAGGGTGAA

DIAPH3

Forward: CTGACGGATGATATGCTGGACA

Reverse: CAGGTTGGGAAGTGGAGGTC

BLM

Forward: CCTCTACCCAACACCACAAA

Reverse: CCTTCGGAGTCTGCAAGAAA

NCAPG

Forward: GCTTGGGATGCTGTGGACTA

Reverse: CCCGAACGTCATCAGTTGGT

RAD51B

Forward: ACAGTGTGAATACCCGGCTG

Reverse: GAAGAACCAGGCCTTCCTCC

CEACAM1

Forward: GATCCTATACCTGCCACGCC

Reverse: ACTGTGGTCTTGCTGGCTTT

TRIM22

Forward: ACGAGGTGGTCAAGGAATGT

Reverse: CTTCTGTCTCTCGATCTGGATATAA

IFIT1

Forward: GAGGAGCCTGGCTAAGCAAA

Reverse: GCTCCAGACTATCCTTGACCTG

18S

Forward: GAGGATGAGGTGGAACGTGT

Reverse: AGAAGTGACGCAGCCCTCTA

Appendix 2: Vector maps

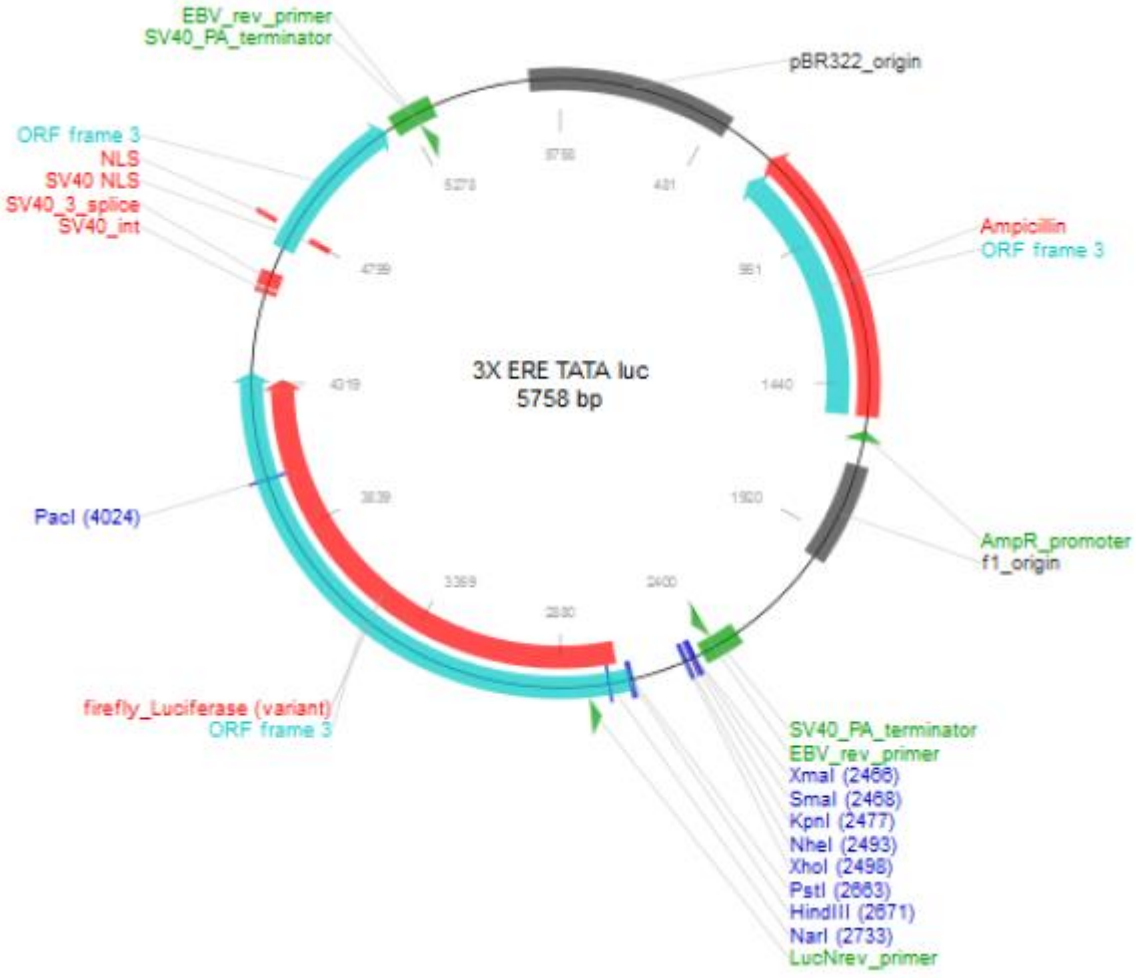

Figure 2.1: Map of ERE-TATA luciferase vector. *This vector was received as a gift from Prof. Rene Bernards, Netherlands Cancer Institute, Amsterdam.*

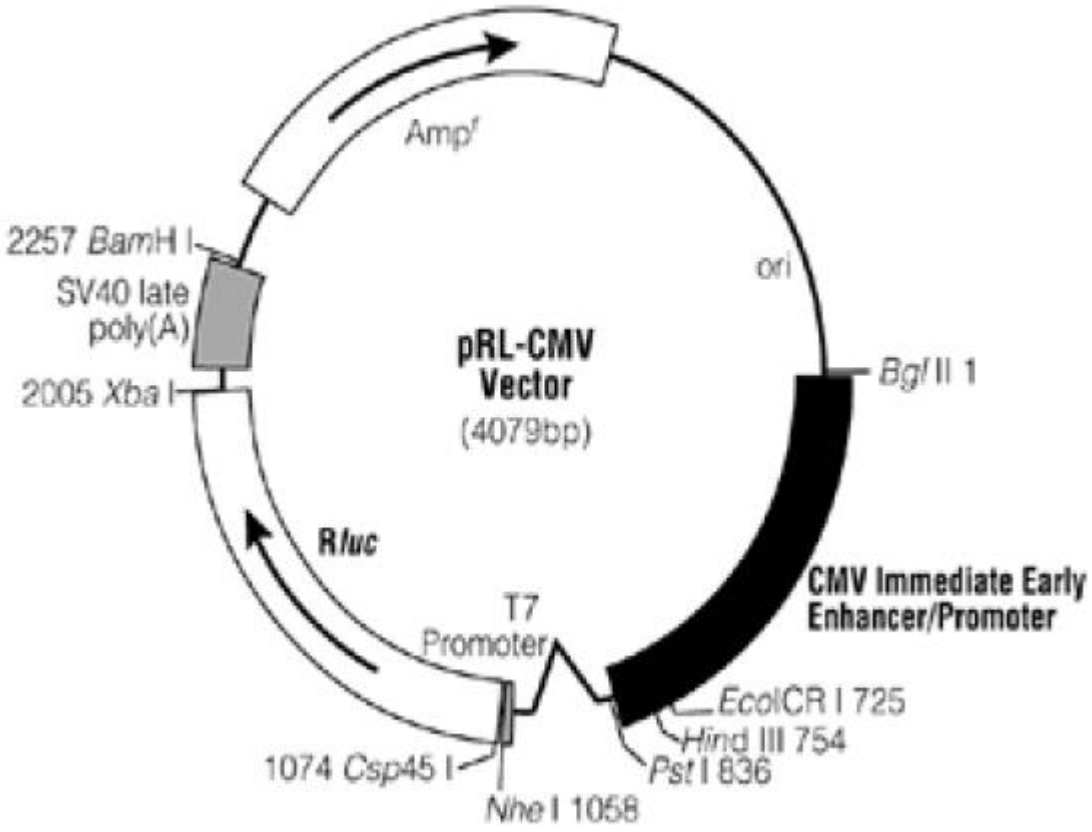

Figure 2.2: Map of pCMV-Renilla luciferase vector. *This vector was received as a gift from Prof. Rene Bernards, Netherlands Cancer Institute, Amsterdam.*

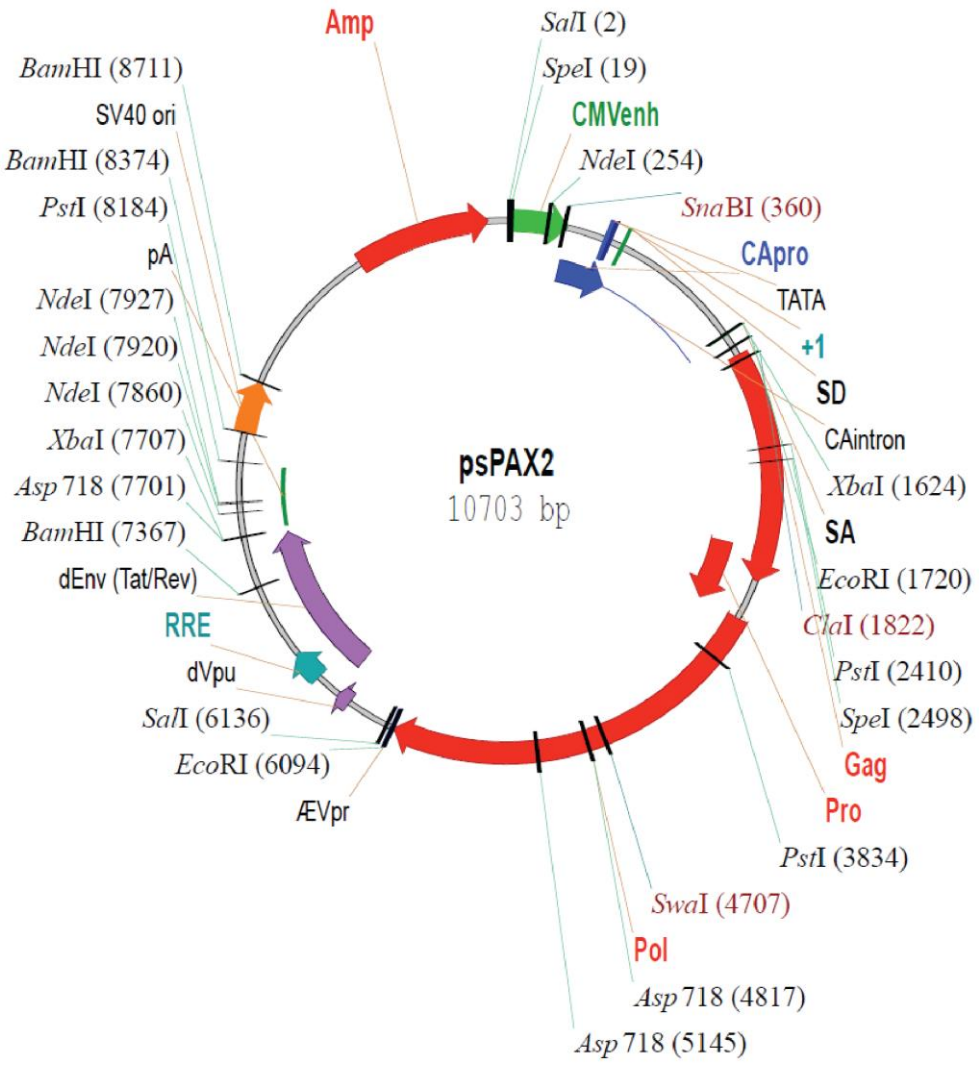

Figure 2.3: Map of psPAX2 viral packaging vector. *This vector was received as a gift from the Trono laboratory, University of Geneva, Switzerland.*

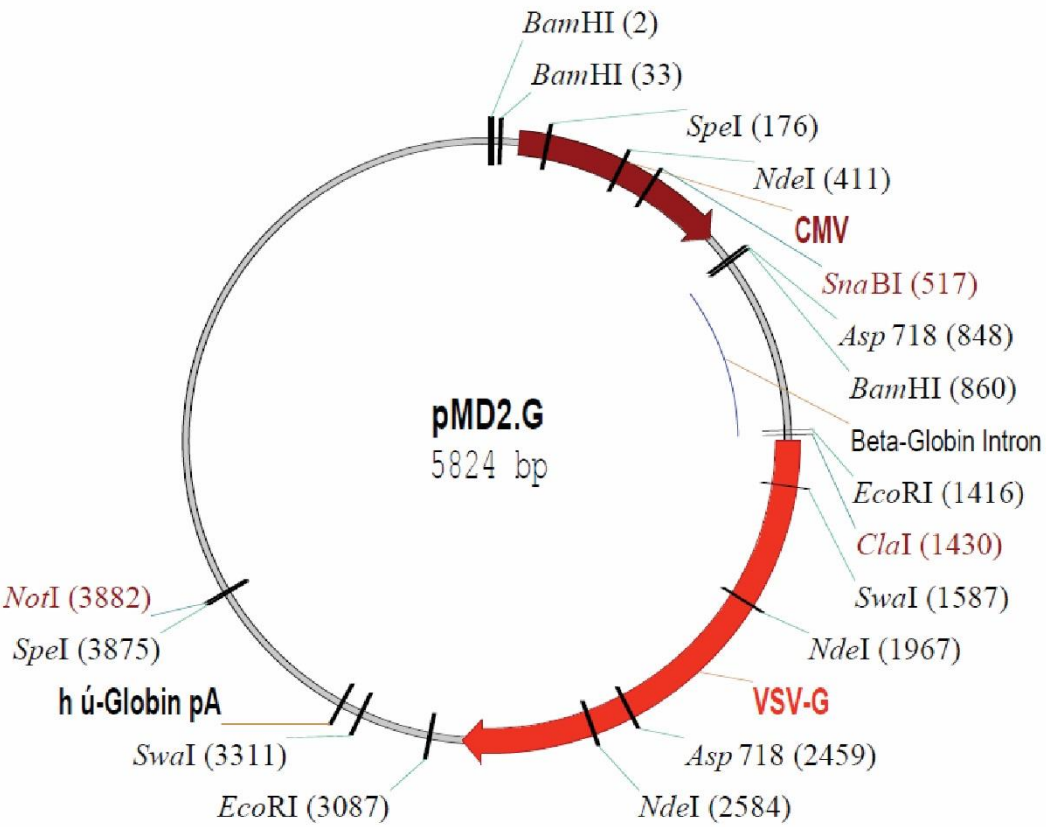

Figure 2.4: Map of pMD2.G viral envelope vector. *This vector was received as a gift from the Trono laboratory, University of Geneva, Switzerland.*

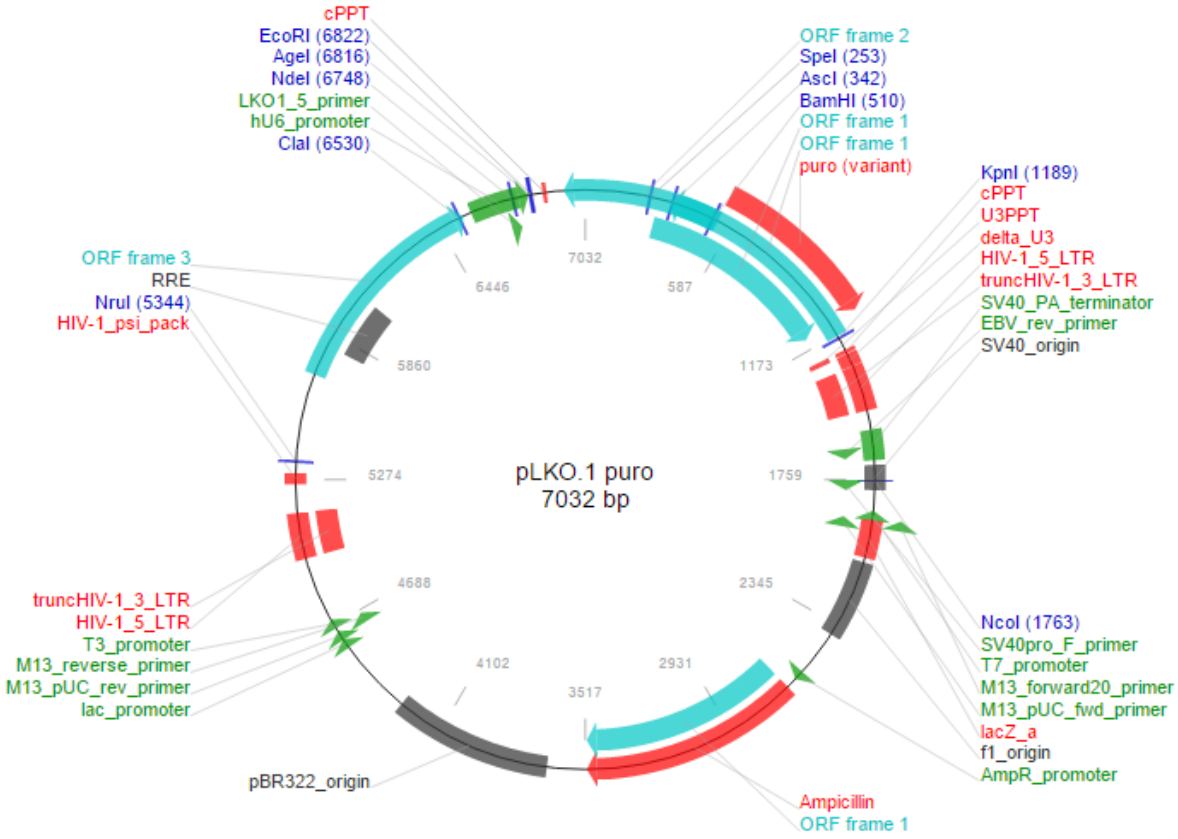

Figure 2.5: Map of pLKO.1-puro (empty vector backbone) (Sigma-Aldrich).

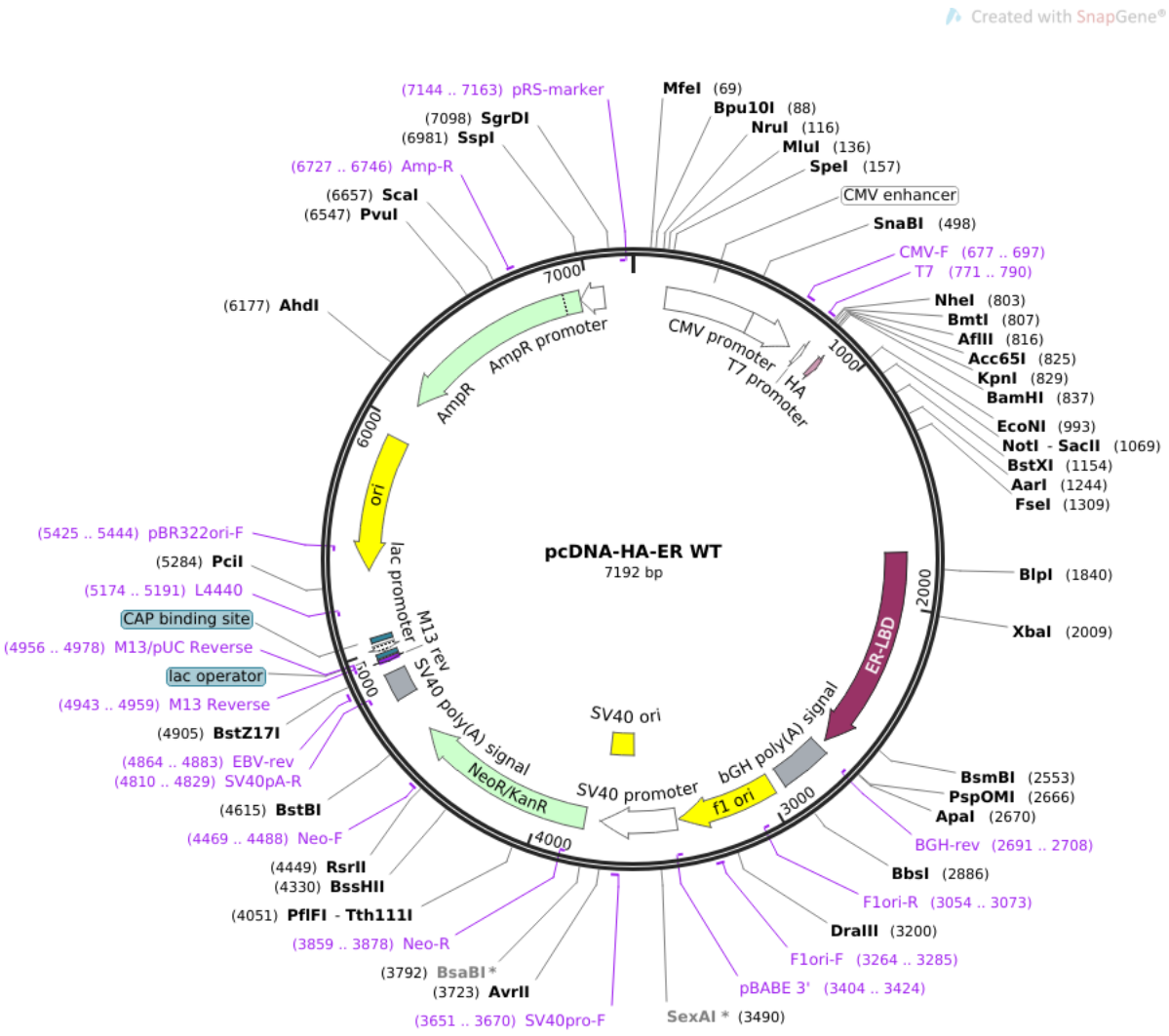

Figure 2.6: pcDNA-HA-ER wild-type vector (addgene 49498).

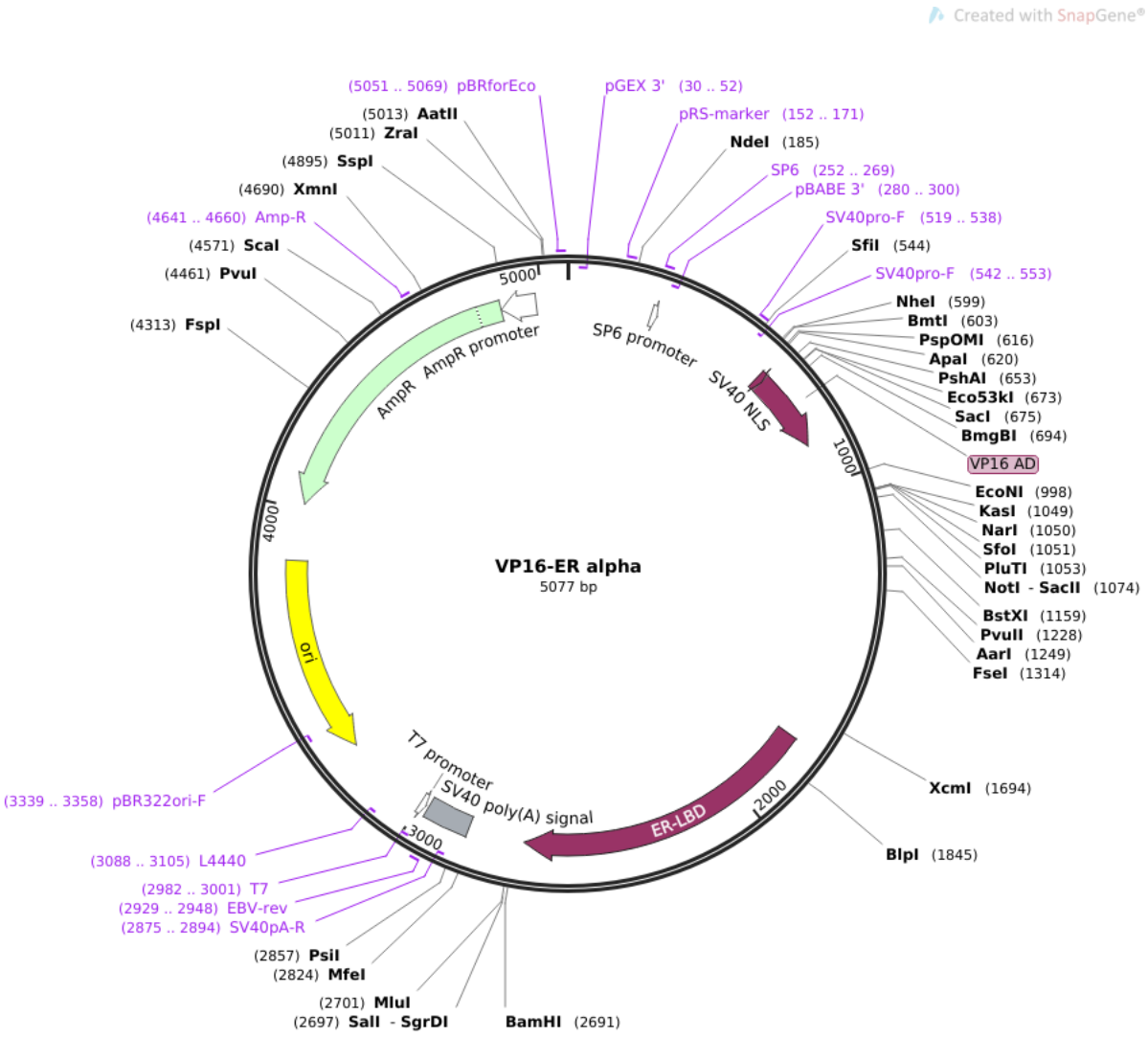

Figure 2.7: VP16 ER alpha wild-type vector (addgene 11351).

Appendix 3: RNA-seq

Table 3.1: Significantly DE genes in LCC1 USP11 knockdown cells versus siRNA control

ENSEMBL_ID	GENE	Log2fold value siUSP11_1 (SI7)	Log2fold value siUSP11_2 (SI8)
ENSG00000102226	USP11	-0.94790471	-0.745616894
ENSG00000163009	C2orf48	-0.727576002	-0.790808116
ENSG00000131747	TOP2A	-0.656130076	-0.810332936
ENSG00000139734	DIAPH3	-0.632055541	-0.737330951
ENSG00000169607	CKAP2L	-0.622623992	-0.820463736
ENSG00000012048	BRCA1	-0.614083512	-0.773251004
ENSG00000197299	BLM	-0.606414787	-0.700348483
ENSG00000109805	NCAPG	-0.598652798	-0.748481025
ENSG00000024526	DEPDC1	-0.589697013	-0.764540583
ENSG00000123219	CENPK	-0.586335589	-0.746013064
ENSG00000129810	SGOL1	-0.57567943	-0.745403668
ENSG00000080986	NDC80	-0.575234994	-0.826924386
ENSG00000163808	KIF15	-0.574489926	-0.75354182
ENSG00000165490	C11orf82	-0.572025015	-0.812857465
ENSG00000011426	ANLN	-0.565728856	-0.686610956
ENSG00000170629	DPY19L2P2	-0.562195526	-0.542432539
ENSG00000143228	NUF2	-0.555749122	-0.689515581
ENSG00000166845	C18orf54	-0.54847179	-0.741794042
ENSG00000138160	KIF11	-0.547488287	-0.661834067
ENSG00000102384	CENPI	-0.547332141	-0.701321929
ENSG00000165244	ZNF367	-0.545875847	-0.728347193
ENSG00000151725	CENPU	-0.544804957	-0.731456451
ENSG00000198826	ARHGAP11A	-0.538163459	-0.729111547
ENSG00000121211	MND1	-0.536545907	-0.664450652
ENSG00000138180	CEP55	-0.536287111	-0.684657727
ENSG00000151835	SACS	-0.53392498	-0.448767424
ENSG00000137812	CASC5	-0.531489774	-0.813715162
ENSG00000118193	KIF14	-0.530620915	-0.701604553
ENSG00000136982	DSCC1	-0.527912643	-0.526196624
ENSG00000148773	MKI67	-0.522850477	-0.737553272
ENSG00000072571	HMMR	-0.520947658	-0.740834083
ENSG00000171320	ESCO2	-0.517031785	-0.636406167

ENSG00000137807	KIF23	-0.516554054	-0.644551302
ENSG00000165480	SKA3	-0.51355679	-0.650807453
ENSG00000126787	DLGAP5	-0.510653122	-0.738190848
ENSG00000100479	POLE2	-0.505507465	-0.584175204
ENSG00000065328	MCM10	-0.502578527	-0.616680539
ENSG00000143476	DTL	-0.502511317	-0.520199568
ENSG00000156802	ATAD2	-0.500787442	-0.647247806
ENSG00000175305	CCNE2	-0.500157545	-0.635591892
ENSG00000051341	POLQ	-0.496101197	-0.804491266
ENSG00000267374	LINC00669	-0.494634912	-0.741006563
ENSG00000163507	KIAA1524	-0.484954715	-0.642559208
ENSG00000156970	BUB1B	-0.481312092	-0.559272505
ENSG00000112742	TTK	-0.480787316	-0.712125316
ENSG00000170312	CDK1	-0.480626331	-0.504247147
ENSG00000142731	PLK4	-0.479904235	-0.657143572
ENSG00000119969	HELLS	-0.477647741	-0.504640972
ENSG00000112029	FBXO5	-0.476832104	-0.578911348
ENSG00000198554	WDHD1	-0.476332318	-0.53869184
ENSG00000100629	CEP128	-0.47227592	-0.626304034
ENSG00000196584	XRCC2	-0.471688987	-0.620377146
ENSG00000119397	CNTRL	-0.467522414	-0.479176792
ENSG00000196550	FAM72A	-0.462252404	-0.404474135
ENSG00000168078	PBK	-0.458454667	-0.592674232
ENSG00000111247	RAD51AP1	-0.454259217	-0.653941899
ENSG00000148019	CEP78	-0.451865012	-0.568972919
ENSG00000176890	TYMS	-0.446956916	-0.511802636
ENSG00000265303	CTD-2510F5.6	-0.446732918	-0.523505367
ENSG00000146918	NCAPG2	-0.446101752	-0.489224957
ENSG00000121621	KIF18A	-0.445841243	-0.752939462
ENSG00000197275	RAD54B	-0.441872009	-0.484168495
ENSG00000171241	SHCBP1	-0.441579507	-0.491965969
ENSG00000169679	BUB1	-0.438030173	-0.525520802
ENSG00000181544	FANCB	-0.436907118	-0.638973282
ENSG00000092470	WDR76	-0.436049649	-0.520069986
ENSG00000136492	BRIP1	-0.436012036	-0.650397424
ENSG00000165891	E2F7	-0.431383742	-0.663971847
ENSG00000132436	FIGNL1	-0.430106354	-0.450133981
ENSG00000136824	SMC2	-0.429413832	-0.739477554
ENSG00000185697	MYBL1	-0.428736931	-0.702044779

ENSG00000035499	DEPDC1B	-0.427635147	-0.5676131
ENSG00000092853	CLSPN	-0.425283006	-0.537490161
ENSG00000175175	PPM1E	-0.423208697	-0.41297136
ENSG00000165304	MELK	-0.422233361	-0.534059444
ENSG00000080839	RBL1	-0.422165171	-0.499741467
ENSG00000188312	CENPP	-0.420271034	-0.643693039
ENSG00000119326	CTNNAL1	-0.419308285	-0.482164721
ENSG00000068489	PRR11	-0.41885867	-0.502553818
ENSG00000122591	FAM126A	-0.418504699	-0.379210673
ENSG00000144354	CDCA7	-0.418083812	-0.530720523
ENSG00000131470	PSMC3IP	-0.415107403	-0.325808219
ENSG00000139354	GAS2L3	-0.414839402	-0.648772716
ENSG00000137804	NUSAP1	-0.413661149	-0.604214053
ENSG00000152253	SPC25	-0.413310783	-0.526401021
ENSG00000122483	CCDC18	-0.412352099	-0.607165089
ENSG00000120539	MASTL	-0.410547822	-0.470420234
ENSG00000094804	CDC6	-0.408926841	-0.444286367
ENSG00000090889	KIF4A	-0.407187153	-0.536061554
ENSG00000176208	ATAD5	-0.405470594	-0.660684276
ENSG00000122966	CIT	-0.401587149	-0.451921604
ENSG00000175322	ZNF519	-0.401379496	-0.46318475
ENSG00000040275	SPDL1	-0.401197472	-0.680099231
ENSG00000163006	CCDC138	-0.400127631	-0.462502176
ENSG00000187951	ARHGAP11B	-0.399875036	-0.583802598
ENSG00000186777	ZNF732	-0.399873807	-0.480407815
ENSG00000183850	ZNF730	-0.399103255	-0.40617587
ENSG00000146263	MMS22L	-0.397194029	-0.586340157
ENSG00000101057	MYBL2	-0.396215652	-0.392055471
ENSG00000105866	SP4	-0.395641071	-0.385669937
ENSG00000103995	CEP152	-0.395166449	-0.586502683
ENSG00000184661	CDCA2	-0.395090598	-0.444049323
ENSG00000170264	FAM161A	-0.392177889	-0.379982246
ENSG00000184445	KNTC1	-0.388578076	-0.508041655
ENSG00000230453	ANKRD18B	-0.384368446	-0.321764758
ENSG00000120802	TMPO	-0.384113888	-0.465540782
ENSG00000094916	CBX5	-0.382583312	-0.371695994
ENSG00000125885	MCM8	-0.381525444	-0.553540801
ENSG00000106804	C5	-0.378467817	-0.454719126
ENSG00000102781	KATNAL1	-0.376077488	-0.331924387

ENSG00000151849	CENPJ	-0.372357286	-0.42573477
ENSG00000188610	FAM72B	-0.371401386	-0.345484167
ENSG00000183137	CEP57L1	-0.370928266	-0.407366582
ENSG00000180336	C17orf104	-0.370332603	-0.456971207
ENSG00000124795	DEK	-0.369617201	-0.544907588
ENSG00000137941	TTLL7	-0.369022933	-0.331707471
ENSG00000085840	ORC1	-0.368386472	-0.307294977
ENSG00000123485	HJURP	-0.368031507	-0.377763594
ENSG00000241472	PTPRG-AS1	-0.367312255	-0.43474131
ENSG00000123473	STIL	-0.367275673	-0.422629841
ENSG00000111788	RP11-22B23.1	-0.366902853	-0.320192961
ENSG00000121957	GPSM2	-0.363233473	-0.505104957
ENSG00000174371	EXO1	-0.36280855	-0.514945391
ENSG00000013810	TACC3	-0.361942914	-0.358332705
ENSG00000268205	CTC-444N24.11	-0.36127814	-0.248227801
ENSG00000144554	FANCD2	-0.360358495	-0.486618808
ENSG00000145386	CCNA2	-0.358709412	-0.448258041
ENSG00000034063	UHRF1	-0.356057364	-0.44426346
ENSG00000135476	ESPL1	-0.355628603	-0.414204641
ENSG00000186185	KIF18B	-0.355285248	-0.54780902
ENSG00000108055	SMC3	-0.355126354	-0.494821461
ENSG00000109674	NEIL3	-0.353636799	-0.573446156
ENSG00000075702	WDR62	-0.353430023	-0.397178269
ENSG00000051825	MPHOSPH9	-0.352657292	-0.393052356
ENSG00000007968	E2F2	-0.350793654	-0.504515614
ENSG00000071794	HLTF	-0.349494804	-0.415749844
ENSG00000118276	B4GALT6	-0.348971311	-0.390396127
ENSG00000187741	FANCA	-0.348355201	-0.451780243
ENSG00000146555	SDK1	-0.347319028	-0.360221388
ENSG00000242265	PEG10	-0.346282488	-0.572767102
ENSG00000114346	ECT2	-0.345923748	-0.491280846
ENSG00000183856	IQGAP3	-0.344547739	-0.470187108
ENSG00000253729	PRKDC	-0.341470074	-0.334477172
ENSG00000154920	EME1	-0.341227598	-0.517642367
ENSG00000029153	ARNTL2	-0.339726608	-0.353891157
ENSG00000053747	LAMA3	-0.336732441	-0.552008741
ENSG00000174442	ZWILCH	-0.336537098	-0.506632368
ENSG00000143401	ANP32E	-0.335861205	-0.526730788
ENSG00000140525	FANCI	-0.335549767	-0.415397009

ENSG00000198901	PRC1	-0.334351847	-0.39873809
ENSG00000149554	CHEK1	-0.333861302	-0.423229092
ENSG00000145375	SPATA5	-0.333034586	-0.439474965
ENSG00000213967	ZNF726	-0.332001963	-0.404643679
ENSG00000155850	SLC26A2	-0.330790452	-0.360362169
ENSG00000117155	SSX2IP	-0.329243173	-0.454653649
ENSG00000117650	NEK2	-0.326253895	-0.392330182
ENSG00000180385	EMC3-AS1	-0.32569368	-0.466392819
ENSG00000088325	TPX2	-0.32521198	-0.363362439
ENSG00000091436	MLTK	-0.322055392	-0.351400077
ENSG00000189308	LIN54	-0.321245006	-0.43953519
ENSG00000121152	NCAPH	-0.321010951	-0.410401343
ENSG00000136108	CKAP2	-0.320611615	-0.419027897
ENSG00000136861	CDK5RAP2	-0.318477532	-0.372705752
ENSG00000237649	KIFC1	-0.318147946	-0.367072432
ENSG00000173542	MOB1B	-0.31811564	-0.321333888
ENSG00000164985	PSIP1	-0.318108748	-0.450196258
ENSG00000109576	AADAT	-0.316747038	-0.337665486
ENSG00000075218	GTSE1	-0.315107128	-0.365648136
ENSG00000101868	POLA1	-0.308372393	-0.413647193
ENSG00000100077	ADRBK2	-0.308352782	-0.297636819
ENSG00000105486	LIG1	-0.30822327	-0.256975083
ENSG00000178202	KDELC2	-0.304772035	-0.384811536
ENSG00000162607	USP1	-0.304734072	-0.424606631
ENSG00000138346	DNA2	-0.301618282	-0.395402239
ENSG00000162636	FAM102B	-0.298120342	-0.266846332
ENSG00000160298	C21orf58	-0.295976711	-0.250057563
ENSG00000005249	PRKAR2B	-0.291582555	-0.21900842
ENSG00000164070	HSPA4L	-0.291464402	-0.428787392
ENSG00000166415	WDR72	-0.290822809	-0.217770132
ENSG00000269728	RP11-145M9.4	-0.290466157	-0.37327429
ENSG00000077684	JADE1	-0.287085092	-0.277888305
ENSG00000116830	TTF2	-0.275808267	-0.360306339
ENSG00000166881	TMEM194A	-0.275113223	-0.415386634
ENSG00000146281	PM20D2	-0.27181617	-0.347063468
ENSG00000106462	EZH2	-0.27030995	-0.382222623
ENSG00000204899	MZT1	-0.256345394	-0.325129779
ENSG00000167081	PBX3	-0.227283041	-0.292016449
ENSG00000109685	WHSC1	-0.191362342	-0.229566092

ENSG00000234127	TRIM26	0.168854592	0.144646572
ENSG00000108669	CYTH1	0.200510052	0.195535422
ENSG00000165861	ZFYVE1	0.207843823	0.290901199
ENSG00000114554	PLXNA1	0.213078706	0.20226955
ENSG00000160695	VPS11	0.213778831	0.203055991
ENSG00000153786	ZDHHC7	0.216487276	0.252088645
ENSG00000013588	GPRC5A	0.22476257	0.384298326
ENSG00000167767	KRT80	0.225914688	0.508387353
ENSG00000072071	LPHN1	0.2266561	0.180367588
ENSG00000059378	PARP12	0.227799766	0.24060334
ENSG00000135631	RAB11FIP5	0.231661565	0.295658274
ENSG00000100439	ABHD4	0.238560232	0.245040885
ENSG00000072121	ZFYVE26	0.241622152	0.158074956
ENSG00000116604	MEF2D	0.24259184	0.283894061
ENSG00000013374	NUB1	0.242993066	0.197654594
ENSG00000128335	APOL2	0.246496454	0.315112636
ENSG00000118960	HS1BP3	0.247480264	0.276945999
ENSG00000105357	MYH14	0.250797799	0.29784751
ENSG00000043143	JADE2	0.250981933	0.200572057
ENSG00000153029	MR1	0.258952917	0.255662872
ENSG00000103042	SLC38A7	0.261903583	0.235039386
ENSG00000135709	KIAA0513	0.262053142	0.346654226
ENSG00000197122	SRC	0.262591997	0.239142978
ENSG00000160271	RALGDS	0.263218336	0.211580669
ENSG00000170581	STAT2	0.263877158	0.253411535
ENSG00000111335	OAS2	0.270967236	0.23112591
ENSG00000197355	UAP1L1	0.274578547	0.255040165
ENSG00000103249	CLCN7	0.282256911	0.25891806
ENSG00000196787	HIST1H2AG	0.284400154	0.33189403
ENSG00000113924	HGD	0.28773101	0.231190726
ENSG00000164713	BRI3	0.293536052	0.211420704
ENSG00000180573	HIST1H2AC	0.293766503	0.320719324
ENSG00000099875	MKNK2	0.293971954	0.250360403
ENSG00000108771	DHX58	0.294289957	0.276590702
ENSG00000123240	OPTN	0.294605007	0.25563707
ENSG00000090238	YPEL3	0.304998904	0.415468988
ENSG00000159792	PSKH1	0.307431746	0.36871072
ENSG00000181830	SLC35C1	0.309172925	0.308681472
ENSG00000089127	OAS1	0.309345205	0.27801525

ENSG00000168016	TRANK1	0.309787755	0.266291647
ENSG00000158373	HIST1H2BD	0.313036188	0.352691555
ENSG00000134326	CMPK2	0.313581809	0.266357078
ENSG00000140464	PML	0.318377558	0.283201662
ENSG00000184678	HIST2H2BE	0.322663078	0.397210994
ENSG00000040531	CTNS	0.327194402	0.272074205
ENSG00000179344	HLA-DQB1	0.331868774	0.307745335
ENSG00000101986	ABCD1	0.331917219	0.32836044
ENSG00000135148	TRAFD1	0.332902653	0.29430297
ENSG00000119986	AVPI1	0.334905629	0.353172682
ENSG00000124201	ZNFX1	0.338039565	0.325221173
ENSG00000205356	TECPR1	0.338962419	0.412775793
ENSG00000068079	IFI35	0.344591198	0.339973811
ENSG00000076864	RAP1GAP	0.345583927	0.228492575
ENSG00000213689	TREX1	0.351156046	0.457926355
ENSG00000183558	HIST2H2AA3	0.359687586	0.393564918
ENSG00000128284	APOL3	0.361047896	0.293387257
ENSG00000102886	GDPD3	0.361646891	0.336920495
ENSG00000181218	HIST3H2A	0.362604801	0.366458017
ENSG00000182179	UBA7	0.375586032	0.379604073
ENSG00000013364	MVP	0.384426557	0.51392541
ENSG00000204525	HLA-C	0.39144286	0.296396285
ENSG00000204592	HLA-E	0.410633945	0.321116846
ENSG00000119917	IFIT3	0.411312572	0.237535517
ENSG00000134321	RSAD2	0.413713032	0.269395461
ENSG00000167614	TTYH1	0.414069248	0.360946116
ENSG00000173821	RNF213	0.415089228	0.195305608
ENSG00000256262	USP30-AS1	0.438484601	0.3628775
ENSG00000146859	TMEM140	0.443403785	0.403316744
ENSG00000149131	SERPING1	0.463123762	0.444477127
ENSG00000100342	APOL1	0.465277112	0.375253626
ENSG00000135114	OASL	0.46855234	0.362777371
ENSG00000234745	HLA-B	0.475912261	0.320999074
ENSG00000026950	BTN3A1	0.488131949	0.254433638
ENSG00000206337	HCP5	0.495371395	0.34404714
ENSG00000187134	AKR1C1	0.496003187	-0.31525007
ENSG00000231389	HLA-DPA-1	0.496462563	0.336817723
ENSG00000111801	BTN3A3	0.49696102	0.333313724
ENSG00000133321	RARRES3	0.507079488	0.369354817

ENSG00000103056	SMPD3	0.524105431	0.381173174
ENSG00000132274	TRIM22	0.528740448	0.298036587
ENSG00000168062	BATF2	0.532638803	0.431895087
ENSG00000172183	ISG20	0.533477984	0.346397979
ENSG00000151632	AKR1C2	0.537147567	-0.30435242
ENSG00000206341	HLA-H	0.543330557	0.365307944
ENSG00000102032	RENBP	0.557960052	0.48630339
ENSG00000204622	HLA-J	0.57404302	0.432386703
ENSG00000079385	CEACAM1	0.686524892	0.415665934
ENSG00000162654	GBP4	0.698127544	0.484694412
ENSG00000136514	RTP4	0.74123899	0.600877039
ENSG00000124256	ZBP1	0.776920784	0.469376034

Table 3.2: Significantly DE genes in LCC9 USP11 knockdown cells versus siRNA control

ENSEMBL_ID	GENE	Log2fold value siUSP11_1 (SI7)	Log2fold value siUSP11_2 (SI8)
ENSG00000102226	USP11	-1.401572943	-1.143216762
ENSG00000182185	RAD51B	-0.399795497	-0.257241896
ENSG00000249001	RP11-742B18.1	-0.382843518	-0.289087732
ENSG00000158373	HIST1H2BD	0.223032863	0.218922214
ENSG00000181381	DDX60L	0.30448582	0.347211758
ENSG00000123609	NMI	0.31931636	0.305719656
ENSG00000138642	HERC6	0.331867357	0.280655319
ENSG00000138496	PARP9	0.332017543	0.23934969
ENSG00000115415	STAT1	0.346544535	0.311301542
ENSG00000107201	DDX58	0.348266849	0.361635287
ENSG00000115267	IFIH1	0.360029486	0.271945224
ENSG00000137628	DDX60	0.3626594	0.266161546
ENSG00000152778	IFIT5	0.379388099	0.321359441
ENSG00000164342	TLR3	0.388537458	0.32766248
ENSG00000188313	PLSCR1	0.395953028	0.267335447
ENSG00000117226	GBP3	0.398850565	0.310008955
ENSG00000156587	UBE2L6	0.406974095	0.229982755
ENSG00000137965	IFI44	0.425202803	0.334722188
ENSG00000089127	OAS1	0.444360732	0.25226463
ENSG00000166710	B2M	0.478344478	0.271681548
ENSG00000137959	IFI44L	0.480976155	0.30628422
ENSG00000111335	OAS2	0.500628629	0.294182601
ENSG00000135114	OASL	0.518000228	0.2818333
ENSG00000132274	TRIM22	0.533315011	0.345993589
ENSG00000185745	IFIT1	0.575796696	0.457481905
ENSG00000119922	IFIT2	0.637920306	0.489224092
ENSG00000134326	CMPK2	0.661854276	0.416886325
ENSG00000134321	RSAD2	0.695528903	0.494618398
ENSG00000119917	IFIT3	0.839972572	0.457880889

Appendix 4: Mass spectrometry

Table 4.1: Proteins significantly upregulated in NTC versus shUSP11_1 +E2

NTC		**shUSP11_1**	
Gene names	Protein names	Gene names	Protein names
SERPINB6	Serpin B6	PON2	Serum paraoxonase/arylesterase 2
MUC6	Mucin-6	POLR1D	DNA-directed RNA polymerases I and III subunit RPAC2
DDX58	Probable ATP-dependent RNA helicase DDX58	MAPK15	Mitogen-activated protein kinase 15
POLD1	DNA polymerase;DNA polymerase delta catalytic subunit	APOD	Apolipoprotein D
SLC27A2	Very long-chain acyl-CoA synthetase	ANXA6	Annexin
GGCT	Gamma-glutamylcyclotransferase	AMPD2	AMP deaminase 2
OAT	Ornithine aminotransferase	AGR2	Anterior gradient protein 2 homolog
MYL3	Myosin light chain 3;Myosin light chain 1/3, skeletal muscle isoform	SERPINA3	Alpha-1-antichymotrypsin
HNRNPA1	Heterogeneous nuclear ribonucleoprotein A1;Heterogeneous nuclear ribonucleoprotein A1, N-terminally processed;Heterogeneous nuclear ribonucleoprotein A1-like 2	ANXA1	Annexin A1;Annexin
MIF	Macrophage migration inhibitory factor	TFF1	Trefoil factor 1
S100A4	Protein S100-A4	FBP1	Fructose-1,6-bisphosphatase 1
AK4	Adenylate kinase 4, mitochondrial	IGFBP2	Insulin-like growth factor-binding protein 2
HNRNPH3	Heterogeneous nuclear ribonucleoprotein H3	AZGP1	Zinc-alpha-2-glycoprotein
TAGLN2	Transgelin-2	NEDD8	NEDD8
ERH	Enhancer of rudimentary homolog	PDZK1	Na(+)/H(+) exchange regulatory cofactor NHE-RF3;Putative PDZ domain-containing protein 1P
FABP5	Fatty acid-binding protein, epidermal	AGR3	Anterior gradient protein 3 homolog
SRSF4	Serine/arginine-rich splicing factor 4	MZB1	Marginal zone B- and B1-cell-specific protein
LBR	Lamin-B receptor	POF1B	Protein POF1B
DNAJC9	DnaJ homolog subfamily C member 9	CORO2A	Coronin-2A
OSBPL8	Oxysterol-binding protein-related protein 8;Oxysterol-binding protein	HGD	Homogentisate 1,2-dioxygenase
FN3K	Fructosamine-3-kinase	GTPBP3	tRNA modification GTPase GTPBP3, mitochondrial
ABRACL	Costars family protein ABRACL	TBC1D23	TBC1 domain family member 23
ANKFY1	Rabankyrin-5		

AK6;TAF9	Adenylate kinase isoenzyme 6		

Table 4.2: Proteins significantly upregulated in NTC versus shUSP11_4 +E2

NTC		**shUSP11_4**	
Gene names	Protein names	Gene names	Protein names
SERPINB6	Serpin B6	DHX29	ATP-dependent RNA helicase DHX29
HEL-S-109	Nucleobindin-2;Nesfatin-1	FHL2	Four and a half LIM domains protein 2
MUC1	Mucin-1;Mucin-1 subunit alpha;Mucin-1 subunit beta	PPAN-P2RY11	Suppressor of SWI4 1 homolog
SULT1A4	Sulfotransferase;Sulfotransferase 1A4;Sulfotransferase 1A3;Sulfotransferase 1A1	POLR1D	DNA-directed RNA polymerases I and III subunit RPAC2
DLGAP4	Disks large-associated protein 4	SLC7A2	Cationic amino acid transporter 2
ABHD16A	Abhydrolase domain-containing protein 16A	SLC35A2	UDP-galactose translocator
MUC6	Mucin-6	NMD3	60S ribosomal export protein NMD3
CTSD	Cathepsin D;Cathepsin D light chain;Cathepsin D heavy chain	APOD	Apolipoprotein D
PSMD10	26S proteasome non-ATPase regulatory subunit 10	TTC39A	Tetratricopeptide repeat protein 39A
MSI2	RNA-binding protein Musashi homolog 2	CD59	CD59 glycoprotein
POLR2H	DNA-directed RNA polymerases I, II, and III subunit RPABC3	SDR16C5	Epidermal retinol dehydrogenase 2
SEC62	Translocation protein SEC62	WBP2	WW domain-binding protein 2
PFN2	Profilin;Profilin-2	PIH1D1	PIH1 domain-containing protein 1
DNPH1	2-deoxynucleoside 5-phosphate N-hydrolase 1	FAAH	Fatty-acid amide hydrolase 1
PCMT1	Protein-L-isoaspartate O-methyltransferase;Protein-L-isoaspartate(D-aspartate) O-methyltransferase	HAT1	Histone acetyltransferase type B catalytic subunit
CCDC12	Coiled-coil domain-containing protein 12	WBSCR22	Probable 18S rRNA (guanine-N(7))-methyltransferase
NDUFAB1	Acyl carrier protein, mitochondrial;Acyl carrier protein	SYNCRIP	Heterogeneous nuclear ribonucleoprotein Q
PGRMC2	Membrane-associated progesterone receptor component 2	ANXA1	Annexin A1;Annexin
ACTN4	Alpha-actinin-4	KRT18	Keratin, type I cytoskeletal 18
GGCT	Gamma-glutamylcyclotransferase	UROD	Uroporphyrinogen decarboxylase
AKR7A3	Aflatoxin B1 aldehyde reductase member 3	PGR	Progesterone receptor
PGLS	6-phosphogluconolactonase	CLU	Clusterin
TOMM40	Mitochondrial import receptor subunit TOM40 homolog	SLC2A1	Solute carrier family 2, facilitated glucose transporter member 1
OAT	Ornithine aminotransferase, mitochondrial;Ornithine aminotransferase, hepatic form;Ornithine aminotransferase,	LCP1	Plastin-2

	renal form		
ATP1B1	Sodium/potassium-transporting ATPase subunit beta-1	AKR1A1	Alcohol dehydrogenase [NADP(+)]
SSB	Lupus La protein	SCP2	Non-specific lipid-transfer protein
P4HB	Protein disulfide-isomerase	PSM8	Proteasome subunit beta type;Proteasome subunit beta type-8
PFN1	Profilin-1	PGM1	Phosphoglucomutase-1
HNRNPA1	Heterogeneous nuclear ribonucleoprotein A1	ATRX	Transcriptional regulator ATRX
ANXA3	Annexin A3;Annexin	NASP	Nuclear autoantigenic sperm protein
CKMT1A;CKMT1B	Creatine kinase U-type, mitochondrial	MRE11A	Double-strand break repair protein MRE11A
ACTN1	Alpha-actinin-1	RAB25	Ras-related protein Rab-25
PLS3	Plastin-3	EPPK1	Epiplakin
MIF	Macrophage migration inhibitory factor	YBX1	Nuclease-sensitive element-binding protein 1
UCHL3	Ubiquitin carboxyl-terminal hydrolase isozyme L3;Ubiquitin carboxyl-terminal hydrolase	PRDX1	Peroxiredoxin-1
VCL	Vinculin	MTM1	Myotubularin
COMT	Catechol O-methyltransferase	RAB31	Ras-related protein Rab-31
HNRNPA2B1	Heterogeneous nuclear ribonucleoproteins A2/B1	KIAA0101	PCNA-associated factor
MAOB	Amine oxidase [flavin-containing] B	BRD3	Bromodomain-containing protein 3
CALR	Calreticulin	RAB35	Ras-related protein Rab-35
BLVRB	Flavin reductase (NADPH)	DHCR24	Delta(24)-sterol reductase
PEBP1	Phosphatidylethanolamine-binding protein 1	NEDD8	NEDD8
HNRNPH3	Heterogeneous nuclear ribonucleoprotein H3	ATP6AP1	V-type proton ATPase subunit S1
SRP14	Signal recognition particle 14 kDa protein	PDCD4	Programmed cell death protein 4
HPCAL1	Hippocalcin-like protein 1;Neuron-specific calcium-binding protein hippocalcin	PKIB	cAMP-dependent protein kinase inhibitor beta
TAGLN2	Transgelin-2	JMJD6	Bifunctional arginine demethylase and lysyl-hydroxylase JMJD6
ECI1;DCI	Enoyl-CoA delta isomerase 1, mitochondrial	BLOC1S2	Biogenesis of lysosome-related organelles complex 1 subunit 2
SLC1A1	Excitatory amino acid transporter 3	SCCPDH	Saccharopine dehydrogenase-like oxidoreductase
PPIC	Peptidyl-prolyl cis-trans isomerase C	SERBP1	Plasminogen activator inhibitor 1 RNA-binding protein
CRKL	Crk-like protein	AGR3	Anterior gradient protein 3 homolog
GYG1	Glycogenin-1	CORO2A	Coronin-2A
GSS	Glutathione synthetase	RFK	Riboflavin kinase
SRP9	Signal recognition particle 9 kDa protein	GTPBP3	tRNA modification GTPase GTPBP3, mitochondrial
HINT1	Histidine triad nucleotide-binding protein 1	TCEAL4	Transcription elongation factor A protein-like 4

GNAQ	Guanine nucleotide-binding protein G(q) subunit alpha	MBOAT7	Lysophospholipid acyltransferase 7
GNG10	Guanine nucleotide-binding protein G(I)/G(S)/G(O) subunit gamma-10;Guanine nucleotide-binding protein subunit gamma	NDC1	Nucleoporin NDC1
ARHGDIB	Rho GDP-dissociation inhibitor 2	MLPH	Melanophilin
HNRNPF	Heterogeneous nuclear ribonucleoprotein F;Heterogeneous nuclear ribonucleoprotein F, N-terminally processed	PPDPF	Pancreatic progenitor cell differentiation and proliferation factor
SEC13	Protein SEC13 homolog	TBC1D23	TBC1 domain family member 23
MTPN	Myotrophin	DDX18	ATP-dependent RNA helicase DDX18
TPI1	Triosephosphate isomerase	CDKN2AIP	CDKN2A-interacting protein
HSPE1	10 kDa heat shock protein, mitochondrial	MAGEC2	Melanoma-associated antigen C2
NUTF2	Nuclear transport factor 2	GNG12	Guanine nucleotide-binding protein G(I)/G(S)/G(O) subunit gamma-12
YWHAE	14-3-3 protein epsilon	UQCR10	Cytochrome b-c1 complex subunit 9
POLR2G	DNA-directed RNA polymerase II subunit RPB7	CDV3	Protein CDV3 homolog
PPIA	Peptidyl-prolyl cis-trans isomerase A	MKL2	MKL/myocardin-like protein 2
FKBP1A	Peptidyl-prolyl cis-trans isomerase FKBP1A	SAMHD1	Deoxynucleoside triphosphate triphosphohydrolase SAMHD1
TUBB4B	Tubulin beta-4B chain	SCIN	Adseverin
PAFAH1B2	Platelet-activating factor acetylhydrolase IB subunit beta		
ERH	Enhancer of rudimentary homolog		
FABP5	Fatty acid-binding protein, epidermal		
HMGCS1	Hydroxymethylglutaryl-CoA synthase, cytoplasmic		
SSBP1	Single-stranded DNA-binding protein, mitochondrial		
CBX3	Chromobox protein homolog 3		
RCN2	Reticulocalbin-2		
SF3B4	Splicing factor 3B subunit 4		
CYP1B1	Cytochrome P450 1B1		
SH3BGRL3	SH3 domain-binding glutamic acid-rich-like protein 3		
PDZK1;PDZK1P1	Na(+)/H(+) exchange regulatory cofactor NHE-RF3;Putative PDZ domain-containing protein 1P		
ACAD10	Acyl-CoA dehydrogenase family member 10		
DNAJC10	DnaJ homolog subfamily C member 10		
MZB1	Marginal zone B- and B1-cell-specific protein		
DNAJC9	DnaJ homolog subfamily C member 9		
TFG	Protein TFG		
DCPS	m7GpppX diphosphatase		

ABHD14B	Alpha/beta hydrolase domain-containing protein 14B		
C12orf57	Protein C10		
HNRNPUL1	Heterogeneous nuclear ribonucleoprotein U-like protein 1		
GLOD4	Glyoxalase domain-containing protein 4		
FAM120C	Constitutive coactivator of PPAR-gamma-like protein 2		
ABRACL	Costars family protein ABRACL		
ENOPH1	Enolase-phosphatase E1		
PYCARD	Apoptosis-associated speck-like protein containing a CARD		
CARHSP1	Calcium-regulated heat stable protein 1		
VPRBP	Protein VPRBP		
COL4A3BP	Collagen type IV alpha-3-binding protein		
HEBP2	Heme-binding protein 2		

Table 4.3: Proteins significantly upregulated in NTC +E2 versus NTC -E2

NTC +E2		**NTC -E2**	
Gene names	**Protein names**	**Gene names**	**Protein names**
SERPINA1	Alpha-1-antitrypsin;Short peptide from AAT	CUL2	Cullin-2
UHRF1	E3 ubiquitin-protein ligase UHRF1	PPAN-P2RY11	Suppressor of SWI4 1 homolog
PEG10	Retrotransposon-derived protein PEG10	POLR1D	DNA-directed RNA polymerases I and III subunit RPAC2
POLD2	DNA polymerase delta subunit 2	RALGAPA1	Ral GTPase-activating protein subunit alpha-1
MUC1	Mucin-1;Mucin-1 subunit alpha;Mucin-1 subunit beta	RBM47	RNA-binding protein 47
IREB2	Iron-responsive element-binding protein 2	EWSR1	RNA-binding protein EWS
HELLS	Lymphoid-specific helicase	ANXA6	Annexin
CLN6	Ceroid-lipofuscinosis neuronal protein 6	PRMT1	Protein arginine N-methyltransferase 1
CTSD	Cathepsin D;Cathepsin D light chain;Cathepsin D heavy chain	SEC23A	Protein transport protein Sec23A
SMN1	Survival motor neuron protein	CNOT2	CCR4-NOT transcription complex subunit 2
DDX58	Probable ATP-dependent RNA helicase DDX58	ERGIC3	Endoplasmic reticulum-Golgi intermediate compartment protein 3
GUK1	Guanylate kinase	NDUFB5	NADH dehydrogenase [ubiquinone] 1 beta subcomplex

			subunit 5, mitochondrial
COX17	Cytochrome c oxidase copper chaperone	TLE3	Transducin-like enhancer protein 3
SCRN3	Secernin-3	GFER	FAD-linked sulfhydryl oxidase ALR;Sulfhydryl oxidase
MRPS34	28S ribosomal protein S34, mitochondrial	IST1	IST1 homolog
POLR2H	DNA-directed RNA polymerases I, II, and III subunit RPABC3	ERBB2	Receptor protein-tyrosine kinase;Receptor tyrosine-protein kinase erbB-2
RFC4	Replication factor C subunit 4	WBP2	WW domain-binding protein 2
DCK	Deoxycytidine kinase	PIH1D1	PIH1 domain-containing protein 1
PCM1	Pericentriolar material 1 protein	DNASE2	Deoxyribonuclease-2-alpha
ALYREF	THO complex subunit 4	PSMD12	26S proteasome non-ATPase regulatory subunit 12
NCAPH	Condensin complex subunit 2	QSOX1	Sulfhydryl oxidase 1
SLC3A2	4F2 cell-surface antigen heavy chain	IRF6	Interferon regulatory factor 6
SEC62	Translocation protein SEC62	SURF4	Surfeit locus protein 4
CDK2	Cyclin-dependent kinase 2	SLC25A20	Mitochondrial carnitine/acylcarnitine carrier protein
ABCA3	ATP-binding cassette sub-family A member 3	SYNCRIP	Heterogeneous nuclear ribonucleoprotein Q
KDM1B	Lysine-specific histone demethylase 1B	BCAS1	Breast carcinoma-amplified sequence 1
		NEBL	Nebulette
CCDC12	Coiled-coil domain-containing protein 12	NDUFB4	NADH dehydrogenase [ubiquinone] 1 beta subcomplex subunit 4
SPC24	Kinetochore protein Spc24	SNX4	Sorting nexin-4
POLD1	DNA polymerase;DNA polymerase delta catalytic subunit	MT-CO3	Cytochrome c oxidase subunit 3
HAX1	HCLS1-associated protein X-1	LMNA	Prelamin-A/C;Lamin-A/C
PGRMC1	Membrane-associated progesterone receptor component 1	CAT	Catalase
HIP1	Huntingtin-interacting protein 1	CSTB	Cystatin-B
UBE2C	Ubiquitin-conjugating enzyme E2 C	ATP1B1	Sodium/potassium-transporting ATPase subunit beta-1
SLC9A3R1	Na(+)/H(+) exchange regulatory cofactor NHE-RF1	KRT18	Keratin, type I cytoskeletal 18
NDC80	Kinetochore protein NDC80 homolog	S100A6	Protein S100-A6;Protein S100
HAT1	Histone acetyltransferase type B catalytic subunit	ANXA5	Annexin A5;Annexin
SLC27A2	Very long-chain acyl-CoA synthetase	GAA	Lysosomal alpha-glucosidase;76 kDa lysosomal alpha-glucosidase

P4HA2	Prolyl 4-hydroxylase subunit alpha-2	CTSA	Carboxypeptidase;Lysosomal protective protein
CA12	Carbonic anhydrase 12	CLU	Clusterin
PRC1	Protein regulator of cytokinesis 1	ACADM	Medium-chain specific acyl-CoA dehydrogenase, mitochondrial
ACTN4	Alpha-actinin-4	NQO1	NAD(P)H dehydrogenase [quinone] 1
MGEA5	Protein O-GlcNAcase	NDUFB7	NADH dehydrogenase [ubiquinone] 1 beta subcomplex subunit 7
BUB1B	Mitotic checkpoint serine/threonine-protein kinase BUB1 beta	CAPN2	Calpain-2 catalytic subunit
GGCT	Gamma-glutamylcyclotransferase	IGFBP2	Insulin-like growth factor-binding protein 2
HMMR	Hyaluronan mediated motility receptor	RAB6A	Ras-related protein Rab-6A;Ras-related protein Rab-6B
CSDE1	Cold shock domain-containing protein E1	PSMB1	Proteasome subunit beta type-1
WDHD1	WD repeat and HMG-box DNA-binding protein 1	PTMS	Parathymosin
RNASEH2A	Ribonuclease H2 subunit A	GATA3	Trans-acting T-cell-specific transcription factor GATA-3
KIF4A	Chromosome-associated kinesin KIF4A	AZGP1	Zinc-alpha-2-glycoprotein
SMC2	Structural maintenance of chromosomes protein 2	PTPN6	Tyrosine-protein phosphatase non-receptor type 6
WHSC1	Histone-lysine N-methyltransferase NSD2	ALDH4A1	Delta-1-pyrroline-5-carboxylate dehydrogenase, mitochondrial
DHFR	Dihydrofolate reductase	ATP5D	ATP synthase subunit delta, mitochondrial
TFRC	Transferrin receptor protein 1;Transferrin receptor protein 1, serum form	COPB2	Coatomer subunit beta
TFF1	Trefoil factor 1	HMGCL	Hydroxymethylglutaryl-CoA lyase, mitochondrial
TK1	Thymidine kinase, cytosolic;Thymidine kinase	CRAT	Carnitine O-acetyltransferase
TYMS	Thymidylate synthase	ACADSB	Short/branched chain specific acyl-CoA dehydrogenase, mitochondrial
SSB	Lupus La protein	ATRX	Transcriptional regulator ATRX
PGR;PR	Progesterone receptor	CDKN1B	Cyclin-dependent kinase inhibitor 1B
CDK1;CDC2	Cyclin-dependent kinase 1	ACADVL	Very long-chain specific acyl-CoA dehydrogenase, mitochondrial
EPHX1	Epoxide hydrolase 1	MRE11A	Double-strand break repair protein MRE11A
P4HB	Protein disulfide-isomerase	PSMD7	26S proteasome non-ATPase regulatory subunit 7
RHOC	Rho-related GTP-binding protein RhoC	HDGF	Hepatoma-derived growth factor

HSP90AB1	Heat shock protein HSP 90-beta	MFAP1	Microfibrillar-associated protein 1
HMBS	Porphobilinogen deaminase	RRP1	Ribosomal RNA processing protein 1 homolog A
MYL3;MYL1	Myosin light chain 3;Myosin light chain 1/3, skeletal muscle isoform	RAB25	Ras-related protein Rab-25
HNRNPA1	Heterogeneous nuclear ribonucleoprotein A1	TMSB4X	Thymosin beta-4;Hematopoietic system regulatory peptide
COX6C	Cytochrome c oxidase subunit 6C	SLC25A11	Mitochondrial 2-oxoglutarate/malate carrier protein
ALDOC	Fructose-bisphosphate aldolase C;Fructose-bisphosphate aldolase	C1QBP	Complement component 1 Q subcomponent-binding protein, mitochondrial
H2AFV	Histone H2A.V	MZT1	Mitotic-spindle organizing protein 1
SLC2A1	Solute carrier family 2, facilitated glucose transporter member 1	AHNAK	Neuroblast differentiation-associated protein AHNAK
TOP2A	DNA topoisomerase 2-alpha	GALNT2	Polypeptide N-acetylgalactosaminyltransferase 2;Polypeptide N-acetylgalactosaminyltransferase 2 soluble form
PCNA	Proliferating cell nuclear antigen	SELENBP1	Selenium-binding protein 1
TPT1	Translationally-controlled tumor protein	PRPF4B	Serine/threonine-protein kinase PRP4 homolog
MIF	Macrophage migration inhibitory factor	ALCAM	CD166 antigen
CCNB1	G2/mitotic-specific cyclin-B1	EIF2B1	Translation initiation factor eIF-2B subunit alpha
STMN1	Stathmin	MESDC2	LDLR chaperone MESD
GJA1	Gap junction alpha-1 protein	GANAB	Neutral alpha-glucosidase AB
CTPS1	CTP synthase 1	NUMA1	Nuclear mitotic apparatus protein 1
DDX5	Probable ATP-dependent RNA helicase DDX5	BRD3	Bromodomain-containing protein 3
HNRNPA2B1	Heterogeneous nuclear ribonucleoproteins A2/B1	TCEAL1	Transcription elongation factor A protein-like 1
IGFBP4	Insulin-like growth factor-binding protein 4	RAB35	Ras-related protein Rab-35
RRM1	Ribonucleoside-diphosphate reductase large subunit	TMED2	Transmembrane emp24 domain-containing protein 2
MCM3	DNA replication licensing factor MCM3	PDCD4	Programmed cell death protein 4
DNMT1	DNA (cytosine-5)-methyltransferase 1	MIA3	Melanoma inhibitory activity protein 3
RPL10	60S ribosomal protein L10	MRPL54	39S ribosomal protein L54, mitochondrial
PPP2R1B	Serine/threonine-protein phosphatase 2A 65 kDa regulatory subunit A beta isoform	CERS6	Ceramide synthase 6
RRM2	Ribonucleoside-diphosphate reductase subunit M2	GALNT7	N-acetylgalactosaminyltransferase 7
DNAJA1	DnaJ homolog subfamily A member 1	GOLM1	Golgi membrane protein 1

HNRNPH3	Heterogeneous nuclear ribonucleoprotein H3	TMEM87A	Transmembrane protein 87A
CKS2	Cyclin-dependent kinases regulatory subunit 2	GALNT6	Polypeptide N-acetylgalactosaminyltransferase 6
MCM4	DNA replication licensing factor MCM4	CDC26	Anaphase-promoting complex subunit CDC26
MCM5	DNA replication licensing factor MCM5;DNA helicase	SLC35B2	Adenosine 3-phospho 5-phosphosulfate transporter 1
MCM7	DNA replication licensing factor MCM7	GNPDA2	Glucosamine-6-phosphate isomerase 2
RFC1	Replication factor C subunit 1	COG1	Conserved oligomeric Golgi complex subunit 1
ARL3	ADP-ribosylation factor-like protein 3	NCSTN	Nicastrin
HPCAL1;HPCA	Hippocalcin-like protein 1;Neuron-specific calcium-binding protein hippocalcin	HGD	Homogentisate 1,2-dioxygenase
FDFT1	Squalene synthase	PHKB	Phosphorylase b kinase regulatory subunit beta
TAGLN2	Transgelin-2	TCEAL4	Transcription elongation factor A protein-like 4
FEN1	Flap endonuclease 1	DYNLL2	Dynein light chain 2, cytoplasmic
RFC3	Replication factor C subunit 3	USMG5	Up-regulated during skeletal muscle growth protein 5
EIF1	Eukaryotic translation initiation factor 1	FAM129B	Niban-like protein 1
TMPO	Lamina-associated polypeptide 2, isoform alpha;Thymopoietin;Thymopentin	CEP44	Centrosomal protein of 44 kDa
RPL35	60S ribosomal protein L35	NUCKS1	Nuclear ubiquitous casein and cyclin-dependent kinase substrate 1
MSH2	DNA mismatch repair protein Msh2	ACBD3	Golgi resident protein GCP60
PPIC	Peptidyl-prolyl cis-trans isomerase C	PPDPF	Pancreatic progenitor cell differentiation and proliferation factor
MKI67	Antigen KI-67	GOLPH3L	Golgi phosphoprotein 3-like
MAPKAPK2	MAP kinase-activated protein kinase 2	PLEKHF2	Pleckstrin homology domain-containing family F member 2
CENPF	Centromere protein F	QTRTD1	Queuine tRNA-ribosyltransferase subunit QTRTD1
SRP9	Signal recognition particle 9 kDa protein	POLR1B	DNA-directed RNA polymerase I subunit RPA2
MCM2	DNA replication licensing factor MCM2	GRPEL1	GrpE protein homolog 1, mitochondrial
KPNA2	Importin subunit alpha-1	EPB41L5	Band 4.1-like protein 5
HNRNPF	Heterogeneous nuclear ribonucleoprotein F	KIF13B	Kinesin-like protein KIF13B;Kinesin-like protein
KIF11	Kinesin-like protein KIF11	DIABLO	Diablo homolog, mitochondrial
PLK1	Serine/threonine-protein kinase PLK1	HEBP1	Heme-binding protein 1
ADAR	Double-stranded RNA-specific adenosine deaminase	UFSP2	Ufm1-specific protease 2

MTPN	Myotrophin	TBC1D23	TBC1 domain family member 23
CKS1B	Cyclin-dependent kinases regulatory subunit 1;Cyclin-dependent kinases regulatory subunit	THUMPD1	THUMP domain-containing protein 1
RPS15A	40S ribosomal protein S15a	MAGEC2	Melanoma-associated antigen C2
RPS6	40S ribosomal protein S6	SLC25A10	Mitochondrial dicarboxylate carrier
TUBB4B	Tubulin beta-4B chain	UQCR10	Cytochrome b-c1 complex subunit 9
PAFAH1B2	Platelet-activating factor acetylhydrolase IB subunit beta	ARMCX3	Armadillo repeat-containing X-linked protein 3
HIST1H3A	Histone H3.1	LIMA1	LIM domain and actin-binding protein 1
MRPS35	28S ribosomal protein S35, mitochondrial	PCYOX1	Prenylcysteine oxidase 1
ERH	Enhancer of rudimentary homolog	CNOT7	CCR4-NOT transcription complex subunit 7
FABP5	Fatty acid-binding protein, epidermal	SLC25A13	Calcium-binding mitochondrial carrier protein Aralar2
HMGCS1	Hydroxymethylglutaryl-CoA synthase, cytoplasmic	TMED3	Transmembrane emp24 domain-containing protein 3
KIF23	Kinesin-like protein KIF23;Kinesin-like protein	SCIN	Adseverin
FKBP4	Peptidyl-prolyl cis-trans isomerase FKBP4		
FPGS	Folylpolyglutamate synthase, mitochondrial		
MAD2L1	Mitotic spindle assembly checkpoint protein MAD2A		
SQSTM1	Sequestosome-1		
TPBG	Trophoblast glycoprotein		
GNL2	Nucleolar GTP-binding protein 2		
CKAP5	Cytoskeleton-associated protein 5		
MCM6	DNA replication licensing factor MCM6		
KIF22	Kinesin-like protein KIF22;Kinesin-like protein		
NCAPD2	Condensin complex subunit 1		
POLD3	DNA polymerase delta subunit 3		
KIF14	Kinesin-like protein KIF14		
SF3B4	Splicing factor 3B subunit 4		
CYP1B1	Cytochrome P450 1B1		
UBE2S	Ubiquitin-conjugating enzyme E2 S		
GREB1	Protein GREB1		
PRRC2B	Protein PRRC2B		
DNTTIP2	Deoxynucleotidyltransferase terminal-interacting protein 2		
NUP188	Nucleoporin NUP188 homolog		
PDZK1;PDZK1P1	Na(+)/H(+) exchange regulatory cofactor NHE-RF3;Putative PDZ domain-containing protein 1P		

RIF1	Telomere-associated protein RIF1		
FMN1	Formin-1		
RPL7L1	60S ribosomal protein L7-like 1		
ACAD10	Acyl-CoA dehydrogenase family member 10		
CDC73	Parafibromin		
INTS5	Integrator complex subunit 5		
ATAD2	ATPase family AAA domain-containing protein 2		
THOC6	THO complex subunit 6 homolog		
HIST2H2AB	Histone H2A type 2-B		
COLGALT1	Procollagen galactosyltransferase 1		
CCNY	Cyclin-Y		
PREX1	Phosphatidylinositol 3,4,5-trisphosphate-dependent Rac exchanger 1 protein		
CKAP2	Cytoskeleton-associated protein 2		
SYNE2	Nesprin-2		
DNAJC9	DnaJ homolog subfamily C member 9		
DHX38	Pre-mRNA-splicing factor ATP-dependent RNA helicase PRP16		
ARHGEF2	Rho guanine nucleotide exchange factor 2		
HMCES	Embryonic stem cell-specific 5-hydroxymethylcytosine-binding protein		
C12orf57	Protein C10		
NCAPG	Condensin complex subunit 3		
MCMBP	Mini-chromosome maintenance complex-binding protein		
KIFC1	Kinesin-like protein KIFC1		
RPAP1	RNA polymerase II-associated protein 1		
LSM14B	Protein LSM14 homolog B		
FANCD2	Fanconi anemia group D2 protein		
PARD6B	Partitioning defective 6 homolog beta		
UCK2	Uridine-cytidine kinase 2		
RACGAP1	Rac GTPase-activating protein 1		
DDX47	Probable ATP-dependent RNA helicase DDX47		
ZNF703	Zinc finger protein 703		
NOL11	Nucleolar protein 11		
ECT2	Protein ECT2		

CELSR2	Cadherin EGF LAG seven-pass G-type receptor 2		
UBE2T	Ubiquitin-conjugating enzyme E2 T		
ANLN	Actin-binding protein anillin		
POLE3	DNA polymerase epsilon subunit 3		
SMC4	Structural maintenance of chromosomes protein 4;Structural maintenance of chromosomes protein		
FANCI	Fanconi anemia group I protein		
P4HTM	Transmembrane prolyl 4-hydroxylase		
GSKIP	GSK3-beta interaction protein		
ANAPC4	Anaphase-promoting complex subunit 4		
HSPB8	Heat shock protein beta-8		
TPX2	Targeting protein for Xklp2		
PYCARD	Apoptosis-associated speck-like protein containing a CARD		
CARHSP1	Calcium-regulated heat stable protein 1		
TMX2	Thioredoxin-related transmembrane protein 2		
AK6;TAF9	Adenylate kinase isoenzyme 6		
PKP3	Plakophilin-3		
HEBP2	Heme-binding protein 2		
MRFAP1	MORF4 family-associated protein 1		
PSAT1	Phosphoserine aminotransferase		
TACC3	Transforming acidic coiled-coil-containing protein 3		

Table 4.4: USP11 ubiquitinome

Proteins significantly upregulated in shUSP11_1	
Protein names	Gene names
Cadherin-1;E-Cad/CTF1;E-Cad/CTF2;E-Cad/CTF3;Cadherin-3	CDH1;CDH3
Cell adhesion molecule 1	CADM1
Elongation factor 1-delta;Elongation factor 1-beta	EEF1D;EEF1B2
Serine/arginine-rich splicing factor 7	SRSF7
Prostate tumor-overexpressed gene 1 protein	PTOV1
Heat shock 70 kDa protein 1B;Heat shock 70 kDa protein 1A;Heat shock 70 kDa protein 6	HSPA1B;HSPA1A;HSPA6

DNA-3-methyladenine glycosylase	MPG
Pituitary tumor-transforming gene 1 protein-interacting protein	PTTG1IP
Polyadenylate-binding protein;Polyadenylate-binding protein 4;Polyadenylate-binding protein 1	PABPC4;PABPC1
60S ribosomal protein L30	RPL30
Cofilin-1	CFL1
Palmitoyltransferase;Palmitoyltransferase ZDHHC3	ZDHHC3
Protein SOGA1;N-terminal form;C-terminal 80 kDa form	SOGA1
Ankyrin repeat domain-containing protein 13A	ANKRD13A
Nucleosome assembly protein 1-like 1	NAP1L1
Nucleosome assembly protein 1-like 1	NAP1L1
Mitochondrial Rho GTPase;Mitochondrial Rho GTPase 1	RHOT1
Butyrophilin subfamily 2 member A1	BTN2A1
GTP-binding nuclear protein Ran	RAN
Eukaryotic elongation factor 2 kinase	EEF2K
CSC1-like protein 1	TMEM63A
Fructose-bisphosphate aldolase A;Fructose-bisphosphate aldolase	ALDOA
Anion exchange protein 2	SLC4A2
Sodium/potassium-transporting ATPase subunit alpha-1	ATP1A1
Galectin-1	LGALS1
Heat shock cognate 71 kDa protein	HSPA8
Inosine-5'-monophosphate dehydrogenase 2	IMPDH2
Nucleoprotein TPR	TPR
Elongation factor 2	EEF2
Ezrin	EZR
Histone H2AX	H2AFX
Voltage-dependent anion-selective channel protein 1	VDAC1
Receptor tyrosine-protein kinase erbB-3	ERBB3

Nucleoside diphosphate kinase;Nucleoside diphosphate kinase B;Putative nucleoside diphosphate kinase	NME1-NME2;NME2;NME2P1
G1/S-specific cyclin-D1	CCND1
Heat shock 70 kDa protein 1-like	HSPA1L
Ubiquitin carboxyl-terminal hydrolase 5	USP5
Ubiquitin carboxyl-terminal hydrolase 5	USP5
Ras GTPase-activating-like protein IQGAP1	IQGAP1
Fatty acid synthase;[Acyl-carrier-protein] S-acetyltransferase;[Acyl-carrier-protein] S-malonyltransferase;3-oxoacyl-[acyl-carrier-protein] synthase;3-oxoacyl-[acyl-carrier-protein] reductase;3-hydroxyacyl-[acyl-carrier-protein] dehydratase;Enoyl-[acyl-carrier-protein] reductase;Oleoyl-[acyl-carrier-protein] hydrolase	FASN
Fatty acid synthase;[Acyl-carrier-protein] S-acetyltransferase;[Acyl-carrier-protein] S-malonyltransferase;3-oxoacyl-[acyl-carrier-protein] synthase;3-oxoacyl-[acyl-carrier-protein] reductase;3-hydroxyacyl-[acyl-carrier-protein] dehydratase;Enoyl-[acyl-carrier-protein] reductase;Oleoyl-[acyl-carrier-protein] hydrolase	FASN
T-complex protein 1 subunit gamma	CCT3
Hsc70-interacting protein;Putative protein FAM10A5	ST13;ST13P5
40S ribosomal protein S20	RPS20
Small ubiquitin-related modifier 2;Small ubiquitin-related modifier 3;Small ubiquitin-related modifier 4	SUMO2;SUMO3;SUMO4
Peptidyl-prolyl cis-trans isomerase A;Peptidyl-prolyl cis-trans isomerase A, N-terminally processed	PPIA
Ubiquitin-40S ribosomal protein S27a;Ubiquitin;40S ribosomal protein S27a	RPS27A
Tubulin alpha-1B chain;Tubulin alpha-1A chain;Tubulin alpha-3C/D chain;Tubulin alpha-3E chain;Tubulin alpha-1C chain	TUBA1B;TUBA1A;TUBA3C;TUBA3E;TUBA1C
Bcl-2-like protein 1	BCL2L1
Neuroblast differentiation-associated protein AHNAK	AHNAK
Leiomodin-3	LMOD3
Syntaxin-4	STX4
Cytoplasmic dynein 1 heavy chain 1	DYNC1H1
Deoxynucleotidyltransferase terminal-interacting protein 2	DNTTIP2
Deoxynucleotidyltransferase terminal-interacting protein 2	DNTTIP2
Neural proliferation differentiation and control protein 1	NPDC1
Focadhesin	FOCAD

TOM1-like protein 2	TOM1L2
Keratinocyte-associated transmembrane protein 2	KCT2
RNA polymerase-associated protein LEO1	LEO1
Protein S100-A13	S100A13
Protein FAM49B	FAM49B
Ataxin-10	ATXN10
Sodium-dependent multivitamin transporter	SLC5A6
Melanoma-associated antigen D1	MAGED1
Suppressor of tumorigenicity 14 protein	ST14

Appendix 5: Awards, presentations and publications

Irish Cancer Society Celebration of Research: Best poster
April 2014

Young Life Scientists' Symposium: Best poster
November 2014

Irish Association for Cancer Research (IACR) Annual Meeting, Irish Cancer Society Scholars and Fellows session: Oral presentation
February 2015 and February 2016

European Association for Cancer Research (EACR) Precision Medicine in Cancer Conference travel bursary: €906
March 2015

Royal Academy of Medicine Section of Biomedical Sciences: Donegan Medal first runner up
June 2015

EACR 24th Biennial Congress travel bursary: €677
July 2016

Irish Association of Pharmacologists Annual Conference: Best oral presentation
November 2016

Irish Cancer Society Researcher of the Year nominee
December 2016

British Association for Cancer Research (BACR)/Cancer Research UK (CRUK) travel bursary to attend American Association for Cancer Research (AACR) Annual Meeting: £1000
April 2017

AACR-Aflac Scholar-in-training Award: $2000
April 2017

AACR Annual Meeting: Oral presentation
April 2017